Mechanism(s) of Ischaemia/Reperfusion Injury and Cardioprotection

A thesis submitted in fulfilment of the requirements for the degree of Doctor of Philosophy

KAI YEE CHIN

Bachelor of Science (Hons)

School of Medical Sciences

College of Science Engineering and Health

RMIT University

August 2015

DECLARATION

I certify that except where due acknowledgement has been made, the work is that of the author alone; the work has not been submitted previously, in whole or in part, to qualify for any other academic award; the content of the thesis is the result of work which has been carried out since the official commencement date of the approved research program; any editorial work, paid or unpaid, carried out by a third party is acknowledged; and, ethics procedures and guidelines have been followed.

KAI YEE CHIN

19th August 2015

ACKNOWLEDGEMENT

This acknowledgement goes out to people who have crossed the path of my PhD journey, making it a wonderful PhD experience for me.

Firstly, I would like to express my greatest gratitude to my primary supervisor, Professor Owen Woodman. I joined Prof Woodman's laboratory in 2010 when I did a mini research project during the final year of my undergraduate studies. I had a very good experience working with Prof Woodman and I decided to continue my Honours studies with Prof Woodman, which was in collaboration with A/Prof Rebecca Ritchie from the Baker IDI Heart and Diabetes Institute. It was a challenging yet rewarding year for me and I received the Dux award for my Honours studies in Bachelor of Biomedical Science. Then, I continued my PhD studies with Prof Woodman. Prof Woodman has been a very supportive, helpful, patient and understanding supervisor. I am extremely grateful to receive research training from him and I owe everything that I have achieved during my PhD studies to him. Thank you!

Secondly, my sincere appreciation goes out to A/Prof Rebecca Ritchie and all members of the Heart Failure Pharmacology Baker IDI Heart and Diabetes Institute, especially Dr Helena Qin. I did my Honours studies and performed several experiments for my PhD studies in A/Prof Ritchie's laboratory. A/Prof Ritchie has always welcomed me to work in her laboratory and has been helpful in my research studies. I have also learnt the Langendorff technique in A/Prof Ritchie's laboratory under Dr Qin's guidance. Dr Qin who is like my big sister has always provided me with immense support. In addition, I would also like to thank my secondary supersivor, A/Prof Ian Darby for his expert advice with regards to the immunohistochemistry technique.

To the current (Saher and Salheen) and previous (Dr Chen Huei Leo) members of the laboratory, and fellow colleague (Dr Simon Potocnik) in the vascular research group, it has been a great pleasure working with each of you in the laboratory. I am extremely grateful to Dr Leo for his constant support and enhancing my Western blot technique. I am also very grateful to Dr Potocnik for his technical assistance and for fixing my broken instrument. I would not be able to carry out my experiments efficiently without his kind assistance.

Last but definitely not least, I would like to thank my family members and friends for their endless support and encouragement. Thank you to each of you for always being there for me whenever I need help or a listening ear during the stressful period. Thank you very much!

PUBLICATIONS

K.Y. CHIN, L. MICHEL, C. QIN, N. CAO, O.L. WOODMAN, R.H. RITCHIE (2015) The HNO donor Angeli's salt offers potential hemodynamic advantages over NO• or dobutamine in ischemia-reperfusion injury in the rat heart *in vitro.* Manuscript submitted to *American Journal of Physiology- Heart and Circulatory Physiology (#H-00637-2015)*

K.Y. CHIN, C. QIN, L. MAY, R.H. RITCHIE, O.L. WOODMAN (2015) New pharmacological approaches to the prevention of myocardial ischemia-reperfusion injury. Accepted manuscript in *Current Drug Targets*

K.Y. CHIN, C. QIN, N. CAO, B.K. KEMP-HARPER, O.L. WOODMAN, R.H. RITCHIE (2014) The concomitant coronary vasodilator and positive inotropic actions of the nitroxyl donor Angeli's salt in the intact rat heart: contribution of soluble guanylyl cyclase-dependent and -independent mechanisms. *British Journal of Pharmacology,*171: 1722-1734

CONFERENCE ABSTRACTS

K.Y. CHIN, L. MICHEL, C. QIN, R.H. RITCHIE, O.L. WOODMAN (2015) Preservation of coronary vasodilator responses to the nitroxyl donor Angeli's salt after ischemia/reperfusion of the rat isolated heart, *The FASEB Journal*, 29 (S1026.1)

K.Y. CHIN, I.A. DARBY, O.L. WOODMAN (2014) Investigation of the mechanism(s) of flavonol-induced cardioprotection, *Proceedings of International Society of Cardiovascular Pharmacotherapy*, Adelaide, Australia, P01

K.Y. CHIN, I.A. DARBY, O.L. WOODMAN (2014) Investigation of the mechanism(s) of flavonol-induced cardioprotection, *Proceedings of College of Science, Engineering and Health Higher Degree by Research Student Conference, RMIT University*, Melbourne, Australia, Oral presentation

K.Y. CHIN, C. QIN, N. CAO, B.K. KEMP-HARPER, O.L. WOODMAN, R.H. RITCHIE (2014) The concomitant coronary vasodilator and positive inotropic actions of the nitroxyl donor Angeli's salt in the intact rat heart: contribution of soluble guanylyl cyclase-dependent and -independent mechanisms, *Proceedings of College of Science, Engineering and Health Higher Degree by Research Student Conference, RMIT University*, Melbourne, Australia, P40

K.Y. CHIN, I.A. DARBY, O.L. WOODMAN (2014) Investigation of the mechanism(s) of flavonol-induced cardioprotection in rat isolated hearts, *The FASEB Journal*, 28 (S652.7)

K.Y. CHIN, C. QIN, N. CAO, B.K. KEMP-HARPER, O.L. WOODMAN, R.H. RITCHIE (2013) The concomitant coronary vasodilator and positive inotropic actions of the nitroxyl donor Angeli's salt in the intact rat heart: contribution of soluble guanylyl cyclase-dependent and -independent mechanisms, *Proceedings of Australian Society of Clinical and Experimental Pharmacologists and Toxicologists*, Melbourne, Australia, P404 and oral presentation

K.Y. CHIN, C. QIN, N. CAO, B.K. KEMP-HARPER, O.L. WOODMAN, R.H. RITCHIE (2013) The concomitant coronary vasodilator and positive inotropic actions of the nitroxyl donor Angeli's salt in the intact rat heart: contribution of soluble guanylyl cyclase-dependent and -independent mechanisms, *Proceedings of Biomed Link Conference,* Melbourne, Australia, P28

R.H. RITCHIE, **K.Y. CHIN**, C. QIN, N. CAO, B.K. KEMP-HARPER, O.L. WOODMAN (2013) Soluble guanylyl cyclase mediates concomitant coronary vasodilator and positive inotropic actions of the HNO donor Angeli's salt in the intact rat heart, *BMC Pharmacology and Toxicology,* 14 (Suppl 1): P57

R.H. RITCHIE, **K.Y. CHIN**, C. QIN, N. CAO, B.K. KEMP-HARPER, O.L. WOODMAN (2012) The nitroxyl donor Angeli's salt elicits concomitant concentration-dependent coronary vasodilatory and inotropic actions in the intact rat heart. *Circulation Research,* 111 (Suppl S): 156

R.H. RITCHIE, **K.Y. CHIN**, C. QIN, N. CAO, B.K. KEMP-HARPER, O.L. WOODMAN (2012) Nitroxyl (HNO), the novel redox sibling of NO•, enhances left ventricular (LV) function and coronary flow via thiol-sensitive and cGMP-dependent actions: impact of diabetes, *Heart, Lung and Circulation,* 21 (Suppl 1): S87

R.H. RITCHIE, **K.Y. CHIN**, C. QIN, N. CAO, B.K. KEMP-HARPER, O.L. WOODMAN (2011) The cardiac actions of the nitroxyl (HNO) donor Angeli's salt are thiol-sensitive and cGMP-dependent: impact of diabetes, *Proceedings of the Australian Physiological Society,* Perth, Australia, 42: P104

TABLE OF CONTENTS

LIST OF FIGURES

CHAPTER 3

CHAPTER 4

CHAPTER 5

CHAPTER 6

LIST OF TABLES

LIST OF ABBREVIATIONS

1-NCA	1-nitrosocyclohexyl acetate
4-AP	4-aminopyridine
ADP	adenosine diphosphate
Akt	protein kinase B
ALARM-HF	acute heart failure global survey of standard treatment
AMP	adenosine monophosphate
ANOVA	analysis of variance
ANT	adenine nucleotide translocase
$ApoE^{-/-}$	apolipoprotein E–deficient
ASK	apoptosis signal-regulating kinase
ATP	adenosine triphosphate
AUC	area under the curve
BAD	Bcl-2-associated death promoter
Bax	Bcl-2-associated X protein
Bcl-2	B-cell lymphoma-2
Bcl-X	Bcl-extra large
BK_{Ca}	calcium-activated potassium channel
BSA	bovine serum albumin
Ca^{2+}	calcium ions
Ca^{2+}-ATPase	calcium pump
$CaCl_2$	calcium chloride
cAMP	cyclic adenosine monophosphate
CaMKII	calcium/calmodulin-dependent kinase II
cGMP	cyclic guanosine monophosphate
CGRP	calcitonin gene-related peptide
$CGRP_{8-37}$	calcitonin gene-related peptide receptor antagonist
CO_2	carbon dioxide
CVD	cardiovascular disease
Cyp-D	cyclophilin D

Da	Dalton
DADLE	D-Ala^2-D-Leu^5-enkephalin
DEA/NO	diethylamine NONOate
DiOHF	3’,4’-dihydroxyflavonol
DMSO	dimethyl sulfoxide
DTT	dithiothreitol
EDTA	ethylenediaminetetraacetic acid
eNOS	endothelial nitric oxide synthase
Erk	extracellular signal-regulated kinase
Fe^{2+}	ferrous ions
Fe^{3+}	ferric ions
GRP78	78 kDa glucose-regulated protein
GSH	glutathione
GSK	glycogen synthase kinase
GSSH	glutathione disulphide
GTN	glyceryl trinitrate
H^+	hydrogen ions
HCO_3^-	bicarbonate ions
HNO	nitroxyl
HO-1	haem oxygenase-1
HRP	horseradish peroxidise
HXC	hydroxocobalamin
I/R	ischaemia/reperfusion
IL	interleukin
IPA/NO	isopropylamine NONOate
JAK	Janus kinase
JNK	*c-jun* N-terminal kinase
K^+	potassium ions
K_{ATP}	ATP-sensitive potassium channel
K_v	voltage-gated potassium channel
KCl	potassium chloride

KH_2PO_4	potassium phosphate monobasic
L-NMMA	N-monomethyl-L-arginine
LDH	lactate dehydrogenase
LVDP	left ventricular developed pressure
LVEDP	left ventricular end-diastolic pressure
LVSP	left ventricular systolic pressure
LVP	left ventricular pressure
MAPK	mitogen-activated protein kinase
MAPKK/ MAP2K/ MEK/ MKK	mitogen-activated protein kinase kinase
MAPKKK/ MAP3K/ MEKK/ MKKK	mitogen-activated protein kinase kinase kinase
MLK	mixed-lineage kinase
mPTP	mitochondrial permeability transition pore
$MgSO_4 \bullet 7H_2O$	magnesium sulphate hepta hydrate
Na^+	sodium ions
Na^+/Ca^{2+} exchanger	sodium-calcium exchanger
Na^+/H^+ exchanger	sodium proton exchanger
Na^+/ HCO_3^- co-transporter	sodium-bicarboante co-transporter
Na^+/ K^+-ATPase	sodium-potassium pump
Na_2HPO_4	sodium phosphate dibasic
$Na_2N_2O_3$	sodium trioxodinitrate
NaCl	sodium chloride
NADH	nicotinamide adenine dinucleotide
NADPH	nicotinamide adenine dinucleotide phosphate
$NaH_2PO_4 \bullet H_2O$	sodium dihydrogen phosphate monohydrate
$NaHCO_3$	sodium bicarbonate
NaOH	sodium hydroxide
NF-κβ	nuclear factor kappa-light-chain-enhancer of activated B cells
NO	nitric oxide
NO^-	nitroxyl ions

NOS	nitric oxide synthase
$\bullet O_2^-$	superoxide anions
O_2	oxygen molecules
ODQ	1H-[1,2,4]oxadiazolo[4,3-a]quinoxalin-1-one
PBS	phosphate buffered saline
PFA	paraformaldehyde
$PhSO_2NHOH$	N-hydroxybenzenesulfonamide
PI3K	phosphatidylinositol 3′-kinase
PLN	phospholamban
PKA	protein kinase A
Raf	proto-oncogene serine/threonine protein kinase
RISK	Reperfusion Injury Salvage Kinase
ROS	reactive oxygen species
RPP	cate pressure product
RyR	ryanodine receptor
SAPK	stress-activated protein kinase
SAFE	Survivor Activating Factor Enhancement
SDS-PAGE	sodium dodecyl sulfate-polyacrylamide gel electrophoresis
SEM	standard error of mean
Ser	serine
SERCA	sarco/endoplasmic reticulum Ca^{2+}-ATPase
sGC	soluble guanylyl cyclase
SR	sarcoplasmic reticulum
STAT	signal transducer and activator of transcription
TBST	Tris buffered saline plus 0.1% Tween-20
TdT	terminal deoxynucleotidyl transferase
TEMED	N,N,N',N'-tetramethylethylenediamine
TGF	transforming growth factor
Thr	threonine
TNF	tumour necrosis factor
Tris	tris(hydroxymethyl) aminomethane

TUNEL	terminal deoxynucleotidyl transferase dUTP nick end labelling
Tyr	tyrosine
U46619	9,11-dideoxy-9α,11α-methanoepoxy prostaglandin $F_{2\alpha}$
WHO	World Health Organisation

SUMMARY

Acute myocardial infarction secondary to coronary artery occlusion is a leading cause of death worldwide. Timely myocardial reperfusion, using either thrombolytic therapy or percutaneous coronary intervention, is the primary treatment for patients with acute ST-segment elevation myocardial infarction. Although this reperfusion strategy is essential for myocardial salvage, it can in itself induce myocardial damage and cardiomyocyte death, a phenomenon termed “myocardial reperfusion injury”. There are no pharmacological strategies to address reperfusion injury that have achieved successful clinical outcome. An emerging strategy to alleviate this ischaemia/reperfusion (I/R) injury is to manipulate the interplay between pro-injurious and pro-survival kinase pathways at the time of reperfusion.

The first part of my PhD study is to determine the temporal change in the expression of pro-injurious kinases implicated during I/R, which include the mitogen-activated protein kinases (MAPKs) *c-jun* N-terminal kinases (JNKs) and p38 MAPK together with calcium/calmodulin-dependent protein kinase (CaMK) II and phospholamban (PLN), as well as kinases that are pro-survival including the MAPK extracellular signal-regulated kinase (Erk) 1/2, protein kinase B (Akt) and signal transducer and activator of transcription (STAT) 3. Langendorff-perfused rat hearts were subjected to 20 min no-flow global ischaemia without reperfusion or followed by either 5, 15 or 30 min reperfusion. The temporal change in the expression of pro-injurious and pro-survival kinases during myocardial I/R was studied using Western blot. It was found that p38 MAPK and CaMKII were phosphorylated during ischaemia and the phosphorylation of p38 MAPK, but not CaMKII, remained elevated throughout 30 min reperfusion. No significant changes in the phosphorylation of pro-injurious kinases JNK 1/2 or protective kinases Erk 1/2, Akt and STAT3 were observed during ischaemia while their phosphorylation was subsequently elevated to be highest at 30 min of

reperfusion. The phosphorylation of PLN was greatest at 5 min of reperfusion and reduced to basal levels 15 min after reperfusion. In conclusion, the expression of most kinases investigated in this study was highest at 30 min of reperfusion, except for PLN where phosphorylation was highest at 5 min of reperfusion. p38 MAPK and CaMKII were phosphorylated during ischaemia and the phosphorylation of p38 MAPK, but not CaMKII remained elevated throughout 30 min reperfusion.

In the second part of my study, the ability of the synthetic flavonol, 3',4'-dihydroxyflavonol (DiOHF) to alter the expression of pro-survival and pro-injurious kinases during myocardial I/R was studied. DiOHF has been demonstrated to confer cardioprotection against myocardial I/R injury in various models including sheep and goat *in vivo* and rats *in vitro*. These data suggest that it has the potential as an adjunctive therapeutic agent for reperfusion injury however the mechanism of DiOHF-induced cardioprotection remains elusive. Isolated rat hearts were subjected to 20 min global, no-flow ischaemia followed by 5 or 30 min reperfusion in the presence of 10 μM DiOHF. The post-ischaemic cardiac relaxation was significantly improved, accompanied by reduced lactate dehydrogenase release, an indicator of cell death, and the number of apoptotic bodies measured using an *in situ* apoptosis detection assay was also decreased with DiOHF treatment compared to its vehicle control. At 5 min reperfusion, DiOHF treatment had no significant effect on the phosphorylation of p38 MAPK, JNK 1/2, CaMKII, Akt, Erk 1/2 and STAT3 compared to its vehicle control, however it significantly reduced the I/R-induced increased phosphorylation of PLN. At 30 min of reperfusion, the phosphorylation of p38 MAPK, Erk 1/2 and STAT3 was also not affected with DiOHF treatment compared to its vehicle control. I/R-induced increased phosphorylation of the pro-injurious kinase JNK 2 at 30 min of reperfusion was significantly reduced with DiOHF treatment. I/R-induced increased phosphorylation of CaMKII also tended to decrease with DiOHF treatment, although not significant, while the

phosphorylation of PLN remained low with DiOHF treatment at 30 min of reperfusion. Interestingly, the I/R-induced increased phosphorylation of the protective kinase Akt was also reduced with DiOHF treatment at 30 min of reperfusion. These data suggest that DiOHF exerted protection against reperfusion injury in rat isolated hearts by inhibiting I/R-induced increased activation of PLN at 5 min of reperfusion while the protective action of DiOHF at 30 min reperfusion was mediated by inhibiting the I/R-induced increased activation of JNK 2 and maintaining the activation of PLN at low levels without affecting the activation of protective kinases Erk 1/2 and STAT3.

After an episode of acute myocardial infarction, patients are highly susceptible to develop acute heart failure. Patients with acute heart failure and a low systolic pressure at admission have a high mortality rate, therefore they are often treated with a positive inotrope. The redox sibling of nitric oxide, nitroxyl (HNO) has been shown to improve cardiac contractility and vasodilatation in normal and failing hearts in a canine model. The mechanism of the cardiac and vascular action of HNO has been investigated in isolated cardiomyocytes and in rat isolated hearts using a constant flow preparation. The third part of my study was to investigate the mechanism of action of the HNO donor Angeli's salt using isolated hearts perfused at constant pressure. Angeli's salt (10 pmol- 10 μmol) elicited concomitant, potent dose-dependent increases in coronary flow and cardiac contractility in normal rats hearts. The mechanism of the dilator and cardiac actions of Angeli's salt was investigated in the presence of various pharmacological agents including the HNO scavenger L-cysteine (4 mM), the nitric oxide scavenger hydroxocobalamin (HXC, 0.1 mM), the calcitonin gene-related peptide (CGRP) receptor antagonist $CGRP_{8-37}$, (0.1 μM), the soluble guanylyl cyclase (sGC) inhibitor 1H-[1,2,4]oxadiazolo[4,3-a]quinoxalin-1-one (ODQ, 10 μM), the voltage-gated potassium channel inhibitor, 4-aminopyridine (4-AP, 1 mM) and the thiol-reducing agent, dithiothreitol (DTT, 100 μM). These scavengers or inhibitors were

added for at least 15 min in the physiological buffer before the dose–response curve to Angeli's salt was carried out. L-cysteine and ODQ caused a rightward shift in (but did not abolish) the dose-response curve of the cardiac and dilator effects induced by Angeli's salt, implicating contributions from HNO and sGC in both the vasodilator and inotropic actions of Angeli's salt. In contrast, neither the HXC, $CGRP_{8-37}$ nor 4-AP affected Angeli's salt actions. In addition, the presence of the DTT attenuated the inotropic, but not the dilator action of Angeli's salt. These data suggest that Angeli's salt induced vasodilatation and cardiac contractility via sGC-dependent and thiol-sensitive mechanisms.

In the fourth part of my study, the acute improvement in cardiac and vascular function by Angeli's salt after myocardial I/R was investigated. The cardiac effect of Angeli's salt was compared to the clinically used inotrope for acute heart failure dobutamine, while its dilator effect was compared with the nitric oxide donor, diethylamine NONOate (DEA/NO). Rat isolated hearts were subjected to 75 min physiological buffer perfusion (sham) or treated with 30 ischaemia followed by 25 min reperfusion. Following pre-constriction of the coronary vasculature with the thromboxane mimetic U46619 (9,11-dideoxy-9α,11α-methanoepoxy prostaglandin $F_{2\alpha}$, 3 μM), dose-response curves to the HNO donor, Angeli's salt (1 nmol- 10 μmol), the nitric oxide donor, DEA/NO (1 nmol- 1 μmol) and the clinically used inotrope for acute heart failure, dobutamine (100 pmol- 100 nmol) were performed. Both Angeli's salt and DEA/NO elicited dose-dependent increases in coronary flow in sham hearts. The vasodilator response to Angeli's salt, but not DEA/NO was preserved in hearts subjected to I/R. Angeli's salt and dobutamine also increased cardiac contractility in sham hearts, however positive inotropic actions caused by both Angeli's salt and dobutamine were impaired in I/R-treated hearts. In addition, tachycardia caused by dobutamine, but not Angeli's salt, was exacerbated in I/R-treated hearts and this may increase the risk of arrhythmias which can cause sudden cardiac death. These data suggest that Angeli's salt may have advantages over the clinically

used inotrope, dobutamine to improve impaired cardiac function after acute myocardial infarction and it also had superior coronary vasodilator capacity after I/R.

In conclusion, these studies provide evidence to support the possible use of DiOHF and HNO in the treatment of acute myocardial infarction to reduce reperfusion injury or to improve cardiac contractility and induce vasodilatation respectively.

Chapter 1

1. Literature Review

1.1 Introduction

Cardiovascular disease (CVD) remains the leading cause of death worldwide. The World Health Organisation (WHO) estimated that in 2012, 17.5 million people died from CVDs, which contributed to 31% of all global deaths. Of these deaths, an estimated of 7.4 million cases were due to coronary heart disease. Coronary heart disease, a disease of blood vessels supplying the heart muscle, is predominantly caused by the formation of atherosclerosis, which is characterized by the accumulation of fatty acids, cholesterols and white blood cells in blood vessels, leading to blockage of blood vessels and cessation of blood flow to the heart. Major complications of coronary heart disease include myocardial infarction and heart failure. Timely reperfusion of the blocked vessel is critical to restore the blood flow to the ischaemic myocardium to salvage myocardial tissues and improve clinical outcomes. Paradoxically, this reperfusion strategy can induce a form of myocardial injury called reperfusion injury.

Myocardial reperfusion injury was first suggested by Jennings and colleagues in 1960 when they observed pathological changes in the canine heart after ischaemia/reperfusion (I/R) (Jennings *et al.*, 1960). The morphological changes in the canine heart included cell swelling, contracture of myofibrils and calcification in the mitochondria. In later years, 4 types of reperfusion-induced cardiac dysfunction have been reported which include: i) reperfusion arrhythmias, ii) microvascular dysfunction, iii) myocardial stunning and iv) lethal reperfusion injury (Yellon & Hausenloy, 2007). The first 3 types of cardiac dysfunction are reversible;

however, lethal reperfusion injury contributes to further myocardial tissue death beyond that generated by ischaemia alone. It has been reported that as much as 50% of the final myocardial infarct size is due to the reperfusion injury (Yellon & Hausenloy, 2007), indicating that pharmacological intervention at the time of reperfusion to resuscitate ischaemic myocardium is a realistic proposition to reduce infarct size. At present, there is no effective pharmacological treatment for reperfusion injury.

1.2 Pathological features of I/R injury

1.2.1 Reperfusion arrhythmias

The detrimental consequences of reperfusion have been realized for well over a century. In one of the earliest known reports from the 19th century, Cohnheim and Von Schulthess-Rechberg (1881) reported ventricular fibrillation (which is defined as asynchronous excitations and contractions in the ventricular region) occurred within seconds of the onset of myocardial reperfusion in an experimental model (Wit & Janse, 2001). The incidence of arrhythmias depends on the species and the duration of the preceding ischaemic period with maximum frequency of arrhythmias after 10 to 30 min of ischaemia (Manning & Hearse, 1984). Elevated levels of reactive oxygen species (ROS) have been the focus of considerable attention as possible initiators of arrhythmias (Kloner *et al.*, 1989). ROS, generated on reperfusion, triggers protein oxidation and lipid peroxidation, which in turn disrupts cell membrane integrity and modifies the activity of a number of ionic translocating proteins in the sarcolemma (Opie, 1989). As a result, electrophysiological alterations including shortening of the action potential, reduced amplitude and maximum rate of depolarization, decreased conduction velocity and abnormal automaticity occur (Opie, 1989). The disturbance in the ionic homeostasis, particularly potassium (K^+) and calcium (Ca^{2+}) ions

and the stimulation of adrenergic receptors may also contribute to reperfusion arrhythmias (Hearse & Bolli, 1992).

1.2.2 Microvascular dysfunction and the "no-reflow" phenomenon

The "no-reflow" phenomenon is defined as inadequate myocardial perfusion through a segment of the coronary circulation without angiographic evidence of mechanical vessel obstruction after the opening of an occluded artery (Kloner *et al.*, 1974). This phenomenon was first described in 1966 by Krug and colleagues where significant portions of the cat inner myocardium were not perfused after temporary occlusions of 60 to 120 min (Krug *et al.*, 1966). In 1974, Kloner and colleagues again demonstrated that after 90 min coronary artery occlusion in the canine heart, myocardial tracers such as carbon black or thioflavin S (a fluorescent stain for endothelium) injected to measure the distribution of coronary arterial flow showed a significant area of the inner half of the damaged myocardium was not penetrated by tracers (Kloner *et al.*, 1974). This suggested that poor or absent perfusion of the previously ischaemic myocardium in the inner ventricular wall had occurred (Kloner *et al.*, 1974). In addition, electron microscopic study showed severe capillary damage and myocardial cell swelling in the poorly perfused area (Kloner *et al.*, 1974). Intraluminal capillary plugging by neutrophils, endothelial protrusions (also called "blebs") and/or microthrombi was also reported (Kloner *et al.*, 1974).

Possible causes of this phenomenon include myocardial cell swelling associated with interstitial edema compressing the microvessel, and capillary occlusion by aggregated platelets and/or neutrophils that limit adequate perfusion on reperfusion (Reffelmann & Kloner, 2002). In addition, vasoconstrictors released by damaged endothelial cells, neutrophils and platelets as well as the overproduction of superoxide anions ($\bullet O_2^-$) due to increased production of xanthine oxidase by neutrophils may cause impaired endothelium-

dependent, nitric oxide (NO)-mediated relaxation and result in sustained vasoconstriction of coronary microcirculation (Niccoli *et al.*, 2009). Microemboli formation from the atherosclerotic plaque debris may also obstruct blood flow and contribute to the development of "no-reflow" phenomenon (Reffelmann & Kloner, 2002).

In the clinical setting, no-reflow has also been reported in patients after thrombolysis or mechanical reperfusion therapy such as percutaneous coronary interventions (Schofer *et al.*, 1985; Bates *et al.*, 1986; Wilson *et al.*, 1989). The no-reflow phenomenon that occurs after a reperfusion strategy has been associated with a higher prevalence of early post-infarction complications such as left ventricular remodeling and rupture, congestive heart failure and death (Eeckhout & Kern, 2001).

1.2.3 Myocardial stunning

Myocardial stunning is the transient mechanical left ventricular dysfunction that persists after reperfusion, despite the absence of irreversible damage (Bolli, 1990). Stunning is a reversible injury which must be distinguished from the irreversible injury of infarction. Evidence for myocardial stunning has emerged from a considerable number of both experimental and clinical studies. In anesthetized dogs, for example, 15 min of myocardial ischaemia followed by reperfusion results in a prolonged decrease in contractility lasting several hours despite all cells remaining viable (Farber *et al.*, 1988). Left ventricular dysfunction consistent with stunning has been demonstrated in many clinical settings, such as that evident in patients subjected to planned periods of global I/R during coronary artery bypass grafting, surgery for coronary artery disease (Ferrari *et al.*, 1990).

The precise mechanism responsible for myocardial stunning requires further investigation, but the following three appear most plausible: i) elevated levels of ROS, ii) Ca^{2+} overload and iii) excitation-contraction uncoupling (Bolli, 1990). It has been suggested

that increased oxidative stress disrupts several proteins involved with Ca^{2+} flux across both the sarcolemma and sarcoplasmic reticulum, which results in reduced Ca^{2+} sequestration from the cell and increased free cytosolic Ca^{2+} concentration. This impairs the contractility in the ischaemic myocardium (Jeroudi *et al.*, 1994). Altered Ca^{2+} homeostasis may also disrupt excitation-contraction uncoupling causing mechanical left ventricular dysfunction (Jeroudi *et al.*, 1994). In addition, the production of ROS may also react with contractile proteins via oxidative modifications (e.g. oxidation of critical thiol groups) and a decrease in the responsiveness of myofilaments to Ca^{2+} may lead to impaired left ventricular contractility (Bolli, 1990). Although myocardial stunning is usually considered transient and reversible, lasting hours rather than days or weeks, the phenomenon of "chronically stunned myocardium" is now emerging, particularly in large, pre-clinical animal models and in patients (Canty & Suzuki, 2012).

1.2.4 Lethal reperfusion injury

Lethal reperfusion injury can be defined as the injury caused by the restoration of blood flow after an ischaemic episode leading to death of cells that were viable at the time of reperfusion. Cardiomyocyte death as a result of I/R injury involves two major types of cell death: apoptosis and necrosis. Necrosis is an irreversible form of cell death that is a direct result of prolonged ischaemia, characterized by irreversible cell membrane rupture with the release of cytosolic components (Bartling *et al.*, 1998). As distinct to necrosis, apoptotic cell death features cell shrinkage, chromatin condensation, formation of cytoplasmic blebs and apoptotic bodies, without loss of membrane integrity or inflammation (Bartling *et al.*, 1998). Both necrosis and apoptosis are evident following post-ischaemic reperfusion; in contrast, necrotic (but not apoptotic) cell death is evident after permanent coronary artery occlusion without reperfusion (Zhao *et al.*, 2000).

Death of cardiomyocytes during I/R appears to be an active process, which can be inhibited with appropriate interventions. Interestingly, mitochondria are emerging as a crucial regulator in all forms of cell death in I/R injury, in particular with respect to the mitochondrial permeability transition pore (mPTP) (Lemasters *et al.*, 1998). Mitochondrial PTPs are voltage-dependent and high conductance channels. Opening of mPTPs can result in the activation of a series of signalling events leading to apoptosis and necrosis (Lemasters *et al.*, 1998). The mPTP can be activated as a result of increased ROS and/or Ca^{2+} overload, as discussed later.

1.3 Mechanisms of I/R injury

There is growing understanding of the pathophysiological mechanisms of myocardial I/R injury that is helping to guide the investigation of new pharmacological approaches to cardioprotection. In particular, ROS overproduction, Ca^{2+} overload and infiltration of inflammatory cells into the site of injury have received considerable attention in their role as important mediators of the direct myocardial I/R injury.

1.3.1 ROS hypothesis of myocardial I/R injury

Molecular oxygen (O_2) is used as a terminal electron acceptor to metabolize organic carbon to provide energy. In the myocardium, 95% of O_2 is reduced by tetravalent reduction to water through the mitochondrial electron transport chain, however a small percentage (<5%) of O_2 consumed can leak from this respiratory chain and result in the formation of various ROS including $\bullet O_2^-$, hydroxyl radicals, hydrogen peroxide, peroxynitrite and hypochlorous acid (Bandyopadhyay *et al.*, 2004). Under physiological conditions, oxygen-derived free radicals are important mediators in signal transduction to induce transcription factor activation, gene expression, cell growth and others; however, they can also promote

oxidation of lipids, proteins and DNA resulting in lethal cell damage (Bandyopadhyay *et al.*, 2004). There are also a group of proteins called antioxidants present in the cell which function is to inhibit oxidation and prevent the oxidation-induced cellular damage (Bandyopadhyay *et al.*, 2004). When the antioxidant defense mechanism fails to counteract the accumulation of ROS, oxidative stress occurs and this could cause cell death.

ROS generation has been documented during ischaemia; however maximal levels of ROS occur during reperfusion. Zweier and colleagues demonstrated that oxygen-centered radical production was detected during ischaemia while a burst of oxygen free radical generation occurred during the first 10 sec of reperfusion in perfused rabbit hearts subjected to global I/R injury (Zweier *et al.*, 1987). Later, Bolli and colleagues also reported that ROS generation was detected during coronary artery occlusion performed in open-chest dogs and this ROS generation increased dramatically after reperfusion (Bolli *et al.*, 1989). This increased ROS production contributed to post-ischaemic contractile dysfunctions in the canine heart (Bolli *et al.*, 1989).

During ischaemia, adenosine triphosphate (ATP) generation is limited due to a lack of O_2 supply and hydrolysis of ATP occurs and results in the production of adenosine diphosphate and adenosine monophosphate (AMP) (Zweier & Talukder, 2006) (Figure 1.1). AMP then undergoes catabolism to produce hypoxanthine. Upon reperfusion, hypoxanthine reacts with O_2 to form uric acid and $\bullet O_2^-$, a reaction catalyzed by xanthine oxidase (Zweier & Talukder, 2006). The activation of this series of events is a major source of ROS generation during I/R (Figure 1.1). There are also a number of potential sources from which ROS may be produced during I/R, such as from the pro-oxidant enzyme xanthine oxidase in endothelial cells, respiratory burst caused by nicotinamide adenine dinucleotide phosphate (NADPH) oxidase in inflammatory cells (especially neutrophils and monocytes), malfunction of the mitochondrial electron transport chain (particularly from complex I and III), as well as the the

uncoupling of the nitric oxide synthases (Bolli, 1988; Duilio *et al.*, 2001; Zhao, 2004; Sugamura & Keaney, 2011). Overproduction of ROS is a key feature of reperfusion arrhythmias, myocardial stunning and endothelial dysfunction; it can also trigger the opening of the mPTP resulting in cell death (Kloner *et al.*, 1989). Moreover, the severity of cell damage post-I/R is proportional to the magnitude of ROS-mediated responses within cardiomyocytes (Ferrari *et al.*, 1993).

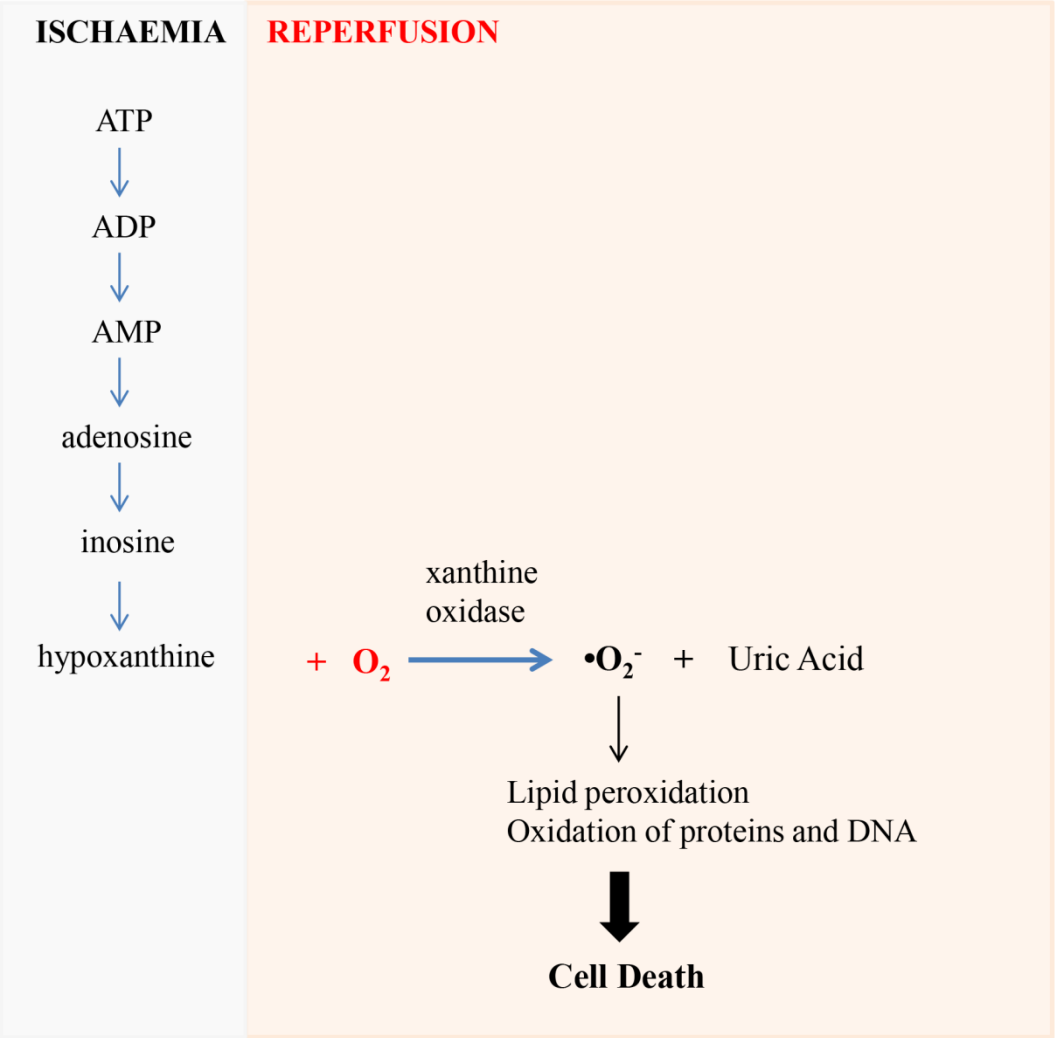

Figure 1.1: The oxygen hypothesis in myocardial ischaemia/reperfusion injury. During ischaemia, hydrolysis of adenosine triphosphate (ATP) takes place resulting in the production of adenosine diphosphate (ADP) and subsequent formation of adenosine monophosphate (AMP). There is an accumulation of AMP during ischaemia. AMP undergoes further breakdown forming hypoxanthine. Upon reperfusion, hypoxanthine reacts with oxygen molecules (O_2) and this generates superoxide anions ($\bullet O_2^-$) and uric acid. The production of $\bullet O_2^-$ can cause oxidation of lipids, proteins and DNA resulting in cell death (Zweier & Talukder, 2006).

1.3.2 Ca^{2+} hypothesis of myocardial I/R injury

Cardiomyocyte Ca^{2+} overload during myocardial I/R is the result of altered metabolism during the ischaemic insult. Under normal conditions, cardiac muscle is a highly aerobic tissue; that is, it obtains virtually all its energy from oxidative metabolism. During ischaemia, cardiomyocyte O_2 supply becomes limited, the heart undergoes anaerobic metabolism producing lactic acid and other products of anaerobic glycolysis resulting in intracellular acidosis and a drop in pH level (Sanada *et al.*, 2011). This rapid intracellular acidosis activates pH-regulating ion transporters, including the sodium proton (Na^+/H^+) exchanger and the sodium-bicarbonate (Na^+/HCO_3^-) co-transporter, which together results in cardiomyocyte Na^+ accumulation (Figure 1.2) (Tani & Neely, 1989; Pierce & Meng, 1992). On the other hand, ATP depletion during ischaemia leads to inactivation of the sodium-potassium pump (Na^+/K^+-ATPase), further enhancing cardiomyocyte Na^+ accumulation (Solaini & Harris, 2005). This Na^+ overload reverses the normal direction of the sarcolemmal Na^+/Ca^{2+} exchanger, resulting in an intracellular Ca^{2+} overload (Tani & Neely, 1989). In addition, extracellular Ca^{2+} may gain access to the cell through leaky cell membranes as a result of lipid peroxidation caused by ROS (Solaini & Harris, 2005). As soon as cytosolic Ca^{2+} rises, sarcoplasmic reticulum (the major intracellular Ca^{2+} store) releases further Ca^{2+}, due to the effect of cytosolic Ca^{2+} on the open probability of the cardiomyocyte ryanodine receptor (RyR) 2. Meanwhile, cytosolic Ca^{2+} removal mechanisms, such as Ca^{2+}-ATPases, are largely impaired during ischaemia as a result of cardiomyocyte ATP depletion and abnormal ion concentrations in the cell (Solaini & Harris, 2005). As a consequence, the cytosolic Ca^{2+} concentration increases dramatically in the ischaemic myocardium and triggers several injurious mechanisms.

During the first few minutes of reperfusion, increased cytosolic Ca^{2+} may bind to myofibrils in the presence of a resupply of oxygen, causing hypercontracture of myocytes

(Braunwald & Kloner, 1985). This can cause mechanical stiffness leading to cell disruption and eventually cell death. Ca^{2+} can also diffuse into mitochondria and mitochondrial Ca^{2+} overload can trigger the opening of the mPTP resulting in apotosis and cell death (Sanada *et al.*, 2011). Finally, increased Ca^{2+} concentrations can also cause smooth muscle contraction, which may lead to vasoconstriction and impaired reperfusion (Zucchi *et al.*, 2001).

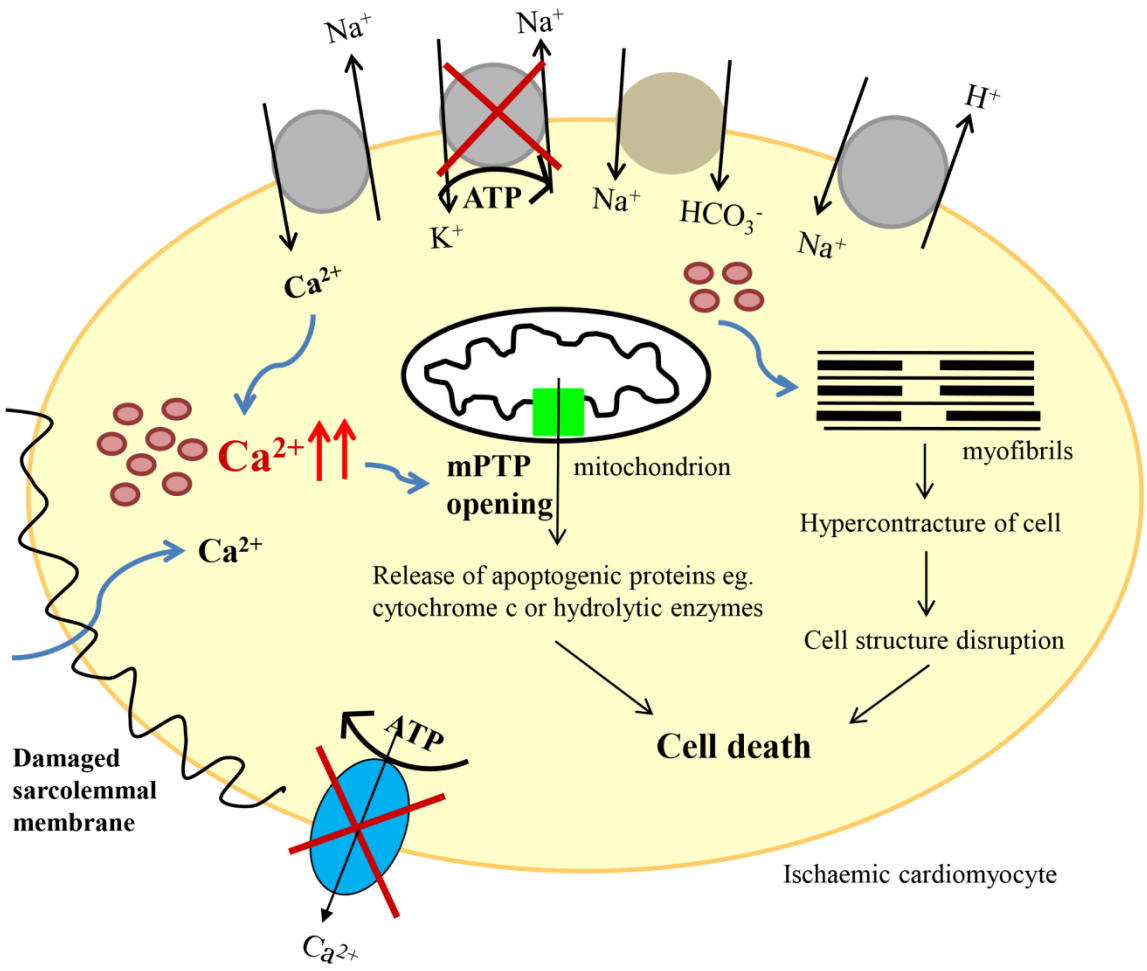

Figure 1.2: The calcium hypothesis in myocardial ischaemia/reperfusion injury. During reperfusion, calcium ions (Ca^{2+}) enter the cell directly through the damaged sarcolemmal membrane and through the reverse mode of the sodium-calcium (Na^{+}/Ca^{2+}) exchanger to normalize the high Na^{+} concentration in the cell. At the same time, cytosolic Ca^{2+} removal mechanisms, such as Ca^{2+}-adenosine triphosphatases (ATPases), are impaired due to ATP depletion during ischaemia. This increases Ca^{2+} concentration in cardiomyocytes. Intracelullar Ca^{2+} overload can result in the activation of a series of injurious events. Ca^{2+} may bind to myofibrils in the presence of a resupply of oxygen, causing hypercontracture of myocytes. This can cause cell structure disruption and result in cell death. Ca^{2+} can also diffuse into mitochondria and mitochondrial Ca^{2+} overload can trigger the opening of the mitochondrial permeability transition pore (mPTP) resulting in apoptosis (Sanada *et al.*, 2011). Na^{+}/CO_3^{-}= sodium-bicarbonate co-transporter; Na^{+}/K^{+} ATPase= sodium-potassium pump; Na^{+}/H^{+}= sodium proton exchanger

1.3.3 Mitochondria in myocardial I/R injury

As mentioned earlier, mitochondria are emerging as the major mediator of cell death during I/R. During I/R, intracellular Ca^{2+} overload and increased oxidative stress, accompanied by other factors such as high phosphate concentrations and the depletion of adenine nucleotides cause the formation of mPTPs in the mitochondrial inner membrane (Halestrap, 2010) (Figure 1.3). Upon stimulation by high Ca^{2+} contents, the key regulator of mPTP, cyclophilin D (Cyp-D) binds to adenine nucleotide translocase (ANT) and causes a conformational change of ANT and converts it into a non-specific pore (Halestrap, 2010). Cyp-D is a peptidyl-prolylcis-trans isomerase which catalyses the inter-conversion between *cis* and *trans* conformations of prolineimidic peptide bonds (Takahashi *et al.*, 1989; Halestrap *et al.*, 2002). This causes the conformational change of ANT and results in pore formation in the mitochondrial membrane (Halestrap *et al.*, 2002). Mitochondrial PTP opening allows solutes with a molecular mass of up to 1.5 kDa to diffuse across the mitochondrial inner membrane freely. This results in the dissipation of mitochondrial membrane potential ($\Delta\Psi m$), uncoupling of oxidative phosphorylation which in turn promotes ATP hydrolysis (Crompton, 1999), together with mitochondrial swelling due to water influx as a result of increased osmotic pressure in the matrix leading to outer membrane rupture and cell death (Halestrap *et al.*, 2002).

Petronilli and colleagues also reported that ROS oxidized the thiol group in the pore protein and triggered the pore opening (Petronilli *et al.*, 2009). Mitochondrial PTP opening may also release pro-apoptotic factors cytochrome C, second mitochondria-derived activator of caspase, also known as DIABLO, which is a caspase co-activator and apoptosis-inducing factor into the cytosol (Zamzami & Kroemer, 2001; Weiss *et al.*, 2003). Cytochrome C binds to apoptotic protease activating factor-1 with deoxy-ATP and caspase-9 to form a complex called the apoptosome (Zou *et al.*, 1999). This triggers the activation of caspase-3 and causes

apoptosis. Therefore, the ability to inhibit the opening of mPTP may prevent apoptosis and necrosis in cells after I/R.

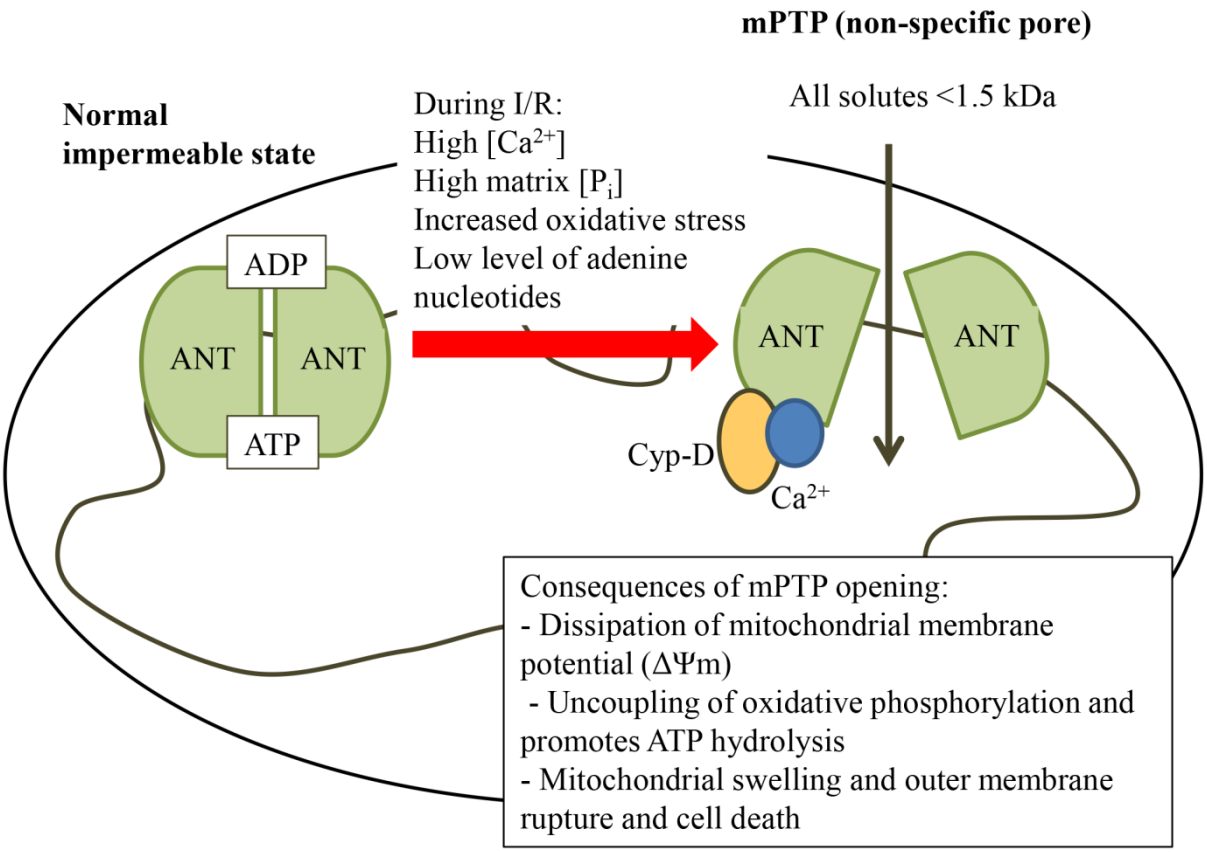

Figure 1.3: A hypothetical diagram of the formation of mitochondrial permeability transition pore (mPTP) during ischaemia/reperfusion (I/R). Intracellular calcium ions (Ca^{2+}) overload, increased oxidative stress, high phosphate levels (P_i) and the depletion of adenine nucleotides during I/R cause the formation of mPTP in the mitochondrial inner membrane. Upon stimulation by a high Ca^{2+} content, cyclophilin D (Cyp-D) binds to adenine nucleotide translocase (ANT) and causes a conformational change of ANT and converts it into a non-specific pore. Mitochondrial PTP opening allows solutes with molecular mass of up to 1.5 kDa to diffuse across the mitochondrial inner membrane freely. This results in the activation of a series of events which can lead to cell death (Halestrap, 2010). ADP= adenosine diphosphate; ATP= adenosine triphosphate

1.3.4 Inflammatory cell-mediated myocardial I/R injury

Although acute inflammation triggered during myocardial I/R is a pathophysiological healing response to I/R injury, accumulating evidence indicates that the inflammatory response which is triggered during ischaemia, and greatly augmented during reperfusion, may itself promote tissue death leading to cardiac dysfunction (Hansen, 1995). Neutrophils, which are the major component of the innate immune system, are now recognised as major mediators of myocardial I/R injury. During I/R, the inflammatory response characterized by neutrophil accumulation and leukocycte infiltration into the ischaemic myocardium is activated. Activated neutrophils may release several mediators, such as oxygen free radicals and proteolytic enzymes, which can directly cause cell injury (Weiss, 1989). They may also plug capillaries causing mechanical obstruction to blood flow and release pro-inflammatory factors (such as platelet activating factor, thromboxane and leukotrienes) which can amplify the inflammatory reaction causing further injury to post-ischaemic tissues (Jordan *et al.*, 1999). Interaction of neutrophils with the endothelium, an action mediated by soluble adhesion molecules such as E-selectin, P-selectin, intracellular adhesion molecules-1, vascular cell adhesion molecule-1 and others, may also result in endothelium dysfunction (Entman & Smith, 1994). In the clinical setting, it has also been reported that higher numbers of white blood cells at admission are associated with high mortality in patients with acute myocardial infarction, indicating a close association between systemic inflammation and a poor prognosis post-myocardial infarction (Grzybowski *et al.*, 2004).

1.4 Signalling pathways that have been implicated during I/R

Increased oxidative stress and Ca^{2+} overload during myocardial I/R could activate a wide range of signal transduction pathways and result in cell death or survival. An emerging strategy to treat myocardial I/R injury is to manipulate the activation of pro-injurious and pro-survival signalling pathways in the myocardium to reduce cardiomyocyte death, at the time of reperfusion.

1.4.1 MAPK signalling pathway

The mitogen-activated protein kinase (MAPK) superfamily consists of a group of highly conserved signal transduction kinases that have diverse roles in cardiac physiological and pathological processes (Cowan & Storey, 2003). The MAPK subfamilies are involved in many cellular processes including cell growth, development, differentiation, cell cycle, death and survival (Feuerstein & Young, 2000). The activation of MAPKs involves a three-tier system (Figure 1.4). Upon stimulation by factors such as inflammatory cytokines or growth factors, the MAPK kinase kinase (MAPKKK, MAP3K, MEKK or MKKK) is activated (Cowan & Storey, 2003). Active MAPKKK then activates its downstream signalling molecule MAPK kinase (MAPKK, MAP2K, MEK or MKK), which is a 'dual-specific' kinase that targets a threonine-X-tyrosine (Thr-X-Tyr) motif on MAPK and phosphorylates MAPK at both serine (Ser)/Thr and Tyr sites (Cowan & Storey, 2003). The activation of MAPK results in a conformational change and a >1000-fold increase in their specific activity (Cowan & Storey, 2003). Active MAPKs in turn phosphorylate their target proteins, many of which are transcription factors. Three best-characterized MAPK subfamilies are extracellular signal-regulated kinase (Erk) 1/2, *c-jun* N-terminal kinases (JNKs) and p38 MAPK (Cowan & Storey, 2003).

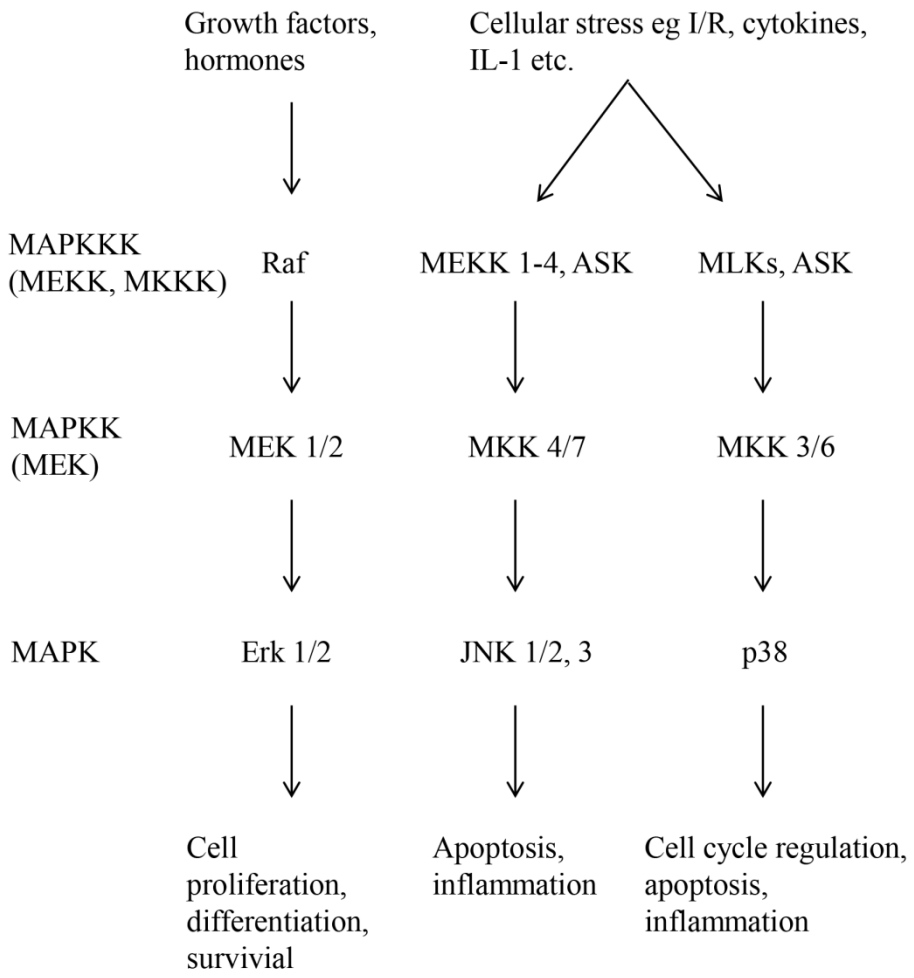

Figure 1.4: Flow chart showing the three major mitogen-activated protein kinase (MAPK) signalling cascades (extracellular signal-regulated kinases, Erks, *c-jun* N-terminal kinases, JNKs and p38 MAPK), including stimuli, three-tier regulatory substrates (mitogen-activated protein kinase kinase kinase, MAPKKK/MEKK/MKKK, mitogen-activated protein kinase kinase, MAPKK/MEK/MKK and MAPK) and the various cellular responses caused by each module (Cowan & Storey, 2003). ASK= apoptosis signal-regulating kinase; I/R= ischaemia/reperfusion; IL= interleukin; MLKs= mixed-lineage kinases; Raf= proto-oncogene serine/threonine protein kinase

1.4.1.1 Erk signalling cascade

The Erk signalling cascade is one of the most widely studied signalling pathways in cellular biology. The two best-studied Erk isomers, Erk 1 and Erk 2, which are 83% identical, share many commonalities in signalling activities, therefore they are usually referred to as Erk 1/2 (Rose *et al.*, 2010). Erk 1/2 respond primarily to growth factors such as transforming growth factor-β1, peptide hormones and neurotransmitters to cause cell survival. Upon stimulation, the small G-protein Ras is activated and active Ras recruits and activates c-Raf which is the MAPKKK in this signalling cascade (Rose *et al.*, 2010) (Figure 1.4). Active Raf then activates MEK 1/2 which in turn phosphorylates Thr and Tyr residues on the Thr-X-Tyr motif (where X is glutamate) on Erk 1/2 (Rose *et al.*, 2010). Once activated, Erk 1/2 will phosphorylate various downstream substrates including 90 kDa ribosomal S6 kinases, MAPK-activated protein kinase-1, (Frodin & Gammeltoft, 1999), cytoplasmic phospholipase A_2 (Lin *et al.*, 1993), as well as the transcription factor Elk-1 (Davis, 1993). These substrates will activate other regulatory molecules such as the transcription factor c-Fos, glycogen synthase kinase (GSK)-3 and others to cause cell proliferation, differentiation and survival (Frodin & Gammeltoft, 1999).

The activation of the Erk 1/2 signalling cascade in myocardial I/R has also been widely reported, and it is well-established to be cardioprotective. A wide range of pharmacological agents infused during I/R exert their cardioprotective effects through the activation of the Erk 1/2 signalling pathway. For example, D-Ala^2-D-Leu^5-enkephalin (DADLE), a delta-opioid receptor agonist, reduced myocardial infarct size in rat hearts *in vivo* by increasing the phosphorylation of Erk 1/2 (Ikeda *et al.*, 2006). The cardioprotective effect of DADLE was abolished in the presence of PD98059, a MEK 1/2 inhibitor, suggesting that the Erk 1/2 signalling pathway is involved in the cardioprotection by DADLE (Ikeda *et al.*, 2006). In rat isolated hearts subjected to I/R, anaesthetic post-conditioning with sevoflurane

reduced myocardial infarct size and improved post-ischaemic cardiac contractility, and these effects were mediated by activation of the Erk 1/2 signalling pathway (Yao *et al.*, 2010). It has also been reported that the activation of Erk 1/2 causes phosphorylation and inhibition of pro-apoptotic proteins such as B-cell lymphoma-2-associated X protein (Bax), B-cell lymphoma-2-associated death promoter (BAD), caspases-3 and -9 resulting in cell survival (Hausenloy & Yellon, 2007).

1.4.1.2 JNK signalling cascade

JNK consists of 3 isoforms i.e. JNK 1, JNK 2 and JNK 3. JNK 1 and JNK 2 are expressed in many tissues, while JNK 3 is predominantly found in the brain (Rose *et al.*, 2010). As a stress-activated protein kinase, JNK is activated in response to various stress stimuli including osmotic shock, UV radiation, oxidative stress, and pro-inflammatory cytokines such as tumour necrosis factor (TNF)-α and interleukin (IL)-1 (Cowan & Storey, 2003). Upon stimulation, JNK is phosphorylated at the Thr-X-Tyr (where X is a proline) motif by the dual-specificity kinases i.e. JNNK 1 and JNNK 2, also known as MKK 4 and MKK 7 (Cowan & Storey, 2003) (Figure 1.4). Upstream signalling proteins of JNNK 1/2 are MAPKKKs including MEKK 1-4 and apoptosis signal-regulating kinase (ASK) 1 (Cowan & Storey, 2003). Once activated, JNK can phosphorylate and activate various downstream signalling substrates including activating transcription factor-2 (van Dam *et al.*, 1995) and ETS domain-containing protein Elk-1, tumor suppressor p53 (Bogoyevitch & Kobe, 2006) and others. JNK strongly phosphorylates *c-jun*, leading to increased activity of the transcription factor activator protein-1 and causes cell death (Shaulian & Karin, 2002).

Reports have suggested that JNK causes apoptosis by inducing the release of apoptogenic factors such as cytochrome C from mitochondria (Aoki *et al.*, 2002). JNK can also phosphorylate and inhibit the activity of the anti-apoptotic protein B-cell lymphoma

(Bcl)-2 (Yamamoto *et al.*, 1999) while promoting apoptosis by phosphorylating pro-apoptotic proteins such as Bim and Bmf (Lei & Davis, 2003; Putcha *et al.*, 2003). In myocardial I/R, inhibition of JNK phosphorylation has been reported to be cardioprotective. The presence of a JNK inhibitor reduces myocardial infarct size after I/R in rats *in vivo* (Ferrandi *et al.*, 2004; Milano *et al.*, 2007). The protective effect of JNK inhibition in myocardial I/R is associated with attenuation of apoptosis-inducing factor translocation to the nucleus thereby preventing apoptosis (Song *et al.*, 2008; Zhang *et al.*, 2009) and inhibition of JNK mitochondrial translocation to reduce ROS generation and mitochondrial dysfunction (Chambers *et al.*, 2013).

1.4.1.3 p38 MAPK signalling cascade

p38 MAPK is a 38 kDa kinase which was first described as a tyrosine phosphorylated protein in response to bacterial lipopolysaccharide stimulation in macrophages (Rose *et al.*, 2010). There are 5 isoforms of p38 MAPK reported to date i.e. p38α, p38β, p38δ, p38γ and p38-2 with isoforms α and β being predominantly found in the heart (Cowan & Storey, 2003). Like other MAPK subfamilies, p38 MAPK signalling is involved in a variety of biological processes including apoptosis and inflammation, as well as cell growth, differentiation and cell cycle regulation (Rose *et al.*, 2010). It has been reported that p38 MAPK signalling has a major role in the immune response. The activation of p38 MAPK increases the expression of pro-inflammatory cytokines IL-1, TNF-α, cell adhesion molecules such as vascular cell adhesion molecule-1 and other inflammation-related molecules (Rose *et al.*, 2010). p38 MAPK, together with JNK, form the stress-activated protein kinase (SAPK) pathway. It is also activated by environmental stresses such as heat, hyperosmotic shock, UV radiation, I/R, as well as TNF receptor signalling (Cowan & Storey, 2003). In response to these stimuli, guanosine triphosphatases such as Rac, the Rho and the cell division control protein 42

homologs, are responsible for the transmission of these stress stimuli to MAPKKKs of this pathway (Cowan & Storey, 2003). MAPKKKs, such as mixed-lineage kinases (MLKs) and ASK 1, are activated and active MAPKKKs phosphorylate and activate their downstream effectors MKK 3 and MKK 6 (Rose *et al.*, 2010) (Figure 1.4). These dual-specificity kinases MKK 3 and MKK 6, then phosphorylate p38 MAPK at the conserved Thr-X-Tyr motif (where X is glycine) (Rose *et al.*, 2010) and active p38 MAPK phosphorylates its downstream signalling substrates such as cyclic adenosine monophosphate (cAMP) response element-binding protein (Tan *et al.*, 1996), activating transcription factor-1 (Tan *et al.*, 1996), MAPK-activated protein kinase 2 (McLaughlin *et al.*, 1996), heat shock protein 27 (Stokoe *et al.*, 1992) and others.

The role of p38 MAPK in myocardial I/R injury is controversial. Numerous studies have shown that the activation of p38 MAPK is cardioprotective in myocardial I/R. For example, pre-treatment with the p38 MAPK inhibitor, SB203580 abolished the cardioprotective effect of erythropoietin in rabbit isolated hearts subjected to global ischaemia and reperfusion (Rafiee *et al.*, 2005). The presence of another p38 MAPK inhibitor, SB202190 also attenuated the cardioprotective effect of resveratrol, a naturally-occurring antioxidant found in grape skins and red wines, in rat hearts *ex vivo* (Das *et al.*, 2006). In transgenic mice over-expressing MKK 6, the recovery of cardiac function after I/R was significantly better compared to the wild type control indicating a protective role of p38 MAPK in I/R (Martindale *et al.*, 2005). The beneficial effect of p38 MAPK in myocardial I/R has been associated with the activation of heat shock protein 27 which causes inactivation of pro-apoptotic proteins such as caspase-3 and Fas (Efthymiou *et al.*, 2005) and the activation of another small heat shock protein α-crystallin B, where it reacts with the voltage-dependent anion channel-1 in the mitochondrial outer membrane to inhibit cytochrome C release (Mitra *et al.*, 2014). In contrast, others have shown that the activation of p38 MAPK is detrimental in

I/R. In several reports, inhibition of the p38 MAPK signalling pathway confers cardioprotection against I/R injury *in vitro* and *in vivo* (Gao *et al.*, 2002; Khan *et al.*, 2006; Schwertz *et al.*, 2007; Becatti *et al.*, 2012). The damaging effect of p38 MAPK is associated with the translocation of the pro-apoptotic protein Bax into mitochondria during ischaemia and induces apoptosis (Capano & Crompton, 2006). Inhibition of p38 MAPK could also reduce the level of pro-inflammatory cytokine TNF-α (Cain *et al.*, 1999), decrease expression of endoplasmic reticulum (ER) stress-related genes (Bian *et al.*, 2011) and inhibit the upregulation of adhesion molecules such as P-selectin and intracellular adhesion molecules-1 during I/R resulting in cell survival (Gao *et al.*, 2002). It has also been reported that there is a differential role of different isoforms of p38 MAPK. p38 MAPKα is reported to exert a deleterious effect in myocardial I/R while p38 MAPKβ is cardioprotective (Bassi *et al.*, 2008). Kim and colleagues reported that the inhibition of p38 MAPKα prevented hypoxia/reoxygenation-induced cell death in isolated cardiacmyocytes while in cardiaomyocytes exhibiting dominant negative p38 MAPKβ, the estrogen-induced cardioprotection against hypoxia/reoxygenation was prevented (Kim *et al.*, 2006).

1.4.2 PI3K/Akt pathway

The phosphatidylinositol 3′-kinase (PI3K)/protein kinase B (Akt) signalling pathway is another signalling cascade involved in cell proliferation, growth and survival. Similar to Erk 1/2, PI3K/Akt pathway is strongly activated by growth factors such as insulin-like growth factor-1 and insulin. In heart tissues, insulin-like growth factor-1 acts on a G-protein coupled receptor and the stimulation of this receptor activates PI3K (Figure 1.5). PI3K then activates its downstream signalling molecule Akt. Experimental evidence has shown that the activation of the PI3K/Akt pathway is protective against myocardial I/R injury. Rat hearts transfected with active Akt using adenoviral vectors were also protected against cardiomyocyte apoptosis

in response to I/R injury (Miao *et al.*, 2000; Matsui *et al.*, 2001). The presence of the PI3K inhibitor, LY294002 or wortmannin blocks the protection elicited by various pharmacological agents such as bradykinin, metformin, adrenomedullin and the adenosine A_1/A_2 agonist 5′-(N-ethylcarboxamido) adenosine during myocardial I/R *in vitro* and *in vivo* (Bell & Yellon, 2003; Okumura *et al.*, 2004; Yang *et al.*, 2004; Bhamra *et al.*, 2008). Akt reacts with various downstream targets which include the phosphorylation and inactivation of GSK-3β and this prevents the opening of mPTP leading to cell survival (Feng *et al.*, 2005; Rahman *et al.*, 2011). Akt also phosphorylates p70S6 kinase to cause cell survival (Jonassen *et al.*, 2001).

1.4.3 The Reperfusion Injury Salvage Kinase (RISK) pathway

PI3K/Akt, together with the Erk 1/2 signalling cascade, are said to form the RISK pathway, the term given to a group of pro-survival protein kinases that confer powerful cardioprotection in myocardial I/R (Hausenloy & Yellon, 2004) (Figure 1.5). Haunseloy and Yellon reported that activation of the RISK pathway could result in the phosphorylation of a wide range of substrates including GSK-3β, pro-apoptotic proteins such as Bax, BAD, Bim, caspases-3 and -9 (Takatani *et al.*, 2004; Bhuiyan *et al.*, 2007; Song *et al.*, 2009) and endothelial nitric oxide synthase (eNOS) (Bell & Yellon, 2003). The phosphorylation and inhibition of GSK-3β and pro-apoptotic proteins, as well as the production of NO from eNOS, could result in the inhibition of the release of mitochondrial cytochrome C and mPTP opening which is a major mediator of cell death in I/R injury, and subsequently enhance cell survival during I/R (Hausenloy & Yellon, 2004). Thus, the ability to manipulate and upregulate the RISK pathway during I/R may provide a potential approach to limit myocardial I/R injury.

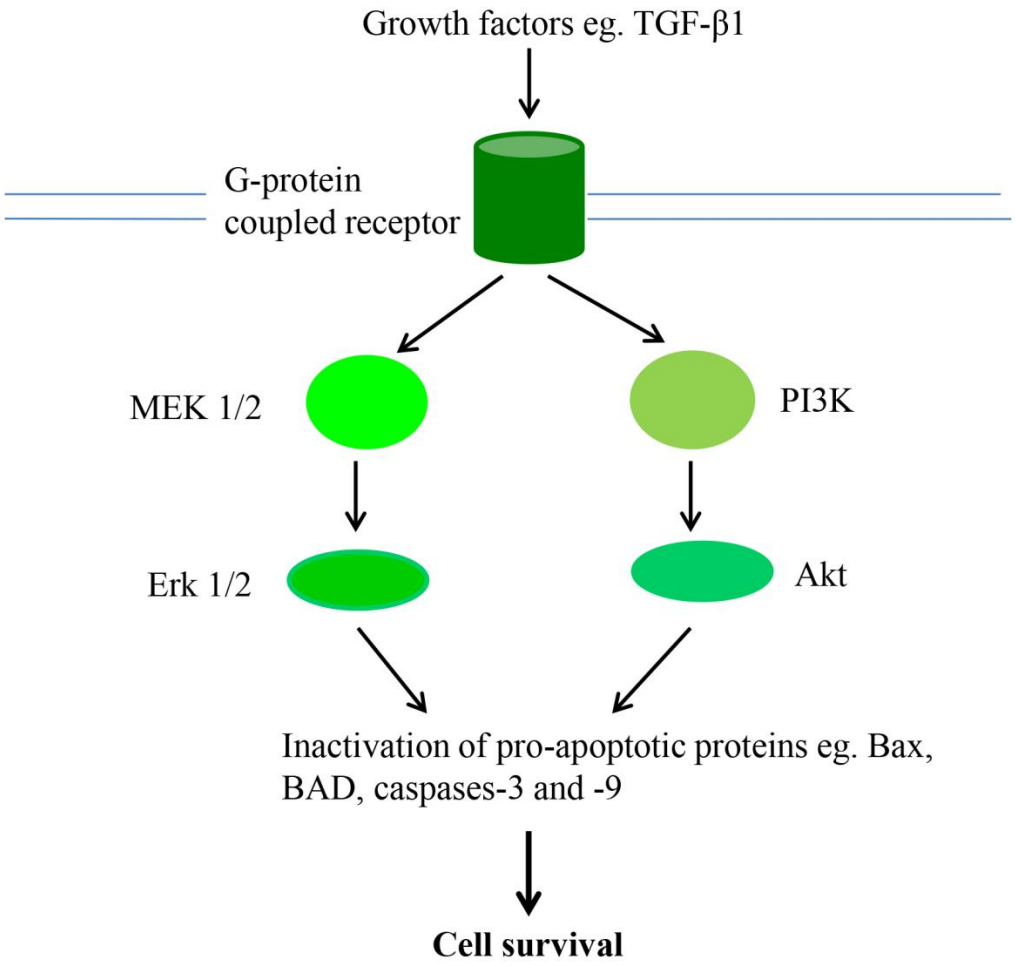

Figure 1.5: Schematic diagram of the Reperfusion Injury Salvage Kinase (RISK) pathway. Upon stimulation of the G-protein coupled receptor by stimuli such as growth factors during ischaemia/reperfusion, two cardioprotective signalling pathways which are extracellular signal-regulated kinases (Erk) 1/2 and phosphatidylinositol 3′-kinase (PI3K)/protein kinase B (Akt) pathways are activated. These two pathways converge at the mitochondria and they phosphorylate and inactivate pro-apoptotic proteins including Bcl-2-associated X protein (Bax) and Bcl-2-associated death promoter (BAD) and result in cell survival (Hausenloy & Yellon, 2004). MEK= mitogen-activated protein kinase kinase; TGF= transforming growth factor

1.4.4 JAK 2/STAT3: the Survivor Activating Factor Enhancement (SAFE) pathway

Another cardioprotective signalling pathway which is elicited during I/R is the SAFE pathway. This pathway involves the activation of the Janus kinase (JAK)/signal transducer and activator of transcription (STAT) signalling pathway (Lecour, 2009) (Figure 1.6). STATs are a group of cytoplasmic transcription factors that mediate intracellular signalling activated by cytokine receptors such as TNF-α and then transmitted to the nucleus (Stephanou, 2004). TNF-α is a cytokine that is generally considered to contribute to cardiac dysfunction in both I/R and heart failure (Mann, 2003). Paradoxically, TNF-α may initiate the activation of protective pathways against reperfusion injury such as the SAFE pathway. The impact of TNF-α on cardioprotection may be concentration-dependent where lower levels of exogenous cardiac TNF-α administration prior to a myocardial I/R insult (0.5 ng/mL) exert cardioprotection and higher concentrations of TNF-α fail to elicit cardioprotection (Lecour *et al.*, 2002). In the heart, TNF-α binds to its receptor on the plasma membrane and this causes homo- or heterodimerization of the receptor (Boengler *et al.*, 2008) (Figure 1.6). The receptor dimerization then causes the phosphorylation and activation of JAKs which are located at the intracellular domain of the receptor (Boengler *et al.*, 2008). Active JAK recruits and phosphorylates STAT proteins on tyrosine residues (Boengler *et al.*, 2008). Once phosphorylated, the STAT protein is released and dimerized followed by translocation to the nucleus to regulate gene transcription (Boengler *et al.*, 2008). There are 7 different subtypes of STAT proteins i.e. STAT1, STAT2, STAT3, STAT4, STAT5α, STAT5β and STAT6 (Boengler *et al.*, 2008). Of these subtypes, STAT1 and STAT3 play an important role in myocardial I/R. It has been reported that STAT1 plays a pro-apoptotic role in myocardial I/R while STAT3 plays an anti-apoptotic role (Stephanou, 2004). Studies have demonstrated that knockout mice of STAT3 are more susceptible to I/R injury with increased cardiac apoptosis, infarct sizes and reduced cardiac function compared to wild type mice (Hilfiker-Kleiner *et al.*,

2004; Frias *et al.*, 2013). The presence of an inhibitor of JAK2, AG-490 or STAT3, static limits the cardioprotection elicited by various pharmacological agents against myocardial I/R injury *in vitro* and *in vivo* (Huang *et al.*, 2011; Das *et al.*, 2012; Ottani *et al.*, 2013). The cardioprotective action of JAK/STAT3 is also mediated by inhibiting the opening of mPTP in cardiomyocytes during I/R (Smith *et al.*, 2010; Frias *et al.*, 2013). By contrast, studies have shown that STAT1 activation is injurious during myocardial I/R (Stephanou *et al.*, 2000; Stephanou *et al.*, 2001). It has been proposed that STAT1 promotes apoptosis by inducing the expression of pro-apoptotic genes such as caspase-1, Fas and Fas ligand and by inhibiting the expression of genes that encode for anti-apoptotic proteins such as Bcl-2 and Bcl-extra large (Bcl-X) leading to cell death (Stephanou *et al.*, 2000; Stephanou *et al.*, 2001). It is also reported that the cardioprotective action of naturally occurring antioxidants including myricetin, delphinidin and epigallocatechin-3-gallate is mediated by inhibition of STAT1 in rat hearts *ex vivo* (Townsend *et al.*, 2004; Scarabelli *et al.*, 2009).

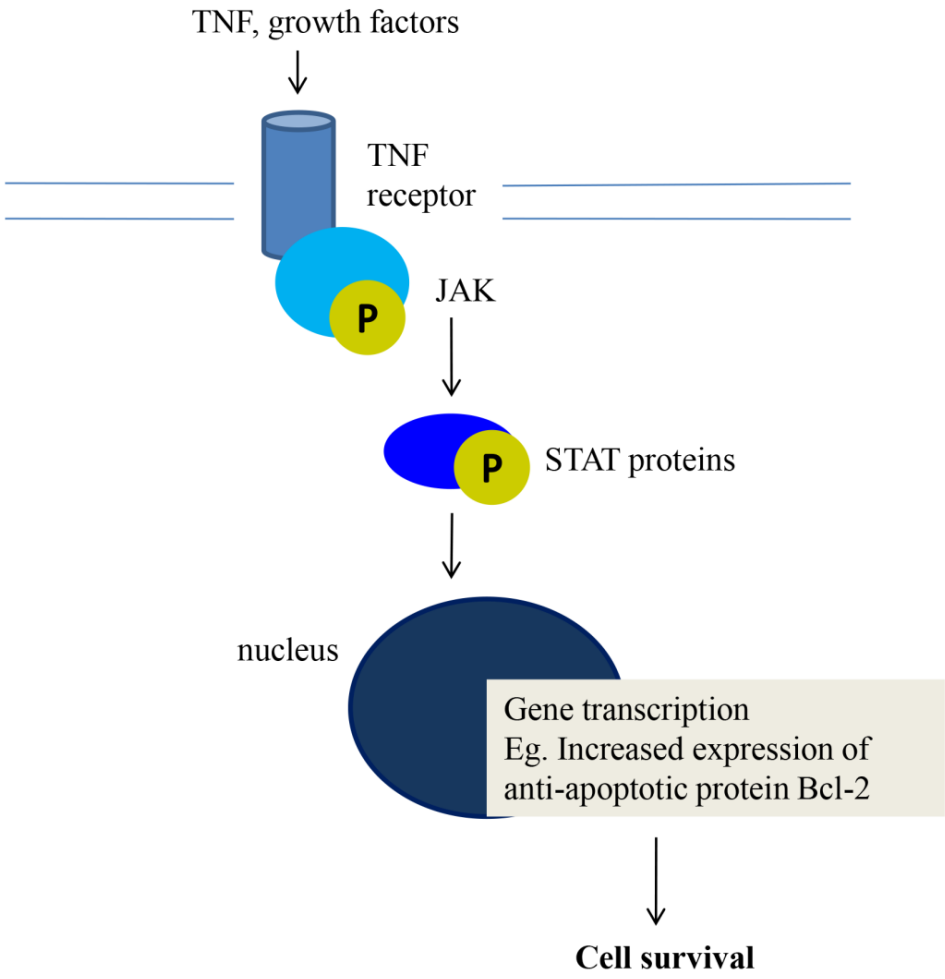

Figure 1.6: Schematic diagram of the Survivor Activating Factor Enhancement (SAFE) pathway. The activation of the tumour necrosis factor (TNF) receptor in the cardiomyocyte causes dimerization and activation of Janus kinase (JAK). This then causes phosphorylation of signal transducer and activator of transcription (STAT) proteins. STAT proteins then move to nucleus to trigger gene transcription such as the anti-apoptotic gene B-cell lymphoma-2 (Bcl-2). This then causes cell survival (Lecour, 2009).

1.4.5 Ca^{2+}/calmodulin-dependent protein kinase (CaMK) II

CaMKII is a multi-functional Ser/Thr protein kinase and is the isoform of CaMK predominantly found in the heart (Maier & Bers, 2007). They are four CaMKII gene products, α, β, γ and δ with the δ isoform predominantly expressed in the heart (Maier & Bers, 2007). CaMKII exists as a holoenzyme complex consisting of 6 to 12 kinase subunits forming a wheel-like structure. Each subunit contains an amino-terminus catalytic domain, a central regulatory domain and a carboxy-terminus association domain which is involved in the oligomerization of CaMKII (Maier & Bers, 2007). Under resting conditions, the catalytic domain is constrained by the pseudosubstrate region within the regulatory domain and causes CaMKII autoinhibition (Anderson *et al.*, 2011). When intracellular Ca^{2+} concentration rises, Ca^{2+} complexes with calmodulin and the Ca^{2+}/calmodulin complex binds to the calmodulin-binding region, adjacent to the pseudosubstrate region in the regulatory domain causing a conformational change (Anderson *et al.*, 2011). This relieves the autoinhibition and activates CaMKII. Once activated, CaMKII undergoes autophosphorylation at Thr 287 and this causes a 1000-fold increase in the affinity of calmodulin binding to CaMKII, a property known as "calmodulin trapping" (Anderson *et al.*, 2011). CaMKII can remain activated even after the Ca^{2+} concentration has declined. Increased oxidative stress can also maintain the autophosphorylated state of CaMKII by inactivating many phosphatases preventing the dephosphorylation of Thr 287 (Anderson *et al.*, 2011). Activated CaMKII can activate various downstream Ca^{2+}-related receptors which include L-type Ca^{2+} channels, RyRs, sarco/endoplasmic reticulum Ca^{2+}-ATPase (SERCA), phospholamban (PLN), and the mitochondrial Ca^{2+} uniporter (Couchonnal & Anderson, 2008).

Under normal physiological conditions, CaMKII regulates myocardial excitation-contraction coupling, however excessive CaMKII activation has been implicated in many pathological conditions such as heart failure, cardiac hyperthrophy and arrhythmias

(Couchonnal & Anderson, 2008). Emerging evidence has also shown that excessive CaMKII activation due to Ca^{2+} overload and increased oxidative stress in the cell during myocardial I/R is deleterious. In 2007, Villa-Petroff and colleagues first reported that CaMKII activation promoted cell death in myocardial I/R (Vila-Petroff *et al.*, 2007). The presence of the CaMKII inhibitor, KN-93 significantly reduced infarct size in rat isolated hearts and improved cell viability in isolated cardiomyocytes after simulated I/R *in vitro* (Vila-Petroff *et al.*, 2007). Others also reported that KN-93 reduces infarct size and improves post-ischaemic cardiac contractility accompanied by reduced expression of pro-apoptotic proteins caspase-3, caspase-9 and cytochrome C, and a reduced Bax/Bcl-2 ratio, an indicator of cell death in rat hearts *ex vivo* (Salas *et al.*, 2010; Adameova *et al.*, 2012; Szobi *et al.*, 2014). In CaMKIIδ knockout mice, hearts had better recovery after I/R *in vivo* compared to wild type mice (Ling *et al.*, 2013). In addition, CaMKII inhibition also reduces I/R-induced arrhythmias (Adameova *et al.*, 2012; Bell *et al.*, 2012). These finding suggest a deleterious role of CaMKII activation in myocardial I/R.

As mentioned earlier, PLN is a downstream target of CaMKII. The role of PLN in myocardial I/R has also been examined. Earlier reports have shown that the phosphorylation of PLN at Thr 17 during myocardial I/R is beneficial as it enhances the Ca^{2+} uptake into the sarcoplasmic reticulum through SERCA2a and improves cardiac relaxation (Vittone *et al.*, 2002; Said *et al.*, 2003). In transgenic PLN-mutant mice, the recovery of Ca^{2+} transient amplitude and myocardial contractile function after myocardial I/R was also prolonged compared to wild type mice suggesting that the activation of PLN delays the recovery of cardiac contractile function during I/R (Valverde *et al.*, 2006). In contrast, recent findings have suggested that the activation of PLN during myocardial I/R may cause damaging effects. Increased phosphorylation of PLN results in increased uptake of Ca^{2+} into the sarcoplasmic reticulum leading to sarcoplasmic reticulum Ca^{2+} overload. This causes Ca^{2+} leak from the

sarcoplasmic reticulum through the RyR and the released Ca^{2+} is taken up by mitochondria via the mitochondrial Ca^{2+} uniporter (Chen *et al.*, 2005; Shintani-Ishida *et al.*, 2012). Excessive mitochondrial Ca^{2+} uptake triggers the opening of the mPTP resulting in apoptosis (Chen *et al.*, 2005; Shintani-Ishida *et al.*, 2012). In addition, Ca^{2+} leak due to increased phosporylation of PLN also contributes to reperfusion-induced arrhythmias (Said *et al.*, 2008). Taken together, inhibition of CaMKII activation and PLN phosphorylation may protect the heart against I/R injury and reduce the incidence of reperfusion-induced arrhythmias.

1.5 Pharmacological intervention to limit myocardial I/R injury

A diverse range of pharmacological agents are being investigated for potential therapeutic use in the treatment of myocardial reperfusion injury, however there are no pharmacological strategies that have achieved successful clinical outcomes. As increased oxidative stress plays a key role in the development of myocardial I/R injury, there has been considerable interest in the potential use of antioxidants, such as flavonoids to attenuate injury.

1.5.1 Flavonoids

Flavonoids are plant-derived polyphenolic compounds that are commonly found in the food such as fruits and vegetables and in beverages such as tea and wine (Pietta, 2000). They comprise a backbone of 15 carbons with two aromatic rings connected to a three carbon bridge, C_6-C_3-C_6 the basic skeleton and labelled as A, B and C (Pietta, 2000) (Figure 1.7). More than 4000 flavonoids have been identified to date and the major subgroups of flavonoids include flavones, flavonols, flavanones, catechins and anthocyanidins. The various subgroups of flavonoids differ from one another by the level of oxidation and pattern of substitution of the C ring, while individual compounds within a subgroup differ in the pattern

of substitution of the A and B rings (Pietta, 2000). For example, flavonols and flavones differ from one another by an extra hydroxyl group at the C3 position in flavonols (Pietta, 2000). The chemical structure, examples and sources for different subgroups of flavonoids are listed in Table 1.1.

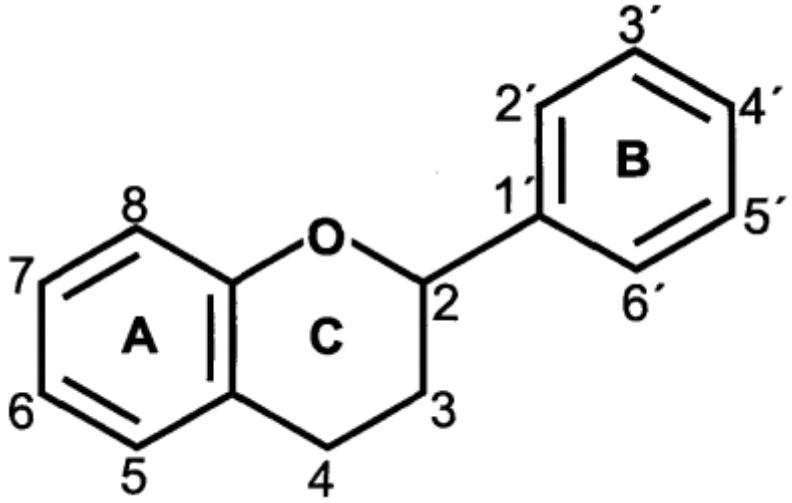

Figure 1.7: Basic flavonoid structure. A flavonoid consists of 2 aromatic rings (A and B) that are bound together by 3 carbon atoms that form an oxygenated heterocycle (ring C) (Pietta, 2000).

Table 1.1: Basic structures, significant sources and examples of main subgroups of flavonoids including flavonols, flavones, flavanols, flavanones and anthocyanidins (Pietta, 2000).

Flavonoids	Chemical structures	Sources	Examples
Flavonols	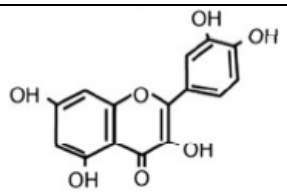	Onions Broccoli	Quercetin Myricetin Kaempferol
Flavones	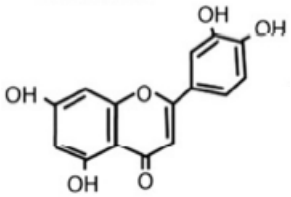	Peppers Celery	Luteolin Apigenin
Flavanols	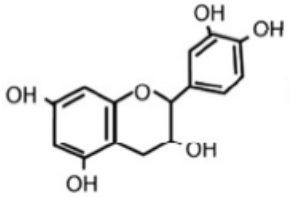	Cocoa Tea Red wines Apples	Epicatechin Catechin
Flavanones	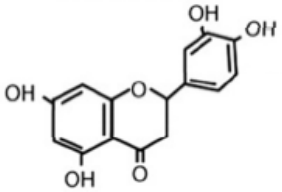	Citrus fruits	Naringenin Hesperetin
Anthocyanidins	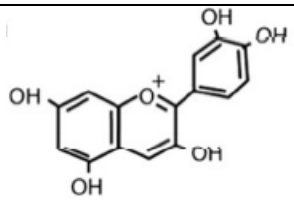	Grapes Blueberries	Cyanidin Delphinidin Malvidin

1.5.2 Epidemiological studies on flavonoids

In 1992, Renaud and de Lorgeril reported that the French population had a lower incidence of coronary heart disease compared to other Western populations, despite the equally high intake of high-fat diet and this phenomenon is described as the "French paradox" (Renaud & de Lorgeril, 1992). It was proposed that the regular consumption of red wine by the French population contained high flavonoid content and played a significant role in cardioprotection (Renaud & de Lorgeril, 1992). A number of epidemiological studies have suggested the beneficial effect of flavonoids in preventing cardiovascular diseases. In the Zutphen Elderly study which involved 805 men aged 65-84 years, there was an inverse correlation between the intake of dietary sources of flavonoids which included tea (61%), onions (13%) and apples (10%), and the mortality from coronary heart disease during a 5-year (Hertog *et al.*, 1993) and 10-year (Hertog *et al.*, 1997) follow up. There was also an inverse association of dietary flavonoid intake with the incidence of myocardial infarction (Hertog *et al.*, 1993). In that study, subjects in the highest tertile of flavonoid intake (42 mg/day) had about a 50% lower relative risk of mortality from coronary heart disease and the incidence of a first myocardial infarction than those in the lowest tertile (12 mg/day) (Hertog *et al.*, 1993). In another cohort study, involving 5133 Finnish men and women aged 30-69 years, increased flavonoid consumption (where major sources of flavonoids were apples and onions) was also associated with a decreased risk of coronary mortality (Knekt *et al.*, 1996). In the Rotterdam Study where 7983 men and women aged ≥55 years were involved, an inverse correlation between tea drinking (source of flavanols) and fatal myocardial infarction was also found after 5.6 years follow-up. Tea drinkers with a daily intake of >375 ml had a lower relative risk of incidence of myocardial infarction than non-tea drinkers (Geleijnse *et al.*, 2002). Mink and colleagues also reported that high flavonoid intake was also associated with a reduced risk of death from coronary heart disease in post-menopausal women (Mink *et al.*, 2007).

1.5.3 Biological properties of flavonoids

Flavonoids possess a number of biological actions which may be beneficial in the prevention of cardiovascular diseases.

1.5.3.1 Antioxidant property

Flavonoids are potent antioxidants. The mechanisms of action include direct scavenging of free radicals, enhancing the expression and/or activity of endogenous antioxidant enzymes and inhibition of pro-oxidant enzymes (Pietta, 2000). Flavonoids are able to reduce highly oxidizing free radicals such as $\bullet O_2^-$, alkoxyl, peroxyl and hydroxyl radicals by donating a hydrogen atom to the radical resulting in the formation of a semiquinone radical (Pietta, 2000). This semiquinone radical can further donate a hydrogen atom to form the stable quinone structure (Pietta, 2000) (Figure 1.8). The free-radical scavenging ability of flavonoids has been extensively studied in both the cell-free medium and biological tissues (Rice-Evans *et al.*, 1995; Salah *et al.*, 1995; Magnani *et al.*, 2000; Woodman *et al.*, 2005; Wang *et al.*, 2006). For example, $\bullet O_2^-$ generated by auto-oxidation of pyrogallol in the cell-free system were scavenged by flavonols and flavones (Magnani *et al.*, 2000) while lipid peroxyl radicals produced in isolated low-density lipoproteins were effectively scavenged by the flavanol catechin (Salah *et al.*, 1995).

Apart from the free-radical scavenging ability, flavonoids can also increase the activity and/or expression of endogenous antioxidant enzymes to improve the antioxidant status in the cell. Chronic consumption of a soy protein-rich diet containing isoflavones, such as genistein and daidzein increased the mRNA level of the antioxidant enzyme superoxide dismutase in adult rats (Mahn *et al.*, 2005). Long-term exposure of adult rats to red wine containing quercetin and myricetin, also improved the glutathione/glutathione disulphide (GSH/GSSH) ratio in rat kidney tissues, suggesting improved antioxidant state in the cell

(Rodrigo *et al.*, 2002). In addition, flavonoids could also inhibit pro-oxidant enzymes such as NADPH oxidase and xanthine oxidase and reduce the generation of ROS. Flavonoids, including baicalein, galangin, kaempferol, luteolin, and naringenin, have been shown to inhibit the activity of xanthine oxidase in a cell-free system (Cos *et al.*, 1998; Nagao *et al.*, 1999; Russo *et al.*, 2000). In rat isolated aorta, quercetin and isorhamnetin are also capable of reducing the angiotension II-induced increased expression of $p47^{phox}$, which is a regulatory subunit of the membrane NADPH oxidase, thereby decreasing ROS generation and preventing endothelial dysfunction (Sanchez *et al.*, 2007; Romero *et al.*, 2009). Due to their favourable antioxidant property, many studies has been perform to investigate the use of flavonoids to ameliorate various pathological conditions such as atherosclerosis, diabetes, dementia, cancer and others where elevated oxidative stress plays a major role in the pathogenesis of these conditions (Nijveldt *et al.*, 2001).

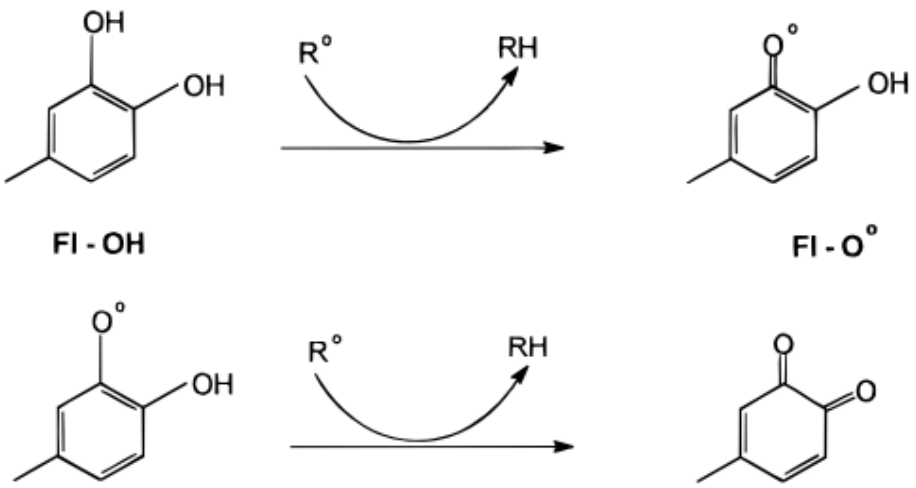

Figure 1.8: Scavenging of reactive oxygen species (R°) by flavonoids (Fl-OH). Fl-OH donates a hydrogen atom to the radical forming a stable quinone structure (Pietta, 2000).

1.5.3.2 Vasodilator property

Flavonoids are also effective vasodilators. Studies have shown that flavonoid-induced vasorelaxation is mainly mediated via endothelium-independent mechanisms. Flavonoids can inhibit contractile responses to extracellular Ca^{2+} influx and in response to the release of Ca^{2+} from intracellular stores to induce endothelium-independent vasorelaxation (Herrera *et al.*, 1996; Chan *et al.*, 2000; Ajay *et al.*, 2003). The flavanone naringenin inhibited the activity of phosphodiesterases (a family of enzymes responsible for the breakdown of cAMP and cyclic guanosine monopshophate (cGMP)) and caused vasorelaxation in rat endothelium-denuded aorta (Orallo *et al.*, 2005); flavonols induced endothelium-independent vasorelaxation via the opening of K^+ channels in the vascular smooth muscle cell causing hyperpolarisation (Qin *et al.*, 2008) while the synthetic flavonol, 3',4'-dihydroxyflavonol decreased vascular contraction via the inhibition of RhoA/Rho-kinase pathway (where activated RhoA could increase myosin light chain phosphorylation and cause smooth musclecontraction) in rat endothelium-denuded aorta (Song *et al.*, 2010b).

Flavonoid-induced vasodilatation may also be partly mediated via an endothelium-dependent pathway. For example, flavonoids may stimulate the Ca^{2+}-dependent NO release from endothelial cells (Martin *et al.*, 2002; Zenebe *et al.*, 2003; Duarte *et al.*, 2004). NO then activates the soluble guanylyl cyclase (sGC)/cGMP pathway in the vascular smooth cell to cause vasorelaxation. In addition, flavonoids may phosphorylate eNOS at Ser^{1177} leading to enhanced NO synthesis and subsequent vasodilatation (Anter *et al.*, 2004). Flavonols, such as quercetin, have also been reported to scavenge superoxide anions and increase the NO bioavailability to cause endothelium-dependent vasorelaxation (Huk *et al.*, 1998).

1.5.3.3 Anti-inflammatory and anti-aggregatory properties

Apart from being potent antioxidants and vasodilators, studies have shown that flavonoids exhibit anti-inflammatory and anti-aggregatory properties. Flavonoids especially flavones, inhibit key enzymes involved in eicosanoid pathways including phospholipase A_2, cyclooxygenase and lipoxygenase, thereby reducing the production of inflammatory mediators such as prostaglandins and leukotrienes (Baumann *et al.*, 1980; Lindahl & Tagesson, 1993; Kimata *et al.*, 2000; Harris *et al.*, 2006). Flavonoids may also inhibit the production of pro-inflammatory cytokines such as TNF-α, IL-1β and IL-6, and soluble adhesion molecules intracellular adhesion molecules-1, vascular cell adhesion molecule-1, E-selectin and P-selectin (Gerritsen *et al.*, 1995; Cho *et al.*, 2003b). For example, in mice *in vivo* and in macrophages *in vitro*, quercetin inhibited lipopolysaccharides-induced TNF-α production (Wadsworth *et al.*, 2001). In the clinical setting activin, a grape seed-derived proanthocyanidin extract, has been shown to reduce plasma levels of vascular cell adhesion molecule-1, intracellular adhesion molecules-1 and E-selectin in patients with systemic sclerosis (Kalin *et al.*, 2002).

1.5.4 Structure activity relationships of flavonoids

As described above, flavonoids possess many biological activities including antioxidant, vasorealxation, anti-inflammation and anti-aggregation. Structure activity relationship studies have reported that the number and orientation of hydroxyl groups on the carbon ring skeleton has an important influence on their biological properties. For example, Herrera and colleagues reported that flavonols with hydroxyl groups at positions 3’ and 4’ in the B ring are potent vasodilators (Herrera *et al.*, 1996). Further, previous study from our laboratory demonstrated that the vasorelaxation activity of flavonol was abolished when the hydroxyl groups at positions 3’ and 4’ in the B ring were substituted with methoxy groups

(Woodman *et al.*, 2005). It has also been reported that hydroxyl groups at C5 and C7 and the double bond between C2 and C3 are required for inhibition of xanthine oxidase which is a pro-oxidant enzyme while hydroxyl groups at 3' and 4' positions on the B ring and at C3 can cause powerful ROS scavenging effect (Cos *et al.*, 1998; Woodman *et al.*, 2005). In addition, it is also reported that substitution of a methoxy group at the 3' position on the B ring abolished the scavenging ability of flavonol (Qin *et al.*, 2008). The structure activity relationship studies of the anti-inflammatory action of flavonoids are however inconsistent. Comalada and colleagues reported that hydroxylation at C5, C7, 3' and 4' positions on the B ring, together with a double bond at C2 and C3, and the B ring at position 2 are required for the strongest anti-inflammatory effect (Comalada *et al.*, 2006). The anti-inflammatory action was mediated by inhibiting the nuclear factor kappa-light-chain-enhancer of activated B cells (NF-κβ) pathway leading to reduced TNF-α production and inducible nitric oxide synthase expression in lipopolysaccharide–induced macrophages (Comalada *et al.*, 2006). In contrast, Lotito and Frei reported that hydroxylation at C5, C7 on the A ring, the C2 and C3 double bond and a keto group at C4 on the C ring are the structural requirement for a flavonoid to inhibit TNFα-induced adhesion molecule expression in human aortic endothelial cells (Lotito & Frei, 2006). Taken together, structure activity relationship studies have shown that the presence of hydroxyl groups at the C3 and 3' and 4' positions on the B ring are required to cause vasorelaxation, antioxidant and anti-inflammatory action.

1.5.5 3'4'-dihydroxyflavonol (DiOHF)

3'4'-dihydroxyflavonol (DiOHF) is a synthetic flavonol with hydroxyl groups at the C3 and 3' and 4' positions on the B ring (Figure 1.9). Studies have shown that it has anti-inflammatory activity and is a more potent antioxidant and vasodilator than naturally occurring flavonols (Chan *et al.*, 2000; Woodman & Chan, 2004). Therefore, having these

properties, DiOHF has the potential as an adjuvant therapeutic agent to reduce I/R injury, possibly by reducing oxidative stress and inflammatory response as well as inhibiting platelet aggregation that are triggered during I/R. DiOHF could also induce vasodilatation to improve perfusion of the heart after an ischaemic episode.

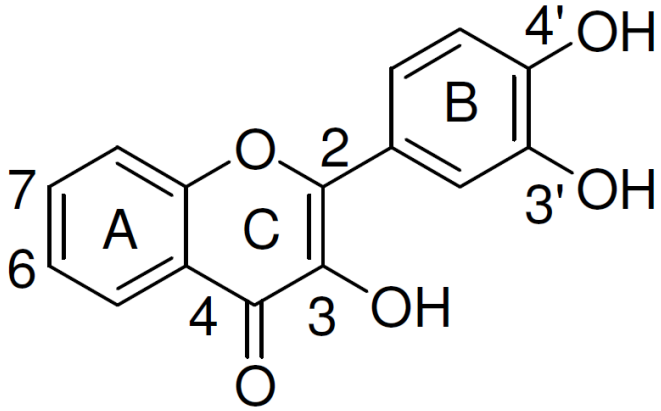

Figure 1.9: Chemical structure of the synthetic flavonol, 3',4'-dihydroxyflavonol (DiOHF). It has hydroxyl groups at the C3 and 3' and 4' positions on the B ring (Woodman & Chan, 2004).

1.5.6 Evidence supporting flavonoids as a potential therapeutic agent for I/R injury

Many studies have shown that flavonoids are cardioprotective in the setting of myocardial I/R injury. Brookes and colleagues demonstrated that oral treatment of rats with the flavonol quercetin (0.033 mg/kg per day, a concentration equivalent to the quercetin content in 1-2 glasses of common red wine consumed by an adult male of 70 kg) for 4 days, improved the post-ischaemic cardiac contractility in rat isolated hearts (Brookes *et al.*, 2002). Treatment with quercetin also protected the heart against myocardial I/R *in vivo* (Annapurna *et al.*, 2009; Jin *et al.*, 2012; Wang *et al.*, 2013), improved post-ischaemic cardiac contractility in the isolated heart (Bartekova *et al.*, 2010) and reduced cell death in isolated cardiomyocytes after anoxia and reoxygenation (Tang *et al.*, 2013). The cardioprotection induced by quercetin has been associated with its ability to reduce oxidative stress as indicated by reduced lipid peroxidation and increased levels of antioxidant enzymes such as superoxide dismutase and catalase in rat hearts after I/R (Annapurna *et al.*, 2009) and reduced mRNA expressions of NADPH oxidase 2 and inducible nitric oxide synthase in rabbit hearts after I/R (Wan *et al.*, 2009). Quercetin may also exert its cardioprotective action by inhibiting the expression of inflammatory protein TNF-α (Jin *et al.*, 2012) and by improving post-ischaemic mitochondrial function which is critical in the generation of ATP and recovery of cell function after I/R (Brookes *et al.*, 2002). The protective action of other flavonols such as kaempferol, myricetin and isorhamnetin against I/R injury has also been reported (Scarabelli *et al.*, 2009; Malakul *et al.*, 2011; Zhang *et al.*, 2011).

In addition, Wang and colleagues demonstrated that the synthetic flavonol DiOHF reduced myocardial infarct size after I/R in anesthetized sheep, with the level of protection similar to that of ischaemic preconditioning, which is a powerful adaptive mechanism that protects the heart against I/R injury (Wang *et al.*, 2004). The cardioprotetive effect of DiOHF against I/R injury is also evident in other species such as goats *in vivo* and rat isolated hearts

(Wang *et al.*, 2009; Qin *et al.*, 2011). Recently, the water soluble pro-drug of DiOHF, NP202 also showed similar beneficial effects against myocardial I/R injury (Thomas *et al.*, 2011; Williams *et al.*, 2011; Lim *et al.*, 2013). The infarct-sparing action of NP202 was accompanied by a reduced number of polymorphonuclear leukocytes and apoptosis in both infarcted and non-infarcted areas of the myocardium in anaesthetized sheep (Thomas *et al.*, 2011).

Studies have also shown that the flavone luteolin protected the heart against I/R injury in rats *in vitro* and *in vivo* (Liao *et al.*, 2011; Sun *et al.*, 2012; Yu *et al.*, 2015). Luteolin-induced cardioprotection may be mediated by reducing oxidative stress as indicated by a decreased level of malondialdehyde, a marker of lipid peroxidation, decreased expression of $p47^{phox}$ of NADPH oxidase and enhanced superoxide dismutase activity (Yu *et al.*, 2015). Luteolin-induced cardioprotection may also be mediated via its anti-inflammatory property by reducing the level of inflammatory cytokines, TNF-α and IL-6 after I/R in diabetic rats (Sun *et al.*, 2012).

Other flavonoids such as flavanol epigallocatechin-3-gallate which is highly abundant in green tea (Aneja *et al.*, 2004; Akhlaghi & Bandy, 2010; Yanagi *et al.*, 2011) and epicatechin extracted from cocoa (Yamazaki *et al.*, 2008; Yamazaki *et al.*, 2014), flavanone naringenin (Testai *et al.*, 2013) and anthocyanidin (Toufektsian *et al.*, 2008) also exert cardioprotection during myocardial I/R. Like flavonols and flavones, their ability to reduce oxidative stress and inflammatory response as well as the ability to improve coronary flow to the heart are reported to contribute to their cardioprotection against I/R injury. Yamazaki and colleagues reported that the ability of epicatechin to preserve mitochondrial bioenergetics, which include increased mitochondrial respiration rate, oxygen consumption and ATP synthesis, and to inhibit mitochondrial Ca^{2+} accumulation after I/R may contribute to its cardioprotective action during I/R (Yamazaki *et al.*, 2014).

1.5.7 Potential signalling pathways of flavonoid-induced cardioprotection

Although it is well-established that flavonoids are protective in myocardial I/R, possibly by reducing oxidative stress, inhibiting inflammatory response and improving blood flow to the heart after ischaemia, increasing evidence have suggested that flavonoids may act as a signalling molecule to modulate signalling pathways in cardiomyocytes to induce cardioprotection.

Studies have shown that quercetin may confer cardioprotection by activating the protective kinase Akt resulting in subsequent improvement of the Bcl/Bax ratio (an indicator of cell survival) (Wang *et al.*, 2013). Kaempferol inhibited the activation of the endoplasmic reticulum stress protein such as 78 kDa glucose-regulated protein, activating transcription factor-6α, X-box binding protein-2, inositol requiring enzyme-1-α and C/EBP homologous protein to improve cell viability in isolated cardiomyocytes after simulated I/R (Kim *et al.*, 2008) while myricetin attenuated the phosphorylation of STAT1 which regulates gene transcription that is involved in apoptosis, to confer cardioprotection against I/R injury (Scarabelli *et al.*, 2009). It is also reported that DiOHF-induced cardioprotection may be mediated by directly inhibiting CaMKII activation causing subsequent inhibition of its downstream signalling pathways, p38 MAPK and JNK, while the expression of protective kinases, Akt and Erk 1/2 was not affected (Thomas *et al.*, 2011; Lim *et al.*, 2013).

The flavone luteolin is reported to exert its cardioprotective action against I/R injury by increasing the expression of Erk 1/2 and suppressing the activation of p38 MAPK and JNK, as well as inhibiting pro-apoptotic proteins, caspases-3, -8 and -9 (Yu *et al.*, 2015). The cardioprotective effect of luteolin may also be dependent on the PI3K/Akt pathway as the presence of the PI3K/Akt inhibitor LY294002 prevented the protective effect of luteolin in isolated hearts and cardiomyocytes (Fang *et al.*, 2011; Sun *et al.*, 2012). In addition, luteolin

may also increase the phosphorylation of PLN and SERCA2a to improve cell survival after I/R (Wu *et al.*, 2013). On the other hand, epigallocatechin-3-gallate and epicatechin-induced cardioprotection involves the activation of mitochondrial ATP-sensitive potassium channels (K_{ATP}), which is one of the major mechanisms of ischaemic preconditioning (Song *et al.*, 2010a) and attenuation of the activation of injurious kinases STAT1 and p38 MAPK (Townsend *et al.*, 2004; Darra *et al.*, 2007; Yanagi *et al.*, 2011), as well as inhibition of JNK phosphorylation (Panneerselvam *et al.*, 2010). Finally, Testai and colleagues reported that flavanone naringenin-induced cardioprotection against I/R was mediated via the activation of the Ca^{2+}-activated K^{+} channel in mitochondria which could reduce the electrical driving force for Ca^{2+} entry into mitochondria (Testai *et al.*, 2013).

1.6 Complication of acute myocardial I/R injury: acute heart failure

Heart failure can be defined as abnormalities in the structure or function of the heart causing failure of the heart to deliver oxygen at a rate commensurate with the requirements of the metabolizing tissues (Hunt *et al.*, 2009). It is a major public health concern due to its high risk of morbidity and mortality (Bui *et al.*, 2011). Bui and colleagues reported that heart failure affects 23 million people worldwide in 2011, and the prevalence may continue to rise each year (Bui *et al.*, 2011). It is also one of the major causes for hospitalizations among the aging population in developed countries and it causes a heavy economic burden (Bui *et al.*, 2011). The aetiology of heart failure includes hypertension, diabetes, dyslipidemia, smoking and others and ischaemic heart disease is the most important risk factor for heart failure (Bui *et al.*, 2011). Heart failure can be classified into 3 major categories which are new-onset heart failure, transient heart failure and chronic heart failure (Hunt *et al.*, 2009). New-onset heart failure or *de novo* heart failure refers to first presentation and patients have with no prior history of heart failure. Transient heart failure refers to symptomatic heart failure over a

limited period of time, although long-term treatment may be indicated. For example, patients with mild myocarditis from which recovery is near complete. Chronic heart failure is defined as worsening of heart failure in patients with a previous diagnosis or hospitalization for heart failure. In all cases, symptoms include shortness of breath, fatigue, fluid retention with clinical signs of fluid retention (pulmonary or peripheral) in the presence of abnormal cardiac function (Hunt *et al.*, 2009).

After an episode of acute myocardial I/R, patients are highly susceptible to acute heart failure. Indeed, according to the EuroHeart Failure Survey II, acute coronary syndrome mainly due to acute myocardial infarction is the major contributing factor for patients' hospitalization with acute heart failure (or *de novo* heart failure) (Nieminen *et al.*, 2006). Population-based studies in Italy and the United Kingdom also reported that a high proportion of patients admitted with acute heart failure have a history of ischaemic heart disease or acute myocardial infarction (Cowie *et al.*, 1999; Fox *et al.*, 2001; Tavazzi *et al.*, 2006). In addition, patients with acute heart failure have a very poor prognosis. The acute heart failure global survey of standard treatment (ALARM-HF) reported that patients with *de novo* heart failure had a higher mortality rate than those with a pre-existing episode of heart failure (Follath *et al.*, 2011).

First-line treatments for acute heart failure are diuretic agents to treat pulmonary oedema and vasodilators such as glyceryl trinitrate or nitroprusside to reduce pre-load and after-load on the heart. In cases where there is low cardiac output and the peripheral vasculature is under-perfused, a positive inotrope will be introduced. In addition, studies have shown that patients with acute heart failure and a lower systolic blood pressure at admission have a higher in-hospital and post-discharge mortality rate (Gheorghiade *et al.*, 2006; Shiraishi *et al.*, 2011). Systolic blood pressure is emerging as an important predictor of in-hospital and post-discharge mortality in acute heart failure (Gheorghiade & Pang, 2009).

Therefore, the ability to increase cardiac output and peripheral perfusion is critical to improve survival in acute heart failure.

1.6.1 Dobutamine

The standard inotropic therapy for acute heart failure is dobutamine (McMurray *et al.*, 2012). Dobutamine is a β_1-adrenergic receptor agonist with weak β_2-adrenergic stimulation. It acts on stimulatory G protein on the myocardium and activates adenylyl cyclase (Steinberg, 1999). Adenylyl cyclase then catalyses the formation of cAMP which then activates protein kinase A (PKA) and this leads to the phosphorylation of regulatory proteins involved in cardiac excitation-contraction coupling and energy metabolism, including L-type Ca^{2+} channels, the sarcoplasmic reticulum membrane protein receptors RyR2, SERCA2a and PLN and myofilament proteins (Steinberg, 1999). The phosphorylation of L-type Ca^{2+} channels allows entry of Ca^{2+} into the cell and this triggers a Ca^{2+}-induced Ca^{2+}-release mechanism from the sarcoplasmic reticulum resulting in enhanced cardiac contraction and relaxation. Dobutamine is infused at a rate of 2-20 μg/kg/min in patients with severely low cardiac output that vital organ perfusion is compromised (McMurray *et al.*, 2012). There is however growing evidence that deleterious effects including cardiac arrhythmias (eg. tachycardia) (Monrad *et al.*, 1986; Burger *et al.*, 2001), increased myocardial oxygen consumption that could lead to myocardial ischaemia (Fujigaki *et al.*, 1989; Vanoverschelde *et al.*, 1993) and a higher mortality rate occurs with dobutamine infusion in patients with acute heart failure compared to the placebo group (Mebazaa *et al.*, 2011).

As the use of dobutamine to improve cardiac output in acute heart failure may develop adverse effects, a few other novel inotropes have also been investiagted in the past 20 years. For example, levosimendan, which is a Ca^{2+} sensitiser, exerts its positive inotropic effects by binding to cardiac troponin C in a Ca^{2+}-dependent manner to enhance the myofilament

responsiveness to Ca^{2+} without increasing intracellular Ca^{2+} concentrations, and milirinone, a phosphodiesterase inhibitor, which prevents the degradation of cAMP resulting in increased contractility of the heart (McMurray *et al.*, 2012). However, studies have shown that they exhibited adverse effects such as arrhythmias which limited their long-term usage (Mebazaa *et al.*, 2007; Parissis *et al.*, 2007). Therefore, the discovery of a novel positive inotrope with limited adverse effects, will improve the prognosis of patients with acute heart failure.

1.7 Nitroxyl (HNO): the reduced congener of NO

HNO is a one-electron reduced and protonated redox sibling of NO. It is a weak acid with a pKa of 11.4 and the predominant species under physiological conditions is HNO rather than nitroxyl anion (NO^-) (Shafirovich & Lymar, 2002). Many reports have shown a distinct chemical, biological and pharmacological profile between HNO and NO. For example, HNO, but not NO, is highly thiolphilic, reacting readily with thiols/thiolates by either reversible or irreversible reactions depending on the conditions, (i.e. the amount of thiols/thiolates present) (Wong *et al.*, 1998). HNO is also resistant to scavenging by superoxide (Miranda *et al.*, 2002). This is in contrast to NO, which is easily scavenged by superoxide forming the highly reactive species peroxynitrite. This resistance to superoxide scavenging is a favourable property of HNO in mammalian systems, as peroxynitrite is cytotoxic and damaging to DNA and protein in cells. Similar to NO, HNO also has an affinity for metal centres of proteins such as iron-containing haem in oxymyoglobin and sGC (Farmer & Sulc, 2005). It coordinates with the ferrous centre in haem forming a stable ferrous-nitrosyl complex (Equation 1), however, different to NO, HNO preferentially targets ferric ion (Fe^{3+}) which predominates in diseases rather than ferrous ion (Fe^{2+}), while NO does not react with Fe^{3+} (Miranda *et al.*, 2003a).

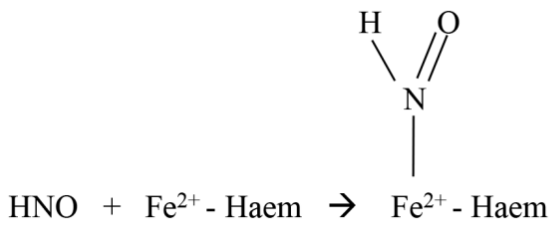

(Equation 1)

1.7.1 Endogenous production of HNO

There is no concrete evidence that HNO is produced endogenously in mammals, however, many predictions have been made of the possibility of endogenous HNO formation.

Several studies exploiting the endothelium-dependent vasodilator acetylcholine to evoke vasodilatation in rodent isolated arteries have shown that the HNO scavenger L-cysteine attenuates the dilator effect of acetylcholine (Ellis *et al.*, 2000; Andrews *et al.*, 2009). This suggests that HNO could be an endothelium-derived relaxing factor. It has been reported that HNO could be generated directly by nitric oxide synthase (NOS) in the absence of its cofactor tetrahydrobiopterin, in non-biological systems (Adak *et al.*, 2000). Oxidative degradation of N-hydroxy-L-arginine, the biosynthetic intermediate of NOS-catalysed oxidation of L-arginine can also produce HNO (Fukuto *et al.*, 1992a; Yoo & Fukuto, 1995). As N-hydroxy-L-arginine is found at a significant level in plasma and some cells *in vitro*, this makes a feasible biosynthetic pathway for HNO (Cho *et al.*, 2003a). From non-NOS sources, HNO may also be generated by the enzymatic reduction of NO in intracellular compartments such as in mitochondria by superoxide dismutase, xanthine oxidase and ubiquinol (Niketic *et al.*, 1999; Poderoso *et al.*, 1999; Saleem & Ohshima, 2004). The reaction of S-nitrosothiols with other thiols such as GSH may also generate HNO (Equation 2) (Wong *et al.*, 1998).

$$RS-NO + R'-SH \rightarrow RSSR' + HNO \qquad \text{(Equation 2)}$$

1.7.2 HNO donors

The naturally-occurring HNO species is transient in nature, as it readily undergoes dimerization to form a hyponitrous acid and decomposes into nitrous acid and water (Equation 3) (Shafirovich & Lymar, 2002). Therefore a HNO donor has to be utilised in biological studies. There are a few commonly used HNO donors (Table 1.2) and the most well-known and studied donor is sodium trioxodinitrate ($Na_2N_2O_3$), more commonly known as Angeli's salt.

$$HNO + HNO \rightarrow [HONNOH] \rightarrow N_2O + H_2O \qquad \text{(Equation 3)}$$

Table 1.2: Nitroxyl (HNO) donors.

HNO donor	Mechanism of action	Properties	References
Angeli's salt ($Na_2N_2O_3$, sodium trioxodinitrate)	- Protonation reaction $N_2O_3^- + H^+$ $\longrightarrow$ **HNO** + NO_2^-	- Reaction occurs at physiological temperature and over a range of pH 4-8 <u>Limitations:</u> - Co-release of nitrite (NO_2^-) - Short half-life (~2-3min)	(Miranda *et al.*, 2005b; DuMond & King, 2011)
Piloty's acid ($PhSO_2NHOH$, N hydroxybenzenesulfonamide)	- Deprotonation reaction $PhSO_2NHOH$ $\longrightarrow$ $PhSO_2^-$ + **HNO**	<u>Limitations:</u> - Releases HNO at pH 13 (non-physiology) - Releases $NO^{\bullet}$ rather than HNO at physiological pH	(DuMond & King, 2011)
Isopropylamine NONOate (IPA/NO, a primary amine diazeniumdiolate)	- Decomposition reaction $[RNH\text{-}N(O)=NO]^-$ $\longleftrightarrow$ $[RN=N(O)\text{-}NHO]^-$ $\longrightarrow$ **HNO** + $RNNO^-$	- Reaction occurs at physiological pH and temperature <u>Limitations:</u> - Short half-life (~2-3mins) - IPA/NO may release NO at neutral pH	(DuMond & King, 2011)

Acyloxy nitroso compound (eg. 1-NCA, 1-Nitrosocyclohexyl acetate)	- Cleavage of ester bond 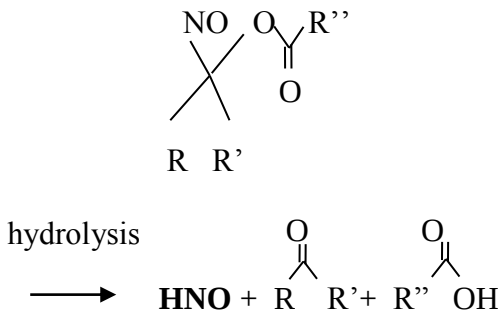 	- Reaction occurs at physiological temperature and over a range of pH 4-8 - Rate of HNO release varies with the structure of the organic/acyl groups - Half-life of > 2h - Newly described class of HNO donor <u>Limitations:</u> - Acyloxy nitroso may compete with HNO to react with thiols - Mechanism of action is not clear yet, and may involve NO release	(Sha *et al.*, 2006; DuMond & King, 2011)

1.7.3 Cardiovascular therapeutic potential of HNO

As discussed above, the primary targets for HNO are thiols and metal centres (eg. the haem group on sGC). The interaction of HNO with these biological moieties has made it a potential therapeutic agent in many biological conditions, especially in cardiovascular pathologies.

1.7.3.1 HNO is a vasodilator

(i) The role of sGC/cGMP signalling

Many reports have shown that HNO elicits vasodilatation. The earliest report by Fukuto and colleagues demonstrated that Angeli's salt induced relaxation in rabbit aorta and bovine intrapulmonary artery, and these responses were inhibited in the presence of the sGC inhibitor, methylene blue (Fukuto *et al.*, 1992b). It was therefore speculated that the vasorelaxation of HNO was mediated by activation of the sGC, and subsequent production of cGMP (Fukuto *et al.*, 1992b) (Figure 1.10). Other studies have shown that Angeli's salt causes relaxation *in vitro* and vasodilatation *in vivo* and *ex vivo*. In rodent isolated thoracic aorta, Angeli's salt induces vasorelaxation through sGC signalling (Ellis *et al.*, 2000; Wanstall *et al.*, 2001). Angeli's salt also exhibits vasodilator activity in the feline pulmonary vascular beds (De Witt *et al.*, 2001), in rat isolated heart *ex vivo* (Favaloro & Kemp-Harper, 2007) and in canine heart *in vivo* (Paolocci *et al.*, 2003).

(ii) The role of potassium channels

More recently, HNO has been reported to cause vasorelaxation through potassium channels. In rat mesenteric arteries, the vasodilator action of HNO is attenuated in the presence of a voltage-dependent potassium channel (K_v) inhibitor, 4-aminopyridine (4-AP) (Irvine *et al.*, 2003). Other studies have shown that the dilator effect of HNO is impaired in

the presence of 4-AP, and is completely abolished in the presence of the sGC inhibitor 1H-[1, 2,4] oxadiazolo [4,3-a] quinoxalin-1-one (ODQ), suggesting the modulation of K_v channels by HNO is downstream of sGC/cGMP signalling (Andrews *et al.*, 2009; Favaloro & Kemp-Harper, 2009) (Figure 1.10). Whether HNO modulates K_v channels by direct interaction, or in a sGC-dependent manner, remains to be elucidated. Yuill and colleagues have recently demonstrated that in rat resistance arteries, HNO-induced vasodilatation could also be mediated through Ca^{2+}-activated K^+ channels (BK_{Ca}) (Yuill *et al.*, 2011) (Figure 1.10). With these findings, it has been suggested that HNO may be the endothelium-derived hyperpolarising factor in resistance arteries. In rat coronary vasculature, Angeli's salt elicits vasorelaxation partly through the K_{ATP} channel, and this action is sGC-dependent (Favaloro & Kemp-Harper, 2007).

(iii) The role of calcitonin gene-related peptide (CGRP)

The vasorelaxation action induced by Angeli's salt has also been shown to be partially mediated through calcitonin gene-related peptide (CGRP) receptors. CGRP is a small neuropeptide that is released from the sensory nerves, to innervate the heart and blood vessels, inducing vasodilatation and cardiac contraction (Katori *et al.*, 2005). Administration of Angeli's salt *in vivo* elevates the plasma levels of CGRP (Paolocci *et al.*, 2003). Favaloro and Kemp-Harper demonstrated that the presence of a CGRP receptor antagonist, $CGRP_{8-37}$, partly attenuated the dilator effect of HNO in the isolated heart *ex vivo*, suggesting CGRP might be partly involved in the vasorelaxation signalling of HNO (Favaloro & Kemp-Harper, 2007) (Figure 1.10). In contrast, in an earlier report by Paolocci and colleagues, the vasodilator action of HNO was not affected by $CGRP_{8-37}$ infusion*in vivo* (Paolocci *et al.*, 2001). Further investigation is needed to determine the role of CGRP in HNO actions.

(iv) HNO does not cause vascular tolerance

As a vasodilator, HNO has pharmacological benefits over NO, in addition to lack of reactivity with superoxide. For example, Angeli's salt, either *in vitro* or *in vivo*, does not induce tolerance to its own actions in blood vessels (Irvine *et al.*, 2007; Irvine *et al.*, 2011). This is favourable over traditional, clinically used NO donors, such as glyceryl trinitrate, which rapidly develop tolerance to their vascular actions (Irvine *et al.*, 2007) and thus are unsuited to long term administration.

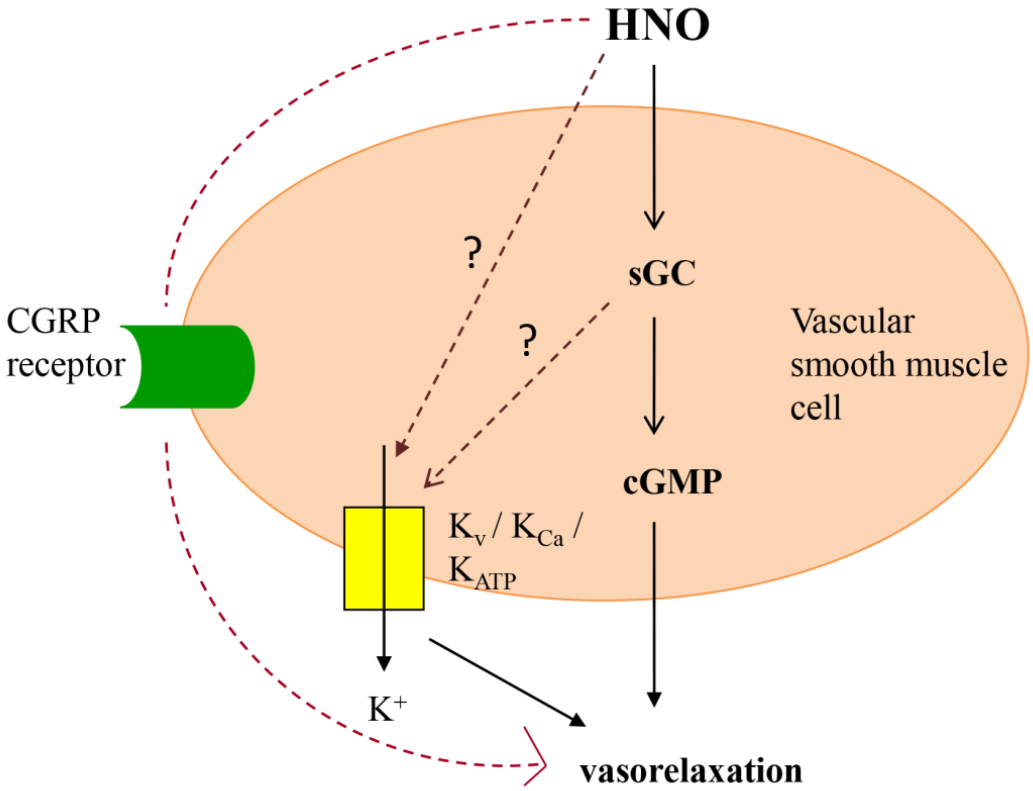

Figure 1.10: Schematic diagram of nitroxyl (HNO) signalling to induce vasorelaxation. HNO induces vasorelaxation primarily via the soluble guanylyl cyclase (sGC)/cyclic guanosine monophosphate (cGMP) pathway. HNO-induced vasorelaxation is also partially mediated through potassium channels (K^+) i.e. voltage-gated potassium channels (K_v) and calcium-activated potassium channel (K_{Ca}) in resistance arteries and adenosine triphosphophate (ATP)-sensitive potasssium channel (K_{ATP}) in coronary vessels. HNO may also cause vasorelaxation by activating the calcitonin gene-related peptide (CGRP) receptor (Irvine *et al.*, 2003; Favaloro & Kemp-Harper, 2007; Yuill *et al.*, 2011).

(v) Potential use of HNO as a vasodilator in disease settings

Bullen and colleagues reported that in isolated common carotid arteries from wild-type and apolipoprotein E–deficient ($ApoE^{-/-}$) mice fed a high-fat diet for 7 weeks (where total plasma cholesterol level or superoxide anion production was elevated), the dilator response to the HNO donor, IPA/NO or the NO donor, glyceryl trinitrate (GTN) was preserved. In the same study, it was also reported that IPA/NO, but not GTN, inhibited collagen-induced platelet aggregation in $ApoE^{-/-}$ mice (Bullen *et al.*, 2011). The dilator response to Angeli's salt in isolated aorta from angiotensin II-induced hypertensive mice was also preserved (Wynne *et al.*, 2012). Angeli's salt and IPA/NO also exhibit arterial pressure-lowering property and this property is preserved in spontaneously hypertensive rats compared to normotensive rats (Irvine *et al.*, 2013a). In addition, vasorelaxation to Angeli's salt in isolated aorta from spontaneously hypertensive rats was similar to that seen in normotensive rats (Irvine *et al.*, 2013a). In streptozotocin-induced type 1 diabetic rats, endogenous HNO-mediated vasodilatation was preserved, while endogenous NO-mediated relaxation was impaired (Leo *et al.*, 2012). These data suggest that HNO can maintain its dilator property in diseases where there is evelated oxidative stress and can be used as a potential therapeutic agent to improve vasodilatation in pathological conditions such as hypertension and diabetes.

1.7.3.2 HNO as antioxidant

The role of HNO in redox biology has also been examined to provide evidence that HNO can act as an antioxidant by inducing the expression and activity of a cytoprotective enzyme, haem oxygenase-1 (HO-1) (Naughton *et al.*, 2002). HO-1 is activated in response to oxidative stress and protects cells from oxidative damage (Naughton *et al.*, 2002). Ritchie and colleagues have also shown that HNO suppresses levels of superoxide in cardiomyocytes,

through inhibition of the superoxide-generating enzyme, NADPH oxidase (Lin *et al.*, 2012; Irvine *et al.*, 2013b).

1.7.3.3 HNO and cardiac function

The reaction between HNO and thiols/thiolates is an important component in the cardio-stimulatory action of HNO.

(i) HNO in I/R injury

One of the earliest discoveries that HNO is beneficial in cardiac conditions was by affording myocardial protection during an I/R event akin to ischaemic preconditioning (Pagliaro *et al.*, 2003). Pagliaro and colleagues have shown that an intracoronary infusion of Angeli's salt on rat isolated hearts before global I/R could confer protection and reduce injury to the heart (Pagliaro *et al.*, 2003). This was indicated by a decrease in left ventricular infarct size and improved post-ischaemic cardiac contractility with Angeli's salt, and the protective effect was thiol-sensitive (Pagliaro *et al.*, 2003). In contrast, Ma and colleagues have shown that when Angeli's salt was administered just before reperfusion (but after ischaemia), it could exacerbate the injury and cause more severe damage to cardiomyocytes, suggesting that the timing is important for administration of Angeli's salt for cardioprotection (Ma *et al.*, 1999a). NO exhibited a completely different profile where it provided a protection when it was administered after ischaemia and before reperfusion (Ma *et al.*, 1999a).

(ii) HNO enhances cardiac contractility and relaxation

Following these discoveries, growing evidence indicates that Angeli's salt can exert a positive cardiac inotropic effect. Paolocci and colleagues demonstrated that Angeli's salt exerted a positive cardiac inotropy in normal canine hearts *in vivo* (Paolocci *et al.*, 2001). In canine tachycardia-induced failing hearts, Angeli's salt enhances cardiac contraction to the same extent as in a normal canine heart, despite the many defective signalling mechanisms that are present (Paolocci *et al.*, 2003). Myocardial relaxation was also improved (Paolocci *et al.*, 2003). In rodent isolated cardiomyocytes, studies have also demonstrated that Angeli's salt increases contractile force and hastens relaxation (Tocchetti *et al.*, 2007; Lancel *et al.*, 2009; Kohr *et al.*, 2010). This positive inotropy induced by Angeli's salt was not seen with the NO donor, diethylamine NONOate (DEA/NO), showing a difference in the behaviour of HNO and NO (Paolocci *et al.*, 2001).

(iii) Mechanism of action of HNO in cardiomyocytes

Numerous studies have been conducted to investigate the mechanism of action of HNO in isolated cardiomyocytes. HNO can regulate Ca^{2+} homeostasis in cardiomyocytes, by targeting specific Ca^{2+}-handling proteins on the sarcoplasmic reticulum through a HNO-thiol interaction (Tocchetti *et al.*, 2007; Kohr *et al.*, 2010). HNO is thought to react with specific thiol groups, called hyperreactive or "critical thiols", on these proteins that are selectively oxidised and reduced, to open and close for Ca^{2+} transport respectively (Zaidi *et al.*, 1989; Cheong *et al.*, 2005; Lancel *et al.*, 2009). HNO reacts with thiol groups on RyR2 on sarcoplasmic reticulum, to trigger the opening of the channel and induce a prompt release of Ca^{2+} (Cheong *et al.*, 2005; Tocchetti *et al.*, 2007; Kohr *et al.*, 2010). This increases the availability of cytoplasmic Ca^{2+} for contraction. To improve cardiomyocyte relaxation, HNO interacts with another thiol-containing protein, SERCA, to increase its opening probability

and accelerate the re-sequestration of Ca^{2+} into the sarcoplasmic reticulum (Tocchetti *et al.*, 2007; Kohr *et al.*, 2010). Further evidence has shown that this reaction occurs via oxidative modification of a single amino acid cysteine 674 on SERCA2a (Lancel *et al.*, 2009). In addition, HNO also covalently modifies the thiol group on PLN, a regulatory protein of SERCA2a to facilitate cardiac relaxation (Karim *et al.*, 1998; Froehlich *et al.*, 2008).

Apart from regulating the Ca^{2+} handling in cardiomyocytes, HNO can also act directly on muscle fibres to enhance cardiac contraction (Dai *et al.*, 2007). The presence of the thiol-reducing agent, dithiothreitol (DTT), blunts this effect, suggesting a thiol interaction is involved (Dai *et al.*, 2007). It has also been hypothesised that HNO reacts with cysteine "hot-spots" in the muscle fibres and causes increased sensitivity of the fibres to Ca^{2+} binding (Dai *et al.*, 2007). It is likely that these cysteine "hot-spots" are present on regulatory contractile proteins such as tropomyosin, troponin C, troponin I and myosin light chain I and II (Dai *et al.*, 2007), as supported by a recent study where depressed myocardial contraction was reversed by HNO, via increasing myofilament sensitisation to Ca^{2+} (Ding *et al.*, 2011).

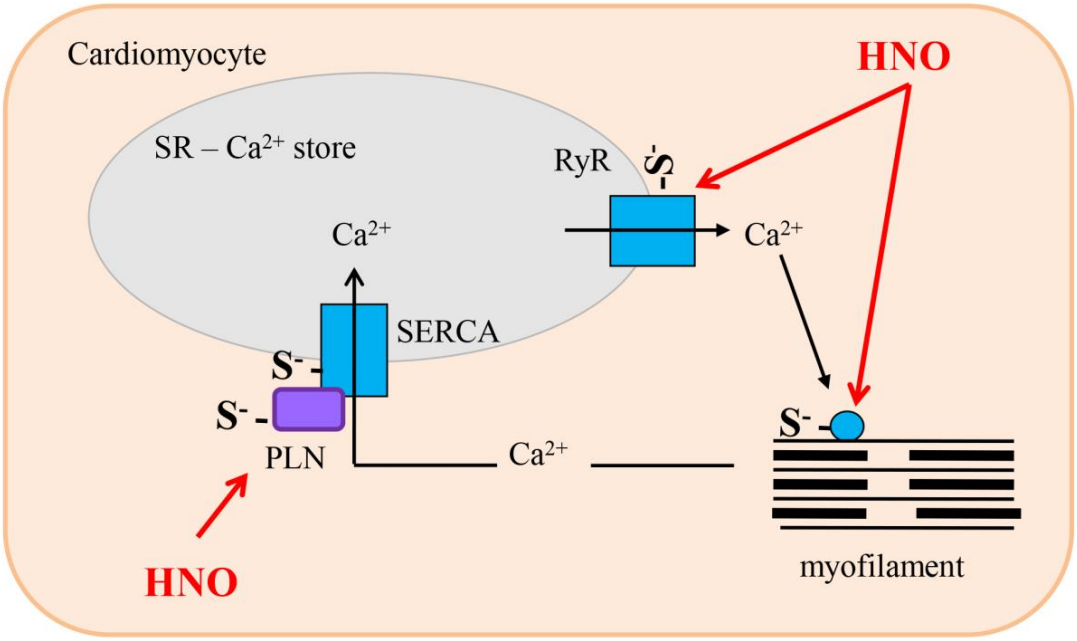

Figure 1.11: Mechanism of action of nitroxyl (HNO) to enhance cardiac contraction and relaxation. HNO reacts with ryanodine receptor (RyR) and myofilament proteins via a thiol interaction (S^-) to enhance cardiac contraction while it acts on sarco/endoplasmic reticulum Ca^{2+}-ATPase (SERCA) and phospholamban (PLN), also through a thiol interaction, to improve relaxation (Dai *et al.*, 2007; Tocchetti *et al.*, 2007). SR= sarcoplasmic reticulum; Ca^{2+}= calcium ions, ATP= adenosine triphosphate

1.7.3.4 Antihypertrophic action of HNO

Studies have shown that HNO exhibited antihypertrophic properties in neonatal rat isolated cardiomyocytes via the sGC/cGMP pathway (Lin *et al.*, 2012; Irvine *et al.*, 2013b). In these studies, on addition of HNO donors, Angeli's salt and IPA/NO, there was a significant reduction in cardiomyocyte size and inhibition of ROS generation that can contribute to cardiac hypertrophy (Lin *et al.*, 2012; Irvine *et al.*, 2013b). In cardiac hypertrophy, there is a switch in fetal genes for contractile proteins to the less efficient β-myosin heavy chain isoform (Lin *et al.*, 2012). Angeli's salt prevented this switch in gene expression (Lin *et al.*, 2012). It also significantly attenuated the activity of a pro-hypertrophic signalling kinase, p38 MAPK (Lin *et al.*, 2012).

1.8 Aims of the project

It is evident that the synthetic flavonol, DiOHF is protective against myocardial I/R injury; however its mechanism of action requires further investigation. The broad aim of the project is to investigate the temporal change in the expression of pro-injurious and pro-survival kinases after myocardial I/R, and the effect of DiOHF on the expression of these kinases after myocardial I/R. It is hypothesized that cardioprotection afforded by DiOHF during I/R is mediated by inhibiting kinases in the injurious pathway without affecting protective kinases. In addition, the mechanism of cardiac and vascular actions of the HNO donor, Angeli's salt in normal hearts as well as its cardiac and vascular effects after acute myocardial infarction will be determined. The hypothesis is that the acute improvement in cardiac and vascular function by the HNO donor, Angeli's salt is preserved after acute myocardial infarction.

The specific aims of this study are

(i) To investigate the temporal change in the expression of pro-injurious and pro-survival kinases after myocardial I/R. The expression of MAPKs, JNKs, p38 MAPK, Erk 1/2, Akt, the multi-functional enzyme CaMKII and PLN after myocardial ischaemia and at various reperfusion time points after ischaemia was investigated.

(ii) To investigate the effect of DiOHF on the expression of injurious and protective kinases after myocardial I/R. DiOHF was added during reperfusion and its effect on myocardial I/R injury was studied. The effect of DiOHF on the expression of JNKs, p38 MAPK, Erk 1/2, Akt, CaMKII and PLN at various reperfusion time points after ischaemia was investigated.

(iii) To investigate the mechanism(s) of cardiac and dilator actions of the HNO donor, Angeli's salt in the more physiological setting of the isolated heart at constant pressure. The cardiac and dilator actions of Angeli's salt on normal hearts were compared to the NO donor, DEA/NO.

(iv) To investigate the acute improvement in cardiac and vascular function by Angeli's salt after myocardial I/R. The cardiac effect of Angeli's salt was compared to dobutamine, a clinically used inotrope for acute heart failure, while its dilator effect was compared with DEA/NO.

Chapter 2

2. General Methods

2.1 Animal Model

Male Sprague-Dawley rats were purchased from either the Monash University Animal Facility (Clayton, VIC, Australia), or the Alfred Medical Research Educational Precinct (AMREP) Animal Facility. All animals were kept in the Research Animal Facility at RMIT University or AMREP under controlled conditions of illumination (12 h light/12 h darkness) and temperature (20–25ºC). All animals were given free access to food (standard pellet diet) and water *ad libitum*. The use of animals was approved by RMIT University and AMREP Animal Ethics Committees and conformed to the National Health and Medical Research Council of Australia code of practice for the care and use of animals for scientific purposes.

2.2 Isolation of Sprague-Dawley rat hearts

Rats (weighing 250-450 g) were anaesthetised with 325 mg/kg sodium pentobarbitone or a mixture of ketamine (100 mg/kg) and xylazine (12 mg/kg) intraperitoneally. Before a surgery was performed, confirmation of anaesthesia of the animal was assessed by checking the pedal pain withdrawal reflex (Skrzypiec-Spring *et al.*, 2007). Once the withdrawal reflex was absent, a thoracotomy was performed by cutting the diaphragm transabdominally. The thoracic cage was cut open on both sides along the axilliary lines and was reflected backwards to expose the heart. The heart was excised and immediately immersed in an ice-cold (4^0C) Krebs' buffer (pH 7.4 composition in mM: NaCl 118, KCl 4.7, $MgSO_4$•$7H_2O$ 1.18, KH_2PO_4 1.2, EDTA 0.5, $CaCl_2$ 1.75, $NaHCO_3$ 25.0 and D-glucose 11) to rinse off any blood on the

heart surface, stop its beating temporarily and to preserve it from ischaemic injury prior to reperfusion. The heart was then transferred onto a dissecting dish containing ice-cold Krebs buffer and any surplus tissues (such as thymus, lungs or fat) surrounding the heart were removed.

2.3 Langendorff-perfused rat hearts

Krebs' buffer was allowed to drip gently from the aortic cannula of the Langendorff system (ADInstrument, Sydney, NSW, Australia) before cannulation of the heart took place to avoid formation of air emboli during the cannulation process. The ascending aorta was gently cannulated at the aortic cannula by holding the aorta with two blunt-ended fine forceps. The aorta was then clamped using an alligator clip and a ligature was quickly tied around the aorta, securing it to the cannula. The cannula was connected to a pressure transducer (ADInstruments) to constantly measure the perfusion (aortic) pressure. The heart was retrogradely perfused with Krebs' buffer bubbled with 95% O_2 and 5% CO_2 at pH 7.4 and 37^0C. Hearts were perfused at a constant flow of ~12 ml/min to generate a perfusion pressure of ~60 mmHg or at a constant pressure of 45 ± 5 mmHg using a negative feedback pressure control loop peristaltic pump system (ADInstruments). The left atrial appendage was removed and a fluid-filled balloon made of thin silicone rubber was inserted into the left ventricle through the left atrium. The balloon was connected to a pressure transducer (ADInstruments) via a catheter to measure left ventricular pressure. The perfusion pressure, coronary flow, heart rate, left ventricular systolic pressure (LVSP), left ventricular end-diastolic pressure (LVEDP), left ventricular developed pressure (LVDP) and its derivative LV±dP/dt were continuously recorded on an ADInstruments PowerLab data acquisition system. Hearts that showed inadequate contractility, i.e. LV+dP/dt <1500 mmHg/sec, heart rate <100 beats/min, or sustained arrhythmias, during the stabilization period were excluded from the study.

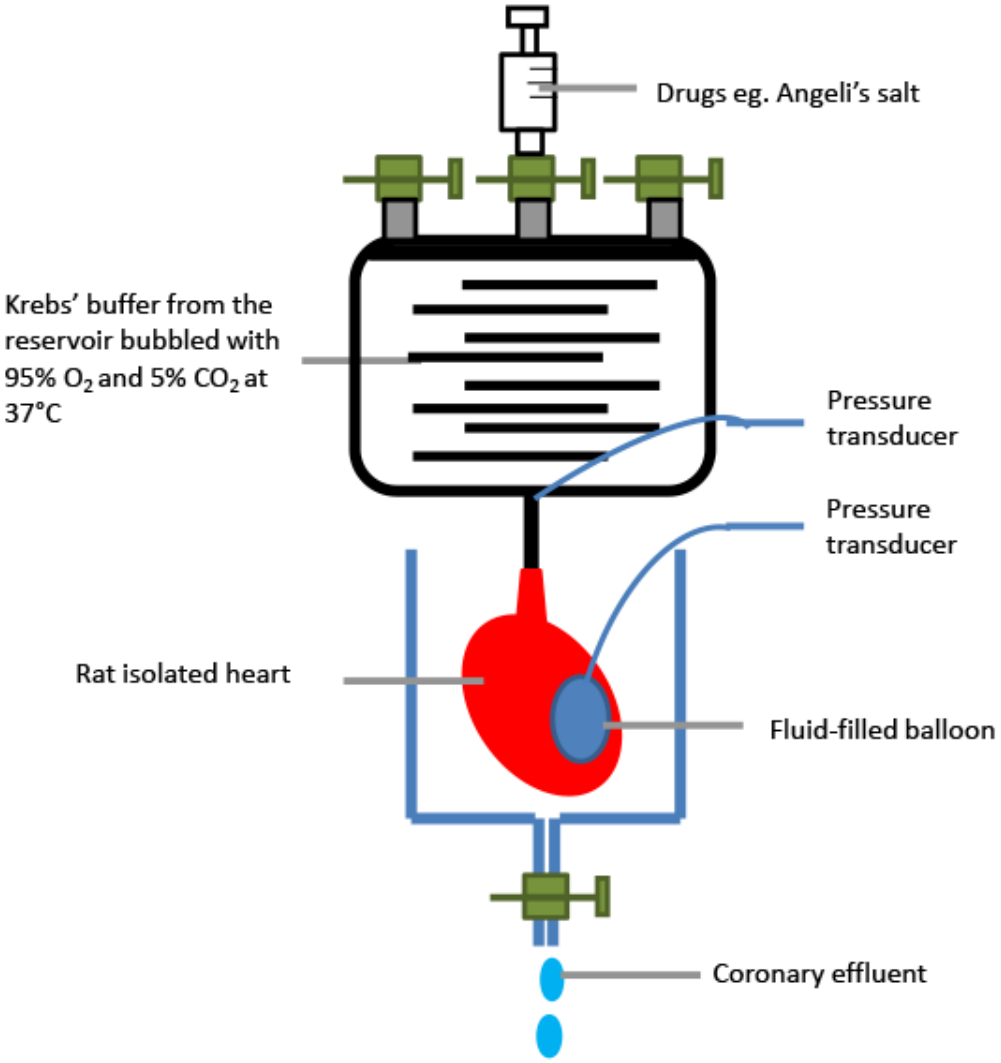

Figure 2.1: Schematic diagram of a rat isolated perfused heart. The heart was retrogradely perfused with Krebs' buffer bubbled with 95% O_2 and 5% CO_2 at pH 7.4 and 37^{0}C. The cannula was connected to a pressure transducer to constantly measure the perfusion (aortic) pressure while a fluid-filled balloon inserted into the left ventricle was connected to a second pressure transducer via a catheter to measure left ventricular pressure (Skrzypiec-Spring *et al.*, 2007). O_2= oxygen molecules; CO_2= carbon dioxide

2.4 Functional experiments

After 20 to 30 min equilibration, hearts were subjected to various treatments. For example, in Chapters 3, 4 and 6, hearts were subjected to global ischaemia followed by reperfusion. Global ischaemia was induced by stopping the Krebs' buffer perfusion to the heart completely. Hearts were immersed in warm (37°C) Krebs' buffer in the organ bath throughout the ischaemic period. Reperfusion was carried out by allowing the flow of Krebs' buffer to the heart again.

At the end of the functional experiment, left ventricular tissues were either snap frozen in liquid nitrogen and stored at -80°C freezer for Western blot analysis or fixed in 4% paraformaldehyde (PFA) overnight for terminal deoxynucleotidyl transferase dUTP nick end labelling (TUNEL) assay.

2.5 Lactate dehydrogenase (LDH) assay

LDH is a soluble cytosolic enzyme that is released following the loss of membrane integrity in the heart tissue into the coronary effluent. The measurement of LDH release, therefore, can be used as an indicator of cellular rupture and severe irreversible cell death.

2.5.1 Collection of LDH samples

Coronary effluent (~1 ml) from rat isolated perfused hearts was collected at various perfusion time points in sham hearts and during equilibration and at various reperfusion time points in I/R-treated hearts (Figure 2.1). Aliquots of samples were stored at -80°C until use.

2.5.2 Measurement of LDH release

On the day of LDH analysis, samples collected from -80°C freezer were warmed to room temperature. Reaction buffer consists of 145 mM sodium dihydrogen phosphate monohydrate ($NaH_2PO_4 \bullet H_2O$) and 1.45 mM sodium pyruvate, pH 7.5 was prepared. 1 mM nicotinamide adenine dinucleotide (NADH) was also prepared on ice and covered with aluminium foil. In a minimal light environment, 700 μL reaction buffer, 100 μL NADH and 200 μL samples were added to a microcuvette and LDH activity was measured every 3 sec for 2 min at 340 nm using a UV/Vis spectrophotometer (Lambda 25; PerkinElmer, Waltham, MA, USA). LDH activity was measured by the rate of reduction in the absorbance value during the conversion of NADH with sodium pyruvate to its oxidized form (NAD^+, equation 1).

$$\text{Pyruvate} + \text{NADH} + \text{H}^+ \xleftrightarrow{\text{LDH}} \text{L-Lactate} + \text{NAD}^+ \qquad \text{(Equation 1)}$$

An LDH standard curve (0.01-1 U/ml) was also constructed using L-LDH extracted from the hog muscle to calculate the LDH concentration in the effluent sample.

2.6 Terminal deoxynucleotidyl transferase dUTP nick end labelling (TUNEL) assay

2.6.1 Left ventricular tissues processing

After fixing in 4% PFA overnight, left ventricular tissues were placed in tissue cassettes which were then placed in a cassette holder (or basket) for tissue processing. Tissue processing was performed in an automated tissue processor (Leica Biosystems, North Ryde, NSW, Australia) where tissues were submerged in 10% neutral buffered formalin, graded concentrations of ethanol, 75%, 90% and 100% for 3 times, xylene for 3 times and melted

paraffin wax for 3 times. Tissues were immersed in each reagent for 30 min at 38°C except for melted paraffin wax at 62°C.

2.6.2 Paraffin wax embedding

Embedding was performed using a modular embedding centre (Shandon Histocentre™ 3, Thermo Electron Corporation, Waltham, MA, USA) which consists of a paraffin wax dispenser, a cold surface and a heated area for storage of moulds and tissue cassettes. Paraffin wax was dispensed into a suitably size mould and the processed tissue was placed in the mould in the correct orientation to provide a good morphology during microscopic examination. The cassette was then attached onto the mould and together they were placed on the cold surface for paraffin wax solidification. Once the paraffin wax had solidified, the mould was removed from the tissue block (left ventricular tissue embedded in paraffin wax).

2.6.3 Sectioning of the tissue block

Tissue blocks were sectioned using a rotary microtome (Leica RM2235 Microtome, Leica Biosystems, North Ryde, NSW, Australia). Trimming of tissue blocks was carried out before sectioning by cutting the block at 15-30 µm. Tissue blocks were then cut at 4 µm and a tissue ribbon was generated which was floated on a thermostatically controlled water bath (50°C) to flatten sections (~30 sec). Individual sections were separated from the ribbon using forceps and were mounted onto glass slides coated with poly-L-lysine. Glass slides containing sections were heated in an oven at 60°C for 1 h to remove any water trapped in the section.

2.6.4 *In situ* detection of apoptosis

Detection of apoptosis was performed using the CardioTACS™ *in situ* apoptosis detection kit (Trevigen, Gaithersburg, MD, USA). Deparaffinization of sections was performed by warming sections on the hot plate at 57°C for 5 min. Sections were dewaxed in xylene for 2 x 5 min followed by immersion in 100%, 95% and 70% ethanol, 5 min each. After 2 x 5 min washes in phosphate buffered saline (PBS; 137 mM NaCl, 2.7 mM KCl, 8 mM Na_2HPO_4 and 2 mM KH_2PO_4, pH = 7.4), sections were incubated with proteinase K solution (20 µg/ml) at room temperature for 20 min to permeabilize tissues. Endogenous peroxidase activity was blocked by incubating sections with 3% hydrogen peroxidase in methanol for 5 min. After washing in distilled water for 1 min, sections were immersed in terminal deoxynucleotidyl transferase (TdT) labelling buffer (0.001% thimerosal, 60 µM 2-mercaptoethanesulfonic acid, 0.05% bovine serum albumin and N-[tris(hydroxymethyl)methyl]-2-aminoethanesulfonic acid sodium salt solution, pH = 7.5) at room temperature for 5 min. The glass slide around the section was dried carefully. Sections were incubated with labelling reaction mix (5µM bionylated deoxynucleotide mix, 0.4 mM manganese cation, TdT enzyme and TdT labelling buffer) in a humidity chamber at 37°C for 1 h. Then, sections were immersed in TdT stop buffer (10 mM EDTA, pH = 8.0) at room temperature for 5 min followed by streptavidin-horseradish peroxidise (HRP) solution incubation for 10 min. TACS Blue Label™ (3,3',5,5'-tetramethylbenzidine in 0.9% dimethyl sulfoxide (DMSO) v/v solution) was then added to sections and it reacted with streptavidin-HRP to generate a dark blue precipitate. After 2 x 5min wash with distilled water, sections were counterstained with Nuclear Fast Red for 2.5 min. Sections were washed in distilled water for 1 min followed by dehydration by sequentially immersing in 95% and 100% ethanol for 1 min each and xylene 2 x 2 min. Sections were then mounted with a synthetic mounting medium DPX and covered with a coverslip. The number of positively stained nuclei in 10

random fields per section was counted under a microscope (at 20x magnification). The number of apoptotic cells was measured as a percentage of total cells.

2.7 Western blot

2.7.1 Protein extraction

Frozen left ventricular tissues were collected from -80^{0}C freezer. Approximately 80 mg left ventricular tissue from each sample was collected and homogenized in 400 µL ice-cold lysis buffer (100 mM NaCl, 10 mM Tris, 2 mM EDTA, 0.5% w/v sodium deoxycholate, 1% vol/vol triton X-100, pH7.4, protease and phosphatase inhibitor cocktails (Roche, Sydney, NSW, Australia)) using the digital homogenizer. Samples were kept on ice throughout the homogenizing process. After all samples were homogenized, tissue homogenates were centrifuged at 3,750 g for 20 min at 4°C. The supernatant was then collected and stored at -80°C until required. This protein extraction yielded a whole (left) ventricle homogenate.

2.7.2 Protein assay

The protein concentration of tissue homogenates was assessed using the Bradford protein assay. Tissue homogenates were diluted 1:200 with PBS to a final volume of 100 µL in a test tube. 100 µL of 0.2 M sodium hydroxide (NaOH) was added to the test tube and incubated for 15 min. 600 µL of MilliQ water followed by 200 µL of red protein assay reagent dye (Bio-Rad, Gladesville, NSW, Australia) were added to the test tube. The solution mixture was vortexed and the mixture turned blue in the presence of protein. 200 µL of the solution was then transferred to a 96-well plate. Each sample was performed in duplicates. The absorbance of samples was measured at 590 nm with a plate reader. A bovine serum albumin (BSA) standard curve (0-20 µg/ml) was also generated and was used to calculate the protein concentration in the unknown sample.

2.7.3 Preparation of samples for sodium dodecyl sulfate-polyacrylamide gel electrophoresis (SDS-PAGE)

An identical amount of protein (50 μg) from each sample was obtained and topped up with MilliQ water so that each sample contained the same total volume (10 μl). The identical volume (10 μl) of 2x Laemmli sample buffer (20% w/v glycerol, 2% SDS, 62.5 mM Tris, 0.05% bromophenol blue and 5% β-mercaptoethanol, pH 6.8) was added to each sample and stored at -80°C until required.

2.7.4 Preparation of gel for SDS-PAGE

Plates were assembled according to the manufacturers' instructions (Bio-Rad, Gladesville, NSW, Australia). The 10% (for Akt, Erk 1/2, STAT3, p38 MAPK, JNK and CaMKII) or 15% (for PLN) resolving gel buffer (30% acrylamide, MilliQ water, 1.5 M Tris, pH 8.8, 10% SDS, 10% ammonium persulfate and N,N,N',N'-tetramethylethylenediamine (TEMED)) was prepared and added into the glass plates using a pipette. Isopropyl alcohol (~20 μL) was also added to remove bubbles and to prevent the top of the gel from drying. The solution was left to polymerize at room temperature for 30-60 min to form an acrylamide-resolving gel. Once the resolving gel had set, the alcohol was removed by dabbing using KimWipes. 4% stacking gel buffer (30% acrylamide, MilliQ water, 0.5 M Tris, pH 6.8, 10% SDS, 10% ammonium persulfate and TEMED) was then added on to the top of the resolving gel and a 15-well comb was inserted. The gel was left to polymerize at room temperature for 20-45 min.

2.7.5 SDS-PAGE

SDS-PAGE was carried out using a mini-PROTEAN apparatus (Bio-Rad, Gladesville, NSW, Australia). Samples collected from -80°C freezer were heated at 95°C for 5 min to denature the protein and centrifuged so that all proteins were concentrated at the bottom of the eppendorff tube. Samples (containing 50 μg protein) and a pre-stained kaleidoscope protein ladder (8 μl, Bio-Rad, Gladesville, NSW, Australia) were loaded into wells followed by electrophoresis of proteins in the running buffer (25 mM Tris, 192 mM glycine, 0.1% SDS, pH 8.3) at 100 V for 1.5-2 h (until the protein separation was completed, Figure 2.2A). Following electrophoresis, gels were placed in an ice-cold transfer buffer (25 mM Tris, 192 mM glycine, 20% methanol, 0.037% SDS, pH 8.3) to remove excess salt and detergents from the running buffer which may increase the conductivity of the transfer buffer. At the same time, Hybond nitrocellulose membranes, filter papers and sponges were also equilibrated in ice-cold transfer buffer. Sponges, filter papers, nitrocellulose membranes and gels were then assembled as shown in Figure 2.2B, for wet transfer to be carried out at 350 mA for 1.5-2 h. Transfer of protein onto the membrane was confirmed by Ponceau S staining.

2.7.6 Immunoblotting

For immunoblotting of phospho-proteins, non-specific binding on the nitrocellulose membrane were blocked in 5% w/v BSA in Tris buffered saline plus 0.1% Tween-20 (TBST) at room temperature for 1 h. Primary antibody (e.g. phospho-Akt raised in rabbit, 1:1000 dilution in 5% BSA/TBST) incubation was carried out at 4°C overnight. The next day, the membrane was washed 3 x 5 min with TBST followed by goat anti-rabbit HRP-conjugated secondary antibody incubation (1:2000 in 5% skim milk/TBST) at room temperature for 1 h (Figure 2.3). The secondary antibody was detected with either enhanced chemiluminescence reagents (Amersham, GE Healthcare, Sydney, NSW, Australia) or Supersignal West Femto

(Thermo Scientific, Waltham, MA, USA) for 1 min, and the chemiluminescence signals on the membrane were detected by the digital image scanner (Bio-Rad Chemidoc). Protein bands were then quantified by densitometry.

After the detection of the phospho-protein, membranes were stripped with stripping buffer (Thermo Scientific, Waltham, MA, USA) according to manufacturer's instructions. To confirm that the membrane was stripped successfully, the membrane was blocked with 5% skim milk/TBST at room temperature for 1 h, followed by goat anti-rabbit HRP-conjugated secondary antibody (1:2000 in 5% skim milk/TBST) incubation at room temperature for 1 h. The membrane was visualized with enhanced chemiluminescence reagents (Amersham, GE Healthcare, Sydney, NSW, Australia) and the loss of protein bands indicated that the stripping was successful. After stripping, the membrane was then probed with the respective total protein (eg. Akt for phospho-Akt) at 4°C overnight. After 3 x 5 min washes with TBST, secondary antibody incubation was carried out followed by chemiluminescence detection and visualization. Protein bands detected were quantified by densitometry.

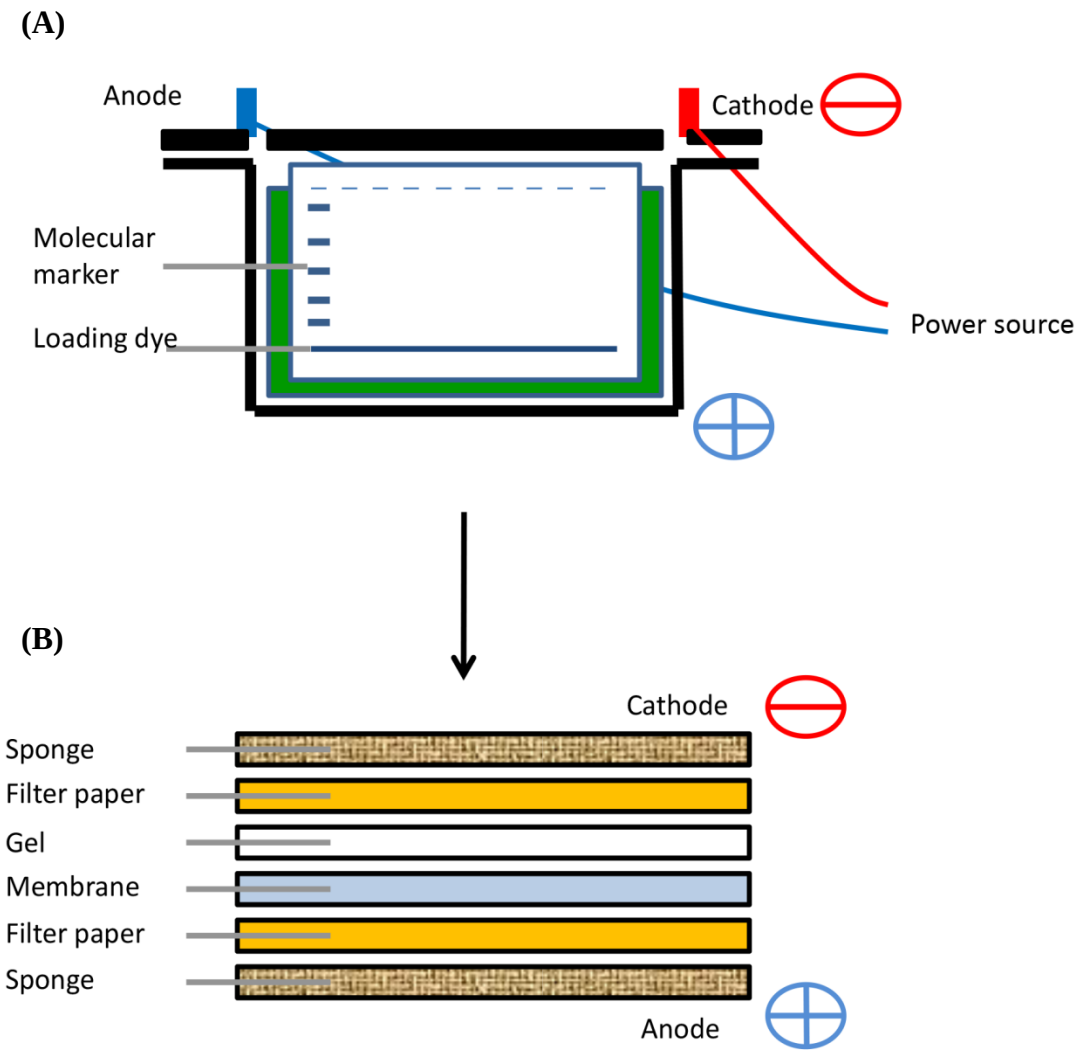

Figure 2.2: (A) Schematic diagram of the mini-PROTEAN apparatus (Bio-rad, Gladesville, NSW, Australia) for sodium dodecyl sulfate-polyacrylamide gel electrophoresis (SDS-PAGE). Negatively charged proteins (denatured in sample buffer containing SDS detergent) will migrate in an electric field through the gel and towards the positive electrode. Having similar charge-to-mass ratio, proteins are separated by size where proteins with lower molecular weight will migrate across the gel faster than higher molecular weight proteins. **(B)** The orientation of the sponge/filter paper/gel/membrane sandwich for wet transfer. This orientation is important for the negatively charged proteins to migrate from the gel onto the membrane when an electric current is applied.

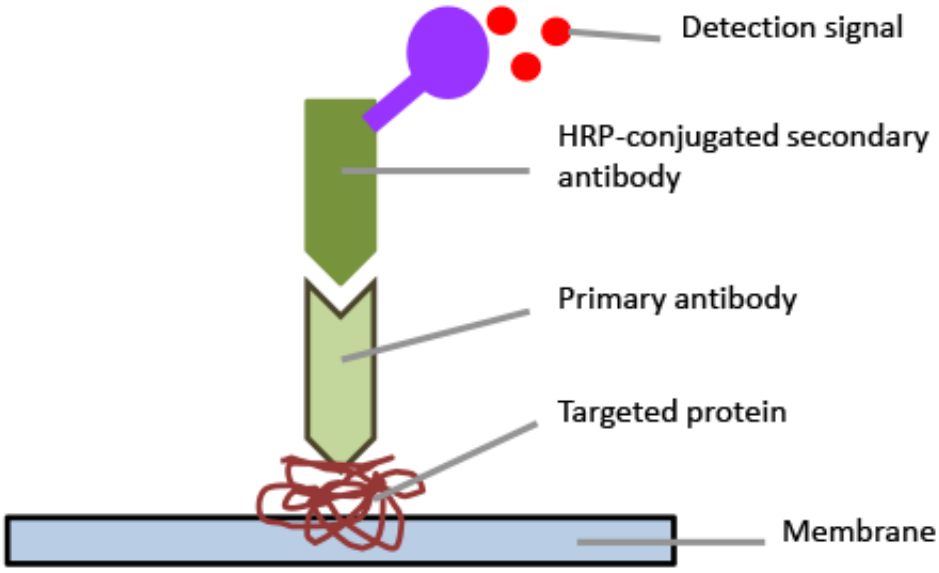

Figure 2.3: Detection of a target protein by the primary antibody followed by the incubation of a horseradish peroxidase (HRP)-conjugated secondary antibody to detect the presence of the primary antibody. The HRP label reacts with chemiluminescent substrates to produce light which is detected using the digital image scanner.

2.8 Assessment of reperfusion-induced arrhythmias

Experimental records of left ventricular pressure (LVP) were used to analyse the incidence of arrhythmias. One of the subtypes of arrhythmia is ventricular fibrillation. According to the Lambeth Conventions (Walker *et al.*, 1988), ventricular fibrillation occurred when beats are no longer distinguishable from one another and the developed pressure is <5 mmHg. The total duration (in sec) of LVP showing a LVDP <5 mmHg in the first 10 min of reperfusion was measured.

2.9 Statistical analysis

All results were expressed as group mean ± standard error of mean (SEM), with the number of independent experiments denoted as 'n'. Data analysis was performed using Graphpad Prism® (version 5.0 or 6.0, La Jolla, CA, USA). Statistical analysis including Student's unpaired *t*-test (Chapters 4, 5 and 6), 1-way ANOVA with Tukey's multiple comparison test (Chapters 3 and 4), 1-way ANOVA with Dunnett's *post hoc* test for multiple comparisons (Chapter 5), 2-way ANOVA with Sidak's multiple comparison test (Chapters 4 and 6) and 2-way ANOVA with Bonferroni *post hoc* test for multiple comparisons (Chapter 5) were performed.

2.10 Drugs and reagents

Sodium chloride (NaCl), potassium chloride (KCl), potassium phosphate monobasic (KH_2PO_4), magnesium sulphate hepta hydrate ($MgSO_4 \bullet 7H_2O$), calcium chloride ($CaCl_2$) sodium bicarbonate ($NaHCO_3$), D-glucose and ethylenediaminetetraacetic acid (EDTA) were all obtained from Sigma-Aldrich (St. Louis, MO, USA). Ketamine was obtained from Parnell Laboratories Aust Pty. Ltd. (Alexandria, NSW, Australia) and xylazine was from Troy Laboratories (Smithfield, NSW, Australia). Sodium pentobarbitone was from Lethabarb,

Virbac Animal Heath (Sydney, NSW, Australia). For LDH assay, L-LDH from hog muscle was from Boehringer Ingelheim (North Ryde, NSW, Australia). Sodium pyruvate, $NaH_2PO_4 \bullet H_2O$, and NADH were purchased from Sigma-Aldrich (St. Louis, MO, USA). For TUNEL assay, ethanol, xylene, hydrogen peroxide and DPX mountant were from Sigma-Aldrich (St. Louis, MO, USA). PFA was from Merck Millipore (Bayswater, VIC, Australia). For Western blot experiments, sodium deoxycholate, NaOH, triton-X, tris(hydroxymethyl) aminomethane (Tris), SDS, β-mercaptoethanol, TEMED, ammonium persulfate, glycine, Tween-20 and methanol were obtained from Sigma-Aldrich (St. Louis, MO, USA). Primary antibodies were all purchased from Cell Signalling Technology (Beverly, MA, USA) except for actin which was purchased from Sigma. Glycerol, bromophenol blue and goat or sheep anti-rabbit and anti-mouse HRP-conjugated secondary antibodies were from Merck Millipore (Bayswater, VIC, Australia). BSA was from Life Technologies (Scoresby, VIC, Australia) and 30% acrylamide was from Bio-Rad Laboratories Pty. Ltd. (Gladesville, NSW, Australia). Ponceau S solution was obtained from Thermo Scientific (Waltham, MA, USA).

Chapter 3

3. Temporal change in the expression of pro-injurious and pro-survival kinases during myocardial I/R

3.1 Introduction

Myocardial infarction remains one of the major health problems in many countries and imposes a heavy economic burden for health expenditure. It is caused by a blockage in the blood vessel supplying the heart and partial or complete occlusion of the blood vessel results in ischaemia of the heart and subsequent cardiomyocyte death (White & Chew, 2008). Early reperfusion to remove the blockage in the blood vessel either by surgery such as percutaneous coronary interventions, or using thrombolytic agents, such as tissue plasminogen activator, is critical to restore the blood flow to the ischaemic myocardium to resuscitate myocardial tissue and improve clinical outcome (White & Chew, 2008). Paradoxically, this revascularization strategy may lead to accelerated and additional myocardial injury beyond that generated by ischaemia alone called myocardial reperfusion injury (Yellon & Hausenloy, 2007). At present, there is no effective pharmacological treatment for reperfusion injury.

A major hypothesis for the mechanism by which myocardial reperfusion causes injury is increased oxidative stress (Yellon & Hausenloy, 2007). Reoxygenation to the ischaemic myocardium produces ROS which are highly reactive molecules that can exert destructive effects on body systems such as damaging cellular DNA, lipids and protein, thereby inhibiting their normal functions and eventually causing cell death (Figure 1.1). A second major contributing factor for myocardial reperfusion injury is the calcium paradox (Yellon &

Hausenloy, 2007). Upon reperfusion, there is an abrupt increase in Ca^{2+} in the cell due to direct entry of Ca^{2+} through the damaged sarcolemmal membrane and the Na^{+}/Ca^{2+} exchanger to normalise pH (Figure 1.2). This can cause Ca^{2+} overload in the cell and induce cardiomyocyte death by causing hypercontracture of the heart cells. Ca^{2+} overload in the mitochondria which results in mitochondrial permeability transition pore (mPTP) opening and cell death has recently received much research attention as a major cause of myocardial reperfusion injury.

Increased oxidative stress and Ca^{2+} overload that occur during myocardial I/R could also activate a wide range of signal transduction pathways and contribute to cell survival or death. Signalling pathways that have been implicated during myocardial I/R include the mitogen-activated protein kinases (MAPKs) and phosphatidylinositol 3′-kinase (PI3K)/protein kinase B (Akt) pathways (Hausenloy & Yellon, 2004; Rose *et al.*, 2010). The best-characterized MAPK subfamilies are extracellular signal-regulated kinase (Erk) 1/2, *c-jun* N-terminal kinases (JNKs) and p38 MAPK. Extensive evidence *in vitro* and *in vivo* has supported a pro-injurious role of JNKs and p38 MAPK activation in myocardial I/R (Ma *et al.*, 1999b; Yue *et al.*, 2000; Ferrandi *et al.*, 2004; Kaiser *et al.*, 2004). The activation of JNKs and p38 MAPK increases the expression of pro-apopoptotic proteins such as Bcl-2-associated X protein (Bax) and Bcl-2-associated death promoter (BAD) as well as decreases the expression of anti-apoptotic proteins such as Bcl-2 and Bcl-X leading to apoptosis and cell death (Javadov *et al.*, 2014). While the activation of JNKs and p38 MAPK are pro-injurious, Hausenloy and Yellon have proposed that the activation of Akt and Erk 1/2 which form the Reperfusion Injury Salvage Kinase (RISK) pathway is involved in protection against myocardial I/R injury (Hausenloy & Yellon, 2004; Hausenloy *et al.*, 2005). Akt and Erk 1/2 phosphorylate several common targets which include pro-apoptotic proteins such as BAD and glycogen synthase kinase (GSK)-3β thereby inactivating them. The inactivation of GSK-3β

inhibits the opening of mPTP and prevents cell death (Hausenloy *et al.*, 2005). Another pro-survival pathway which has been implicated during I/R is the Survivor Activating Factor Enhancement (SAFE) pathway (Lecour, 2009). It involves the activation of the TNF-α, Janus kinase (JAK) and signal transducer and activator of transcription (STAT) 3 to promote cell survival., The relative activation of these kinase signalling pathways could influence the fate of cardiomyocytes to either undergo cell survival or death.

ROS and intracellular Ca^{2+} overload could also activate a multi-functional protein called Ca^{2+}/calmodulin-dependent protein kinase (CaMK) II (Couchonnal & Anderson, 2008). Elevated intracellular Ca^{2+} concentration promotes Ca^{2+} binding onto calmodulin and this calcified calmodulin then binds to CaMKII causing a conformational change and autophosphorylation (Couchonnal & Anderson, 2008). Activated CaMKII will in turn activate various downstream Ca^{2+}-related receptors including ryanodine receptors (RyRs), sarco/endoplasmic reticulum Ca^{2+}-ATPase (SERCA) and phospholamban (PLN) which is the regulatory protein for SERCA2a on the sarcoplasmic reticulum (Couchonnal & Anderson, 2008). Phosphorylation of PLN promotes SERCA resulting in the uptake of Ca^{2+} into the sarcoplasmic reticulum (Mattiazzi & Kranias, 2014). It is well known that CaMKII regulates myocardial excitation-contraction coupling under normal physiological conditions (Couchonnal & Anderson, 2008); however excessive CaMKII activation has been associated with various cardiac diseases including heart failure, cardiac hypertrophy and arrhythmias (Zhang & Brown, 2004; Couchonnal & Anderson, 2008). Emerging evidence has shown that CaMKII could also be a mediator of myocardial I/R injury (Vila-Petroff *et al.*, 2007; Joiner *et al.*, 2012).

In this study, we aimed to explore the temporal change in the activation of pro-injurious kinases p38 MAPK and JNKs as well as the activation of CaMKII and its

downstream target PLN, and the activation of protective kinases Akt and Erk 1/2 in the RISK pathway and STAT3 in the SAFE pathway during myocardial I/R.

3.2 Methods

This investigation conforms with the National Health and Medical Research Council of Australia code of practice for the care and use of animals for scientific purposes. All the procedures involved in this project were approved by the RMIT University Animal Ethics Committee.

3.2.1 Langendorff heart preparation

Hearts isolated from adult male Sprague-Dawley rats (250-300g) anaesthetized with 325 mg/kg sodium pentobarbitone were Langendorff-perfused as described in Chapter 2.3. Rat isolated hearts were perfused at a constant flow of ~12 ml/min to generate a perfusion pressure of 62 ± 5 mmHg. Hearts were equilibrated for 30 min before any intervention was carried out.

3.2.2 Temporal change in the expression of kinases during myocardial I/R

Rat isolated hearts were randomly assigned to one of the following five groups. The first group was (i) sham (S1) where hearts were perfused with Krebs' buffer for a total time of 50 min without any further intervention. This is the time-matched control for hearts subjected to ischaemia without reperfusion. The following 2-5 groups were subjected to I/R treatment. After 30 min equilibration, hearts were subjected to 20 min global ischaemia. Ischaemia was carried out as described in Chapter 2.4. Hearts were then reperfused for either (ii) 0, (iii) 5, (iv) 15 or (v) 30 min with Krebs' buffer in the presence of 0.5% dimethyl sulfoxide (DMSO),

which is the vehicle for DiOHF. At the end of the experiment, left ventricular tissues from all groups were snap frozen in liquid nitrogen and stored at -80°C until use.

3.2.3 Western blot

Western blots were performed as described in Chapter 2.7. In brief, protein sample (50 µg) was separated using SDS-PAGE and transferred onto a nitrocellulose membrane. After blocking in 5% BSA/TBST or skim milk/TBST for 1 h at room temperature, membranes were incubated with primary antibody (phospho^{Ser473}-Akt, Akt, phospho$^{Thr202/Tyr204}$-Erk 1/2, Erk 1/2, phospho^{Tyr705}-STAT3, STAT3, phospho$^{Thr183/Tyr185}$-JNK, JNK, phospho$^{Thr180/Tyr182}$-p38 MAPK, p38 MAPK, phospho$^{Thr286/287}$-CaMKII, CaMKII phospho$^{Ser16/Thr17}$-PLN, PLN or actin 1:1000) at 4ºC overnight. The next day, HRP-conjugated secondary antibody (1:2000) incubation was carried out for 1 h at room temperature and detection of the secondary antibody was carried out using the digital image scanner. Protein bands were then quantified by densitometry. The increase or decrease in the activity of a protein was measured by normalising the degree of phosphorylation of the protein to its total protein. Actin which is the loading control is used to normalise the level of total protein.

3.2.4 Statistical analysis

All results were expressed as group mean ± SEM, with the number of independent experiments denoted as ‘n’. Data analysis was performed using Graphpad Prism® (version 6.0, La Jolla, CA, USA). All Western blot data were analysed using 1-way ANOVA with Tukey’s multiple comparison test. In all cases, $p<0.05$ was considered statistically significant.

3.2.5 Drugs and reagents

All chemical reagents were purchased from Sigma-Aldrich (St. Louis, MO, USA) and dissolved in distilled water unless otherwise stated. All primary antibodies were purchased from Cell Signalling Technology (Beverly, MA, USA) except for actin which was purchased from Sigma. Secondary antibodies were from Merck Millipore (Bayswater, VIC, Australia). Primary and secondary antibodies were all diluted in 5% BSA/TBST.

3.3 Results

3.3.1 Temporal change in the expression of pro-injurious kinases during myocardial I/R

Rat isolated hearts were perfused with Krebs' buffer for 50 min without any further intervention (S1, n=5) or subjected to 20 min global ischaemia followed by reperfusion for 4 different time periods i.e. 0 (n=5), 5 (n=7), 15 (n=6) and 30 min (n=8) to determine the temporal change in kinase activation. The pro-injurious kinase p38 MAPK was phosphorylated during ischaemia and its phosphorylation remained elevated throughout reperfusion (Figure 3.1). In contrast, the phosphorylation of JNK 1/2 occurred during reperfusion but not ischaemia (Figure 3.2). The phosphorylation of JNK 2 at 54 kDa was highest at 30 min of reperfusion while the phosphorylation at 46 kDa (JNK 1) started to peak at 15 min of reperfusion.

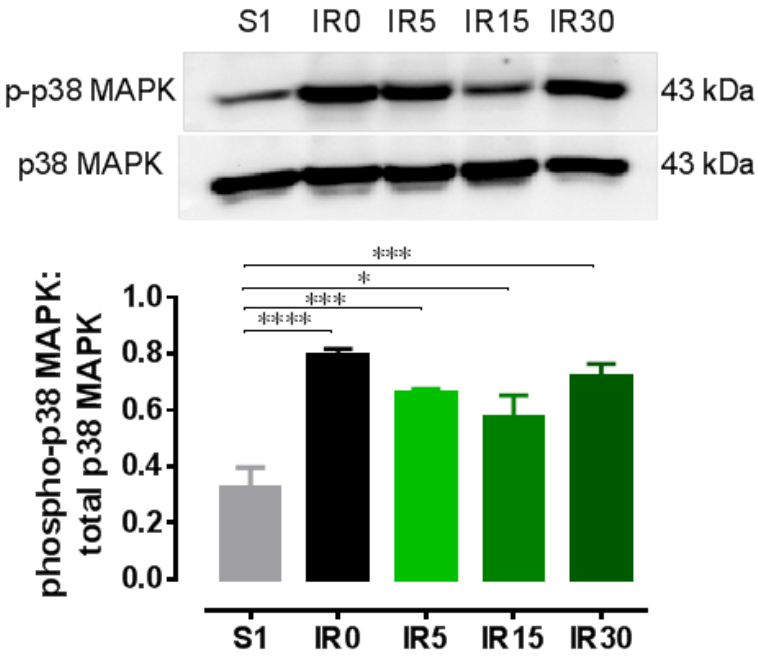

Figure 3.1: Isolated hearts were subjected to 50 min Krebs' buffer perfusion (S1) or subjected to 20 min global ischaemia followed by 0 (IR0), 5 (IR5), 15 (IR15) or 30 min (IR30) reperfusion in the presence of 0.5% DMSO (n= 5-8 per group). The phosphorylation of p38 MAPK at various reperfusion time points was assessed using Western blot. The phosphorylation of these proteins was normalised against total protein. *p<0.05, ***p<0.001, ****p<0.0001 vs corresponding time point, 1-way ANOVA with Tukey's multiple comparisons test. Data are expressed as mean ± SEM.

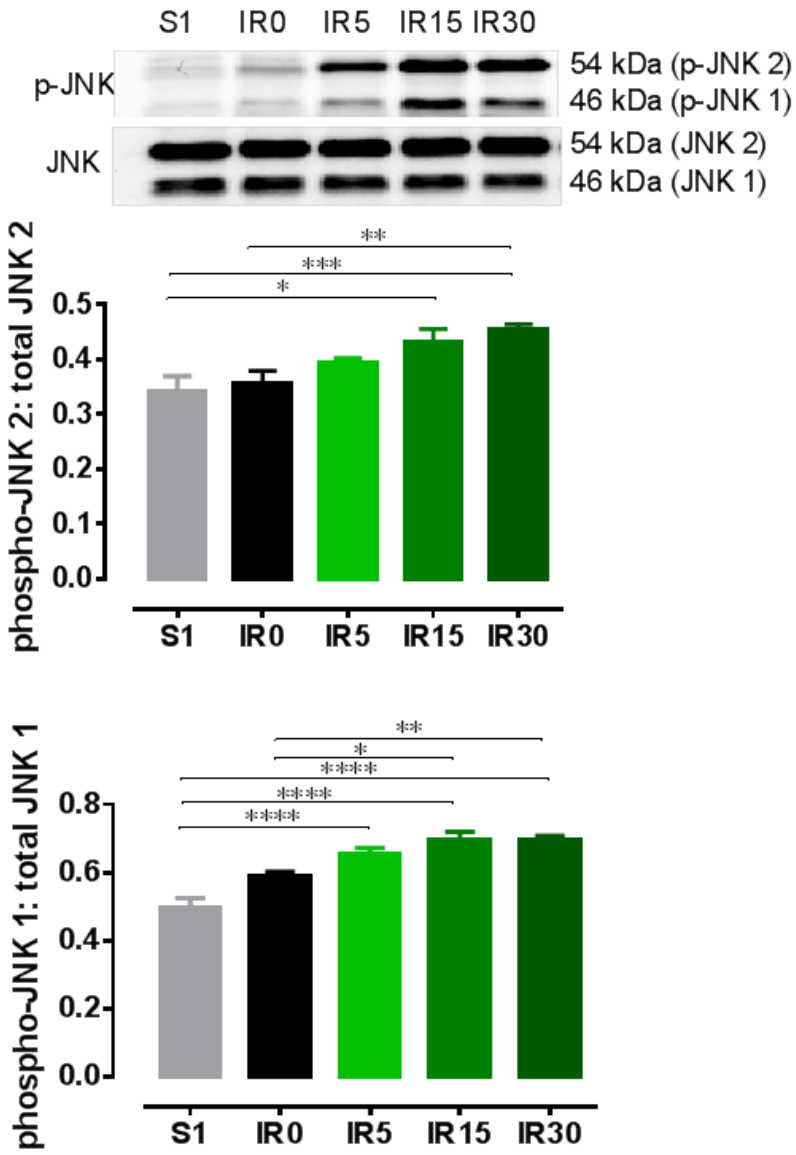

Figure 3.2: Isolated hearts were subjected to 50 min Krebs' buffer perfusion (S1) or subjected to 20 min global ischaemia followed by 0 (IR0), 5 (IR5), 15 (IR15) or 30 min (IR30) reperfusion in the presence of 0.5% DMSO (n= 5-8 per group). The phosphorylation of JNK 1/2 at various reperfusion time points was assessed using Western blot. The phosphorylation of these proteins was normalised against total protein. *p<0.05, **p<0.01, ***p<0.001, ****p<0.0001 vs corresponding time point, 1-way ANOVA with Tukey's multiple comparisons test. Data are expressed as mean ± SEM.

3.3.2 Temporal change in in the expression of multi-functional enzyme CaMKII and its downstream target PLN during myocardial I/R

The multi-functional enzyme CaMKII was phosphorylated during ischaemia; however its phosphorylation from 5 to 30 min reperfusion was not different to sham (Figure 3.3A). The level of total CaMKII tended to increase during ischaemia compared to sham and during reperfusion (Figure 3.3B). The phosphorylation of the downstream target of CaMKII, PLN was greatest at 5 min of reperfusion and reduced to basal level by 15 min after reperfusion (Figure 3.4).

(A)

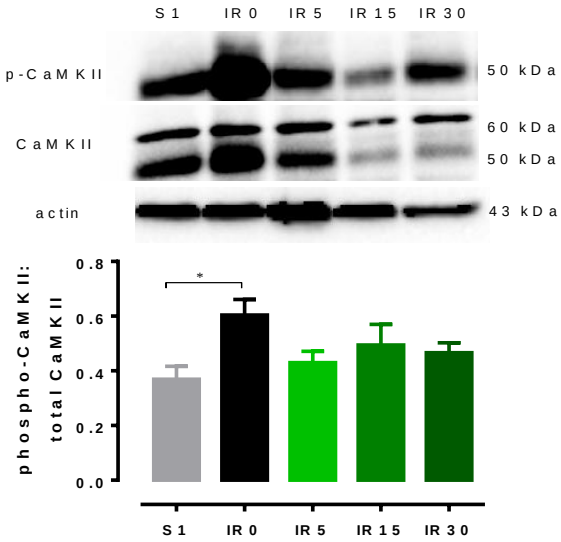

(B)

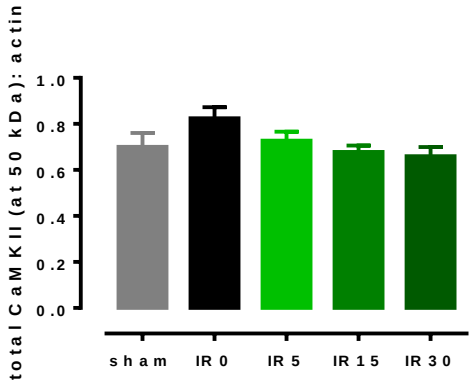

Figure 3.3: Isolated hearts were subjected to 50 min Krebs' buffer perfusion (S1) or subjected to 20 min global ischaemia followed by 0 (IR0), 5 (IR5), 15 (IR15) or 30 min (IR30) reperfusion in the presence of 0.5% DMSO (n= 5-8 per group). The phosphorylation of CaMKII at various reperfusion time points was assessed using Western blot. (A) The phosphorylation of these proteins was normalised against total protein while (B) the level of total protein was normalised against the loading control actin. *$p<0.05$ vs corresponding time point, 1-way ANOVA with Tukey's multiple comparisons test. Data are expressed as mean ± SEM.

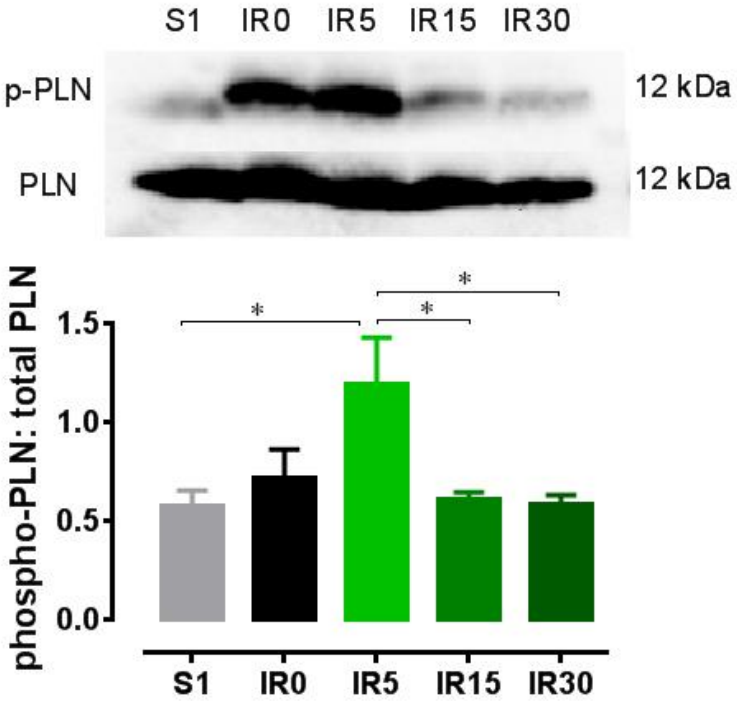

Figure 3.4: Isolated hearts were subjected to 50 min Krebs' buffer perfusion (S1) or subjected to 20 min global ischaemia followed by 0 (IR0), 5 (IR5), 15 (IR15) or 30 min (IR30) reperfusion in the presence of 0.5% DMSO (n= 5-8 per group). The phosphorylation of PLN at various reperfusion time points was assessed using Western blot. The phosphorylation of these proteins was normalised against total protein. *$p<0.05$vs corresponding time point, 1-way ANOVA with Tukey's multiple comparisons test. Data are expressed as mean ± SEM.

3.3.3 Temporal change in the expression protective kinases during myocardial I/R

Protective kinases Akt and Erk 1/2 in the RISK pathway were not phosphorylated during ischaemia, but their phosphorylation increased progressively during reperfusion. The phosphorylation of Akt and Erk 1/2 was highest at 30 min of reperfusion (Figures 3.5 and 3.6).

Similarly, the protective kinase STAT3 in the SAFE pathway was not phosphorylated during ischaemia, but did show a significant increase in phosphorylation during reperfusion. The phosphorylation of STAT3 was also highest at 30 min of reperfusion (Figure 3.7A). Figure 3.7B showed that the level of total STAT3 was not significantly different across different treatment groups.

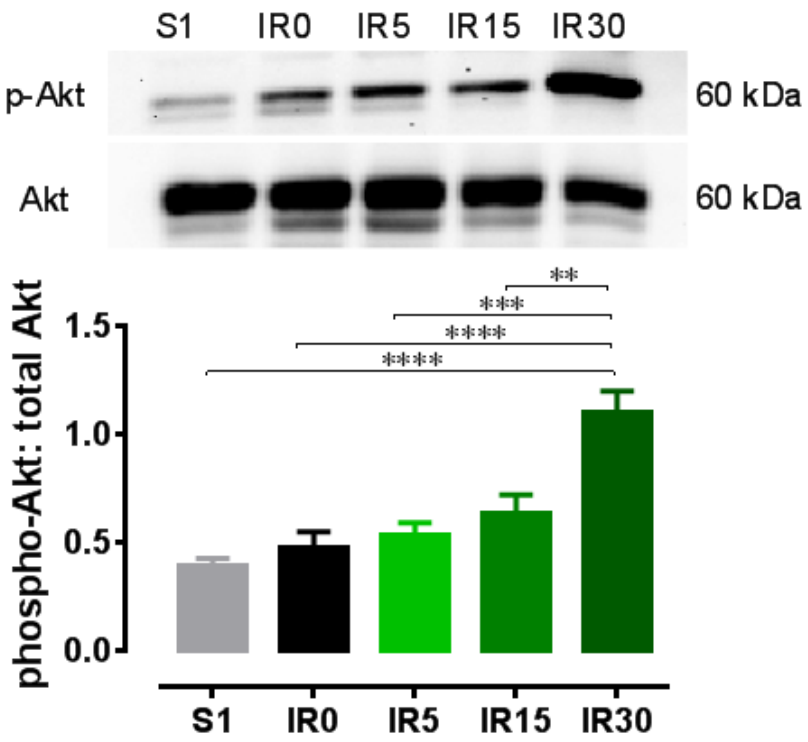

Figure 3.5: Isolated hearts were subjected to 50 min Krebs' buffer perfusion (S1) or subjected to 20 min global ischaemia followed by 0 (IR0), 5 (IR5), 15 (IR15) or 30 min (IR30) reperfusion in the presence of 0.5% DMSO (n= 5-8 per group). The phosphorylation of Akt in the RISK pathway at various reperfusion time points was assessed using Western blot. The phosphorylation of these proteins was normalised against total protein. **p<0.01, ***p<0.001, ****p<0.0001 vs corresponding time point, 1-way ANOVA with Tukey's multiple comparisons test. Data are expressed as mean ± SEM.

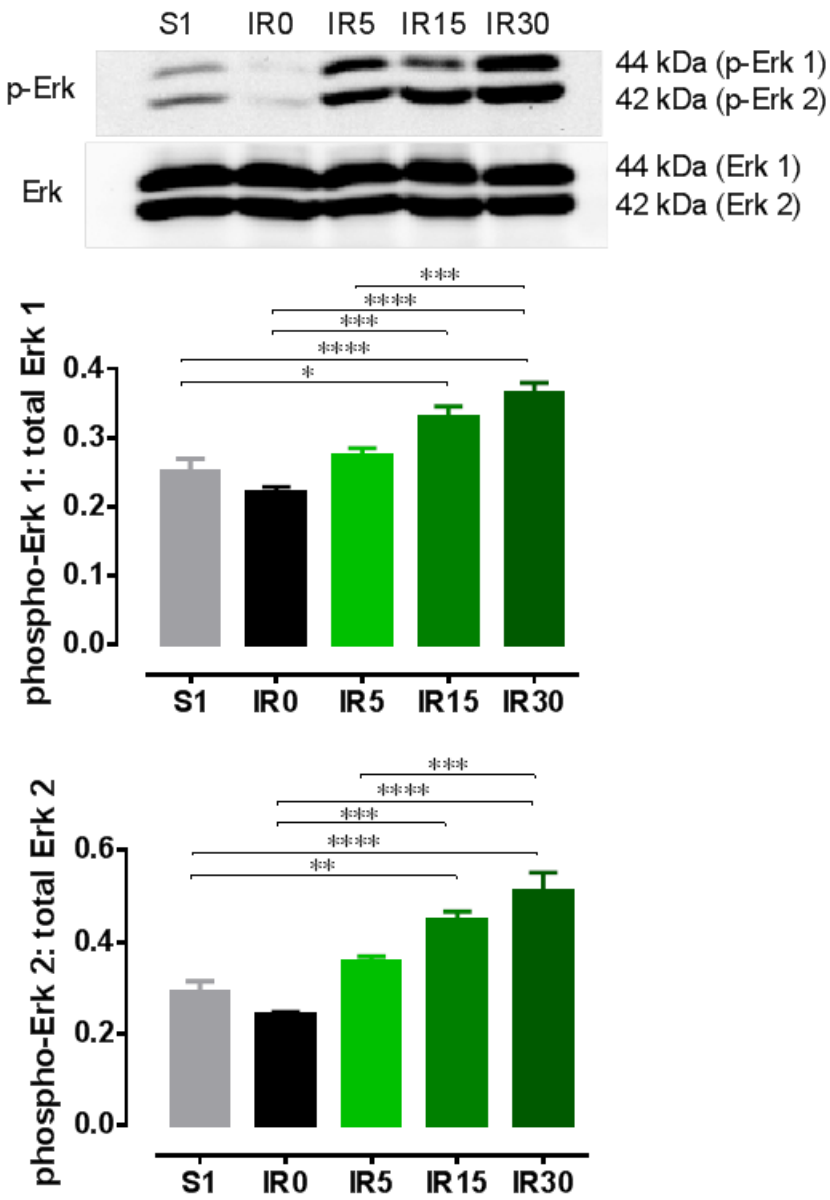

Figure 3.6: Isolated hearts were subjected to 50 min Krebs' buffer perfusion (S1) or subjected to 20 min global ischaemia followed by 0 (IR0), 5 (IR5), 15 (IR15) or 30 min (IR30) reperfusion in the presence of 0.5% DMSO (n= 5-8 per group). The phosphorylation of Erk 1/2 in the RISK pathway at various reperfusion time points was assessed using Western blot. The phosphorylation of these proteins was normalised against total protein. *p<0.05, **p<0.01, ***p<0.001, ****p<0.0001 vs corresponding time point, 1-way ANOVA with Tukey's multiple comparisons test. Data are expressed as mean ± SEM.

(A)

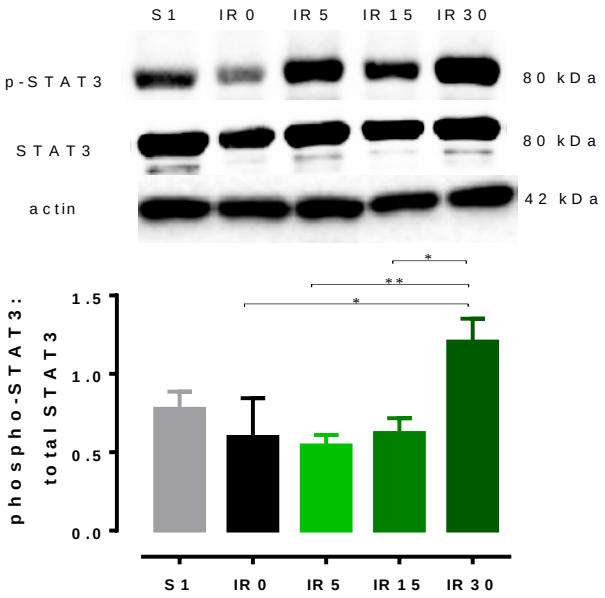

(B)

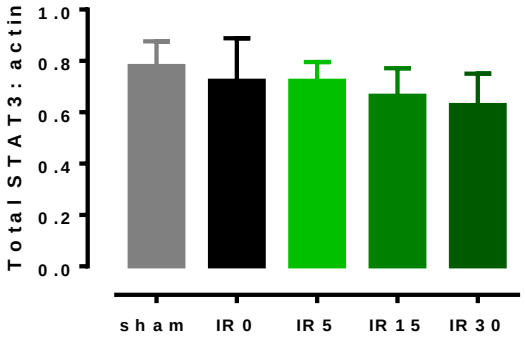

Figure 3.7: Isolated hearts were subjected to 50 min Krebs' buffer perfusion (S1) or subjected to 20 min global ischaemia followed by 0 (IR0), 5 (IR5), 15 (IR15) or 30 min (IR30) reperfusion in the presence of 0.5% DMSO (n= 5-8 per group). The phosphorylation of STAT3 in the SAFE pathway at various reperfusion time points was assessed using Western blot. (A) The phosphorylation of these proteins was normalised against total protein, while (B) the level of total protein was normalised against the loading control actin. *$p<0.05$, **$p<0.01$ vs corresponding time point, 1-way ANOVA with Tukey's multiple comparisons test. Data are expressed as mean ± SEM.

3.4 Discussion

This study demonstrated that pro-injurious kinases JNK 1/2 were activated during reperfusion but not ischaemia, and the activation of JNK 1 and 2 was highest at 15 and 30 min after reperfusion respectively. By contrast, p38 MAPK and CaMKII were activated during ischaemia. The activation of p38 MAPK, but not CaMKII remained elevated throughout reperfusion. The activation of the downstream target of CaMKII, PLN was greatest at 5 min reperfusion. The activation of protective kinases Akt, Erk 1/2 and STAT3 was highest 30 min after reperfusion.

In response to ischaemia and reperfusion, cardiomyocytes in the ischaemic region may die, however the surviving cardiomyocytes may undergo hypertrophy to compensate for the lost contractile capacity. It is suggested that the activation of kinases in this salvageable surviving cardiomyocyte is the major determinant of the final myocardial injury after I/R (Toledo-Pereyra *et al.*, 2008). Therefore, a better understanding of the activation of kinases implicated during I/R may provide further insights into the molecular mechanism that causes cell survival or death following I/R.

A previous study has demonstrated that the translocation of JNK 1 from the cytosol to nucleus occurred during ischaemia while JNK 1 activation occurred during reperfusion (Mizukami *et al.*, 1997). This finding was supported by the observation that an increased phosphorylation of its downstream transcription factor *c-jun* occurred during reperfusion in the nucleus (Mizukami *et al.*, 1997). Other reports also showed that no activation of JNK 1 or JNK 2 isoforms occurred during ischaemia but a progressive increase in the activation of JNK 1/2 during reperfusion was observed (Bogoyevitch *et al.*, 1996; Yin *et al.*, 1997; Tao *et al.*, 2011; Lim *et al.*, 2013). These findings on the temporal change in the activation of JNK during myocardial I/R are similar to our observation in this study. Consistent with these studies (Bogoyevitch *et al.*, 1996; Seko *et al.*, 1997; Ma *et al.*, 1999b), we have also shown

that p38 MAPK was activated during ischaemia. The activation of p38 MAPK was maintained during the ensuing reperfusion period for at least 20 min (Bogoyevitch *et al.*, 1996).

In previous studies, increased CaMKII phosphorylation and activity was observed at 1 min and 3 min of reperfusion respectively (Said *et al.*, 2011; Ling *et al.*, 2013). It has been reported that the activation of CaMKII occurred during ischaemia and a greater increase in CaMKII activation in the first few minutes of reperfusion contributes to reperfusion arrhythmias (Bell *et al.*, 2014). In this study, we demonstrated that CaMKII was activated during ischaemia, however its activation tended to decrease 5 min after reperfusion. The level of total CaMKII also tended to decrease with increased reperfusion time. Previous studies have reported that CaMKII was found abundantly in intracellular compartments such as mitochondria and nucleus to induce mitochondrial fission leading to apotosis and excitation-transcription coupling, respectively (Mattiazzi *et al.*, 2015, Ong and Hausenloy *et al*., 2010). In this study, translocation of CaMKII into mitochondria to trigger apoptosis at a later time point of reperfusion could have taken place. As mentioned earlier, the phosphorylation of CaMKII could activate its downstream substrate PLN. Reports have demonstrated that the phosphorylation of PLN at Thr 17 peaked at 3 min of reperfusion and dephosphorylated with longer reperfusion time (Vila-Petroff *et al.*, 2007; Di Carlo *et al.*, 2014). In this study, we demonstrated the activation of PLN was highest at 5 min of reperfusion and had returned to basal levels by 15 min.

Consistent with other reports, the activation of the protective kinase Akt in the RISK pathway occurred during reperfusion but not during ischaemia (Means *et al.*, 2007; Lim *et al.*, 2013). There was a progressive increase in the phosphorylation of Akt during reperfusion and its activation was highest at 15 to 30 min after reperfusion (Means *et al.*, 2007; Lim *et al.*, 2013). One hour after reperfusion, the phosphorylation of Akt has trended towards basal

levels (Means *et al.*, 2007; Lim *et al.*, 2013). It has been reported that the upstream substrate of Erk 1/2 (another protective kinase in the RISK pathway), Raf-1 was activated 5 min after hypoxia in isolated crdiomyocytes and decreased to basal levels by 30 min (Seko *et al.*, 1996). Raf-1 was again activated 5 min after reperfusion (Seko *et al.*, 1996). The activation of Erk 1/2 occurred during reperfusion but not ischaemia (Takeishi *et al.*, 1999; Means *et al.*, 2007; Lim *et al.*, 2013), a finding similar to our observation in this study. The phosphorylation of Erk 1/2 was highest at 15 to 30 min reperfusion and decreased to basal levels by 1 h (Means *et al.*, 2007; Lim *et al.*, 2013).

It has been reported that the phosphorylation of STAT3, the protective kinase in the SAFE pathway, from 2.5 to 30 min reperfusion in rat isolated heart after 35 min regional ischaemia was not different from sham (Smith *et al.*, 2010). In this study, we have shown that the activation of STAT3 during 0 to 15 min reperfusion was not different to sham, however at 30 min reperfusion, its activation was significantly increased compared to ischaemia alone and 5 and 15 min after reperfusion.

In conclusion, the activation of most kinases investigated in this study including Akt, Erk 1/2, STAT3 and JNK 2 was highest 30 min after reperfusion. JNK 1 activation was highest 15 min after reperfusion. p38 MAPK and CaMKII were activated during ischaemia while the phosphorylation of PLN was greatest at 5 min of reperfusion.

Limitation of the study:

In this study, the whole ventricle homogenate was used to measure the expression of proteins and the expression of proteins in subcellular fractions including nucleus, mitochondria and sarcoplasmic reticulum was not measured. Translocation of proteins within subcellular fractions with activation or inactivation during I/R could have occurred.

Chapter 4

4. The mechanism(s) of flavonol-induced cardioprotection

4.1 Introduction

Flavonoids are a group of plant-derived polyphenols that are known to exhibit biological effects including causing vasodilatation, scavenging free radicals, lowering plasma levels of low-density lipoproteins as well as inhibiting platelet aggregation (Gerritsen *et al.*, 1995; Chan *et al.*, 2000; Woodman *et al.*, 2005; Harris *et al.*, 2006). Epidemiological studies have reported that there was an inverse correlation between the intake of dietary flavonoids and the mortality from coronary heart disease during a 5-year follow-up (Hertog *et al.*, 1993) or the incidence of myocardial infarction (Geleijnse *et al.*, 2002). In addition, experimental data also showed that flavonoid inhibited atherosclerotic plaque development in apolipoprotein E–deficient ($ApoE^{-/-}$) mice fed a high-fat diet for 8 weeks, compared to its vehicle control (Luo *et al.*, 2015). Daily consumption of the flavonol quercetin for 7 days also reduced blood pressure in hypertensive rats (Jalili *et al.*, 2006). This suggests that flavonoids may exert beneficial effects in cardiovascular diseases.

Previous studies from our laboratory have examined the actions of 3',4'-dihydroxyflavonol (DiOHF), a synthetic flavonol with more potent antioxidant and vasodilator than a number of naturally occurring flavones and flavonols (Chan *et al.*, 2000; Woodman & Chan, 2004). The beneficial effect of DiOHF on cardiovascular diseases has also been demonstrated in experimental models. DiOHF prevented diabetes-induced endothelial dysfunction in large conduit and resistance arteries (Woodman & Malakul, 2009; Leo *et al.*,

2011). It also prevented diastolic dysfunction and cardiac remodelling in type 1 diabetic rats (Khong *et al.*, 2011). In addition, DiOHF delayed thrombus formation in type 1 diabetic mice (Mosawy *et al.*, 2013).

There is growing evidence that DiOHF is cardioprotective against myocardial I/R injury, a phenomenon where myocardial reperfusion after a prolonged period of ischaemia causes additional myocardial injury beyond that generated by ischaemia alone (Wang *et al.*, 2004; Wang *et al.*, 2009; Qin *et al.*, 2011; Williams *et al.*, 2011). In anaesthetised sheep subjected to myocardial I/R, the administration of intravenous DiOHF improved post-ischaemic cardiac contractile function and reduced myocardial infarct size with the level of protection being similar to that of ischaemic preconditioning, which is regarded as the most effective protection against reperfusion injury to date (Wang *et al.*, 2004). Daily treatment of goats with DiOHF over 4 weeks reperfusion after ischaemia also significantly reduced infarct size, prevented post-myocardial infarction left ventricular remodelling and reduced apoptosis in the non-infarcted area (Wang *et al.*, 2009). The expression of apoptosis-related proteins, including caspase-3, cytochrome C and Bax, was reduced with DiOHF after 4 weeks of reperfusion (Wang *et al.*, 2009). Recently, studies also showed that the administration of NP202, a pro-drug converted to DiOHF, reduced infarct size in anesthetized sheep after I/R (Thomas *et al.*, 2011; Lim *et al.*, 2013). This protective effect was accompanied by inhibition of polymorphonuclear leucocyte accumulation and myocyte apoptosis identified using TUNEL assay. Importantly, the protective action of NP202 was maintained in sheep even after a longer period of ischaemia of 3 h (which mimics the clinical situation of ischaemic periods of 3-5 h) before the restoration of coronary perfusion (Thomas *et al.*, 2011).

Although the protective action of DiOHF has been known for almost a decade, the precise mechanism of its cardioprotective action remains elusive. An earlier report has suggested that DiOHF may improve post-ischaemic myocardial function in sheep *in vivo* via

its free-radical scavenging ability which may increase the nitric oxide bioavailability causing subsequent improvement in blood flow during reperfusion (Wang *et al.*, 2004). Emerging evidence has shown that DiOHF may protect the heart against I/R injury independent of its antioxidant property. DiOHF may modulate cellular signalling pathways that are crucial in mediating cell death or survival in various diseases (Mansuri *et al.*, 2014). Indeed, in anesthetized sheep, Lim and colleagues demonstrated that NP202, the pro-drug of DiOHF inhibited the activation of pro-injurious kinases, p38 MAPK and JNK at 30 min reperfusion after 1 h ischaemia and this inhibitory action contributed to the protective action of NP202 against I/R injury *in vivo* (Lim *et al.*, 2013). DiOHF may also inhibit the activation of CaMKII and result in the subsequent inhibition of p38 MAPK and JNK pathways (Lim *et al.*, 2013). The activation of protective kinases in the RISK pathway, Akt and Erk 1/2 at 30 min of reperfusion was however not affected with NP202 treatment (Lim *et al.*, 2013). It has been reported that a large number of cardiomyocyte death due to reperfusion injury occurs in the first minutes of reperfusion (Rodriguez-Sinovas *et al.*, 2007), therefore the activation of kinases at earlier reperfusion time points e.g. 5 min of reperfusion has attracted research interest. In this study, the aim was to investigate the effect of DiOHF on kinase activation including protective kinases, Akt, Erk 1/2 and the pro-survival kinase in the SAFE pathway STAT3, pro-injurious kinases p38 MAPK and JNKs as well as CaMKII and its downstream target PLN at 5 and 30 min reperfusion.

4.2 Methods

This investigation conforms with the National Health and Medical Research Council of Australia code of practice for the care and use of animals for scientific purposes. All the procedures involved in this project were approved by the RMIT University Animal Ethics Committee.

4.2.1 Langendorff heart preparation

Hearts isolated from adult male Sprague-Dawley rats (250-300g) anaesthetized with 325 mg/kg sodium pentobarbitone were Langendorff-perfused as described in Chapter 2.3. Rat isolated hearts were perfused at a constant flow of ~12 ml/min to generate a perfusion pressure of 62 ± 5 mmHg.

4.2.2 DiOHF treatment protocol

Rat isolated hearts were randomly assigned to one of the following three groups. The first group was (i) sham (S2) where hearts were perfused with Krebs' buffer for 80 min without any further intervention. The following two groups were subjected to I/R treatment. In I/R-treated groups, hearts were equilibrated for 30 min followed by 20 min global ischaemia. Ischaemia was carried out as described in Chapter 2.4. Hearts were then reperfused for either (ii) 5 or (iii) 30 min with Krebs' buffer in the presence of 10 μM DiOHF. This concentration of DiOHF was chosen as previous study from our laboratory has shown that it is effective in ameliorating I/R injury in rat isolated hearts (Qin *et al*, 2011). Time control for 5 min reperfusion (S1) and vehicle control for DiOHF at 5 min and 30 min reperfusion using 0.5% DMSO experiments had been carried out in Chapter 3. At the end of the experiment, left ventricular tissues were dissected into four pieces where two pieces were snap frozen in liquid nitrogen and stored at -80°C until use while the other two pieces of left ventricular tissue were fixed in 4% PFA for TUNEL assay.

4.2.3 Lactate dehydrogenase (LDH) assay

LDH assay was carried out as described in Chapter 2.5. Coronary effluent from sham hearts (S2) and hearts reperfused for 30 min in the presence of 0.5% DMSO (Chapter 3) or 10 μM DiOHF was collected at 9 time points (i.e. 29th, 50th, 51st, 52nd, 55th, 60th, 75th, 80th and

90th min perfusion in S2 hearts and 29th min during equilibration, 10s, 1, 2, 5, 10, 15, 20 and 30 min after reperfusion in I/R-treated hearts). The concentration of LDH in the effluent sample was calculated using the LDH standard curve (0.01-1 U/ml) constructed using L-LDH extracted from the hog muscle.

4.2.4 Assessment of reperfusion-induced arrhythmias

Assessment of reperfusion-induced arrhythmias was performed as described in Chapter 2.8. Experimental records from left ventricular pressure (LVP) were used to analyse the incidence of arrhythmias. The total duration (in sec) of LVP showing a LVDP <5 mmHg (indicative of ventricular fibrillation) in the first 10 min of reperfusion was measured.

4.2.5 Western blot

Western blots were performed as described in Chapter 2.7. Analysis of protein expression using antibodies including phospho^{Ser473}-Akt, Akt, phospho$^{Thr202/Tyr204}$-Erk 1/2, Erk 1/2, phospho^{Tyr705}-STAT3, STAT3, phospho$^{Thr183/Tyr185}$-JNK, JNK, phospho$^{Thr180/Tyr182}$-p38 MAPK, p38 MAPK, phospho$^{Thr286/287}$-CaMKII, CaMKII phospho$^{Ser16/Thr17}$-PLN, PLN and actin were performed. The increase or decrease in the activity of a protein was measured by normalising the degree of phosphorylation of the protein to its total protein. Actin which is the loading control is used to normalise the level of total protein.

4.2.6 TUNEL assay

The detection of apoptosis in left ventricular tissues from sham hearts (S2) and hearts treated with 0.5% DMSO (Chapter 3) and 10 µM DiOHF for 30 min during reperfusion was performed using the CardioTACS^{TM} *in situ* apoptosis detection kit as described in Chapter 2.6.

4.2.7 Statistical analysis

Myocardial function was expressed as the percentage change from the pre-ischaemic value. Rate-pressure product (RPP) was calculated as the product of heart rate and LVDP. All results were expressed as group mean ± SEM, with the number of independent experiments denoted as 'n'. Data analysis was performed using Graphpad Prism® (version 6.0, La Jolla, CA, USA). Myocardial function and time point LDH data were analysed using 2-way ANOVA with Sidak's multiple comparison test. Area-under-the-curve (AUC) and reperfusion arrhythmias data were analysed using Student's unpaired *t*-test. All Western blot data, total LDH assay and quantitative data for CardioTACS™ assay were analysed using 1-way ANOVA with Tukey'smultiple comparison test. In all cases, $p<0.05$ was considered statistically significant.

4.2.8 Drugs and reagents

All chemical reagents were purchased from Sigma-Aldrich (St. Louis, MO, USA) and dissolved in distilled water unless otherwise stated. DiOHF was from Indofine Chemicals Co. (Hillsborough, NJ, USA) and was dissolved in equal amounts of 100% DMSO and Krebs' buffer to give a final concentration of 0.5% DMSO. L-LDH from hog muscle was from Boehringer Ingelheim (North Ryde, NSW, Australia) and CardioTACS™ was purchased from Trevigen (Gaithersburg, MD, USA).

4.3 Results

4.3.1 Effect of DiOHF during reperfusion on post-ischaemic myocardial function

DiOHF treatment during reperfusion significantly improved myocardial function in rat isolated hearts subjected to global ischaemia and reperfusion. During ischaemia, there was a

100% decrease in LV+dP/dt, LV-dP/dt, RPP and perfusion pressure in both vehicle-and DiOHF-treated hearts compared to their pre-ischaemic values. The recovery (15 min after reperfusion) for LV+dP/dt tended to increase in DiOHF-treated hearts (although not significant) compared to its vehicle control (Figure 4.1A). The recovery for LV-dP/dt was significantly improved in DiOHF-treated hearts compared to its vehicle control ($p<0.05$, Figure 4.1B). The recovery of RPP was comparable in both treatment groups (Figure 4.1C). Perfusion pressure was elevated during reperfusion in vehicle-treated hearts and DiOHF treatment significantly reduced the I/R-induced increase in perfusion pressure by ~25% during early reperfusion ($p<0.05$, Figure 4.1D). Thirty min after reperfusion, the recovery in LV+dP/dt and LV-dP/dt in vehicle- and DiOHF-treated hearts was ~70% and ~82% respectively (Figures 4.1A and B). The area-under-the curve (AUC) for LV+dP/dt tended to increase in DiOHF-treated hearts compared to its vehicle control while there was a significant improvement in AUC for LV-dP/dt in DiOHF-treated hearts compared to its vehicle control ($p<0.05$, Figure 4.2).

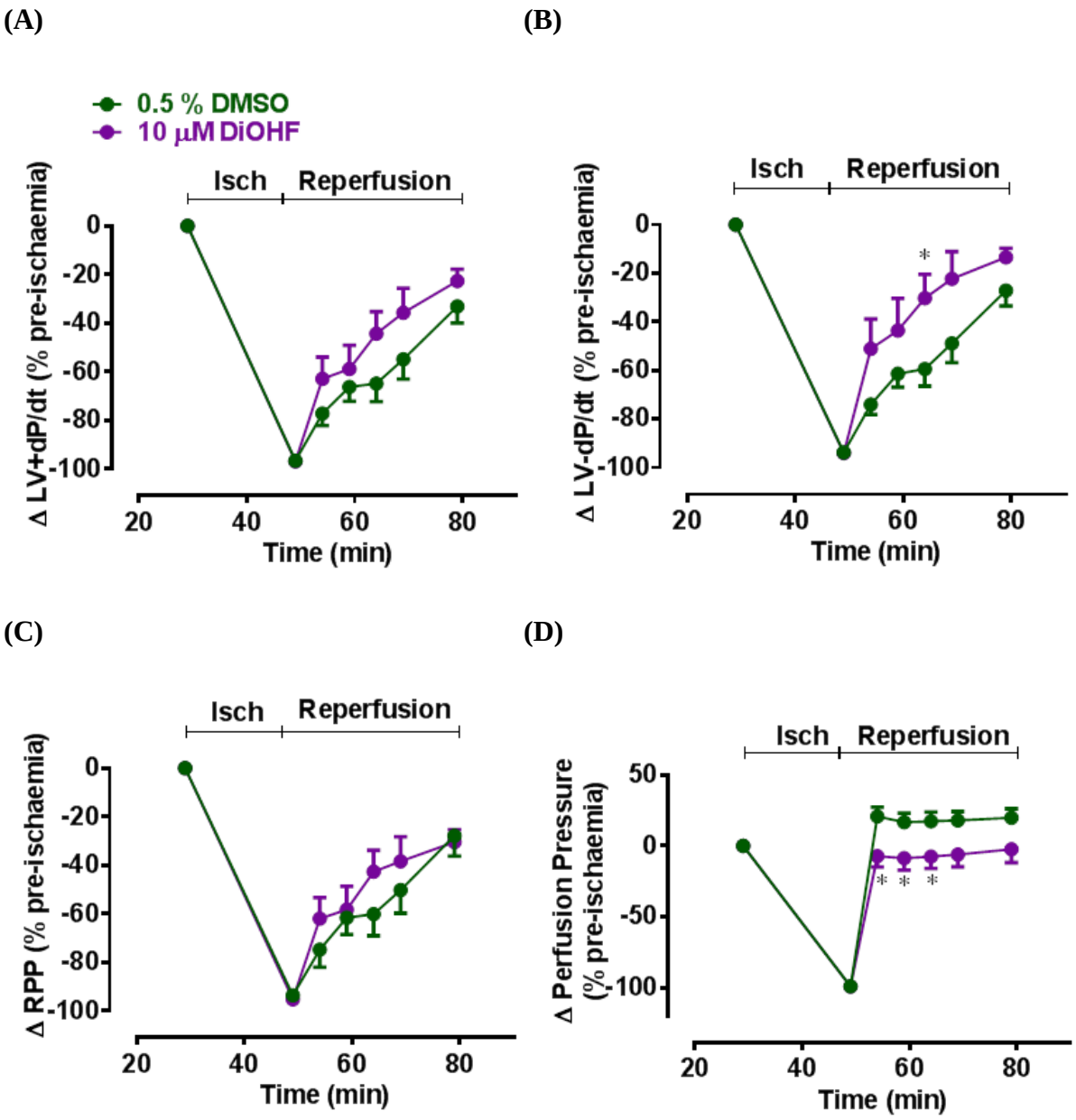

Figure 4.1: The change in the **(A)** positive rate of change in left ventricular pressure (LV+dP/dt), **(B)** negative rate of change in left ventricular pressure (LV-dP/dt), **(C)** rate-pressure product (RPP) and **(D)** perfusion pressure as a percentage of pre-ischaemic values in rat hearts subjected to 20 min ischaemia and 30 min reperfusion in the presence of 0.5% DMSO (n=8) or 10 µM DiOHF (n=7). *p<0.05 vs 0.5% DMSO, 2-way ANOVA with Sidak's multiple comparison test. Data are expressed as mean ± SEM. Isch= ischaemia

(A)

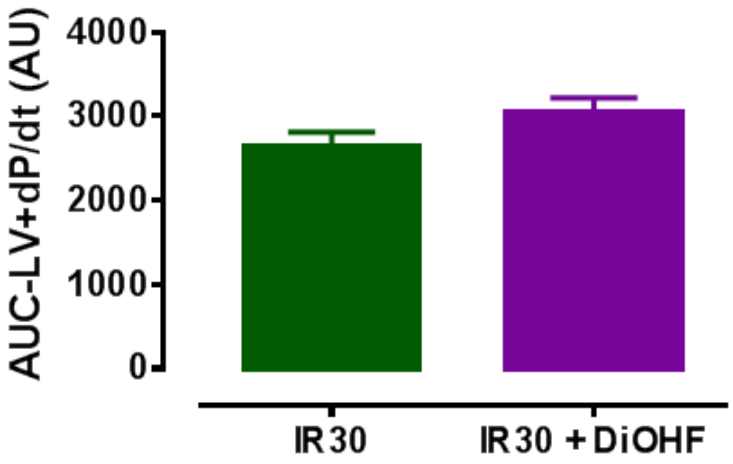

(B)

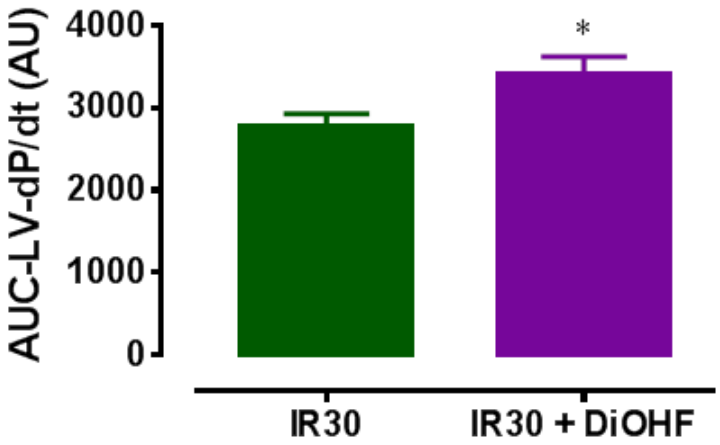

Figure 4.2: Area-under-the-curve (AUC) for **(A)** LV+dP/dt and **(B)** LV-dP/dt in rat hearts subjected to 20 min ischaemia and 30 min reperfusion in the presence of 0.5% DMSO (IR30, n=8) or 10 µM DiOHF (IR30 + DiOHF, n=7). *p<0.05 vs IR30, Student's unpaired *t*-test. Data are expressed as mean ± SEM.

4.3.2 Effect of DiOHF on cell death, apoptosis and reperfusion-induced arrhythmias after I/R

Myocardial injury was assessed by the release of LDH into the coronary effluent. DiOHF treatment during reperfusion caused a significant reduction in LDH release as early as 1 min of reperfusion compared to its vehicle control (Figure 4.3A). The total LDH release in the vehicle-treated heart over 30 min of reperfusion was significantly elevated compared to sham hearts ($p<0.001$, Figure 4.3B) and this increase in LDH release was also significantly reduced by DiOHF ($p<0.01$).

The number of apoptotic cells was also significantly elevated in vehicle-treated hearts ($p<0.001$). DiOHF treatment also significantly reduced the I/R-induced increase in the number of apoptotic cells in the rat isolated heart 30 min after reperfusion ($p<0.05$, Figure 4.4).

Reperfusion-induced arrhythmias (specifically of ventricular fibrillation) during the first 10 min of repefusion were examined. The duration of ventricular fibrillation during the first 10 min of reperfusion in vehicle-treated hearts was 156 ± 44 sec while in DiOHF-treated hearts, the duration of ventricular fibrillation during the first 10 min of reperfusion was 54 ± 34 sec (Figure 4.5). There was a reduction in the duration of reperfusion-induced ventricular fibrillation with DiOHF treatment although this was not significant.

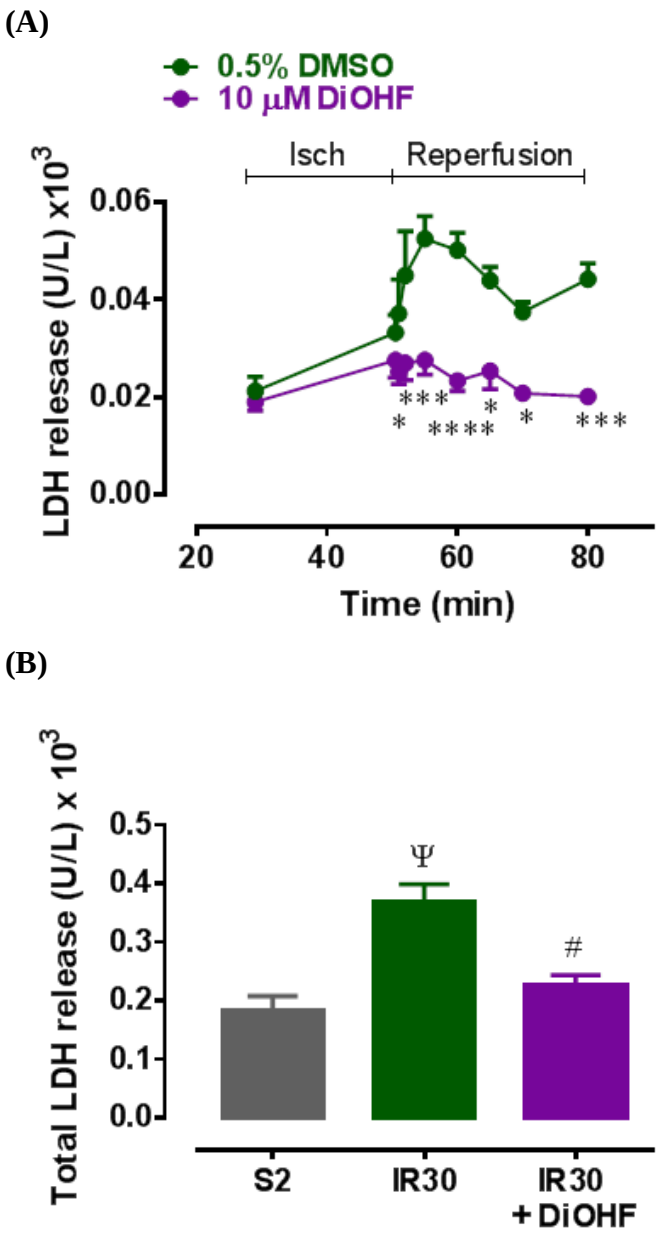

Figure 4.3: (A) Time course release of lactate dehydrogenase (LDH) in I/R-treated hearts with 0.5% DMSO (n=8) or 10 µM DiOHF (n=7) during reperfusion. **(B)** Total LDH release after 80 min perfusion in sham hearts (S2, n=7) and hearts subjected to 20 min ischaemia and 30 min reperfusion in the presence of 0.5% DMSO (IR30) or 10 µM DiOHF (IR30 + DiOHF). *p<0.05, ***p<0.001, ****p<0.0001 vs 0.5% DMSO, 2-way ANOVA with Sidak's multiple comparisons test. Ψp<0.001 vs S2, #p<0.01 vs IR30, 1-way ANOVA with Tukey's multiple comparisons test. Data are expressed as mean ± SEM. Isch= ischaemia

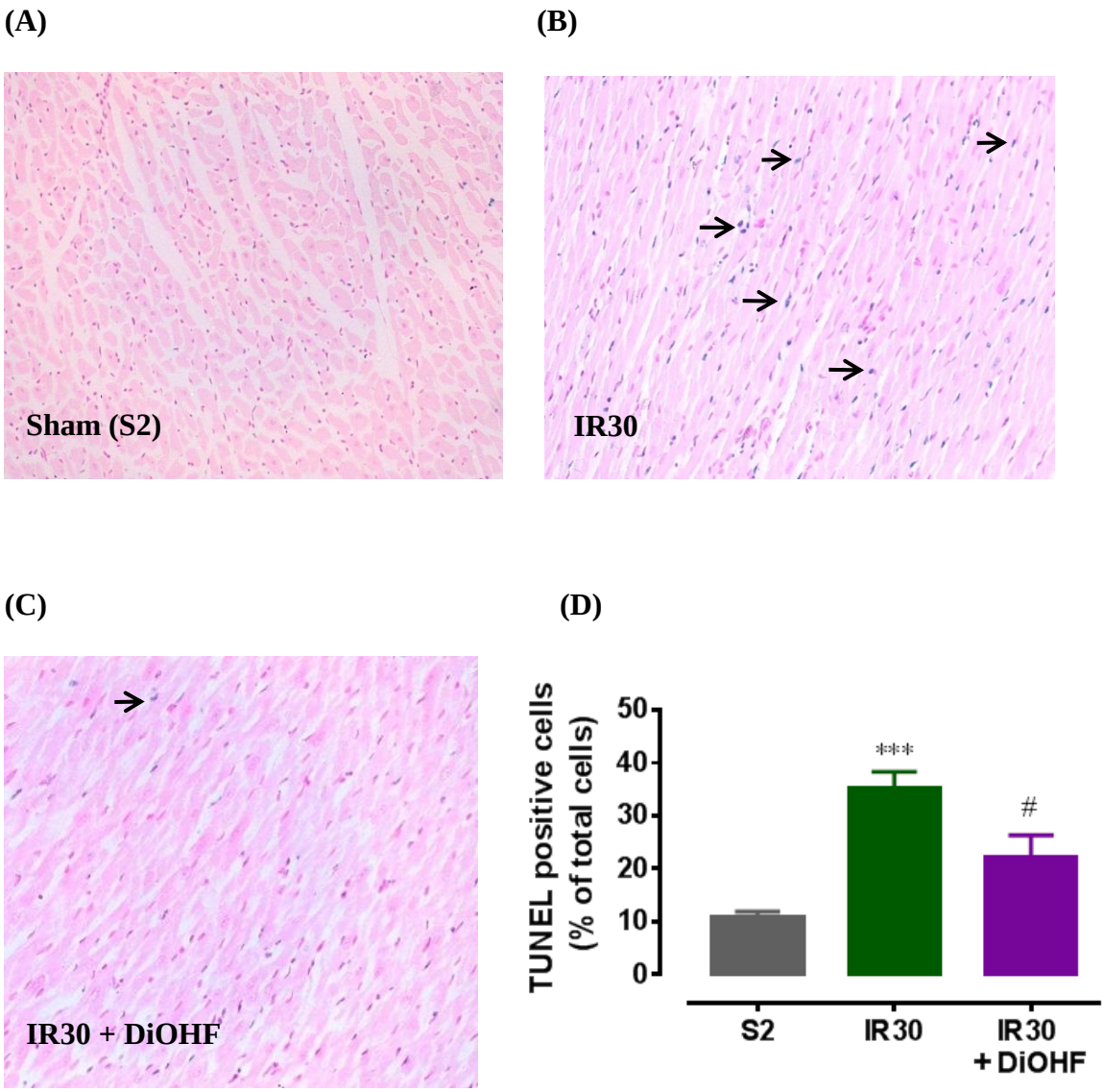

Figure 4.4: Representative images of TUNEL labelling of sections from **(A)** sham hearts (S2), hearts subjected to 20 min ischaemia followed by 30 min reperfusion in the presence of **(B)** 0.5% DMSO (IR30) or **(C)** 10 µM DiOHF (IR30 + DiOHF). Positive apoptotic nuclei were stained blue (indicated with arrows). **(D)** Quantitative data for TUNEL positive cells in sections from sham (S2), vehicle-treated and DiOHF-treated hearts (n= 4-5 per group). TUNEL positive cells were expressed as a percentage of total cells in the section. ***$p<0.001$ vs S2, #$p<0.05$ vs IR30, 1-way ANOVA with Tukey's multiple comparisons test. Data are expressed as mean ± SEM. Original magnification x200.

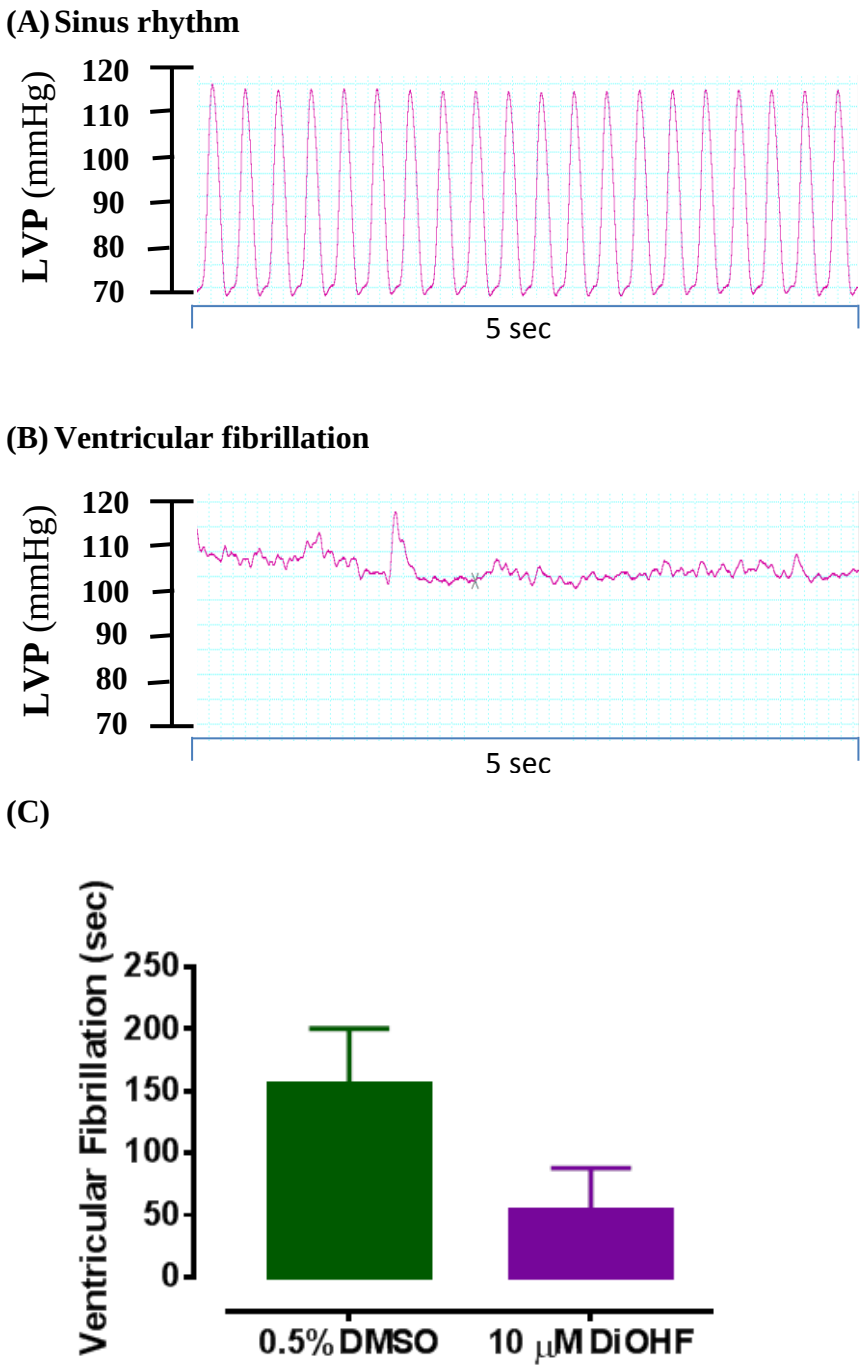

Figure 4.5: Duration of ventricular fibrillation during the first 10 min of reperfusion in hearts subjected to 20 min ischaemia followed by 30 min reperfusion in the presence of 0.5% DMSO or 10 μM DiOHF. Representative traces from the left ventricular pressure (LVP) showing **(A)** sinus rhythm and **(B)** ventricular fibrillation in reperfused hearts. **(C)** Panel C data are mean ± SEM (n= 7-8 per group), analysed by Student's *t*-test, p=ns.

4.3.3 Effects of DiOHF on the expression of pro-injurious kinases during myocardial I/R

The phosphorylation of the pro-injurious kinase p38 MAPK at 5 and 30 min of reperfusion in vehicle-treated hearts was significantly increased compared to sham, S1 and S2 respectievly, while DiOHF treatment had no effect on the I/R-induced increase in phosphorylation of p38 MAPK at both time points (Figure 4.6).

The phosphorylation of injurious kinases JNK 1/2 at 5 min of reperfusion in vehicle-treated hearts was also significantly increased compared to sham (S1) and similarly, DiOHF treatment had no effect on the I/R-induced increased phosphorylation of JNK 1/2 at 5 min reperfusion (Figure 4.7A). At 30 min of reperfusion, DiOHF treatment significantly reduced the I/R-induced increased phosphorylation of JNK 2 ($p<0.05$), while the phosphorylation of JNK 1 was comparable in all groups at 30 min reperfusion (Figure 4.7B).

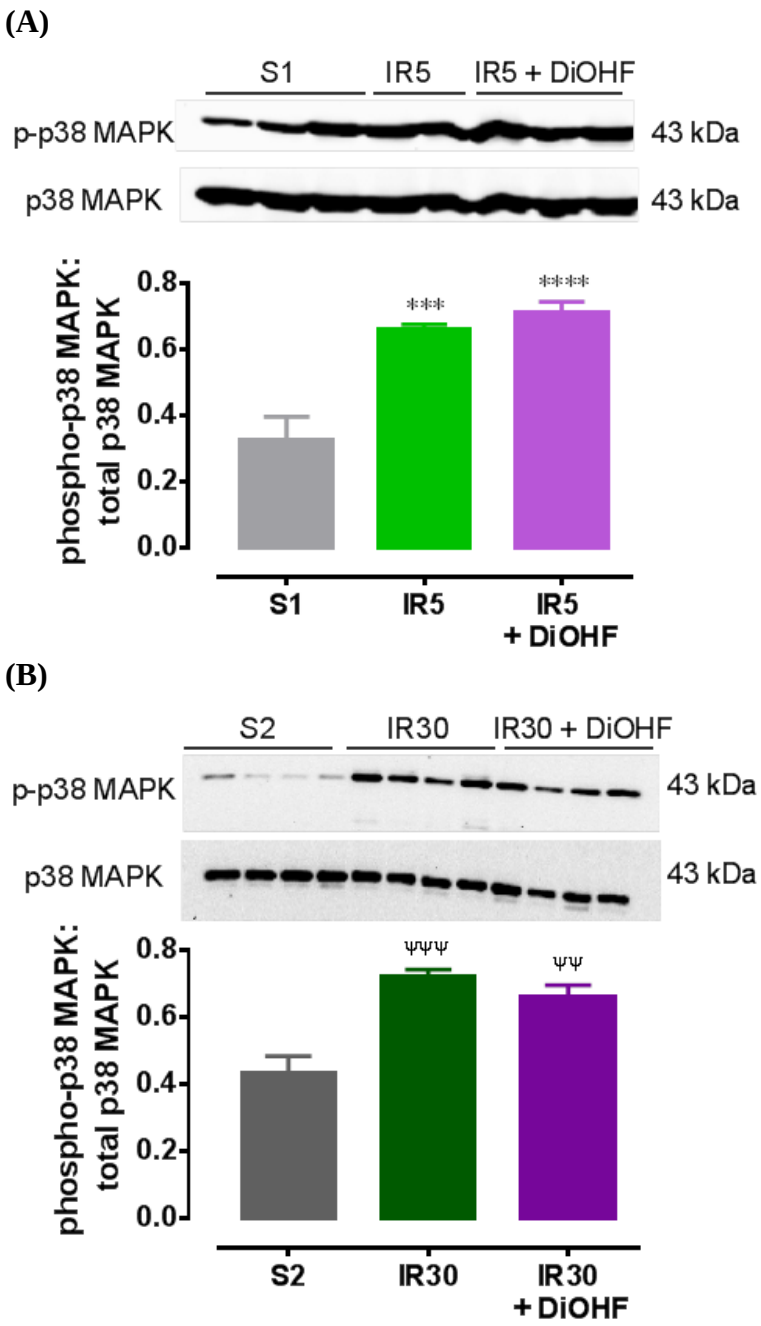

Figure 4.6: Expressions of pro-injurious kinase p38 MAPK in sham hearts, S1 or S2 and hearts subjected to 20 min ischaemia followed by **(A)** 5 min or **(B)** 30 min reperfusion in the presence of 0.5% DMSO (IR5 or IR30) or 10 µM DiOHF (IR5 + DiOHF or IR30 + DiOHF), n= 6-8 per group. Representative immunoblots and densitometric analysis are shown. The phosphorylation of the protein was normalised against total protein. ***p<0.001, ****p<0.0001 vs S1, ΨΨp<0.01, ΨΨΨp<0.001 vs S2, 1-way ANOVA with Tukey's multiple comparisons test. Data are expressed as mean ± SEM.

(A)

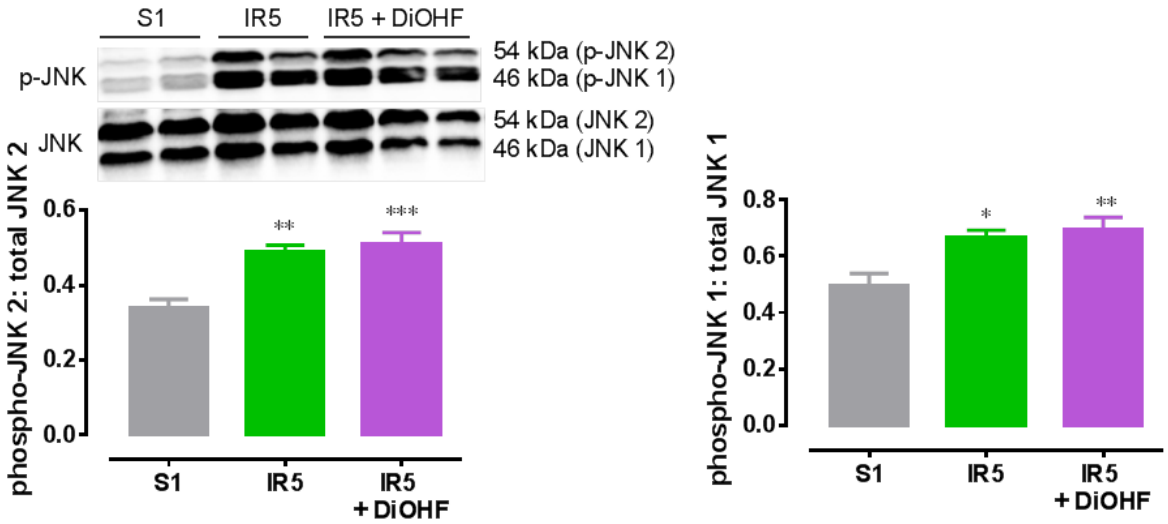

(B)

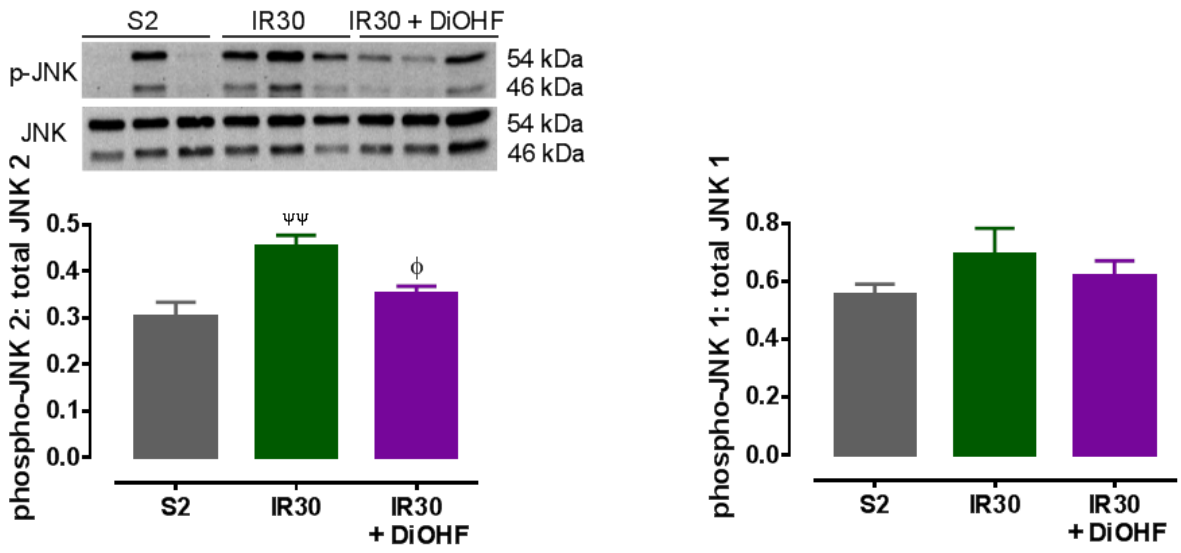

Figure 4.7: Expressions of pro-injurious kinases JNK 1/2, in sham hearts, S1 or S2 and hearts subjected to 20 min ischaemia followed by **(A)** 5 min or **(B)** 30 min reperfusion in the presence of 0.5% DMSO (IR5 or IR30) or 10 µM DiOHF (IR5 + DiOHF or IR30 + DiOHF), n= 6-8 per group. Representative immunoblots and densitometric analysis are shown. The phosphorylation of the protein was normalised against total protein. *p<0.05, **p<0.01, ***p<0.001vs S1, ΨΨp<0.01 vs S2, ϕp<0.05 vs IR30, 1-way ANOVA with Tukey's multiple comparisons test. Data are expressed as mean ± SEM.

4.3.4 Effects of DiOHF on the expression of CaMKII and its downstream target PLN during myocardial I/R

At 5 min of reperfusion, the phosphorylation of the multi-functional enzyme CaMKII was comparable in all groups (Figure 4.8A). At 30 min of reperfusion, the phosphorylation of CaMKII in vehicle-treated hearts was significantly increased compared to sham ($p<0.01$, Figure 4.8B) and this increase in phosphorylation of CaMKII tended to be reduced with DiOHF treatment, although that effect was not significant. Figure 4.8C showed that total CaMKII tended to decrease in hearts subjected to ischaemia and reperfusion compared to sham.

DiOHF during reperfusion significantly reduced the I/R-induced increased phosphorylation of PLN at 5 min of reperfusion ($p<0.05$, Figure 4.9A). The phosphorylation of PLN in vehicle-treated hearts at 30 min of reperfusion was comparable to basal level while DiOHF treatment significantly reduced this activation ($p<0.05$, Figure 4.9B). Interestingly, the reduction in PLN phosphorylation by DiOHF was lower than sham.

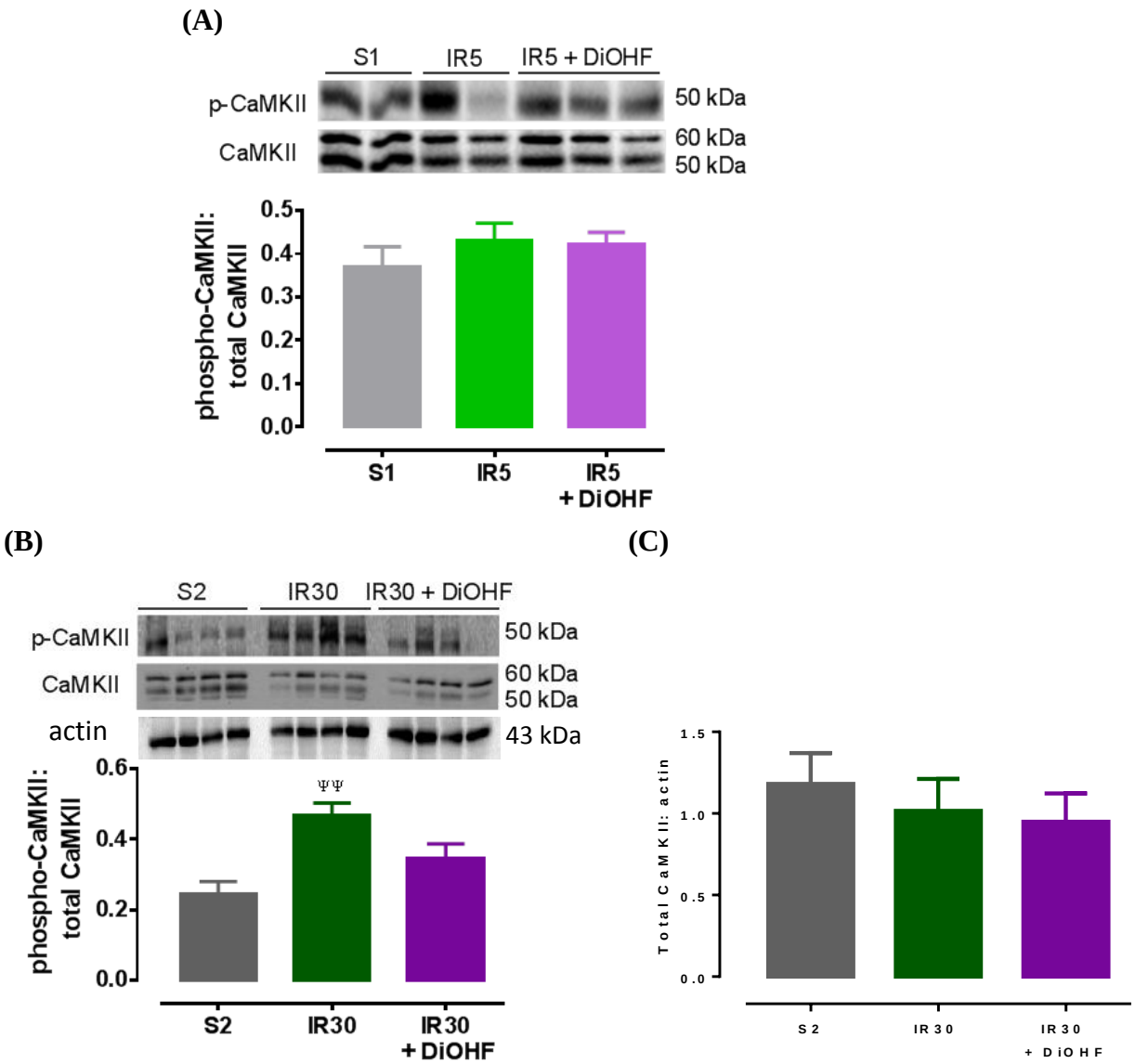

Figure 4.8: Expressions of the multi-functional enzyme CaMKII in sham hearts, S1 or S2 and hearts subjected to 20 min ischaemia followed by **(A)** 5 min or **(B)** 30 min reperfusion in the presence of 0.5% DMSO (IR5 or IR30) or 10 µM DiOHF (IR5 + DiOHF or IR30 + DiOHF), n= 6-8 per group. Representative immunoblots and densitometric analysis are shown. The phosphorylation of the protein was normalised against total protein. (C) Total CaMKII in sham hearts (S2) and hearts subjected to 20 min ischaemia followed by 30 min in the presence of 0.5% DMSO or 10 µM DiOHF was normliased against actin. ΨΨp<0.01 vs S2, 1-way ANOVA with Tukey's multiple comparisons test. Data are expressed as mean ± SEM.

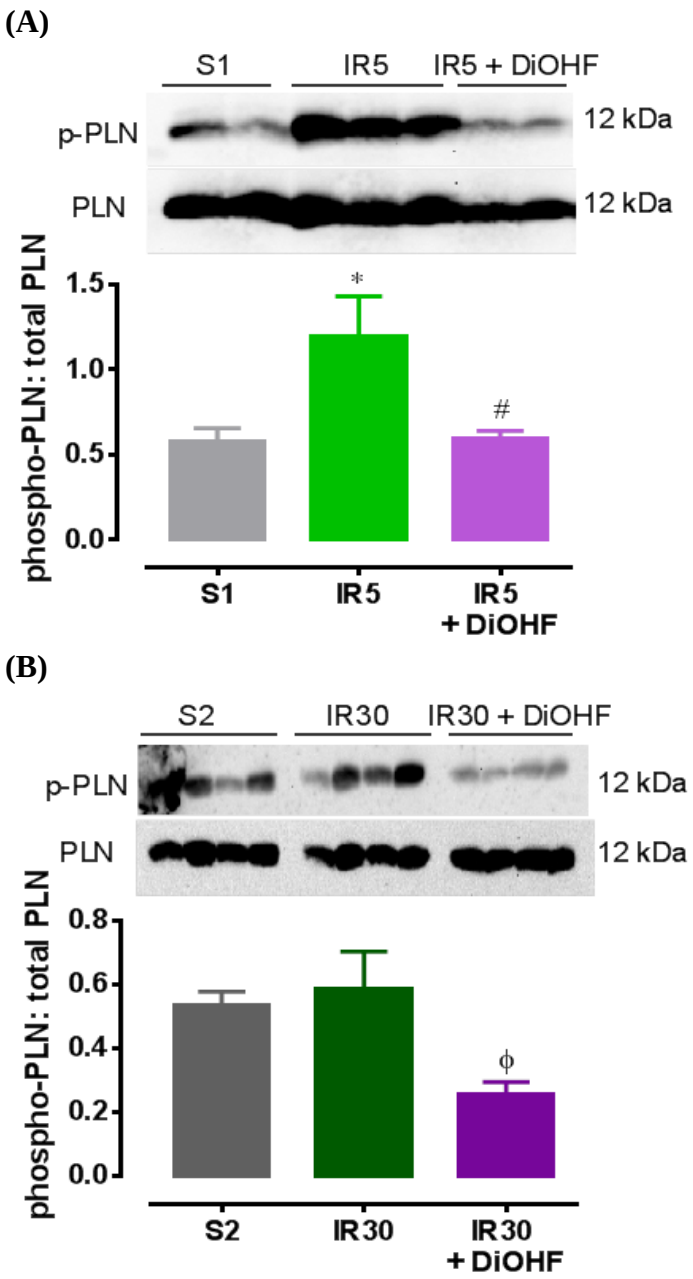

Figure 4.9: Expressions of PLN in sham hearts, S1 or S2 and hearts subjected to 20 min ischaemia followed by **(A)** 5 min or **(B)** 30 min reperfusion in the presence of 0.5% DMSO (IR5 or IR30) or 10 µM DiOHF (IR5 + DiOHF or IR30 + DiOHF), n= 6-8 per group. Representative immunoblots and densitometric analysis are shown. The phosphorylation of the protein was normalised against total protein. *p<0.05 vs S1, #p<0.05 vs IR5, ϕp<0.05 vs IR30, 1-way ANOVA with Tukey's multiple comparisons test. Data are expressed as mean ± SEM.

4.3.5 Effects of DiOHF on the expression of protective kinases during myocardial I/R

Five minutes after reperfusion, the phosphorylation of the protective kinase in the RISK pathway, Akt in vehicle-treated hearts was not significantly different from sham (S1) (Figure 4.10A). DiOHF during reperfusion significantly increased the phosphorylation of Akt compared to sham at 5 min ($p<0.05$). At 30 min of reperfusion, the phosphorylation of Akt was significantly increased in the vehicle-treated group compared to sham (S2) ($p<0.001$, Figure 4.10B), however DiOHF treatment significantly reduced the I/R-induced increased phosphorylation of Akt ($p<0.05$).

The phosphorylation of another kinase in the RISK pathway, Erk 1/2 in vehicle-treated hearts was also not significantly different from sham (S1) at 5 min of reperfusion. Similarly, DiOHF treatment significantly increased the phosphorylation of Erk 1/2 compared to sham at 5 min ($p<0.05$, Figure 4.11A). At 30 min of reperfusion, the phosphorylation of Erk 1 was comparable in all groups while the phosphorylation of Erk 2 in vehicle-treated hearts was significantly increased compared to sham (S2). DiOHF had no effect on the I/R-induced increased phosphorylation of Erk 2 at this time point (Figure 4.11B).

At 5 min of reperfusion, the phosphorylation of the protective kinase STAT3 in the SAFE pathway in the vehicle-treated hearts tended to reduce compared to sham (S1) while DiOHF treatment increased the phosphorylation of STAT3, although neither change was statistically significant (Figure 4.12A). At 30 min of reperfusion, STAT3 phosphorylation also tended to increase in vehicle-treated hearts compared to sham (S2) and DiOHF treatment significantly increased the phosphorylation of STAT3 compared to sham ($p<0.05$, Figure 4.12B).

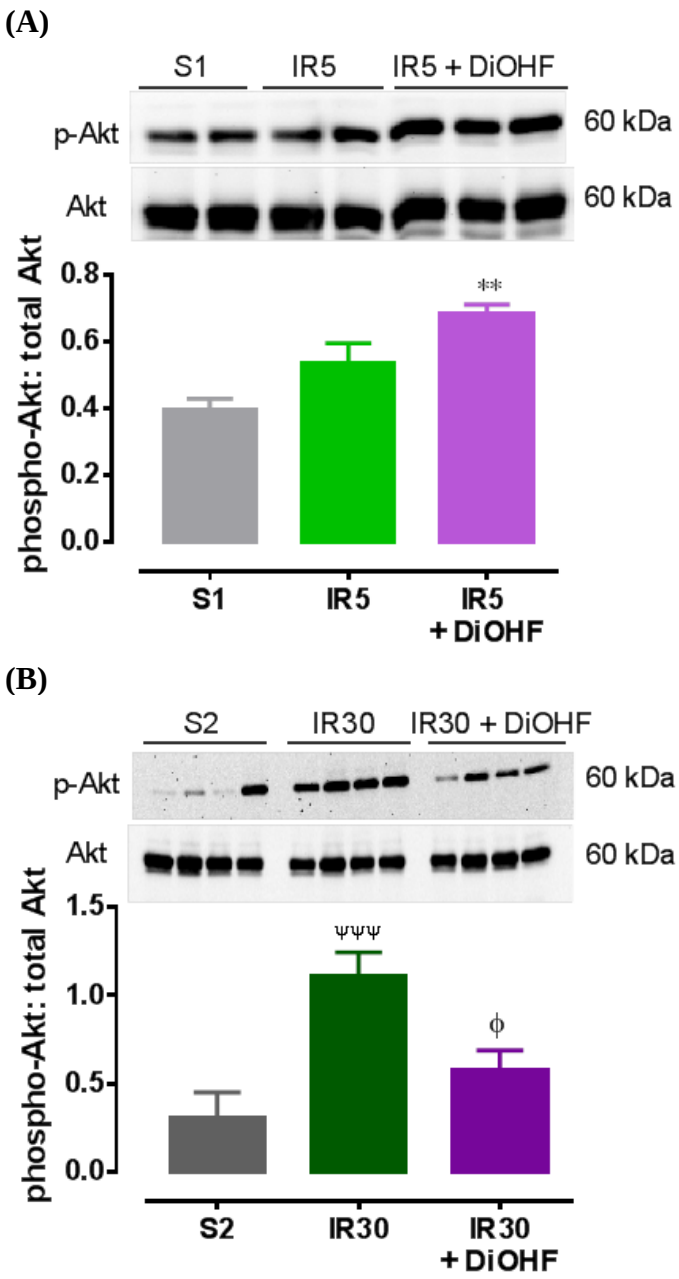

Figure 4.10: Expressions of the protective kinase Akt in sham hearts S1 or S2 and hearts subjected to 20 min ischaemia followed by **(A)** 5 min or **(B)** 30 min reperfusion in the presence of 0.5% DMSO (IR5 or IR30) or 10 µM DiOHF (IR5 + DiOHF or IR30 + DiOHF), n= 6-8 per group. Representative immunoblots and densitometric analysis are shown. The phosphorylation of the protein was normalised against total protein. **p<0.001 vsS1, ΨΨΨp<0.0001 vs S2, ϕp<0.05 vs IR30, 1-way ANOVA with Tukey's multiple comparisons test. Data are expressed as mean ± SEM.

(A)

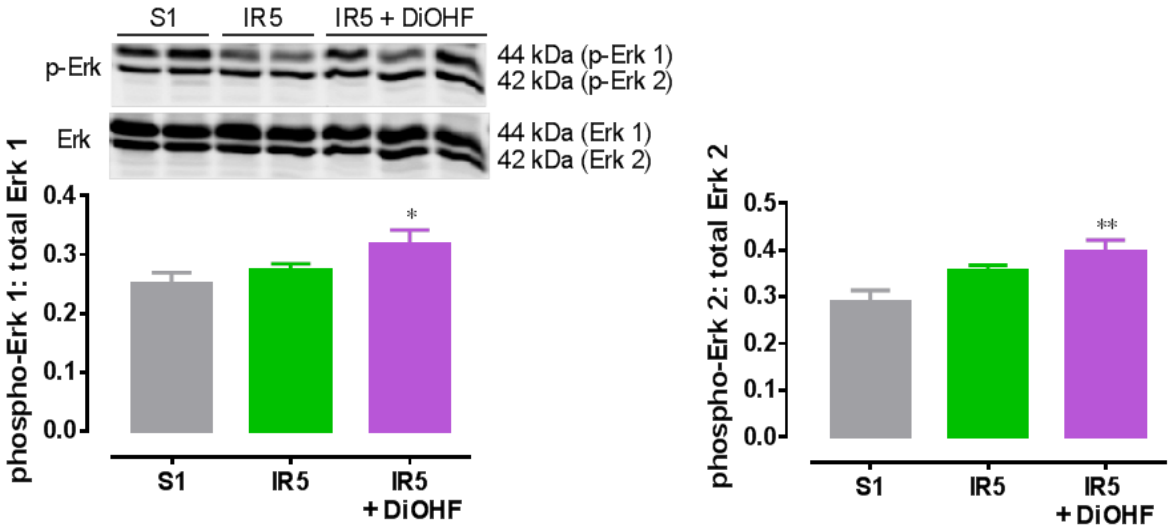

(B)

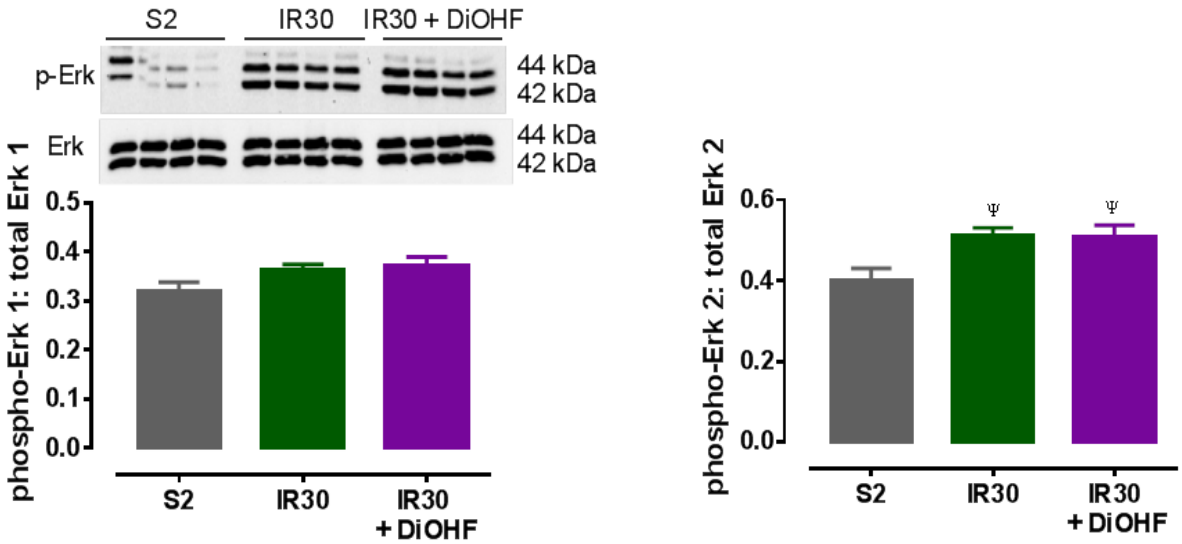

Figure 4.11: Expressions of protective kinases Erk 1/2 in sham hearts S1 or S2 and hearts subjected to 20 min ischaemia followed by **(A)** 5 min or **(B)** 30 min reperfusion in the presence of 0.5% DMSO (IR5 or IR30) or 10 µM DiOHF (IR5 + DiOHF or IR30 + DiOHF), n= 6-8 per group. Representative immunoblots and densitometric analysis are shown. The phosphorylation of the protein was normalised against total protein. *$p<0.05$, **$p<0.001$ vsS1, Ψ$p<0.05$ vs S2, 1-way ANOVA with Tukey's multiple comparisons test. Data are expressed as mean ± SEM.

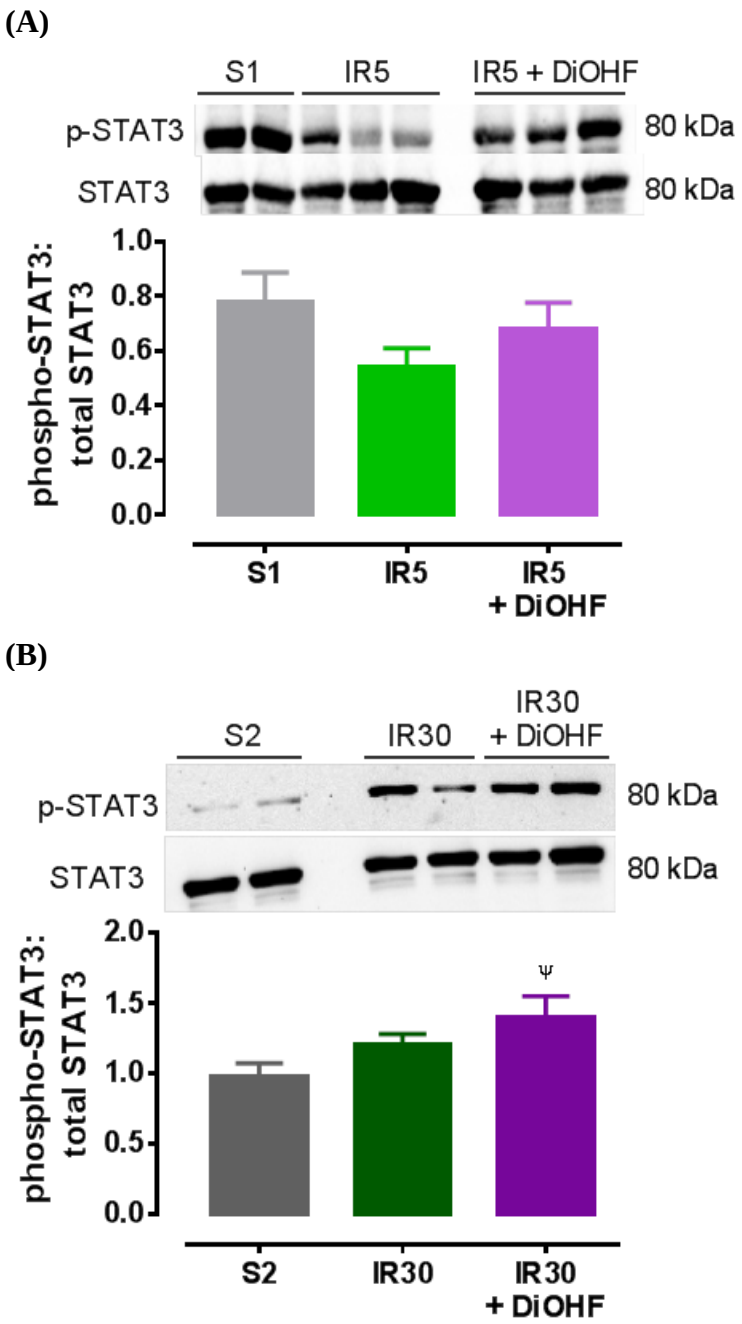

Figure 4.12: Expressions of the protective kinase STAT3 in sham hearts, S1 or S2, and hearts subjected to 20 min ischaemia followed by **(A)** 5 min or **(B)** 30 min reperfusion in the presence of 0.5% DMSO (IR5 or IR30) or 10 µM DiOHF (IR5 + DiOHF or IR30 + DiOHF), n= 6-8 per group. Representative immunoblots and densitometric analysis are shown. The phosphorylation of the protein was normalised against total protein. ψp<0.05 vs S2, 1-way ANOVA with Tukey's multiple comparisons test. Data are expressed as mean ± SEM.

4.4 Discussion

This study demonstrated that DiOHF treatment during reperfusion significantly improved post-ischaemic myocardial function as indicated by an improvement in LV-dP/dt and reduced coronary perfusion pressure compared to its vehicle control. DiOHF treatment also reduced cell death as early as 1 min after the initiation of reperfusion and decreased the amount of apoptosis 30 min after reperfusion. DiOHF significantly increased the phosphorylation of the protective kinases Akt and Erk 1/2 during 5 min reperfusion compared to sham but it had no effect on the increased phosphorylation of pro-injurious kinases JNK 1/2 and p38 MAPK at the same time. Increased phosphorylation of PLN 5 min after reperfusion was significantly reduced by DiOHF. At 30 min of reperfusion, DiOHF reduced the I/R-induced increased phosphorylation of Akt. DiOHF had no effect on the increased phosphorylation of Erk 2 at 30 min of reperfusion although it significantly increased the phosphorylation of STAT3 compared to sham. The I/R-induced increased phosphorylation of p38 MAPK was also not affected by DiOHF. In contrast, DiOHF significantly reduced the I/R-induced increased phosphorylation of JNK 2 and tended to reduce the increased phosphorylation of CaMKII at 30 min of reperfusion. The phosphorylation of the downstream target of CaMKII, PLN was also significantly reduced with DiOHF treatment compared to its vehicle control. Taken together, DiOHF treatment during reperfusion is protective against myocardial I/R injury *in vitro*, and this protective effect may be mediated by inhibiting the activation of PLN at 5 min reperfusion and reducing the activation of both PLN and JNK 2 at 30 min reperfusion.

In this study, DiOHF treatment during reperfusion, which is a clinical-relevant time point, protected the heart against myocardial I/R injury by reducing cardiomyocyte necrosis and apoptosis while improving post-ischaemic cardiac relaxation and reducing coronary perfusion pressure. Although DiOHF significantly improved post-ischaemic cardiac

relaxation, its effect on cardiac contraction was not significantly different compared to its vehicle control. This is consistent with a previous study from our laboratory (Qin *et al.*, 2011). It that study, it was reported that DiOHF treatment during reperfusion in rat isolated heart subjected to global ischaemia and reperfusion, had no significant effect on the post-ischaemic myocardial contractility (Qin *et al.*, 2011), which was considered to be due to the negative inotropic action of DiOHF which is mediated by its calcium utilisation inhibitory property that limits cardiac contraction (Qin *et al.*, 2011). Biochemical analysis using LDH assay however showed that DiOHF treatment significantly reduced cell death, a finding similar to our observation in this study, and preserved eNOS expression which may increase the production of nitric oxide (NO) and prevent the opening of mitochondrial permeability transition pore (mPTP) (Hausenloy *et al.*, 2005). This suggests that DiOHF is protective against myocardial I/R injury (Qin *et al.*, 2011).

As mentioned earlier, the protective action of NP202, the pro-drug converted to DiOHF against I/R in anaesthetized sheep was mediated by inhibiting the activation of CaMKII and this resulted in subsequent inhibition of JNK/*c-jun* and p38 MAPK/MAPK-activated protein kinase 2 pathways without affecting the activation of protective kinases Akt and Erk 1/2 (Lim *et al.*, 2013). In that study, the effect of NP202 on kinase activation was examined 30 min after reperfusion where a maximum level of kinase activation was observed (Lim *et al.*, 2013). As myocardial injury followed by cardiomyocyte death is detected as early as minutes after the onset of reperfusion (Ruiz-Meana & Garcia-Dorado, 2009), the effect of DiOHF on kinase activation at earlier reperfusion time points i.e. 5 and 30 min reperfusion was investigated in this study.

In this study, DiOHF treatment during reperfusion tended to increase the activation of Akt and Erk 1/2 at 5 min; however the activation of Akt, but not Erk 1/2, was decreased at 30 min of reperfusion by DiOHF. This finding is in contrast to the effect of NP202 in

anesthetised sheep where the increased phosphorylation of both Akt and Erk 1/2 after 1 h ischaemia followed by 30 min reperfusion or 3 h ischaemia followed by 3 h reperfusion was not altered with NP202 treatment (Thomas *et al.*, 2011; Lim *et al.*, 2013). In another study, in murine isolated cardiomyocytes, pre-treatment with NP202 before simulated I/R using hydrogen peroxide significantly increased the phosphorylation of Akt and Erk 1/2 (Thomas *et al.*, 2015). Interestingly, in the same study, it was shown that in the presence of specific inhibitors for PI3K/Akt and mitogen/extracellular signal-regulated kinase (MEK 1/2)/Erk 1/2 pathways, LY294002 and PD98059 respectively, the cardioprotection induced by NP202 in anesthetised sheep subjected to 1 h ischaemia and 3 h reperfusion was impaired in the presence of PD98059 but not LY294002 (Thomas *et al.*, 2015). This suggested that the MEK 1/2/Erk 1/2, but not the PI3K/Akt pathway is crucial in mediating the protective action of DiOHF against I/R injury. This may explain the reduced activation of Akt by DiOHF at 30 min reperfusion in this study as DiOHF-induced cardioprotection at this time point (but not at 5 min reperfusion) could be mediated by other protective mechanisms, and there was no role for Akt. In another cellular model, DiOHF has also been shown to inhibit RhoA/Rho-kinase pathway and resulted in decreased vascular contraction in rat isolated aorta (Song *et al.*, 2010b). Inhibition of RhoA/Rho-kinase pathway has been shown to mitigate the progression of heart failure and protect the heart against I/R injury (Sanada *et al.*, 2004; Chau *et al.*, 2011). Active RhoA could activate its downstream molecule, focal adhesion kinase resulting in the activation of PI3K and subsequent Akt activation (Del Re *et al.*, 2008). DiOHF may reduce Akt activation via a RhoA-dependent mechanism. The effect of DiOHF on Akt requires further investigation.

The phosphorylation of the protective kinase, STAT3 tended to increase with DiOHF treatment at 5 min of reperfusion while it significantly increased the activation of STAT3 at 30 min of reperfusion compared to sham. This is consistent with the reported effects of other

flavonols, such as myricetin and delphinidin, which conferred protection against myocardial I/R injury by attenuating the phosphorylation of STAT1, which is pro-apoptotic without affecting the activation of STAT3, which is anti-apoptotic (Scarabelli *et al.*, 2009).

As mentioned earlier, CaMKII could be a direct target of DiOHF and the inhibition of CaMKII activation by DiOHF results in cardioprotection (Lim *et al.*, 2013). In this study, DiOHF tended to reduce the I/R-induced increased activation of CaMKII at 30 min reperfusion although this effect was not significant. In addition, an increased activation of CaMKII was observed during ischaemia and the activation of CaMKII tended to decrease at 5 min of reperfusion (Chapter 3). DiOHF treatment had no effect on the activation of CaMKII at 5 min. It is possible that the action of DiOHF on the activity of CaMKII occurred at a very early time point of reperfusion (i.e. <5 min, which was not investigated in this study) as reports showed that increased CaMKII activation was observed at 1 to 3 min of reperfusion (Said *et al.*, 2011; Ling *et al.*, 2013). Another possible reason is that once CaMKII is activated during ischaemia, it is translocated into subcellular fraction such as mitochondria to trigger apoptosis. In addition, the I/R-induced increased phosphorylation of the downstream target of CaMKII, PLN was reduced by DiOHF at 5 min of reperfusion. There are conflicting data regarding the role of CaMKII and PLN in myocardial I/R. Earlier reports demonstrated that the presence of the inhibitor of CaMKII, KN-93 reduced the phosphorylation of PLN at Thr 17 during early reperfusion which was associated with a better mechanical recovery after ischaemia (Vittone *et al.*, 2002; Said *et al.*, 2003). PLN phosphorylation during I/R enhanced Ca^{2+} uptake through SERCA2a and could improve Ca^{2+} handling in the cell (Said *et al.*, 2003). In transgenic PLN-mutant mice, the recovery of Ca^{2+} transient amplitude and myocardial contractile function was also delayed compared to wild type (Said *et al.*, 2003; Valverde *et al.*, 2006). More recent data has shown that CaMKII inhibition were protective in myocardial I/R. Vila-Petroff and colleagues demonstrated that KN-93 treatment before

ischaemia and during early reperfusion reduced myocardial infarct size and prevented Ca^{2+} oscillations, a consequence of sarcoplasmic reticulum Ca^{2+} overload (Vila-Petroff *et al.*, 2007). It is suggested that sarcoplasmic reticulum Ca^{2+} overload due to the increased phosphorylation of PLN at Thr 17, could result in sarcoplasmic reticulum Ca^{2+} leak (Vila-Petroff *et al.*, 2007). These Ca^{2+} were taken up by mitochondria and excessive mitochondrial Ca^{2+} uptake could trigger the opening of the mPTP resulting in apoptosis (Chen *et al.*, 2005; Vila-Petroff *et al.*, 2007; Shintani-Ishida *et al.*, 2012). Other reports also showed that CaMKII inhibition improved post-ischaemic cardiac contractile recovery, reduced sarcoplasmic reticulum Ca^{2+} overload, cytochrome C release and Ca^{2+}-induced mitochondrial swelling and subsequent cell death (Salas *et al.*, 2010; Szobi *et al.*, 2014). In addition, treatment with KN-93 reduced the incidence of reperfusion arrhythmias, a severe and life-threatening condition which occurs within seconds of the onset of myocardial reperfusion (Adameova *et al.*, 2012; Bell *et al.*, 2012). It is also suggested that phosphorylation of PLN during early reperfusion caused sarcoplasmic reticulum Ca^{2+} leak and contributed to reperfusion arrhythmias (Said *et al.*, 2008).

In this study, the increased phosphorylation of JNK 2, another possible downstream target of CaMKII, at 30 min of reperfusion was significantly reduced with DiOHF treatment. This is consistent with the finding in anesthetized sheep (Lim *et al.*, 2013). DiOHF reduced the oxidative stress-induced increased activation of MKK 4 and 7, two protein kinases upstream of JNK and the phosphorylation of the transcription factor *c-jun* (Lim *et al.*, 2013). Cardioprotection caused by JNK inhibition is associated with a reduction in caspase-3 activity and cytochrome C release thereby preventing apoptosis (Milano *et al.*, 2007). This is in accordance with the finding in this study where reduced number of apoptotic cells was observed in DiOHF-treated hearts at 30 min of reperfusion. In contrast to previous reports that DiOHF-induced cardioprotection was also mediated via the inhibition of p38 MAPK

activation (Thomas *et al.*, 2011; Lim *et al.*, 2013), this report showed no effect of DiOHF treatment on the activation of p38 MAPK in myocardial I/R. Although it is generally thought that p38 MAPK, which can initiate a series of inflammatory response is pro-injurious during I/R, studies have also reported that the activation of p38 MAPK is protective against myocardial I/R injury (Das *et al.*, 2006; Khan *et al.*, 2006). It has also been reported that the different isoforms of p38 MAPK has different role in myocardial I/R where p38 MAPKα has a deleterious effect on myocardial I/R while p38 MAPKβ is cardioprotective (Otsu *et al.*, 2003; Bassi *et al.*, 2008).

In conclusion, it is proposed that DiOHF may confer protection against myocardial I/R injury by inhibiting PLN-induced sarcoplasmic reticulum Ca^{2+} leaks and subsequent reperfusion-induced arrhythmias. The DiOHF-induced cardioprotection may also be mediated by inhibiting JNK 2 activation to reduce apoptosis while maintaining the activation of protective kinases Erk 2 and STAT3 at 30 min reperfusion.

Chapter 5

5. The mechanism(s) of cardiac and dilator actions of Angeli's salt

5.1 Introduction

One of the major consequences of acute myocardial infarction is acute heart failure. When there is a low cardiac output and the peripheral vasculature is under-perfused, a positive inotrope will be introduced. Currently available positive inotropes to improve cardiac output in acute heart failure include dobutamine, levosimendan, milirone and etc., however the use of these inotropes to may develop adverse effects such as cardiac arrhythmias resulting in increased mortality rate. Therefore, the discovery of a novel positive inotrope with limited adverse effects is highly desirable.

Nitroxyl (HNO) is the one-electron reduced and protonated redox sibling of NO. Its therapeutic potential was first suggested when the effects of the anti-alcoholism drug, cyanamide, were found to be attributed to the release of HNO (Nagasawa *et al.*, 1990). HNO is a transient species, readily undergoing dimerisation to form hyponitrous acid with subsequent decomposition into nitrous acid and water (DuMond & King, 2011). Therefore, HNO donors are utilised in pharmacological studies, often with the prototypical HNO donor, sodium trioxodinitrate ($Na_2N_2O_3$) or Angeli's salt (Miranda *et al.*, 2005a). In recent years, HNO has emerged as a novel regulator of cardiovascular function, with vasoprotective (vasodilator, anti-aggregatory) and cardioprotective (i.e. positive inotrope, anti-hypertrophic) properties (Irvine *et al.*, 2008; Bullen *et al.*, 2011; Tocchetti *et al.*, 2011; Lin *et al.*, 2012). Interestingly, HNO serves as a positive cardiac inotrope and is protective in an experimental

model of heart failure (Paolocci *et al.*, 2001; Paolocci *et al.*, 2003), an action not shared by NO. HNO also exhibits antihypertrophic actions in the myocardium, an effect mediated via inhibition of NADPH oxidase-derived superoxide generation (Lin *et al.*, 2012) and attenuation of the activity of a pro-hypertrophic signalling pathway, p38 MAPK (Wanstall *et al.*, 2001; Favaloro & Kemp-Harper, 2009; Lin *et al.*, 2012). As such, recent interest in the therapeutic potential of HNO has focused on cardiovascular disorders, such as vascular dysfunction, cardiac dysfunction, cardiac remodelling and heart failure (Irvine *et al.*, 2007; Irvine *et al.*, 2008; Ritchie *et al.*, 2009; El-Armouche *et al.*, 2010; Bullen *et al.*, 2011; Ding *et al.*, 2011; Yuill *et al.*, 2011; Lin *et al.*, 2012).

In contrast to NO, HNO possesses several unique pharmacological properties. Firstly, HNO is resistant to scavenging by the ROS, superoxide (levels of which are commonly elevated in cardiovascular pathologies), whereas NO is highly reactive with superoxide, forming a second ROS, peroxynitrite (Miranda *et al.*, 2002). In addition, tolerance does not develop to HNO's vasodilator actions, a favourable benefit over traditional clinically-used nitrovasodilators (Irvine *et al.*, 2007; Irvine *et al.*, 2011). HNO reacts readily with metal centres of proteins such as iron-containing haem in oxymyoglobin and sGC, and in contrast to NO, preferentially targets ferric (Fe^{3+}) rather than ferrous (Fe^{2+}) haem groups and thus may activate these proteins when their iron is in the oxidised state (Miranda *et al.*, 2003b). Furthermore, HNO (but not NO) is highly thiolphilic, directly targeting thiol-containing proteins. Such an action of HNO underlies many of its unique properties in the cardiovascular system (Fukuto & Carrington, 2011). Indeed, the interaction of HNO with cysteine residues on Ca^{2+}-cycling proteins (i.e. RyR, SERCA) on the sarcoplasmic reticulum of cardiomyocytes leads to enhanced cardiac contractility (Fukuto & Carrington, 2011; Tocchetti *et al.*, 2011). The therapeutic advantages of HNO over NO are likely evident in settings where nitrogen oxides are exposed to significant levels of ROS, limiting the bioavailability of NO but not of

HNO (Irvine *et al.*, 2008; Ritchie *et al.*, 2009; Bullen *et al.*, 2011), and/or where specific HNO interactions with key cysteine residues confers protection (e.g. on SERCA, a property not shared by NO (Fukuto & Carrington, 2011; Tocchetti *et al.*, 2011). It is anticipated that HNO donors would thus be comparable to NO donors in other settings such as via inhalation for pulmonary hypertension (De Witt *et al.*, 2001). The distinct pharmacological profile of HNO suggests however it offers favourable therapeutic advantages over its free radical sibling, NO, in vascular dysfunction, cardiac dysfunction, cardiac remodelling and heart failure.

NO predominantly utilises sGC/cGMP to mediate vasodilatation and suppression of cardiomyocyte hypertrophy. In contrast, HNO has been shown to signal via both sGC-dependent and -independent pathways in the vasculature and myocardium. The mechanism of vasodilator actions of the HNO donor, Angeli's salt are largely sGC-dependent (Fukuto *et al.*, 1992b; Ellis *et al.*, 2000; Irvine *et al.*, 2003; Favaloro & Kemp-Harper, 2007; Irvine *et al.*, 2007; Andrews *et al.*, 2009), with a smaller contribution from K^+ channels (K_v and K_{ATP}) and calcitonin gene-related peptide (CGRP) evident in the resistance (Irvine *et al.*, 2003; Favaloro & Kemp-Harper, 2009) and coronary vasculature (Favaloro & Kemp-Harper, 2007), respectively. These vasodilator properties are evident in both large (e.g. aorta) as well as smaller vessels such as in rodent isolated thoracic aorta, rodent isolated mesenteric arteries or isolated hearts *in vitro* (Ellis *et al.*, 2000; Wanstall *et al.*, 2001; Irvine *et al.*, 2003; Favaloro & Kemp-Harper, 2007). The antihypertrophic actions of HNO donors in isolated cardiomyocytes are similarly cGMP-dependent (Lin *et al.*, 2012), whereas the superoxide-suppressing actions have been variably reported as cGMP dependent (Lin *et al.*, 2012) or cGMP-independent (Bullen *et al.*, 2011), in cardiomyocytes and arteries respectively. In contrast, the acute enhancement of cardiac contractility elicited by HNO donors in the intact heart have been regarded as cGMP-independent, as no detectable changes in plasma cGMP content were observed *in vivo* (Paolocci *et al.*, 2003). These studies in the intact heart have

not however investigated HNO actions on cardiac contractility in the presence of cGMP inhibition. Most importantly, cardiac contractility is acutely enhanced by HNO donors in failing and normal hearts to an equivalent extent (Paolocci *et al.*, 2001; Paolocci *et al.*, 2003).

The vasodilator and cardiac inotropic effects of HNO donors have been commonly attributed to cGMP-dependent and -independent mechanisms, respectively. The concomitant effects of an HNO donor on vascular and cardiac function, and the net mechanism(s) of these actions, however remain unresolved. The objective of the present study was to thus test the hypothesis that the concomitant vasodilator and inotropic actions induced by the HNO donor, Angeli's salt, are sGC-dependent and sGC-independent, respectively in the rat isolated heart.

5.2 Methods

This investigation conforms with the National Health and Medical Research Council of Australia code of practice for the care and use of animals for scientific purposes. All the procedures involved in this project were approved by The Alfred Medical Research Educational Precinct Animal Ethics Committee.

5.2.1 Langendorff heart preparations

Hearts isolated from male Sprague-Dawley rats (350-450 g) under, ketamine-xylazine anaesthesia (100 and 12 mg/kg i.p., respectively) were Langendorff-perfused as described in Chapter 2.3. Rat isolated hearts were perfused under constant pressure, using the ADInstruments Langendorff System. The STH Pump Controller (ADInstruments) continuously detected coronary flow, in addition to maintaining a constant perfusion pressure (set to achieve coronary flow at baseline of 10 ml/min).

5.2.2 Vasodilatation and contractile function experiments

After 30 min equilibration, the thromboxane A_2 mimetic U46619 (9,11-dideoxy-9α,11α-methanoepoxy prostaglandin $F_{2\alpha}$, 3 μM) was continuously infused into the aorta via a syringe infusion pump (0.1-2.5 ml/min), via a port just above the aortic cannula, to pre-contract the coronary vasculature with a ~50% reduction in baseline coronary flow-rate (i.e. from ~10 ml/min to ~5ml/min). A single bolus dose of NaOH (10 mM, vehicle for Angeli's salt) was then administered to the heart via an injection port just above the aortic cannula, followed by a serial dose-response curve to Angeli's salt (10 pmol - 10 μmol), constructed by administering bolus doses of the HNO donor to the heart via a second injection port just above the aortic cannula, in increasing doses 1 min apart. All parameters of contractile function had returned to baseline levels achieved with U46619 pre-constriction. For coronary flow, this had either returned to baseline levels or had stabilised to a plateau, prior to the addition of the next bolus dose of Angeli's salt. In a parallel series of experiments, hearts were administered serial bolus doses of the equivalent volume of 10 mM NaOH, as a vehicle control.

Subsequent experiments were performed to examine the mechanism of the haemodynamic effects of Angel's salt in the intact heart, in which dose-response curves to Angeli's salt were performed in the presence of various selective pharmacological inhibitors, added to the reservoir of Krebs' perfusion buffer. The relative contribution of HNO and NO to the actions of Angeli's salt was investigated in the presence of the HNO scavenger L-cysteine (4 mM), the NO scavenger hydroxocobalamin (HXC, 0.1 mM) or the thiol dithiothreitol (DTT, 100 μM). Parallel experiments utilised the sGC inhibitor, 1H-[1,2,4]oxadiazolo[4,3-a]quinoxalin-1-one (ODQ, 10 μM), the CGRP antagonist $CGRP_{8-37}$ (0.1 μM), or the K_v channel inhibitor 4-aminopyridine (4-AP, 1 mM) to further examine the

mechanisms of Angeli's salt actions. For comparison, dose–response curves to the pure NO donor diethylamine NONOate (DEA/NO) were also performed.

5.2.3 Data analysis

Changes in all haemodynamic variables induced by each vasodilator dose were measured as the change (Δ) in each response relative to that elicited by the vehicle control (10 mM NaOH for Angeli's salt). All results were expressed as group mean ± SEM, with the number of independent experiments denoted as 'n'. Data analysis was performed using Graphpad Prism® (version 5.0, USA). Vasorelaxant responses were fitted to a sigmoidal logistic equation, to derive the pEC_{50} (vasodilator dose eliciting 50% maximal response, expressed as –log mol) and R_{max} (maximal vasodilator response). The coefficient of variation, R^2, for vasodilator responses was consistently >0.8 in all hearts studied. Dose-response curves to Angeli's salt in the absence and presence of each pharmacological inhibitor were compared on 2-way ANOVA, with the Bonferroni *post hoc* test. Baseline haemodynamic variables and the pEC_{50} and R_{max} for Angeli's salt in the absence and presence of various inhibitors, were analysed using 1-way ANOVA with Dunnett's *post hoc* test for multiple comparisons. The pEC_{50} and R_{max} for DEA/NO in the absence and presence of the inhibitor were analysed using Student's unpaired *t*-test. In all cases, $p<0.05$ was considered statistically significant.

5.2.4 Drugs and reagents

All chemical reagents were purchased from Sigma-Aldrich (St. Louis, MO, USA) and dissolved in distilled water unless otherwise stated. Sodium trioxodinitrate (Angeli's salt), U46619, ODQ and DEA/NO were obtained from Cayman Chemical Company (Ann Arbor, MI, USA). All stock and working solutions of Angeli's salt or DEA/NO were prepared fresh daily in 10 mM NaOH, and kept on ice until required. Aliquots of U46619 (1 mM in 100%

ethanol) were stored at -20^{0}C, and were further diluted on the day of use in Krebs' buffer. Stock solutions of ODQ were prepared fresh daily (1 mM in 100% ethanol) with further dilution in Krebs' buffer. Aliquots of $CGRP_{8-37}$ (0.1 mM in distilled water) were stored at -20^{0}C, with subsequent dilution in Krebs' buffer on the day of use. L-cysteine, HXC, 4-AP and DTT solutions were all prepared in Krebs' buffer.

5.3 Results

5.3.1 Angeli's salt elicits HNO/sGC-dependent vasodilator actions in the whole heart

The baseline characteristics of all buffer-perfused rat hearts used in this study, at the end of equilibration, prior to commencement of any interventions, are shown in Table 5.1. Haemodynamic variables after the commencement of infusion with pharmacological inhibitors are also whon in Table 5.1 while haemodynamic characteristics after U46619 pre-constriction are shown in Table 5.2. Baseline coronary flow prior to commencement of any interventions, as well as that immediately following U46619 pre-constriction, was generally comparable across all experimental groups. A representative recording of all haemodynamic parameters on construction of a dose-response curve to Angeli's salt is shown in Figure 5.1. In the presence of U46619 pre-constriction, the HNO donor, Angeli's salt (10 pmol - 10 μmol) elicited a dose-dependent vasodilatation, with pEC_{50} (-log mol) of 8.55 ± 0.24 and R_{max} (ml/min) of 5.14 ± 0.69 (Table 5.3, Figure 5.2). Significant increases in coronary flow were evident with doses of Angeli's salt $\geq$ 10 nmol. The selective HNO scavenger L-cysteine (4 mM, n=6) caused a rightward shift in the dose-response curve of the vasodilator actions of Angeli's salt, with significant reductions in both the pEC_{50} and R_{max}. In contrast, the selective NO scavenger HXC (100 μM, n=5) not only failed to blunt the vasodilator effect of Angeli's salt, but actually tended to enhance the vasorelaxant Angeli's salt effect (Figure 5.2). The thiol DTT (100 μM, n=5) did not affect the Angeli's salt dose-response curve.

As shown in Figure 5.3, the selective sGC inhibitor, ODQ (10 μM, n=6) also caused a rightward shift in the dose-response curve of the vasodilator actions of Angeli's salt, with significant reduction in the pEC_{50} (Figure 5.3). The R_{max} to Angeli's salt was not significantly affected by ODQ (Table 5.3). Both the selective CGRP receptor antagonist $CGRP_{8-37}$ (0.1 μM, n=5) and the K_v channel inhibitor 4-AP (1 mM, n=5) failed to affect the vasodilator actions of Angeli's salt (Figure 5.3). Furthermore, serial bolus doses of 10 mM NaOH vehicle failed to elicit significant haemodynamic response (Figure 5.3). As shown in Table 5.1, neither L-cysteine, HXC alone nor other pharmacological inhibitors had any significant effect on basal vascular function, although DTT tended to enhance coronary flow and heart rate. For comparison, the NO donor DEA/NO (10 pmol - 10 μmol) elicited a dose-dependent vasodilatation which was also shifted rightwards by HXC (both n=5, Figure 5.4 and Table 5.3).

Table 5.1: Characteristics of all hearts in each experimental group, at each of baseline (at the end of the equilibration period) and after pre-treatment with each pharmacological inhibitor alone (prior to the commencement of U46619 infusion and the addition of Angeli's salt or DEA/NO, shown as mean ±SEM). *p<0.05, **p<0.01 vs the analogous timepoint in hearts allocated to treatment with Angeli's salt alone 1-way ANOVA (Dunnett's *post-hoc* test).

Experimental group	Timepoint	Haemodynamic Variable Prior to Vasodilator Dose-Response Curve								n
		Coronary flow (ml/min)	Perfusion pressure (mmHg)	Heart rate (beats/min)	LVSP (mmHg)	LVDP (mmHg)	LVEDP (mmHg)	LV+dP/dt (mmHg/s)	LV-dP/dt (mmHg/s)	
Angeli's salt (AS)	Baseline	10.6 ± 0.4	44.8 ± 1.3	242 ± 21	75.6 ± 6.2	76.7 ± 7.0	-1.1 ± 1.8	1963 ± 94	-1855 ± 101	8
AS + L-cysteine	Baseline	10.2 ± 1.0	43.0 ±1.6	268 ± 19	57.8 ± 6.0	52.6 ± 6.0*	5.2 ± 1.3*	1687 ± 105	-1435 ± 83	6
	L-cysteine	11.7 ± 1.1	42.3 ± 3.5	201 ± 23	57.5 ± 7.3	52.1 ± 6.6	5.4 ± 1.2	1635 ± 149	-1366 ± 120	
AS + HXC	Baseline	10.5 ± 0.4	45.2 ± 1.5	296 ± 21	53.3 ± 5.0*	55.2 ± 3.9*	-2.0 ± 1.4	1949 ± 153	-1232 ± 131**	5
	HXC	9.1 ± 0.5	46.4 ± 2.0	280 ± 14	56.9 ± 7.9	61.0 ± 6.2	-4.1 ± 2.0	2138 ± 211	-1267 ± 58	
AS + DTT	Baseline	11.2 ± 0.4	50.5 ± 0.6*	291 ± 25	55.1 ± 1.3*	50.7 ± 1.4*	4.1 ± 1.3	1687 ± 218	-1150 ± 81**	5
	DTT	16.5 ± 1.2**	50.0 ±2.1	299 ± 9	52.5 ± 4.1	52.3 ± 4.8	0.2 ±2.0	1818 ± 193	-1211 ± 92	
AS + ODQ	Baseline	10.2 ± 0.7	41.6 ± 0.9	294 ± 18	54.1 ± 4.5*	51.0 ± 3.0*	3.2 ± 1.2	1832 ± 177	-1578 ± 180	6
	ODQ	10.4 ± 0.6	42.6 ± 0.9	244 ± 20	69.5 ± 6.3	67.3 ± 5.4*	2.2 ± 1.7	2047 ± 186	-1812 ± 211	
AS + $CGRP_{8-37}$	Baseline	10.1 ± 0.3	41.4 ± 0.3	239 ± 16	64.8 ± 3.8	64.7 ± 2.9	0.1 ± 1.4	1674 ± 66	-1320 ± 21	5
	$CGRP_{8-37}$	10.1 ± 0.2	43.2 ± 1.6	255 ± 16	69.6 ± 3.4	71.6 ± 3.0	-2.0 ± 1.5	1758 ± 116	-1505 ± 99	
AS + 4-AP	Baseline	10.1 ± 0.8	46.1 ± 1.6	295 ± 19	53.5 ± 3.6*	53.7 ± 3.4*	-0.2 ± 1.5	1718 ± 43	-1500 ± 89	5
	4-AP	8.4 ± 1.5	52.0 ± 2.1	241 ± 9*	72.7 ± 13.9	76.1 ± 15.2	-3.4 ± 2.1	2324 ± 348	-2079 ± 314	
DEA/NO	Baseline	10.4 ± 0.4	51.9 ± 3.1	254 ± 12	63.9 ± 6.7	58.6 ± 8.1	5.3 ± 2.6	1956 ± 248	-1109 ± 57	5
DEA/NO + HXC	Baseline	10.6 ± 0.3	47.8 ± 2.2	271 ± 12	54.3 ± 2.4	55.5 ± 1.6	-1.2 ± 3.4	1834 ± 66	-1203 ± 92	5
	HXC	10.8 ± 1.4	46.8 ± 2.3	257 ± 10	48.0 ± 7.6	50.5 ± 7.1	-2.5 ± 3.2	1705 ± 193	-1079 ± 63	

Table 5.2: Characteristics of all hearts in each experimental group, after the commencement of U46619 infusion (prior to the addition of Angeli's salt or DEA/NO, shown as mean ±SEM). *p<0.05, **p<0.01 vs the analogous timepoint in hearts allocated to treatment with Angeli's salt alone 1-way ANOVA (Dunnett's *post-hoc* test).

Experimental group	Haemodynamic Variable Prior to Vasodilator Dose-Response Curve								n
	Coronary flow (ml/min)	Perfusion pressure (mmHg)	Heart rate (beats/min)	LVSP (mmHg)	LVDP (mmHg)	LVEDP (mmHg)	LV+dP/dt (mmHg/s)	LV-dP/dt (mmHg/s)	
Angeli's salt (AS)	5.7 ± 0.5	51.1 ± 2.2	217 ± 18	55.9 ± 6.9	56.4 ± 8.4	0.6 ± 2.0	1721 ± 165	-1617 ± 185	8
AS + L-cysteine	7.2 ± 0.8	49.2 ± 3.5	187 ± 18	51.8 ± 5.9	47.1 ± 6.1	4.7 ± 0.8	1533 ± 98	-1280 ± 82	6
AS + HXC	5.7 ± 0.5	48.7 ± 1.5	269 ± 11	41.7 ± 8.5	44.7 ± 7.9	-3.0 ± 1.8	1588 ± 242	- 968 ± 96	5
AS + DTT	8.8 ± 0.5*	54.9 ± 1.7	318 ± 19**	42.4 ± 3.4	41.5 ± 3.6	0.9 ± 1.6	1530 ± 156	1123 ± 118	5
AS + ODQ	5.5 ± 0.5	47.4 ± 1.8	208 ± 22	55.8 ± 9.5	52.6 ± 9.0	3.1 ± 1.1	1636 ± 192	-1372 ± 222	6
AS + $CGRP_{8-37}$	5.3 ± 0.2	49.9 ± 1.9	233 ± 14	53.7 ± 1.3	54.6 ± 1.5	-0.8 ± 1.1	1481 ± 82	-1201 ± 71	5
AS + 4-AP	4.5 ±0.9	56.3 ± 2.2	226 ± 20	47.9 ± 11.5	47.9 ± 12.4	-0.0 ± 1.8	1549 ± 319	-1362 ± 245	5
DEA/NO	5.6 ± 0.3	57.9 ± 3.2	267 ± 10	51.5 ± 4.5	47.2 ± 6.2	4.3 ± 2.6	1637 ± 177	- 978 ± 67	5
DEA/NO + HXC	7.0 ± 1.2	50.5 ± 1.8	250 ± 11	44.7 ± 5.6	46.8 ± 3.9	-2.1 ± 2.7	1589 ± 117	-1080 ± 49	5

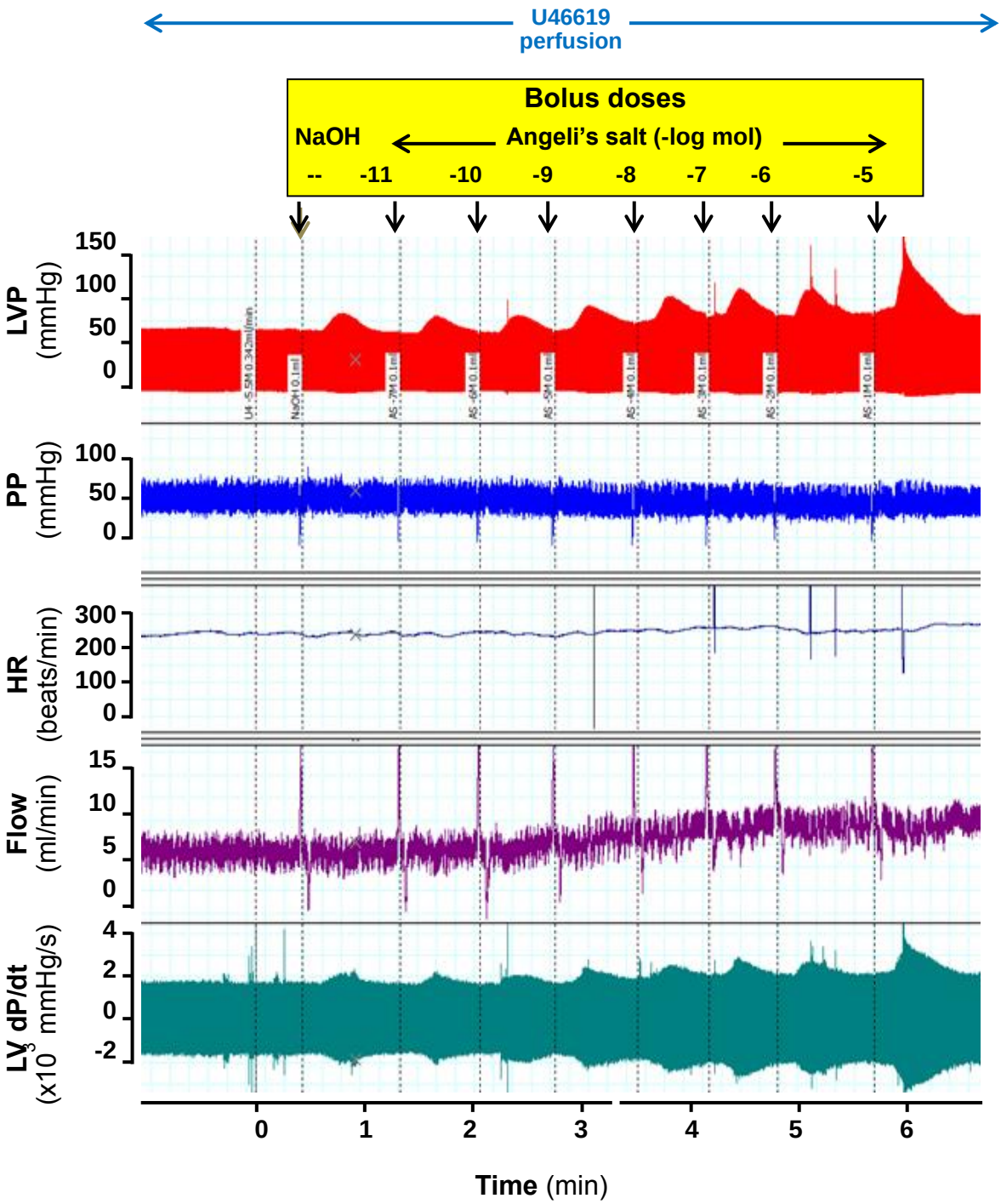

Figure 5.1: Representative dose-response curve to Angeli's salt, showing impact on each of left ventricular pressure (LVP), perfusion pressure (PP), heart rate (HR), coronary flow and LV dP/dt.

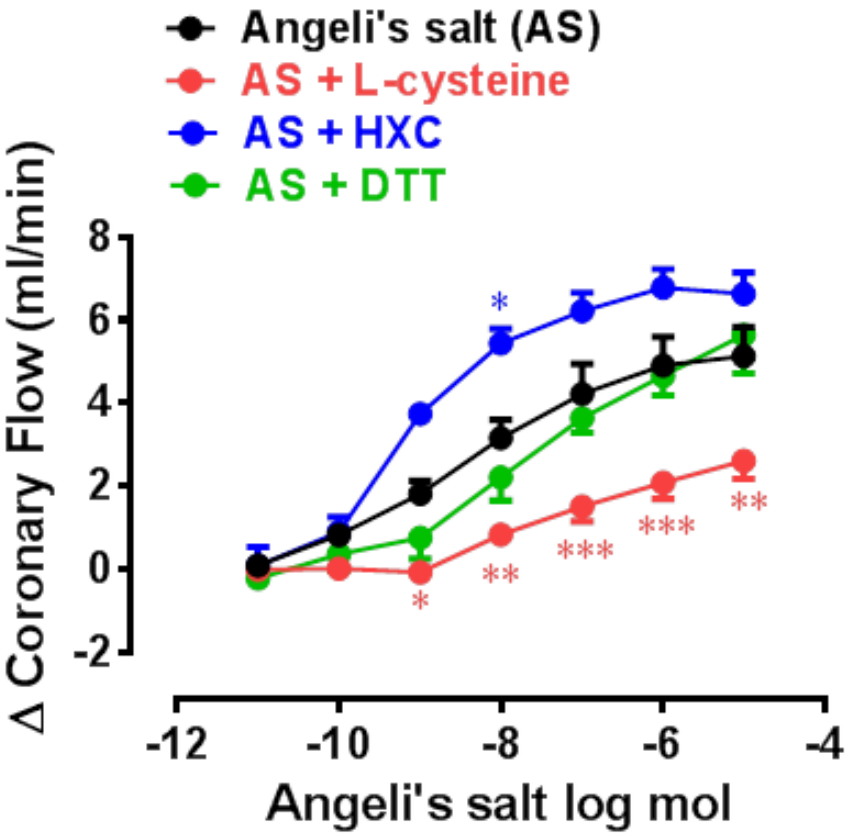

Figure 5.2: Dose-response curves to Angeli's salt (n=8) on coronary flow in the absence and presence of the HNO scavenger L-cysteine (4 mM, n=6), the NO scavenger hydroxocobalamin (HXC, 100 µM, n=5) or the reducing agent dithiothreitol (DTT, 100 µM, n=5). *p<0.05, **p<0.01, ***p<0.001 vs Angeli's salt alone on 2-way ANOVA with Bonferroni *post-hoc* test for multiple comparisons. Data are expressed as mean ± SEM.

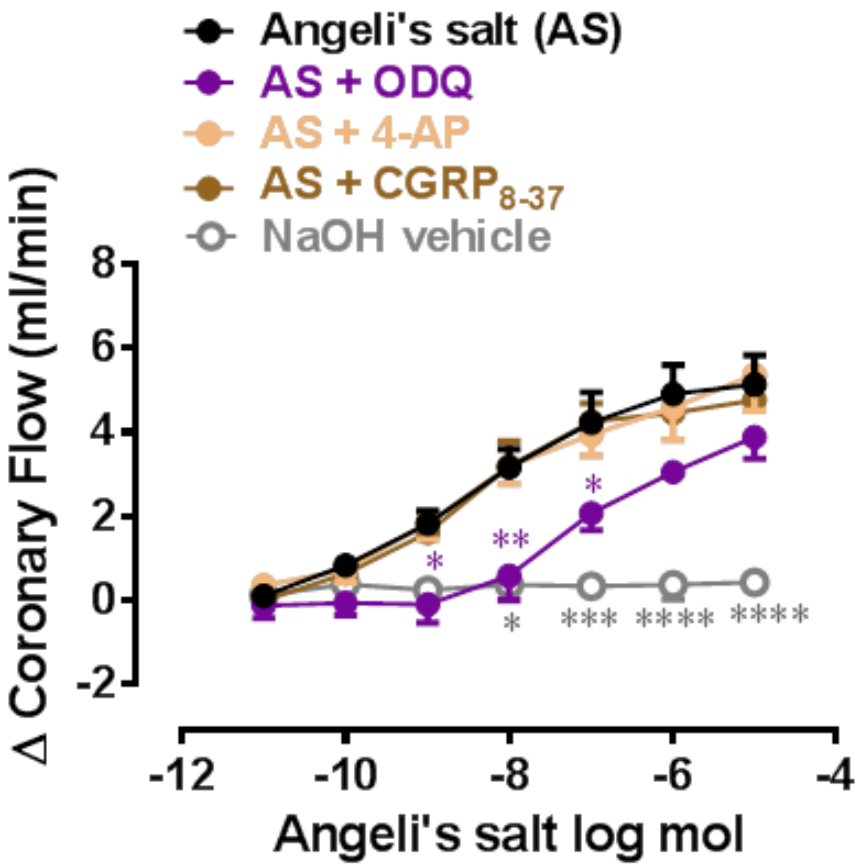

Figure 5.3: Dose-response curves to Angeli's salt (n=8) on coronary flow in the absence and presence the sGC inhibitor ODQ (10 µM, n=6), the CGRP receptor antagonist $CGRP_{8-37}$ (0.1 µM, n=5) and the K_v channel inhibitor 4-AP (1 mM, n=5). Serial bolus doses of 10 mM sodium hydroxide (NaOH) vehicle are shown for comparison (n=3). *p<0.05, **p<0.01, ***p<0.001, ****p<0.0001 vs Angeli's salt alone on 2-way ANOVA with Bonferroni *post-hoc* test for multiple comparisons. Data are expressed as mean ± SEM.

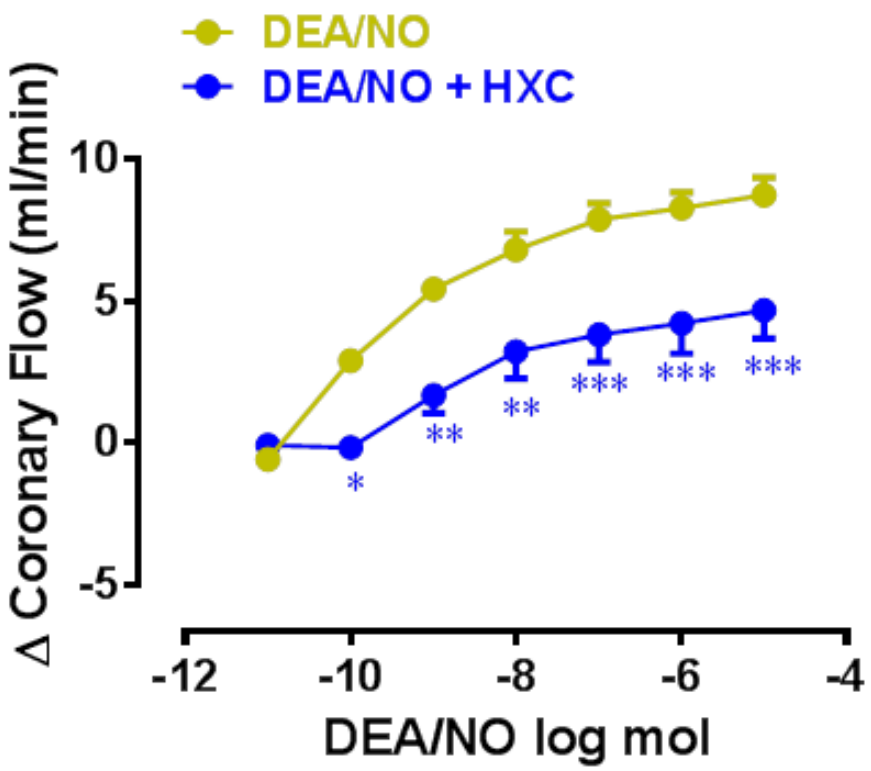

Figure 5.4: Dose-response curves to DEA/NO (n=5) on coronary flow in the absence and presence of hydroxocobalamin (HXC, 100 µM, n=5). *p<0.05, **p<0.01, ***p<0.001 vs DEA/NO alone on 2-way ANOVA with Bonferroni *post-hoc* test for multiple comparisons. Data are expressed as mean ± SEM.

Table 5.3: Sensitivity (pEC_{50}) and maximal relaxation response (R_{max}) for dose–response curves to Angeli's salt and DEA/NO on coronary flow, in the absence and presence of selective inhibitors. *p<0.05, **p<0.01 vs Angeli's salt alone, 1-way ANOVA with Dunnett's *post hoc* test for multiple comparisons and $^{\#\#}$p<0.01 vs DEA/NO alone, Student's unpaired *t*-test. Data are expressed as mean ± SEM.

Experimental group	**pEC_{50} (-log mol)**	**R_{max} (ml/min)**	**n**
Angeli's salt (AS)	8.55 ± 0.24	5.14 ± 0.69	8
AS + L-cysteine	7.53 ± 0.18**	2.62 ± 0.44*	6
AS + HXC	9.12 ± 0.12	6.85 ± 0.47	5
AS + DTT	7.85 ± 0.40	5.65 ± 0.93	5
AS + ODQ	7.36 ± 0.29**	3.88 ± 0.52	6
AS + $CGRP_{8-37}$	8.49 ± 0.26	4.76 ± 0.52	5
AS + 4-AP	8.40 ± 0.30	5.36 ± 0.85	5
DEA/NO	9.60 ± 0.18	8.82 ± 0.61	6
DEA/NO + HXC	8.56 ± 0.19$^{\#\#}$	4.77 ± 1.01$^{\#\#}$	5

5.3.2 Relative contribution of HNO/sGC (but not NO) to the inotropic effects of Angeli's salt

The vasorelaxant effect of Angeli's salt was accompanied by concomitant dose-dependent enhancement of myocardial inotropic function. Significant increases in LVSP, LVDP and LV+dP/dt (Figures 5.5A, B and C), parameters of cardiac contractile function, were evident from $\geq$ 10 nmol Angeli's salt. Both L-cysteine and DTT (but not HXC) markedly blunted the impact of Angeli's salt on each of LVSP, LVDP and LV+dP/dt (Figures 5.5A, B and C). Maximal increases in parameters of cardiac contractility induced by Angeli's salt were suppressed by ~60 % in the presence of L-cysteine. Interestingly, HXC exaggerated the LV+dP/dt response to Angeli's salt (Figure 5.5C). Angeli's salt also tended to increase heart rate at the highest dose studied (by 59 ± 7 beats/min), this was unaffected by either L-cysteine or HXC. Further, no evidence of arrhythmic events was observed at any time. Inhibition of sGC with ODQ also markedly blunted (but did not abolish) the positive inotropic effect of Angeli's salt, on each of LVSP, LVDP and LV+dP/dt (Figures 5.6A, B and C), by ~50 %. In contrast, inhibition of CGRP receptors or K_v channels failed to suppress the positive inotropic actions of Angeli's salt. Interestingly, the LV+dP/dt response tended to be exaggerated by 4-AP. For comparison, the NO donor DEA/NO elicited comparatively modest increases in LVSP, LVDP and LV+dP/dt (Figures 5.7A, B and C), evident at higher doses of DEA/NO, which were insensitive to HXC (both n=5). None of these inhibitors alone (L-cysteine, DTT, HXC, ODQ, $CGRP_{8-37}$ and 4-AP) affected these parameters of contractile function prior to the construction of the dose-response curve to Angeli's salt, as shown in Table 5.1.

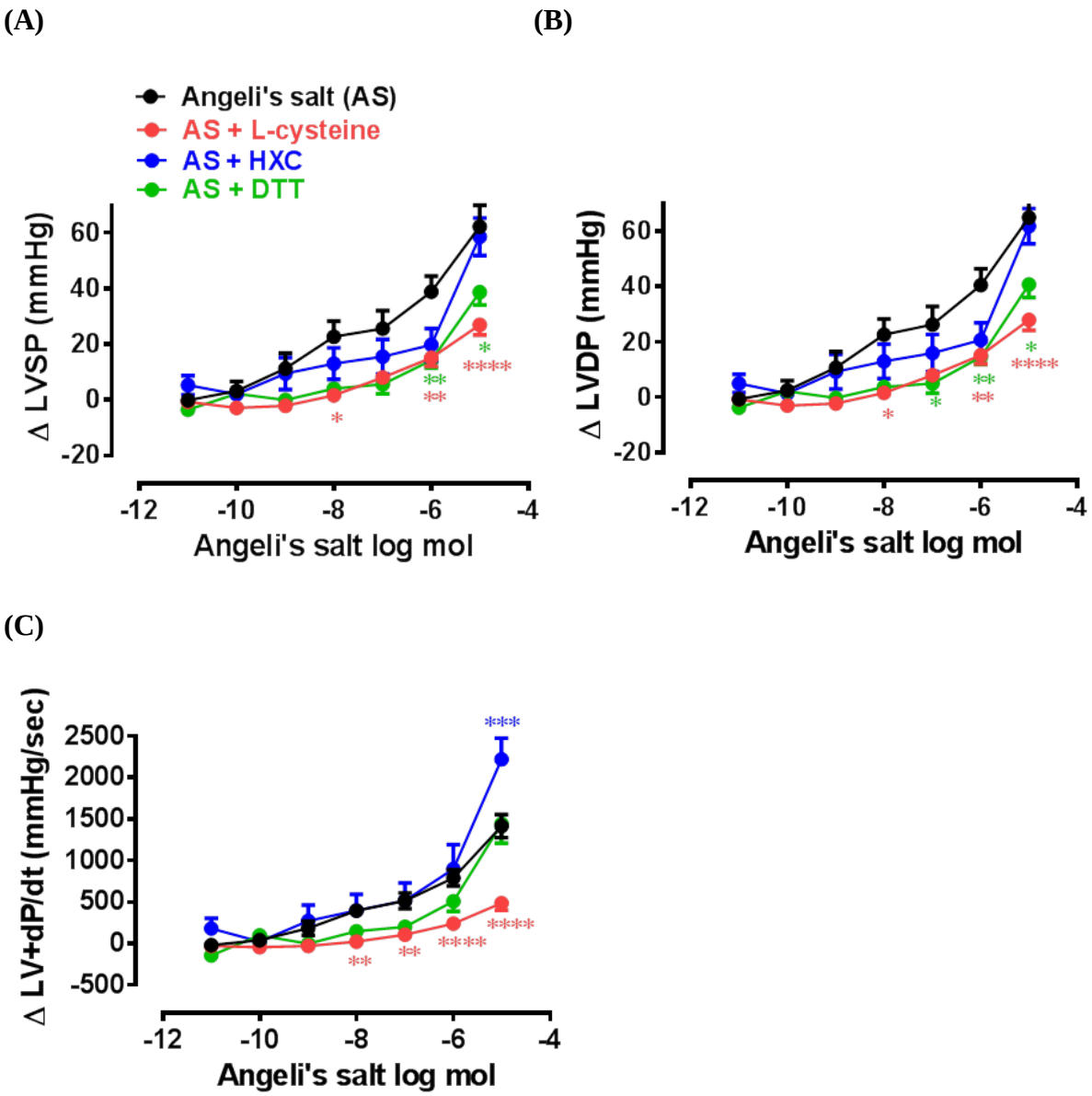

Figure 5.5: Dose-response curves to Angeli's salt (n=8) on **(A)** LVSP, **(B)** LVDP and **(C)** LV+dP/dt in the absence and presence of L-cysteine (n=6), hydroxocobalamin (HXC, n=5) or dithiothreitol (DTT, n=5). *p<0.05, **p<0.01, ***p<0.001, ****p<0.0001 vs Angeli's salt alone on 2-way ANOVA with Bonferroni *post-hoc* test for multiple comparisons. Data are expressed as mean ± SEM.

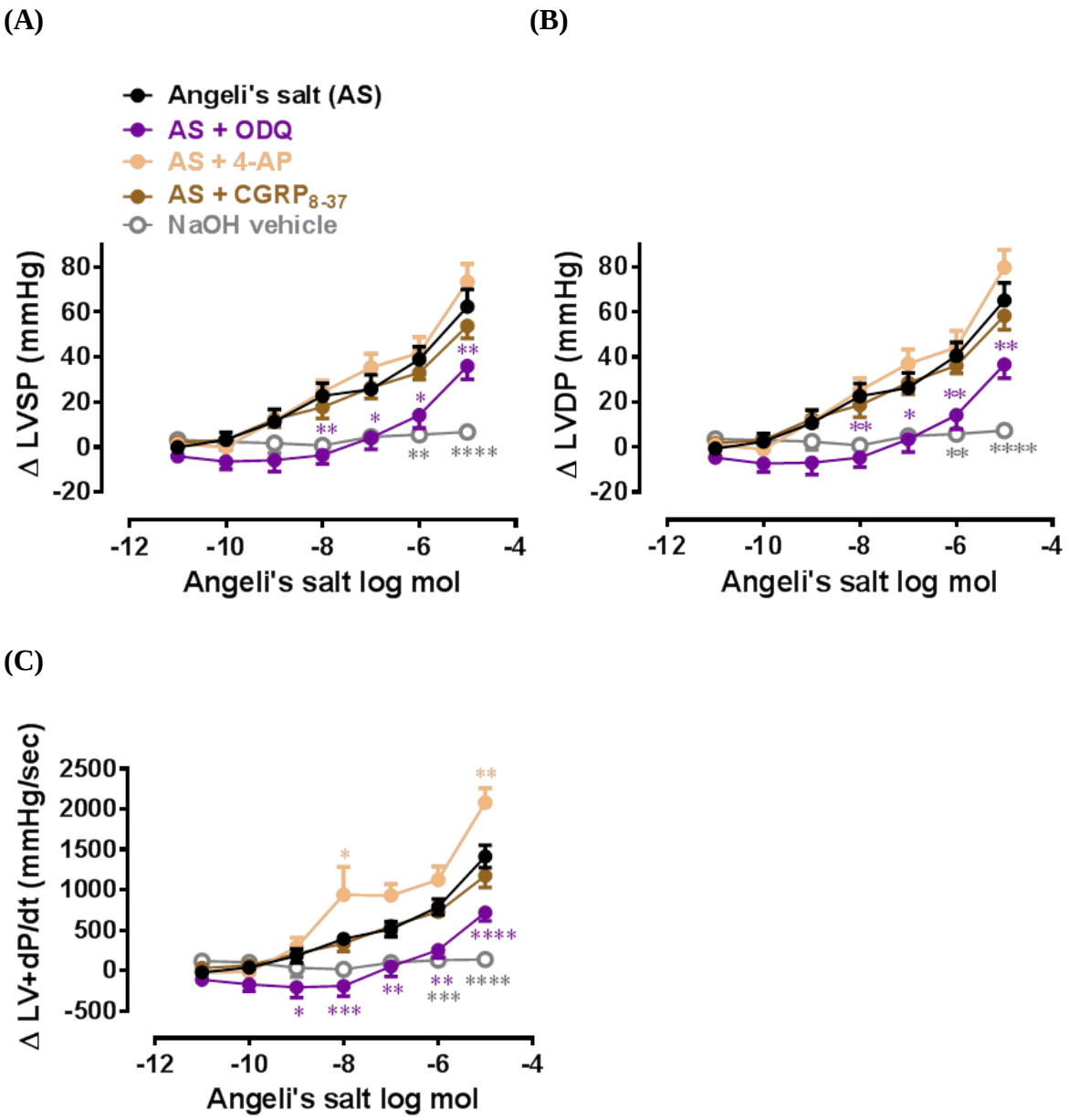

Figure 5.6: Dose-response curves to Angeli's salt (n=8) on **(A)** LVSP, **(B)** LVDP and **(C)** LV+dP/dt in the absence and presence of sGC inhibitor ODQ (10 µM, n=6), the CGRP receptor antagonist $CGRP_{8\text{-}37}$ (0.1 µM, n=5) and the K_v channel inhibitor 4-AP (1 mM, n=5). Serial bolus doses of 10 mM NaOH vehicle are shown for comparison (n=3). *p<0.05, **p<0.01, ***p<0.001, ****p<0.0001 vs Angeli's salt alone on 2-way ANOVA with Bonferroni *post-hoc* test for multiple comparisons. Data are expressed as mean ± SEM.

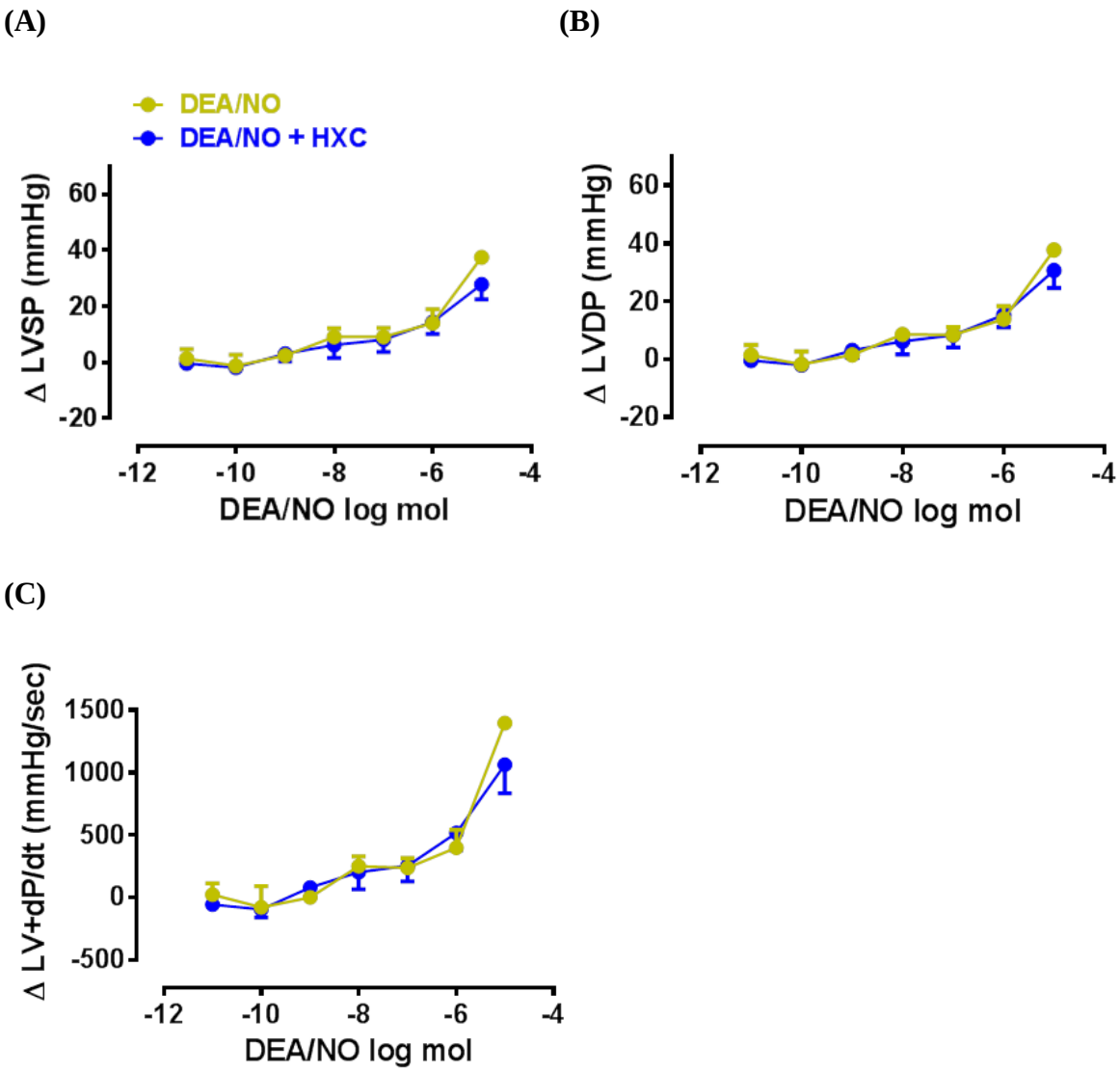

Figure 5.7: Dose-response curves to DEA/NO (n=5) on **(A)** LVSP, **(B)** LVDP and **(C)** LV+dP/dt in the absence and presence of hydroxocobalamin (HXC, 100 µM, n=5). Data are expressed as mean ± SEM.

5.3.3 Contribution of HNO/sGC to the impact of Angeli's salt on cardiac relaxation

Angeli's salt elicited dose-dependent enhancement of myocardial lusitropic function, with progressive reduction in LVEDP (Figure 5.8A) and potentiation of LV-dP/dt (Figure 5.8B). These actions were blunted by L-cysteine, DTT and ODQ (Angeli's salt enhancement of LV-dP/dt was particularly sensitive to these inhibitors), but not by 4-AP (which tended to enhance the Angeli's salt effect) (Figures 5.8 and 5.9). HXC or $CGRP_{8-37}$ was without impact on the cardiac relaxation response to Angeli's salt (Figures 5.8 and 5.9). For comparison, the NO donor DEA/NO also elicited modest improvement in cardiac relaxation as indicated by a slight potentiation in LV-dP/dt (Figure 5.10B), evident at higher doses of DEA/NO, which was also insensitive to HXC (both n=5). None of these inhibitors alone (L-cysteine, DTT, HXC, ODQ, $CGRP_{8-37}$ and 4-AP) affected these parameters of cardiac relaxation alone, prior to the construction of the dose-response curve to Angeli's salt (Table 5.1).

(A)

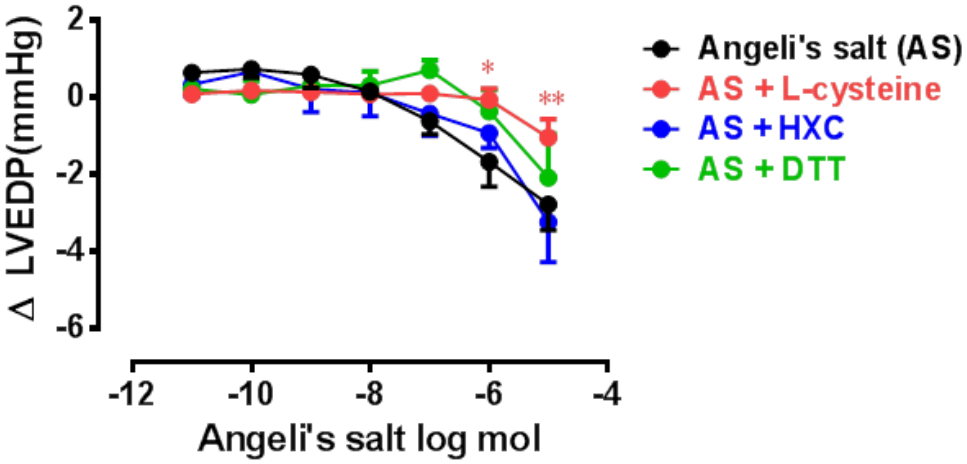

(B)

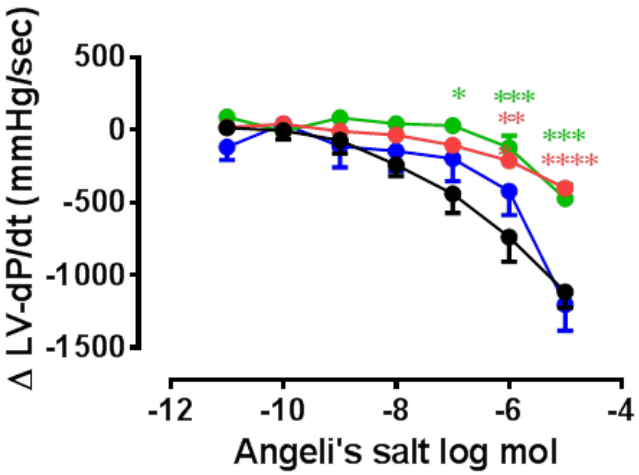

Figure 5.8: Dose-response curves to Angeli's salt (n=8) on **(A)** LVEDP and **(B)** LV-dP/dt in the absence and presence of L-cysteine (n=6), HXC (n=5) or DTT (n=5). *p<0.05, **p<0.01, ***p<0.001, ****p<0.0001 vs Angeli's salt alone on 2-way ANOVA with Bonferroni *post-hoc* test for multiple comparisons. Data are expressed as mean ± SEM.

(A)

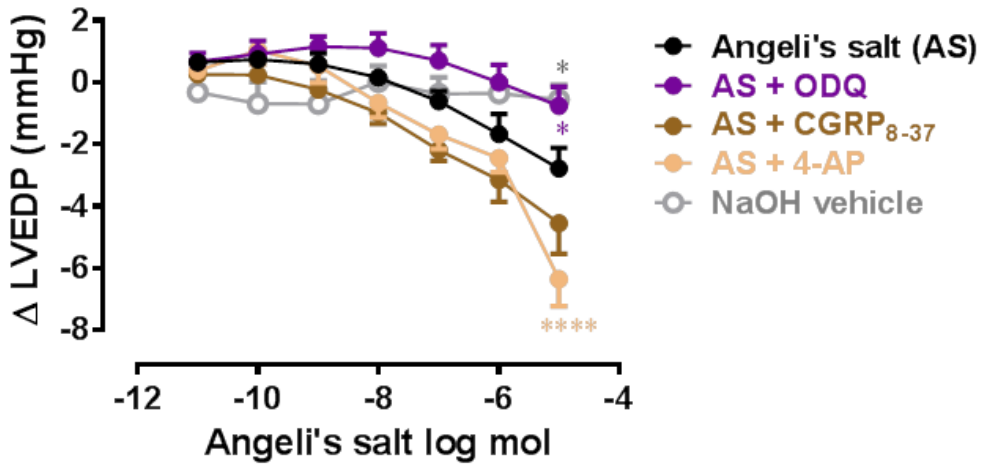

(B)

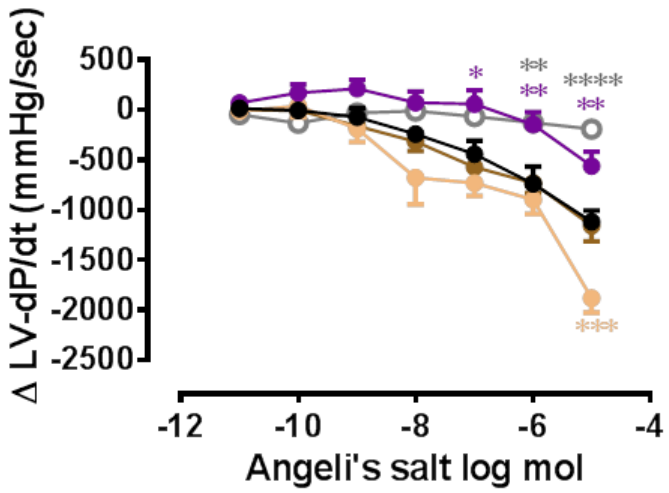

Figure 5.9: Dose-response curves to Angeli's salt (n=8) on **(A)** LVEDP and **(B)** LV-dP/dt in the absence and presence of ODQ (n=6), $CGRP_{8-37}$ (n=5) and 4-AP (n=5). Serial bolus doses of 10 mM NaOH vehicle are shown for comparison (n=3). *p<0.05, **p<0.01, ***p<0.001, ****p<0.0001 vs Angeli's salt alone on 2-way ANOVA with Bonferroni *post-hoc* test for multiple comparisons. Data are expressed as mean ± SEM.

(A)

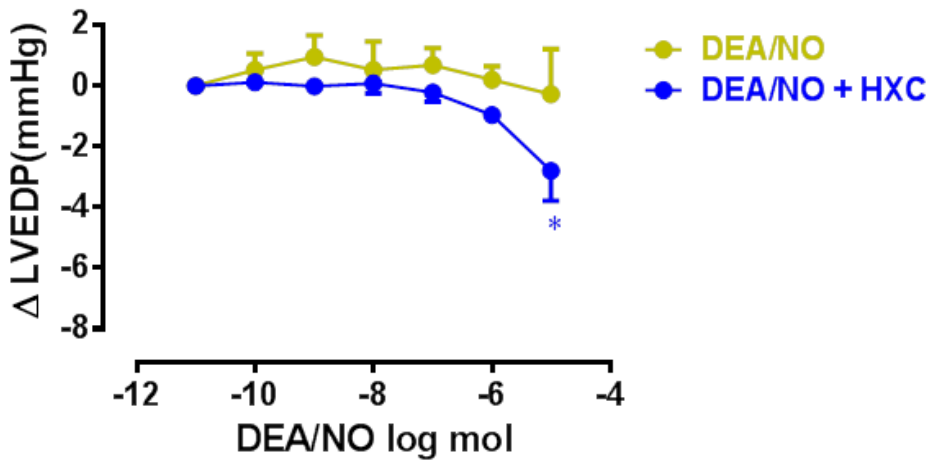

(B)

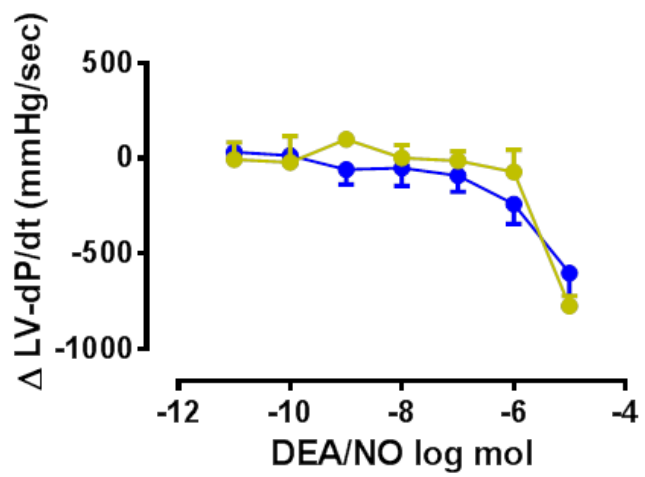

Figure 5.10: Dose-response curves to DEA/NO (n=5) on **(A)** LVEDP and **(B)** LV-dP/dt in the absence and presence of HXC (100 µM, n=5). *p<0.05 vs DEA/NO alone on 2-way ANOVA with Bonferroni *post-hoc* test for multiple comparisons. Data are expressed as mean ± SEM.

5.4 Discussion

The key findings of the present study are that the HNO donor, Angeli's salt, elicits concomitant coronary vasodilator, inotropic and lusitropic actions in the intact rat heart, all of which are mediated by L-cysteine-sensitive, HNO-dependent mechanisms, with a significant contribution mediated via sGC. There appeared to be no role for extracellular oxidation of HNO to NO, or for CGRP receptors or K_v channels in the haemodynamic responses to Angeli's salt. These results are the first evidence that sGC may contribute, at least in part, to the inotropic and/or lusitropic action of HNO in the intact heart.

In this study, it is shown that Angeli's salt induces HNO/sGC-mediated, dose-dependent vasodilatation in the intact rat heart. This is consistent with previous reports in isolated large conduit and smaller resistance-like vessels *in vitro* (Irvine *et al.*, 2003; Favaloro & Kemp-Harper, 2009), as well as in the intact heart studied under conditions of constant flow *ex vivo* (Favaloro & Kemp-Harper, 2007). Although coronary vascular tone under basal, physiological conditions is largely regulated by K_v channels (Leblanc *et al.*, 1994; Shimizu *et al.*, 2000), no role for K_v signalling in the vasodilator response to Angeli's salt in the rat coronary vasculature is observed in this study, consistent with previous observations (Irvine *et al.*, 2003; Favaloro & Kemp-Harper, 2007). In contrast, the vasorelaxant actions of Angeli's salt are mediated, in part, via K_v channels in the mesenteric circulation (Irvine *et al.*, 2003; Andrews *et al.*, 2009), perhaps due to regional differences in K^+ channel subtype distribution. Although K_{ATP} channels may also play a role in coronary vasodilatation in response to Angeli's salt (Favaloro & Kemp-Harper, 2007), this was not investigated in the present study.

Previous studies have suggested a potential contribution of CGRP to the coronary vasodilator response to Angeli's salt, as described in the isolated rat heart studied under constant flow conditions *ex vivo* (Favaloro & Kemp-Harper, 2007), but not to the peripheral arterial or venous vasorelaxation, as reported in a canine model *in vivo* (Paolocci *et al.*, 2001).

Although no contribution of CGRP-dependent signalling to the vasodilator actions of Angeli's salt in the isolated rat heart studied under constant pressure conditions *ex vivo* is detected in this study, the reason for this discrepancy remains unresolved. Angeli's salt co-releases both HNO and nitrite at physiological pH (Miranda *et al.*, 2005b), HNO rather than nitrite likely mediates the vasodilator responses observed here. Firstly, the HNO-selective scavenger, L-cysteine, markedly impaired these responses, and secondly, nitrite has almost negligible dilator activity in the rat coronary vasculature, with 15000-fold less potency than Angeli's salt (Irvine *et al.*, 2003; Favaloro & Kemp-Harper, 2007). Given that a residual, modest Angeli's salt-induced vasodilatation remains in the presence of L-cysteine, there is possibility of oxidation of HNO to NO under the experimental conditions in this study. The inability of the NO-selective scavenger HXC to blunt the vasodilator response to Angeli's salt however suggests this is unlikely, at least in the extracellular milieu. Intriguingly, this vasodilator response was actually augmented in the presence of HXC; whether this reflects a loss of endogenous NO and thus an increased responsiveness of sGC to stimulation by HNO was however not determined.

The positive cardiac inotropic and lusitropic actions of HNO donors are well-established, both in the intact heart *in vivo*, as well as in isolated cardiomyocytes and trabeculae *in vitro* (Paolocci *et al.*, 2001; Tocchetti *et al.*, 2007; Kohr *et al.*, 2010). It is now confirmed that the prototypical HNO donor, Angeli's salt, potently enhances both cardiac contraction and relaxation in the intact rat heart *ex vivo*. These actions were markedly attenuated by both L-cysteine and DTT, specifically implicating HNO. The positive inotropic and dilator effects of Angeli's salt are not likely to be mediated by co-release of nitrite, as this has no appreciable effect on cardiomyocyte contractility (Kohr *et al.*, 2010). Early reports describing the positive inotropic actions implicated the neuropeptide CGRP at least in part in this mechanism of action, based on sensitivity to the CGRP receptor antagonist, $CGRP_{8-37}$

(Paolocci *et al.*, 2001). CGRP itself elicits positive inotropic and lusitropic effects via activation of cAMP/PKA/L-type Ca^{2+} channel signalling (Huang *et al.*, 1999). These actions are however dependent on β-adrenoceptor signalling (Katori *et al.*, 2005), in contrast to those of HNO, which are β-adrenoceptor-independent (Paolocci *et al.*, 2003). Results here are consistent with the absence of a role for CGRP in the inotropic and lusitropic actions of Angeli's salt.

As the myocardial effects of Angeli's salt are all evident even at relatively low doses (e.g. from 10 nmol), concomitant with doses required to elicit vasodilatation, this raises the possibility that these myocardial effects are a secondary effect to vasorelaxation, in accordance with the Gregg effect (Westerhof *et al.*, 2006). The vasodilator response however plateaus at ~1 μmol, whereas the enhancement of left ventricular contractility and relaxation induced by Angeli's salt continue to further progress with increasing doses of the HNO donor, Angeli's salt. Given that previous reports suggest that the vasodilator actions of Angeli's salt are evident at markedly lower concentrations (e.g. 0.1 μM) than required for effects on cardiomyocyte function (e.g. 500 μM) (Favaloro & Kemp-Harper, 2007; Tocchetti *et al.*, 2007), it remains likely that Angeli's salt-mediated vasodilatation occurs at lower concentrations while the contractile effect of Angeli's salt occurs only at higher concentrations. This suggests that the contractile effect of Angeli's salt appears independent of its dilatory effect.

The cardiac inotropic and lusitropic effects of HNO donors have been traditionally attributed to cGMP-<u>independent</u> mechanisms, through a thiol-mediated interaction with the sarcoplasmic reticulum Ca^{2+}-handling proteins, RyR and SERCA (Tocchetti *et al.*, 2007; Kohr *et al.*, 2010). These previous reports concluded that the myocardial actions of HNO were cGMP-independent on the basis of an absence of detectable increases in plasma cGMP *in vivo* (Paolocci *et al.*, 2001), as well as a perceived lack of sensitivity to ODQ (Tocchetti *et*

al., 2007). Of note, the only previous investigation of the role for cGMP in the cardiac inotropic and lusitropic effects of HNO donors utilised isolated cardiomyocytes rather than the intact heart, and the concentration of HNO donor (1 mM) far exceeded that used for ODQ (10 µM) (Tocchetti *et al.*, 2007). ODQ is considered an oxidiser (rather than a competitive inhibitor) of sGC, which irreversibly inhibits the enzyme. There is however one report that suprapharmacological concentrations of Angeli's salt (1 mM) may still be able to stimulate any residual sGC still in its reduced state (Zeller *et al.*, 2009). In the present study, the effects of HNO on left ventricular contractility and relaxation were determined in the intact heart, concomitantly with its vasorelaxant effects. Administration of ODQ under these conditions significantly attenuated (but did not abolish) the left ventricular inotropic and lusitropic effects of Angeli's salt, suggesting for the first time that HNO may mediate a part of these actions via sGC/cGMP-dependent signalling.

Although the impact of both NO and sGC on cardiac contractile function has been previously examined in a broad range of scenarios, no consensus has yet been reached, with negative inotropic (Balligand *et al.*, 1993; Brady *et al.*, 1993; Grocott-Mason *et al.*, 1994; Weyrich *et al.*, 1994; Kojda *et al.*, 1996; Sandirasegarane & Diamond, 1999; Muller-Strahl *et al.*, 2000; Gonzalez *et al.*, 2008; Cawley *et al.*, 2011; Derici *et al.*, 2012), positive inotropic (Klabunde & Ritger, 1991; Smith *et al.*, 1991; Kojda *et al.*, 1995; Kojda *et al.*, 1996; Kojda *et al.*, 1997; Sarkar *et al.*, 2000; Layland *et al.*, 2002; Langer *et al.*, 2003) or no change observed (Ritchie *et al.*, 2006; Ritchie *et al.*, 2009). Indeed, the relationship between NO/sGC and myocardial force may be differentially modulated by concentration, whereby smaller increases in NO/sGC levels elicit positive inotropic effects either secondary to phosphodiesterase-3 inhibition (elevating cAMP), while high concentrations elicit a cGMP-mediated negative inotropic effect, perhaps secondary to formation of S-nitrosothiols on key cardiomyocyte Ca^{2+}-handling proteins such as RyR, SERCA and PLN (Smith *et al.*, 1991;

Kojda *et al.*, 1996; Kojda *et al.*, 1997; Zahradnikova *et al.*, 1997; Paolocci *et al.*, 2000; Layland *et al.*, 2002; Langer *et al.*, 2003; Gonzalez *et al.*, 2007; Rastaldo *et al.*, 2007; Gonzalez *et al.*, 2008; Wang *et al.*, 2008; Ziolo, 2008). It is also likely that distinct cardiomyocyte pools of cGMP also contribute to this lack of consensus with respect to the nature of any possible impact of NO/sGC on inotropic mechanisms, as has been suggested for natriuretic peptide receptors (Qvigstad *et al.*, 2010). There is however consensus with respect to cardiac relaxation, which is enhanced by NO (Paulus *et al.*, 1994; Carnicer *et al.*, 2013). In our study DEA/NO (which releases two NO molecules per molecule of DEA/NO) did tend to enhance systolic function, but this was more modest than that achieved by the equivalent concentration of Angeli's salt (despite it only releasing a single HNO molecule per molecule of Angeli's salt). It has previously been demonstrated that HNO donors such as Angeli's salt and IPA/NO do not increase cardiomyocyte cAMP or CGRP content (Lin *et al.*, 2012; Irvine *et al.*, 2013b).

In this study, the thiols L-cysteine and DTT were similarly effective at blunting the Angeli's salt enhancement of inotropic and lusitropic function at the concentrations used (4 mM vs 0.1 mM). In contrast, only L-cysteine (and not DTT) blunted the vasodilatation response. L-cysteine is conventionally used as an HNO scavenger (Tocchetti *et al.*, 2011), blocking both Angeli's salt-induced coronary vasodilator and positive inotropic actions by removing available HNO. HNO is considered to enhance cardiac contractility and relaxation by inducing a reversible oxidation of key thiol residues on <u>specific</u> cardiomyocyte Ca^{2+} cycling/sensitisation proteins (e.g. RyR and SERCA), without altering net thiol redox status (i.e. GSH/GSSG ratio) (Fukuto & Carrington, 2011). Findings in this study with both thiols are perhaps consistent then with the Angeli's salt-induced vasodilatation dependent on HNO and sGC (but not proteins implicated in Ca^{2+} cycling/sensitisation), whereas its enhancement

of cardiac contractility and relaxation may be mediated at least in part by both sGC-dependent and sGC-independent mechanisms (such as HNO-mediated oxidation of RyR and SERCA).

The thiol modification induced by HNO is quite distinct to that induced by NO. NO leads to S-nitrosation via an indirect action, as it is initially oxidised to nitrous anhydride which then reacts with protein thiol groups to form protein-SNO (Lima *et al.*, 2010; Heinrich *et al.*, 2013). In contrast, the interaction of HNO with thiols is direct and thus extremely rapid (Jackson *et al.*, 2009), first generating the intermediate, N-hydroxysulphenamide, which can then either be irreversibly arranged to form N-hydroxysulphenamide, or alternatively can reversibly interact with an additional thiol, to form a disulphide and hydroxylamine. The predominant thiol modification induced by HNO is thus considered formation of a sulphinamide or disulphide, rather than S-nitrosation (Fukuto & Carrington, 2011). As Angeli's salt only releases NO at a very acidic pH (Miranda *et al.*, 2005b), together with our finding that the coronary vasodilator action of Angeli's salt was not diminished in the presence of the NO scavenger HXC, it is highly unlikely that Angeli's salt will form S-NO in the presence of thiols such as L-cysteine. Thus, in contrast to NO donors, Angeli's salt dose-dependent enhancement of cardiac contractility and relaxation is unlikely to result from S-nitrosation of Ca^{2+}-handling proteins.

In conclusion, the HNO donor Angeli's salt elicits dose-dependent enhancement of left ventricular systolic and diastolic function, with vasodilatation, in the intact rat heart. These effects are all L-cysteine-sensitive and mediated by HNO, with contributions from both sGC-dependent and s-GC-independent mechanisms. No role for CGRP, NO or K_v in Angeli's salt cardiac effects was evident. HNO thus acutely modulates both left ventricular contractile function and left ventricular relaxation, whilst concomitantly unloading the heart. These properties, in combination with the powerful antihypertrophic and superoxide-suppressing

actions we have previously demonstrated, may favour HNO donors as a potential strategy for managing heart failure (alone or in addition to standard care).

Chapter 6

6. The acute improvement in cardiac and vascular function by Angeli's salt after I/R

6.1 Introduction

After an acute episode of myocardial infarction, patients are highly susceptible to heart failure. Several studies have shown that patients with acute heart failure and a lower systolic blood pressure at admission have a higher rate of in-hospital and post-discharge mortality (Gheorghiade *et al.*, 2006; Shiraishi *et al.*, 2011). First-line treatments for acute heart failure are diuretic agents to treat pulmonary oedema which is the most common clinical presentation in heart failure and vasodilators such as glyceryl trinitrate (GTN) or nitroprusside to reduce pre-load and after-load in the heart (McMurray *et al.*, 2012). In cases where there is a low cardiac output and the peripheral vasculature is under-perfused, a positive inotrope will be introduced, commonly dobutamine, a potent β-adrenoceptor agonist (McMurray *et al.*, 2012). Dobutmaine is a well-established therapeutic agent in patients with heart failure, however numerous studies indicate deleterious effects including cardiac arrhythmias (eg. tachycardia) and increased myocardial oxygen consumption that could lead to myocardial ischaemia (Sonnenblick *et al.*, 1979; Monrad *et al.*, 1986; Sato *et al.*, 1997). A higher mortality rate with dobutamine infusion in patients with congestive heart failure compared to placebo grouphas been observed (O'Connor *et al.*, 1999). Further, Unverferth and colleagues showed that patients may develop tolerance to dobutamine after 3 days of continuous infusion (Unverferth *et al.*, 1980).

In addition, a major limitation of treating heart failure patients with nitric oxide (NO) donors such as GTN, to induce vasodilatation is that early development of tolerance occurs to the action of NO donors with loss of effectiveness during sustained treatment may occur (Munzel *et al.*, 2005). This phenomenon is called nitrate tolerance. Nitrate tolerance is associated with increased reactive oxygen species production, endothelial dysfunction and increased sensitivity to vasoconstrictors (Munzel *et al.*, 2005). Pre-treatment of rabbits with GTN increased the vascular production of superoxide anions and this reduced the NO bioavailability and contributed to the attenuated relaxation response to NO donors GTN and 3-morpholino-sydnonimine and acetylcholine (Munzel *et al.*, 1995). Concomitant treatment with antioxidants such as ascorbic acid preserved the sensitivity of the vasculature to NO donors (Bassenge *et al.*, 1998). The vasodilator response to acetylcholine and the vasoconstrictor response to the non-selective inhibitor for nitric oxide synthase (NOS), N-monomethyl-L-arginine (L-NMMA) were also inhibited in the forearm vasculature of healthy male subjects after 6 days with GTN treatment (Gori *et al.*, 2001). Five days of continuous transdermal GTN treatment also resulted in acetylcholine-induced vasoconstriction, instead of endothelium-dependent dilatation suggesting impaired endothelial function (Caramori *et al.*, 1998). The reduction in forearm blood flow induced by angiotensin II and the α-adrenoceptor agonist phenylephrine was enhanced in patients with stable coronary artery disease pre-treated with GTN for a 48-h period compared to the placebo group (Heitzer *et al.*, 1998). This suggests a hypersensitivity to vasoconstrictors with GTN pre-treatment.

In Chapter 5, it is reported that the HNO donor, Angeli's salt simultaneously increases cardiac contractility and coronary flow in normal rat hearts (Chin *et al.*, 2014). Further, Paolocci and colleagues demonstrated that Angeli's salt enhanced cardiac contractility in canine failing hearts to the same extent as in a normal canine heart, despite many defective signalling mechanisms (Paolocci *et al.*, 2003). In contrast, NO donors,

DEA/NO or GTN, either reduced or showed no effect on cardiac contractility in canine failing hearts (Paolocci *et al.*, 2003). In addition, Angeli's salt administration did not induce tachycardia or cardiac arrhythmias in hearts *in vitro* or *in vivo* (Paolocci *et al.*, 2003; Favaloro & Kemp-Harper, 2007). Therefore, the HNO donor Angeli's salt may be a potential therapeutic agent to increase cardiac output and improve blood flow in heart failure. In this study, we tested the hypothesis thatthe cardiac contractile and vasodilator actions of Angeli's salt are preserved in acute heart failure secondary to myocardial I/R.

6.2 Methods

This investigation conforms with the National Health and Medical Research Council of Australia code of practice for the care and use of animals for scientific purposes. All the procedures involved in this project were approved by RMIT University andAlfred Medical Research Educational Precinct Animal Ethics Committees.

6.2.1 Langendorff heart preparations

Hearts isolated from adult male Sprague-Dawley rats (250-300g) anaesthetized with 325 mg/kg sodium pentobarbitone were Langendorff-perfused as described in Chapter 2.3. Rat isolated hearts were perfused at a constant pressure of 45 ± 5 mmHg to achieve a basal coronary flow of about 10 ml/min.

6.2.2 Experimental protocols

After 20 min equilibration, rat isolated hearts were assigned to one of two groups:

sham: hearts were continuously perfused with Krebs' buffer for a total period of 80 min;

I/R: hearts were subjected to 30 min global ischaemia followed by 30 min reperfusion.

Ischaemia and reperfusion were carried out as described in Chapter 2.4.

At 5 min before the completion of 80 min perfusion in sham hearts or 30 min reperfusion in I/R-treated hearts, hearts were infused with the thromboxane A_2 mimetic U46619 (3 μM, 0.1-1.5 ml/min) continuously via a port just above the aortic cannula, to contract the coronary vasculature reducing basal coronary flow rate by ~50% (i.e. from ~10 ml/min to ~5ml/min). A single dose of the vehicle for the HNO donor, Anegli's salt or the NO donor, DEA/NO, 10 mM NaOH or the vehicle for the clinically used inotrope for acute heart failure, dobutamine, Krebs' buffer, was then added to the heart via a second injection port. The construction of the respective dose-response curve to Angeli's salt (1 nmol- 10 μmol), DEA/NO (1 nmol- 1 μmol) or dobutamine (100 pmol- 100 nmol) was then carried out in randomized order as shown in Figure 6.1. The dose-response curve was performed by administering bolus doses of drugs to the heart in increasing doses 1 min apart. A 5 min wash-out with Krebs' buffer was carried out between dose-response curve for each dilator allowing all parameters of contractile function and coronary flow to return to baseline levels.

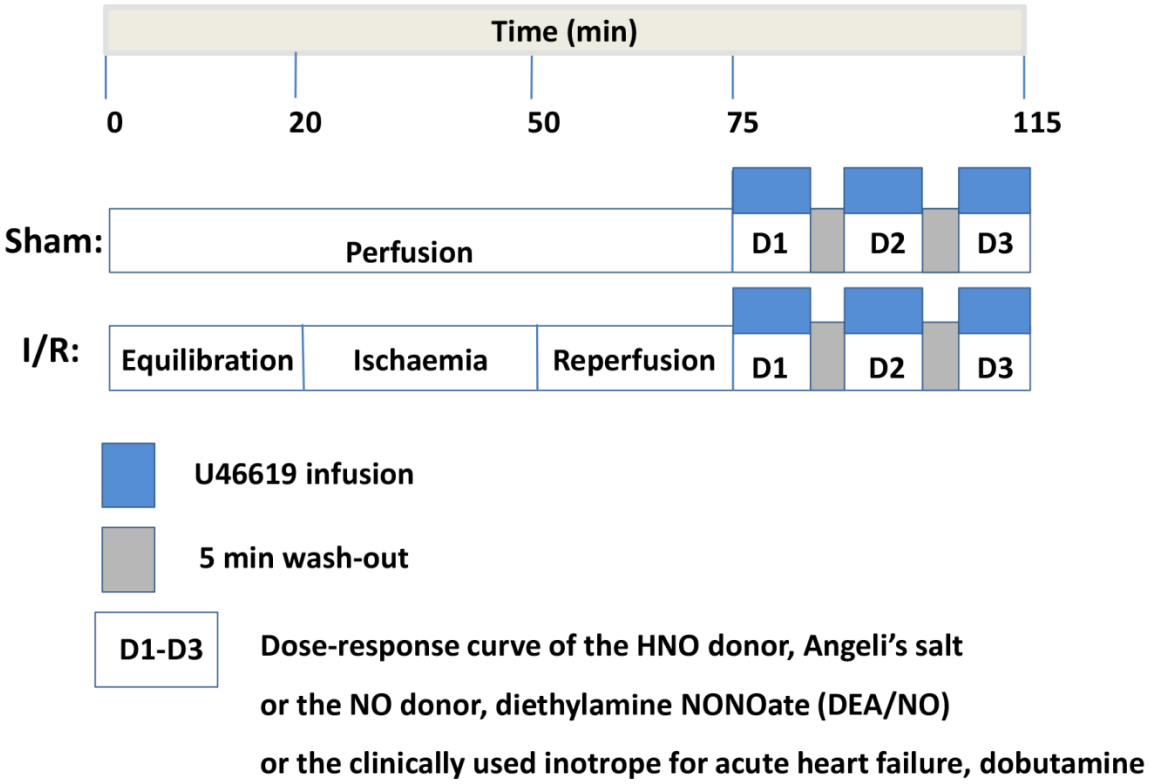

Figure 6.1: Schematic diagram showing the experimental protocol. Rat isolated hearts were subjected to sham or I/R treatment followed by the construction of dose-response curve to the HNO donor, Angeli's salt, NO donor, DEA/NO and clinically used itnotrope for acute heart failure, dobutamine with U46619 pre-constriction in randomized order.

6.2.3 LDH assay

LDH assay was carried out as described in Chapter 2.5. Coronary effluent from sham hearts or I/R-treated hearts was collected at 5 time points (i.e. 51st, 52nd, 55th, 60th, 75th min perfusion in sham hearts and 1, 2, 5, 10 and 15 min reperfusion in I/R-treated hearts).

6.2.4 Assessment of reperfusion-induced arrhythmias

Assessment of reperfusion-induced arrhythmias was performed as described in Chapter 2.8. Experimental records of left ventricular pressure (LVP) from I/R-treated hearts were used to analyse the incidence of arrhythmias. The total duration (in sec) of LVP showing a LVDP <5 mmHg (indicative of ventricular fibrillation) in the first 10 min of reperfusion was measured.

6.2.5 Statistical analysis

All results were expressed as group mean ± SEM, with the number of independent experiments denoted as 'n'. Data analysis was performed using Graphpad Prism® (version 6.0, USA). The vasodilator and cardiac contractile responses to each drug were expressed as percentage change from the baseline value. The difference between the response in control and I/R-treated hearts was analysed using 2-way ANOVA with Sidak's multiple comparisons test. LDH assay and all haemodynamic values were compared using Student's unpaired *t*-test. In all cases, $p<0.05$ was considered statistically significant.

6.2.6 Drugs and reagents

All chemical reagents were purchased from Sigma-Aldrich (St. Louis, MO, USA) and dissolved in distilled water unless otherwise stated. Angeli's salt, DEA/NO and U46619 were

obtained from Cayman Chemical Company (Ann Arbor, MI, USA) and were prepared as described in Chapter 5.2.4. Dobutamine was dissolved in distilled water with gentle heating.

6.3 Results

6.3.1 Basal haemodynamic characteristics in sham and I/R-treated hearts

Basal haemodynamic characteristics of all buffer-perfused rat hearts used in this study, at the end of the 20 min equilibration, prior to any sham or I/R treatment are shown in Table 6.1. There were no significant differences in basal haemodynamic values in sham and I/R-treated groups, although LVSP and LVEDP tended to be higher in I/R-treated hearts.

Table 6.1: Basal haemodynamic characteristics of hearts at the end of 20 min equilibration from sham (n=8) and I/R-treated groups (n=7), prior to any ischaemic insult in the I/R-treated group. Data are expressed as mean ± SEM.

Parameters	**Sham (n=8)**	**I/R (n=7)**
LVSP (mmHg)	73 ± 5	86 ± 5
LVEDP (mmHg)	1.6 ± 3.1	5.9 ± 1.3
LVDP (mmHg)	71 ± 4	80 ± 6
LV+dP/dt (mmHg/s)	2246 ± 126	2218 ± 158
LV-dP/dt (mmHg/s)	-1391 ± 59	-1661 ± 166
Heart rate (beats/min)	253 ± 15	261 ± 7
Coronary flow (ml/min)	9.9 ± 0.3	10.1 ± 0.1

6.3.2 Effect of I/R on cardiac function, cell death and arrhythmias

Haemodynamic values of hearts from sham at the end of the 75 min perfusion (n=8) or I/R-treated hearts at the end of 25 min reperfusion (n=7) were shown in Table 6.2. LVSP and LVEDP were significantly higher in I/R-treated hearts compared to sham ($p<0.001$) while reduced LVDP, LV±dP/dt and coronary flow were observed in I/R-treated hearts at the end of 25 min reperfusion compared to sham hearts at the similar time point ($p<0.05$). The heart rate was not significantly different between the two groups.

Myocardial cell death was assessed by the release of LDH following the loss of membrane integrity in the heart tissue into the coronary effluent. The total release of LDH from hearts subjected to 30 min ischaemia followed by 30 min reperfusion was significantly elevated compared to sham hearts ($p<0.0001$, Figure 6.2).

Early reperfusion-induced ventricular fibrillation occurred in four of the seven hearts subjected to I/R (mean duration of ventricular fibrillation 271 ± 99 sec), but in none of the sham hearts.

Table 6.2: Haemodynamic characteristics of hearts from sham after 75 min perfusion (n=8) and I/R-treated groups after 25 min reperfusion (n=7), prior to the commencement of U46619 infusion and the construction of dose-response curves. *p<0.05, ***p<0.001, ****p<0.0001 vs sham hearts, Student's unpaired *t*-test. Data are expressed as mean ± SEM

Parameters	**Sham (n=8)**	**I/R (n=7)**
LVSP (mmHg)	67 ± 10	119 ± 5 ***
LVEDP (mmHg)	2.4 ± 5	77 ± 4 ****
LVDP (mmHg)	68 ± 6	42 ± 8 *
LV+dP/dt (mmHg/s)	2116 ± 113	971 ± 236 ***
LV-dP/dt (mmHg/s)	-1258 ± 84	-623 ± 129 ***
Heart rate (beats/min)	229 ± 18	181 ± 30
Coronary flow (ml/min)	9.1 ± 0.7	1.7 ± 0.6 ****

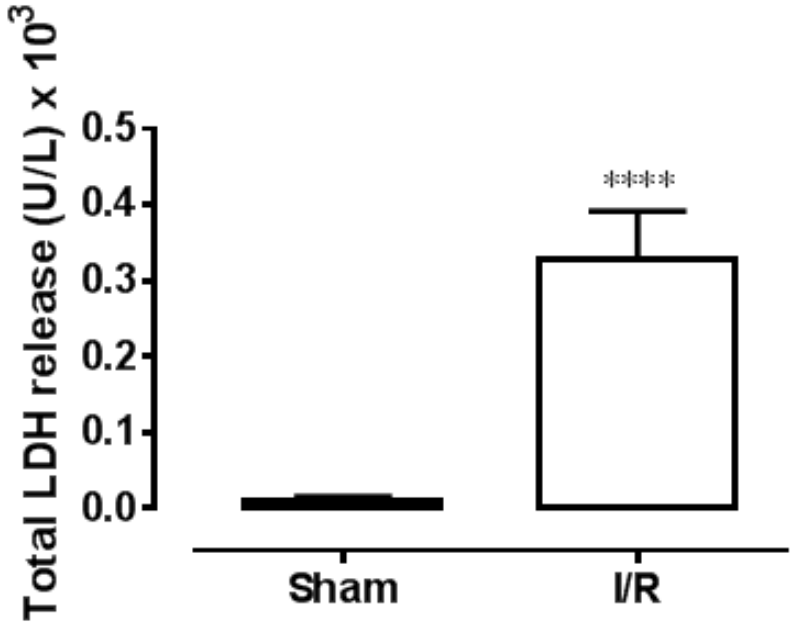

Figure 6.2: Total lactate dehydrogenase (LDH) release after 80 min perfusion in sham hearts (n=8) and hearts subjected to 30 min ischaemia followed by 30 min reperfusion (n=7). ****p<0.0001 vs sham, Student's unpaired *t*-test. Data are expressed as mean ± SEM.

6.3.3 Vasodilator action of Angeli's salt, DEA/NO and dobutamine in sham and I/R-treated hearts

In sham hearts, the HNO donor, Angeli's salt (1 nmol-10 μmol) and the NO donor, DEA/NO (1 nmol-1 μmol) caused a dose-dependent vasodilatation in the coronary vasculature pre-constricted with U46619 (Figures 6.3A and B). There was a ~80% increase in flow at highest doses, 10 μmol and 1 μmol of Angeli's salt and DEA/NO respectively. Bolus addition of dobutamine at lower doses (0.1-1 nmol) reduced flow, while higher doses of dobutamine (10-100 nmol) induced vasodilatation in sham hearts (Figure 6.3C). The increase in flow by dobutamine was much less (by ~50%) than that induced by Angeli's salt and DEA/NO.

In hearts subjected to 30 min ischaemia and 30 min reperfusion, the vasodilator action of Angeli's salt and dobutamine was preserved (Figures 6.3A and C). In contrast, I/R significantly impaired the increase in flow by DEA/NO by ~50% compared to sham hearts ($p<0.05$, Figure 6.3B).

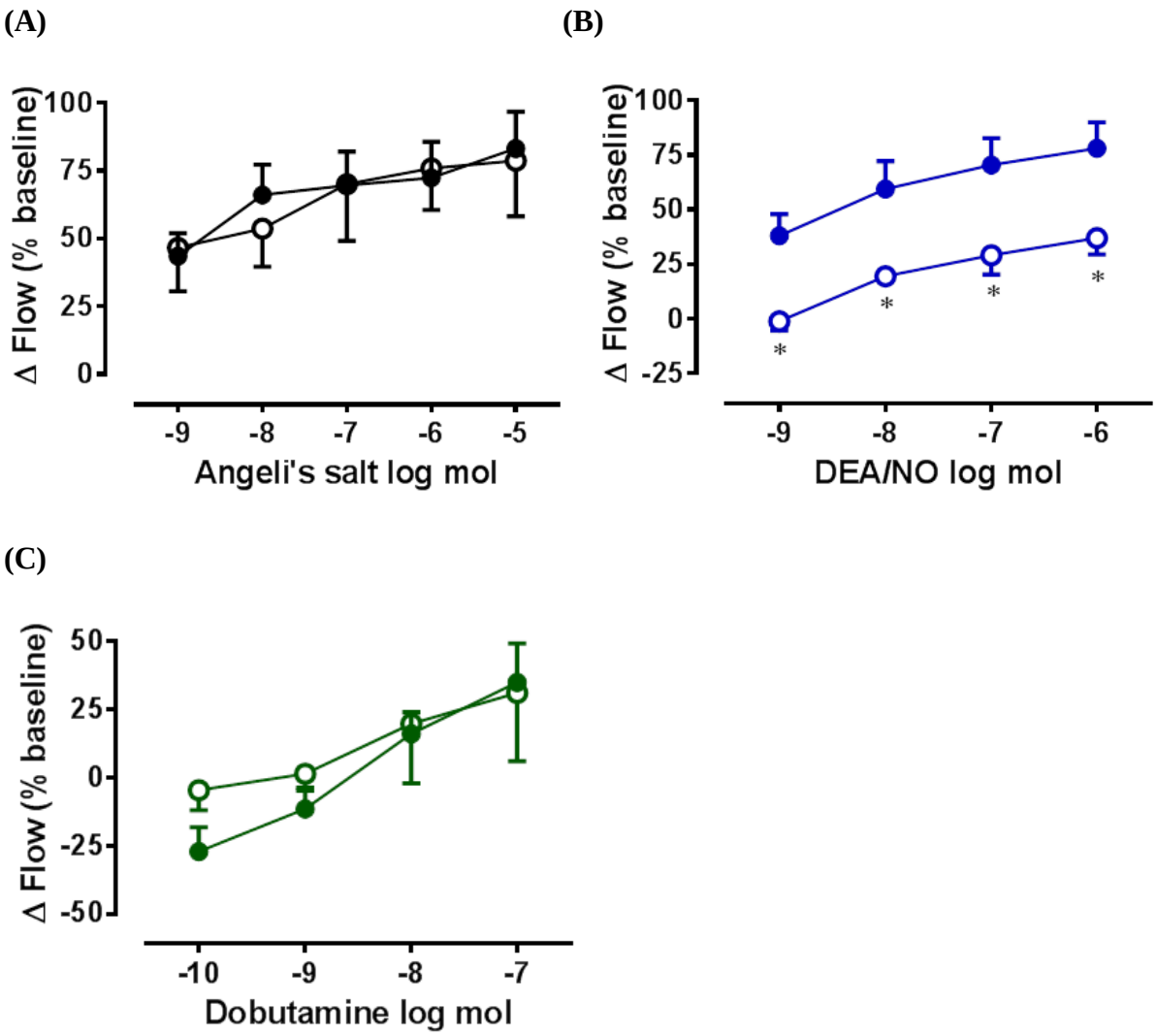

Figure 6.3: The vasodilator response to **(A)** Angeli's salt, **(B)** DEA/NO and **(C)** dobutamine in rat isolated hearts perfused for 80 min with Krebs' buffer (filled symbols, n=8) or subjected to 30 min ischaemia and 30 min reperfusion (open symbols, n=7). *$p<0.05$ vs sham hearts, 2-way ANOVA with Sidak's multiple comparisons test. Data are expressed as mean ± SEM.

6.3.4 Positive inotropic action of Angeli's salt, DEA/NO and dobutamine in sham and I/R-treated hearts

In sham hearts, Angeli's salt caused a dose-dependent increase in cardiac contraction (Figures 6.4A, 6.5A and 6.6A). Angeli's salt at the highest dose used in this study (10 μmol), increased LVSP, LVDP and LV+dP/dt by ~80% of the basal value. Similarly, dobutamine exerted a positive inotropic action in sham hearts (Figures 6.4C, 6.5C and 6.6C). The maximum increase in LVSP, LVDP and LV+dP/dt by 10 nmol of dobutamine was ~60% of basal values (Figures 6.4C and 6.5C). Conversely, DEA/NO had no significant effect on cardiac contraction in sham hearts ((Figures 6.4B, 6.5B and 6.6B).

In I/R-treated hearts, the increase in cardiac contraction caused by Angeli's salt was significantly reduced by ~80% ($p<0.0001$, Figures 6.4A, 6.5A and 6.6A). Similarly, the maximum increase in cardiac contraction caused by dobutamine was significantly reduced by ~75% in I/R-treated hearts ($p<0.001$, Figures 6.4C, 6.5C and 6.6C). I/R caused a reduction in LV+dP/dt when DEA/NO at 1 μmol was administrated ($p<0.05$, Figure 6.6B).

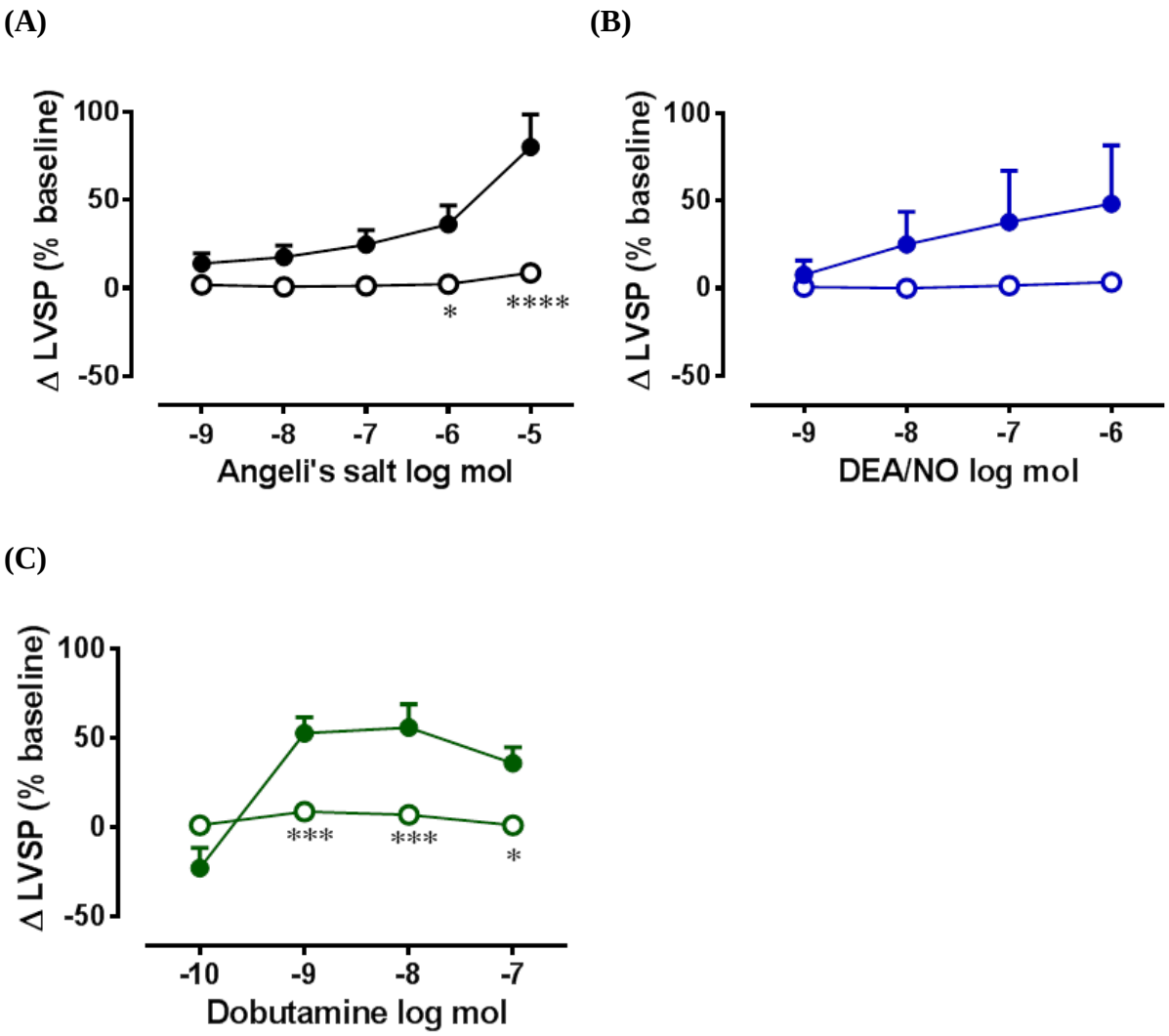

Figure 6.4: The inotropic action expressed as a percentage change in LVSP exerted by **(A)** Angeli's salt, **(B)** DEA/NO and **(C)** dobutamine in rat isolated hearts perfused with 80 min Krebs' buffer (filled symbols, n=8) or subjected to 30 min ischaemia and 30 min reperfusion (open symbols, n=7). *p<0.05, ***p<0.001, ****p<0.0001 vs sham hearts, 2-way ANOVA with Sidak's multiple comparisons test. Data are expressed as mean ± SEM.

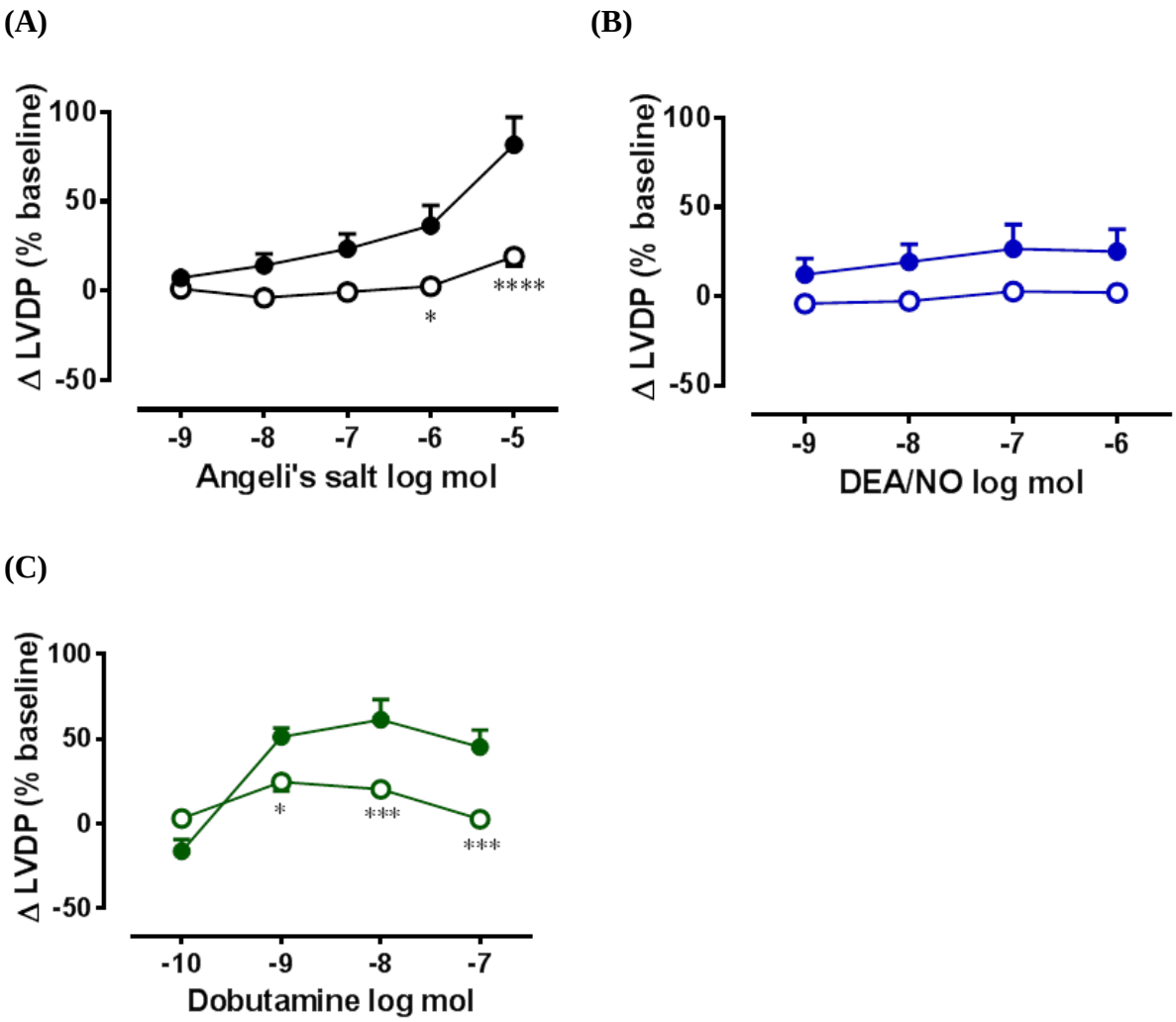

Figure 6.5: The inotropic action expressed as a percentage change in LVDP exerted by **(A)** Angeli's salt, **(B)** DEA/NO and **(C)** dobutamine in rat isolated hearts perfused with 80 min Krebs' buffer (filled symbols, n=8) or subjected to 30 min ischaemia and 30 min reperfusion (open symbols, n=7). *p<0.05, ***p<0.001, ****p<0.0001 vs sham hearts, 2-way ANOVA with Sidak's multiple comparisons test. Data are expressed as mean ± SEM.

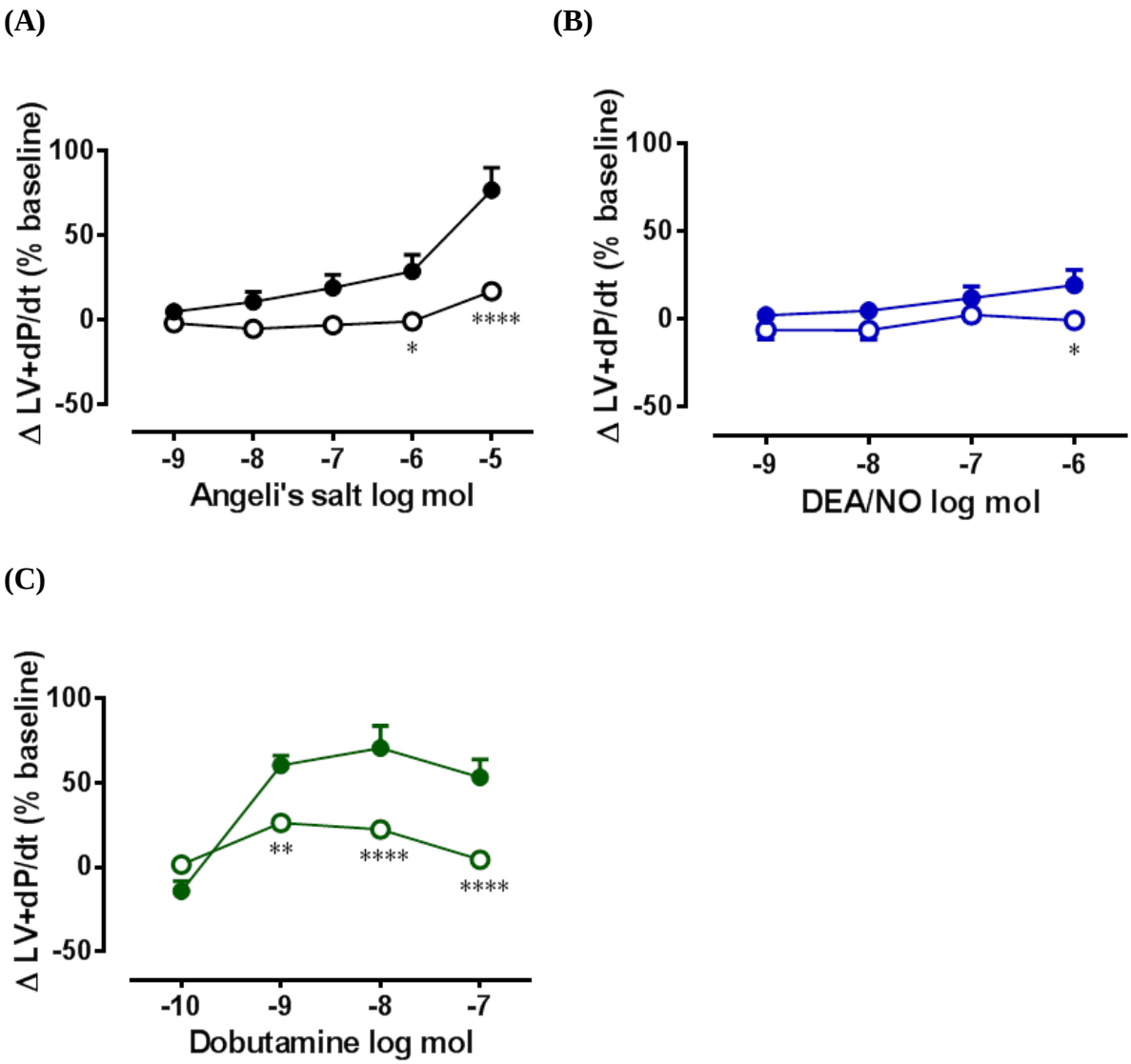

Figure 6.6: The inotropic action expressed as a percentage change in positive rate of change of left ventricular pressure (LV+dP/dt) exerted by **(A)** Angeli's salt, **(B)** DEA/NO and **(C)** dobutamine in rat isolated hearts perfused with 80 min Krebs' buffer (filled symbols, n=8) or subjected to 30 min ischaemia and 30 min reperfusion (open symbols, n=7). *p<0.05, **p<0.01, ***p<0.001, ****p<0.0001 vs sham hearts, 2-way ANOVA with Sidak's multiple comparisons test. Data are expressed as mean ± SEM.

6.3.5 Cardiac relaxation caused by Angeli's salt, DEA/NO and dobutamine in sham and I/R-treated hearts

In sham hearts, Angeli's salt also caused a dose-dependent increase in cardiac relaxation (Figures 6.7A and 6.8A). Angeli's salt at 10 μmol, improved LV-dP/dt by ~55% of the basal value (Figure 6.8A). Similarly, dobutamine increased cardiac relaxation in sham hearts (Figures 6.7C and 6.8C). The maximum improvement in LV-dP/dt by dobutamine at 10 nmol was ~125% of the basal value (Figures 6.8C). DEA/NO had no significant effect on cardiac relaxation in sham hearts ((Figures 6.7B and 6.8B).

In I/R-treated hearts, the increase in cardiac relaxation caused by Angeli's salt and dobutamine was significantly impaired. The improved LV-dP/dt caused by Angeli's salt (10 μmol) was abolished by I/R ($p<0.01$, Figure 6.8A), however the change in LVEDP induced by Angeli's salt in I/R-treated hearts was not different from sham hearts (Figure 6.7A). The maximum enhancement in LV-dP/dt by 10 nmol dobutamine was also impaired by 50% in I/R-treated hearts ($p<0.001$, Figure 6.8C), and the reduction in LVEDP (suggesting better cardiac relaxation) caused by dobutamine was almost abolished in I/R-treated hearts (Figure 6.7C).

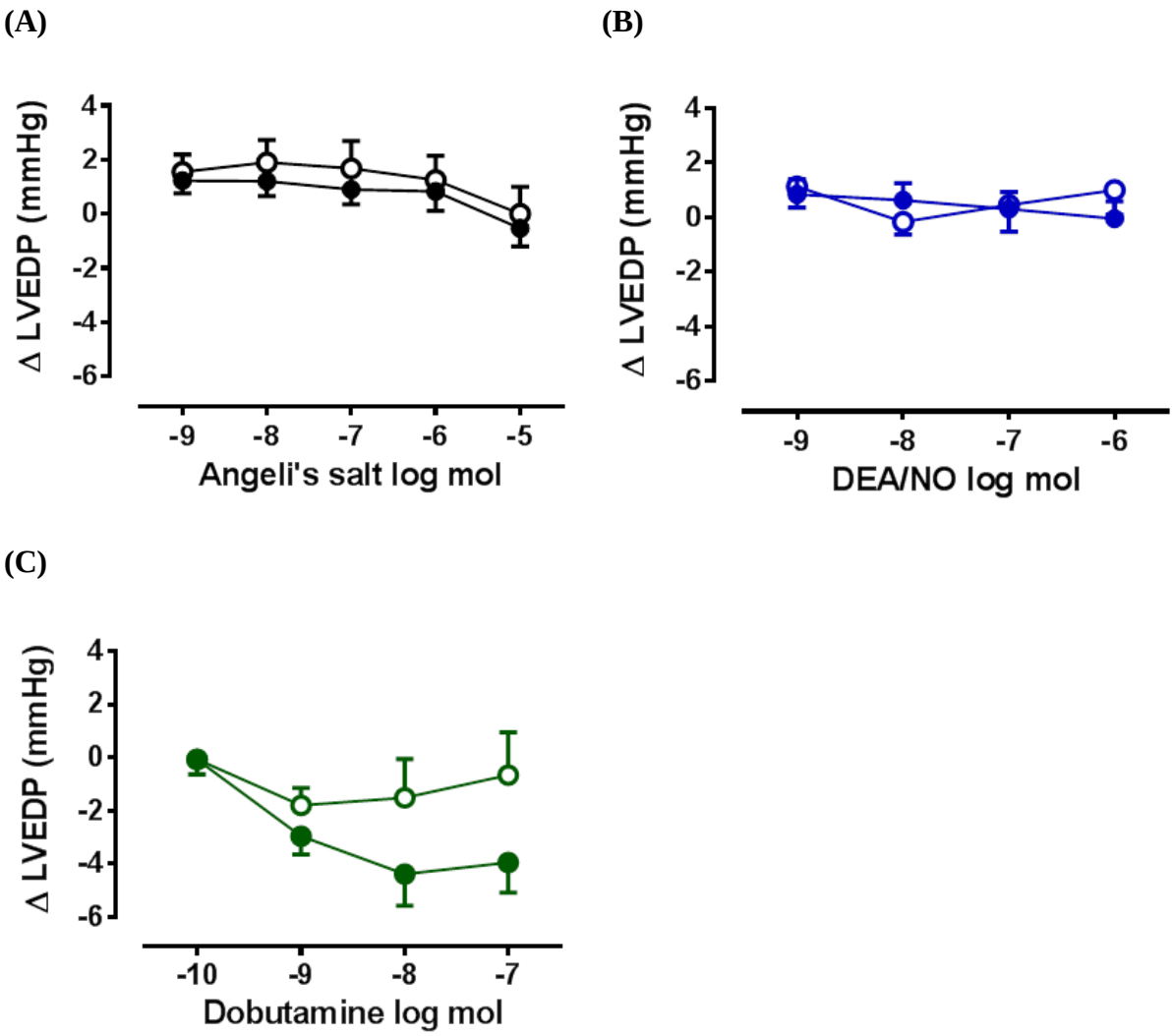

Figure 6.7: The effect of 30 min ischaemia and 30 min reperfusion (open symbols, n=7) and 80 min perfusion in sham hearts (filled symbols, n=8) on the cardiac relaxation expressed as a change in LVEDP affected by **(A)** Angeli's salt, **(B)** DEA/NO and **(C)** dobutamine. 2-way ANOVA with Sidak's multiple comparisons test, p=ns. Data are expressed as mean ± SEM.

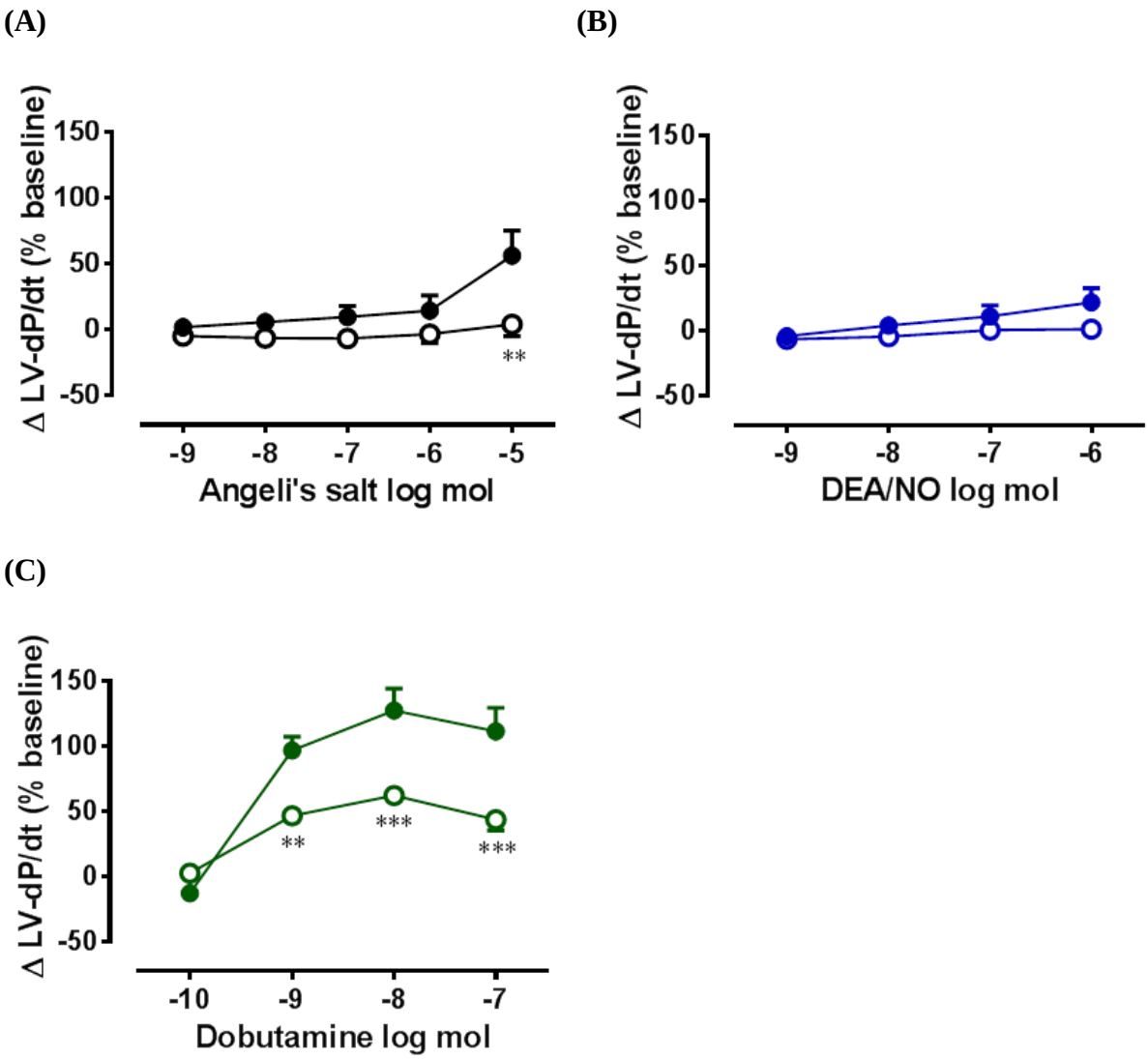

Figure 6.8: The effect of 30 min ischaemia and 30 min reperfusion (open symbols, n=7) and 80 min perfusion in sham hearts (filled symbols, n=8) on the cardiac relaxation expressed as a percentage change in negative rate of change of left ventricular pressure (LV-dP/dt) affected by **(A)** Angeli's salt, **(B)** DEA/NO and **(C)** dobutamine. **p<0.01, ***p<0.001 vs sham hearts, 2-way ANOVA with Sidak's multiple comparisons test. Data are expressed as mean ± SEM.

6.3.6 Heart rate response to Angeli's salt, DEA/NO and dobutamine in sham and I/R-treated hearts

In sham hearts, both Angeli's salt and dobutamine increased heart rate while DEA/NO had no effect (Figures 6.9A and C). The increase in heart rate caused by Angeli's salt was not affected by I/R while I/R increased the dobutamine-induced tachycardia ($p<0.01$, Figure 6.9C). A reduction in heart rate was observed at the highest dose of DEA/NO (1 μmol) in I/R-treated hearts compared to sham hearts ($p<0.001$, Figure 6.9B).

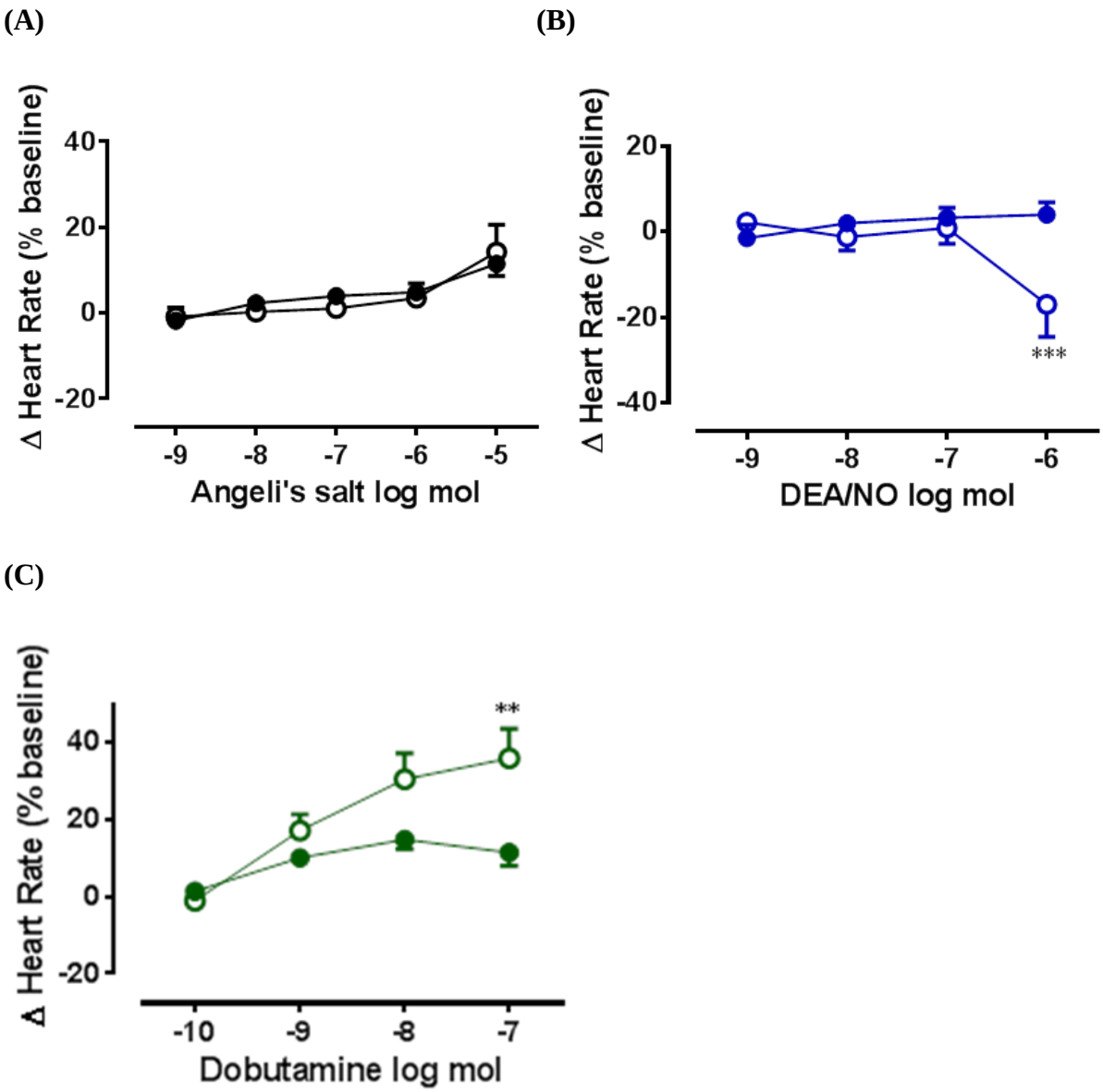

Figure 6.9: The effect of 30 min ischaemia and 30 min reperfusion (open symbols, n=7) and 80 min perfusion in sham hearts (filled symbols, n=8) on the heart rate affected by **(A)** Angeli's salt, **(B)** DEA/NO and **(C)** dobutamine. **p<0.01, ***p<0.001 vs sham hearts, 2-way ANOVA with Sidak's multiple comparisons test. Data are expressed as mean ± SEM.

6.4 Discussion

The key findings of this study are that the vasodilator action of the HNO donor, Angeli's salt, but not the NO donor, DEA/NO, was preserved in hearts after I/R. Both the cardiac contractile action of Angeli's salt and dobutamine were markedly impaired by I/R while the dobutamine-induced tachycardia was exacerbated in I/R-treated hearts.

After myocardial I/R, endothelial dysfunction has been reported to occur due to a decrease in NO availability consequent to oxygen-derived free radical generation during reperfusion (Lefer *et al.*, 1991; Hein *et al.*, 2003; Seal & Gewertz, 2005; Rani *et al.*, 2013). This results in impaired endothelium-dependent vasorelaxation after I/R and likely contributes to increased accumulation of neutrophils in the microvasculature which can form aggregates with platelets that plug capillaries, further impairing coronary flow to the myocardium (Schwartz & Kloner, 2012). This restricts blood flow to the myocardium even after a revascularization strategy has been performed, a condition called "no-reflow" phenomenon. Galiuto and colleagues reported that in 24 patients with acute myocardial infarction, no-reflow, measured using myocardial contrast echocardiography 24 h after successful percutaneous coronary intervention, was detected in 65% of patients (Galiuto *et al.*, 2003). At one month follow-up, sustained no-reflow with left ventricle remodelling was observed in 50% of these patients (Galiuto *et al.*, 2003). A pharmacological intervention to restore the blood flow to the basal level after I/R is desirable.

In this study, Angeli's salt and DEA/NO were both effective dilators of coronary vasculature in the normal rat intact heart. The dilator response to Angeli's salt was preserved after I/R, in contrast to DEA/NO where responses were markedly impaired. One reason for this discrepancy could be the increased oxidative stress after I/R. It is reported that oxidative stress remained elevated and a marked reduction in endogenous antioxidant enzymes level was present up to weeks after reperfusion in hearts after acute myocardial infarction (Hill &

Singal, 1996). Studies have shown that HNO is resistance to scavenging by superoxide anions while NO reacts readily with reactive oxygen species resulting in the formation of the highly reactive species peroxynitrite which is cytotoxic (Miranda *et al.*, 2002). We also reported in rat isolated aorta with pyrogallol-induced increased oxidative stress, the vasodilator action of Angeli's salt was unaffected while the dilator action to DEA/NO was attenuated (Leo *et al.*, 2012). In the same study, it is also reported that in diabetic rats, where increased vascular oxidative stress is evident, endogenous NO-mediated vasorelaxation was impaired while the HNO-mediated relaxation was preserved (Leo *et al.*, 2012). The dilator response to Angeli's salt in isolated aorta from angiotensin II-induced hypertensive mice, where superoxide level is usually increased, is also preserved (Wynne *et al.*, 2012). The vascular action of NO donors in hypertension is however controversial. A preserved dilator response to the NO donor, sodium nitroprusside in isolated aorta from spontaneously hypertensive rats compared to that in normotensive rats was reported (Fukami *et al.*, 1998). In isolated perfused mesenteric arteries from rats with portal hypertension, the vasodilator response to the NO donor, 3-morpholino-sydnonimine was enhanced compared to the control (Heinemann & Stauber, 1996). A recent study by Irvine and colleagues has demonstrated that the vasodepressor ability of Angeli's salt and DEA/NO was also preserved in conscious hypertensive rats (Irvine *et al.*, 2013a). In contrast, in isolated aorta from renal hypertensive rats, the dilator action to sodium nitroprusside was impaired (Bonaventura *et al.*, 2011). Elevation of intra-luminal pressure in resistance arteries from 50 mmHg to 120 mmHg for 1 h before resetting to basal 50 mmHg attenuated the vasodilator response to the NO donor, S-nitroso-N-acetyl-D,L-penicillamine (Christensen *et al.*, 2007). This impaired activity was due to the increased formation of superoxide anions by NADPH oxidase in response to elevated intra-luminal pressure (Christensen *et al.*, 2007).

Both Angeli's salt and DEA/NO induces vasodilatation via a sGC-dependent signalling pathway (Chin *et al.*, 2014), activating sGC by interacting with the iron-containing haem protein in the sGC forming a ferrous-nitrosyl complex (Miranda *et al.*, 2003a; Stasch *et al.*, 2006). It was reported that HNO preferentially targets ferric ion (Fe^{3+}) which predominates in diseased states where there is high oxidative stress (Miranda *et al.*, 2003b; Stasch *et al.*, 2006). NO, in contrast has a preferential affinity for ferrous ion (Fe^{2+}) and has limited reaction with Fe^{3+} (Miranda *et al.*, 2003b; Stasch *et al.*, 2006). In patients with acute heart failure and peripheral oedema, resistance to glyceryl trinitrate treatment to reduce systemic vascular resistance has been reported (Magrini & Niarchos, 1980). It is proposed that the oxidation of the sGC due to increased oxidative stress in acute heart failure (or in the setting of I/R), shifted the redox state of iron in the prosthetic haem from Fe^{2+} (ferrous haem) to Fe^{3+} (ferric haem), and resulted in this sGC-NO-resistant state (Münzel *et al.*, 2007). A further advantage of HNO is the absence of tolerance. It is reported that tolerance to GTN treatment (where improved haemodynamic variables including pulmonary wedge pressure and right atrial pressure was lost and levels returned to baseline values) was seen within the first 24 h of therapy in patients with congestive heart failure (Elkayam *et al.*, 1992). Treatment with HNO, which is able to react with oxidised sGC and does not develop tolerance to its own action may be favourable over NO to increase venous compliance in this disease setting (Irvine *et al.*, 2007).

The cardiac contractile response to both Angeli's salt and dobutamine after global I/R was markedly impaired. HNO released from Angeli's salt is reported to exert its positive inotropic effect and improved cardiac relaxation by acting directly on sarcoplasmic reticulum proteins (i.e. SERCA, RyR and PLN) via a thiol-interaction (Tocchetti *et al.*, 2007; Froehlich *et al.*, 2008). Dobutamine which is a β1-adrenoceptor agonist, exerts positive inotropic and cardiac relaxation action via the activation of the cAMP/PKA-dependent signalling pathway

(Steinberg, 1999). The activation of PKA leads to the phosphorylation of regulatory proteins involved in cardiac excitation-contraction coupling including L-type Ca^{2+} channels and sarcoplasmic reticulum proteins and causes cardiac contraction and relaxation (Steinberg, 1999). The reduced number of intact sarcoplasmic reticulum proteins and impaired Ca^{2+} uptake and release activities in rat isolated hearts after acute myocardial infarction, as a consequence of increased oxidative stress during I/R, have been reported (Osada *et al.*, 1998; Temsah *et al.*, 2000; French *et al.*, 2006). In female guinea pigs, reduced β-adrenoreceptor binding affinity and impaired sensitivity to β-adrenergic stimulation of the surviving, non-infarcted myocardium 3 days post acute myocardial infarction have also been reported (Baumann *et al.*, 1981). The blunted response to dobutamine in hearts after I/R is also consistent with previous finding by Vleeming and colleagues (Vleeming *et al.*, 1991). These defective mechanisms may contribute to decreased cardiac contractile response to Angeli's salt and dobutamine after I/R.

Although depressed β-adrenergic stimulation after myocardial I/R is reported, electrophysiological disturbances resulting in ventricular tachycardia and fibrillation, caused by elevated cAMP levels and subsequent increase in cytosolic Ca^{2+} concentration in hearts after l/R have also been reported (Podzuweit *et al.*, 1978; Lubbe *et al.*, 1992). In this study, dobutamine which is able to increase the level of cAMP in the heart may worsen these electrophysiological changes and result in cardiac arrhythmias. By contrast, Angeli's salt-induced tachycardia was not affected by I/R. In our previous study, we have reported that the Angeli's salt-induced tachycardia was independent of HNO as the presence of the HNO scavenger, L-cysteine had no effect on the Angeli's salt-induced tachycardia in rat intact hearts (Chin *et al.*, 2014). In addition, infusion of Angeli's salt in dog failing hearts *in vivo* did not cause any cardiac arrhythmias (Paolocci *et al.*, 2003). This is favourable to prevent the

adverse effect of arrhythmias that occur with most of current clinically used inotropes including dobutamine and levosimendan (Mebazaa *et al.*, 2007).

In conclusion, one beneficial action of Angeli's salt is its coronary vasodilator capacity which importantly was maintained after I/R. The positive inotropic action of Angeli's salt was impaired by I/R similarly to observations with dobutamine, an agent currently used to treat cardiogenic shock in patients with acute heart failure. The post-acute myocardial infarction dilator capacity plus the inotropic action suggest Angeli's salt may have advantages over dobutamine.

Chapter 7

7. General Discussion

7.1 The effect of DiOHF on the temporal change in the expression of pro-injurious and pro-survival kinases during myocardial I/R

Early reperfusion of the myocardium after a prolonged period of ischaemia is essential for myocardial salvage; however this reperfusion strategy can itself induce myocardial injury and reduce the benefit of myocardial reperfusion. Cardioprotection using pharmacological or non-pharmacological interventions reduces infarct size and improves post-ischaemic cardiac contractile function in experimental models of I/R suggesting that this reperfusion injury is not inevitable and can be reduced with cardioprotective interventions. Unfortunately, there is no treatment that has achieved successful outcomes in the clinical setting, therefore, the development of a novel cardioprotective agent to reduce I/R injury may improve patient outcomes after I/R.

It is now evident that DiOHF confers cardioprotection against myocardial I/R injury. DiOHF exerted cardioprotection against I/R injury in rodent isolated hearts and large animals such as sheep and goats *in vivo* (Wang *et al.*, 2004; Wang *et al.*, 2009; Qin *et al.*, 2011). DiOHF is an effective antioxidant and vasodilator and an earlier report suggested that DiOHF-induced cardioprotection is mediated by its ability to scavenge superoxide radicals that are found abundantly during myocardial I/R (Wang *et al.*, 2004). DiOHF also increases NO bioavailability and preserves vasodilator reserve after I/R (Chan *et al.*, 2003). Increasing evidence has demonstrated that DiOHF can protect against I/R injury independent of its antioxidant and dilator effects. DiOHF may act as a signalling molecule to activate a series

signalling pathways resulting in cell survival or cell death. Together with the study by Lim and colleagues (Lim *et al.*, 2013), we found that DiOHF-induced cardioprotection during 5 min and 30 min reperfusion may be mediated by distinct signalling mechanisms. During 5 min reperfusion, we found that DiOHF reduced the activation of PLN (Chapter 4) and this may prevent the sarcoplasmic reticulum Ca^{2+} leak resulting in arrhythmias and mPTP opening. Indeed, it is reported that DiOHF treatment during ischaemia and before reperfusion inhibited the Ca^{2+}-induced mPTP opening in isolated cardiac mitochondria after ischaemia during 15 min reperfusion in anaesthetized rats (Woodman *et al.*, 2014). Mitochondrial PTP opening which is a major mediator of cell death occurs within minutes after the onset of reperfusion and this marks the first window of opportunity for cardioprotection. In the later phase of cardioprotection (30 min reperfusion), DiOHF prevented cell death by inhibiting the activation of kinases involved in apoptosis or necrosis such as JNKs and p38 MAPK. I/R-induced activation of protective kinases Erk 1/2 and STAT3, but not Akt was sustained with DiOHF treatment and this may be important for the protective action of DiOHF in myocardial I/R. The reduction in myocardial infarct size and cell death after I/R *in vivo* and *in vitro* respectively was evident with DiOHF treatment at 30 min reperfusion. It has also been reported that DiOHF may bind directly onto the multi-functional enzyme, CaMKII (which is the upstream kinase of JNKs and p38 MAPK) and inhibit its activation. This resulted in subsequent inhibition of the activation of JNK and p38 MAPK signalling pathways. However, further experiments are required to confirm this observation.

The clinical application of flavonol as an adjunctive therapy for I/R injury in humans is limited due to their poor water solubility. Recently, the development of the water soluble derivative of DiOHF, NP202, which has the similar cardioprotective capacity as DiOHF has the potential as a therapeutic agent for clinical use (Thomas *et al.*, 2011; Lim *et al.*, 2013). Although there is improvement in the treatment for acute myocardial I/R injury, the prognosis

of patients remains poor. This may be due to the presence of many complications of acute myocardial infarction.

7.2 The effect of I/R on the cardiac and vascular actions by the HNO donor, Angeli's salt

One of the major complications of acute myocardial I/R is acute heart failure. A major manifestation of acute heart failure is systolic dysfunction where the heart fails to pump blood to meet the requirement of metabolizing tissues and this can result in multiple organ failure. A number of inotopic agents have been introduced to improve ejection fraction in patients with acute heart failure, however the prognosis of these patients remains poor as these inotropic agents can result in adverse effects particularly cardiac arrhythmia. Therefore, there is a necessity to develop new inotropic agents without causing any adverse effects to improve the prognosis of patients with acute heart failure.

HNO which is a positive inotrope may have advantages over dobutamine as the HNO donor, Angeli's salt- (but not dobutamine) induced tachycardia, was not aggravated by I/R (Chapter 6). In addition, the Angeli's salt–induced tachycardia in normal rat hearts was not affected by the presence of the HNO scavenger suggesting that HNO has no effect on the increased heart rate by Angeli's salt (Chapter 5). Increased oxidative stress in hearts after I/R may react with the NO produced by DEA/NO and reduce the dilator action of DEA/NO whereas the vascular action of Angeli's salt was not affected. This suggests that Angeli's salt may have a superior dilator capacity after I/R. Improved vasodilatation during acute heart failure may reduce and pre-load and after-load of the heart and increase stroke volume leading to improved perfusion of peripheral vasculatures; however the application should be strictly monitored to prevent adverse effects such as hypotension.

7.3 Future directions

In this study, the effect of DiOHF on I/R injury was investigated using an *ex vivo* isolated heart model. This preparation is denervated and experiments are carried out in the absence of other confounding factors of other organs. This may be advantageous as the effect of DiOHF on I/R injury and its mechanism of action are cardiac-specific, however, the disadvantage of this technique is that it is one step further away from the *in vivo* state where systemic circulation and a host of peripheral effects including neurohormonal regulation are present. Therefore, a myocardial I/R *in vivo* model in rats could be established to study the effect of DiOHF against myocardial I/R injury. Myocardial I/R *in vivo* is established by temporary occlusion of the left coronary artery and DiOHF can be infused during reperfusion when the occlusion is relieved. The mechanism of DiOHF-induced cardioprotection could be investigated at different time points of reperfusion.

DiOHF has shown to inhibit the activation of PLN on sarcoplasmic reticulum (Chapter 4), however its effect on other Ca^{2+}-related receptors and downstream targets of CaMKII such as RyRs and SERCA has not been investigated. The effect of DiOHF on endoplasmic reticulum stress could also be investigated using endoplasmic reticulum stress markers such as 78 kDa glucose-regulated protein, X-box binding protein-1 and C/EBP homologous protein which are activated during I/R. These will further improve our understanding of the mechanism of DiOHF-induced cardioprotection in I/R.

The effect of DiOHF on I/R injury can be studied in a more complex model of cardiovascular disease with co-morbid conditions of diabetes, hypertension and atherosclerosis to mimic the situation in the clinical setting where most patients presenting with acute myocardial infarction have a co-morbid illness. The presence of these disease states may affect the response of the heart to cardioprotection during I/R.

The mechanism of cardiac and vascular action of Angeli's salt, as well as dobutamine and DEA/NO during I/R can be investigated. The mechanism of action can be investigated in the presence of the HNO and NO scavengers to confirm the action of Angeli's salt and DEA/NO is mediated via HNO and NO respectively; β-adrenoceptor antagonist timolol, sGC inhibitor ODQ, the non-competitive inhibitor of SERCA thapsigargin and the RyR blocker ruthenium red could also be used to investigate the mechanism of action of dobutamine, DEA/NO and Angeli's salt.

7.4 Conclusion

The investigation of the signalling pathway activated by DiOHF during I/R improves our understanding of the mechanistic action of DiOHF. This is important before its translation into the clinical setting as an adjunctive therapy for reperfusion injury. In addition, further investigations on the mechanism(s) of cardiac and vascular actions of Angeli's salt in the setting of I/R are required before it can be used as a therapeutic agent to improve left ventricular ejection fraction in acute heart failure.

REFERENCES

Adak S, Wang Q, Stuehr DJ (2000). Arginine conversion to nitroxide by tetrahydrobiopterin-free neuronal nitric-oxide synthase. Implications for mechanism. *J Biol Chem* 275**:** 33554-33561.

Adameova A, Carnicka S, Rajtik T, Szobi A, Nemcekova M, Svec P, *et al.* (2012). Upregulation of CaMKIIδ during ischaemia-reperfusion is associated with reperfusion-induced arrhythmias and mechanical dysfunction of the rat heart: involvement of sarcolemmal Ca^{2+}-cycling proteins. *Can J Physiol Pharmacol* 90**:** 1127-1134.

Ajay M, Gilani AU, Mustafa MR (2003). Effects of flavonoids on vascular smooth muscle of the isolated rat thoracic aorta. *Life Sci* 74**:** 603-612.

Akhlaghi M, Bandy B (2010). Dietary green tea extract increases phase 2 enzyme activities in protecting against myocardial ischemia-reperfusion. *Nutr Res* 30**:** 32-39.

Anderson ME, Brown JH, Bers DM (2011). CaMKII in myocardial hypertrophy and heart failure. *J Mol Cell Cardiol* 51**:** 468-473.

Andrews KL, Irvine JC, Tare M, Apostolopoulos J, Favaloro JL, Triggle CR, *et al.* (2009). A role for nitroxyl (HNO) as an endothelium-derived relaxing and hyperpolarizing factor in resistance arteries. *Br J Pharmacol* 157**:** 540-550.

Aneja R, Hake PW, Burroughs TJ, Denenberg AG, Wong HR, Zingarelli B (2004). Epigallocatechin, a green tea polyphenol, attenuates myocardial ischemia reperfusion injury in rats. *Mol Med* 10**:** 55-62.

Annapurna A, Reddy CS, Akondi RB, Rao SR (2009). Cardioprotective actions of two bioflavonoids, quercetin and rutin, in experimental myocardial infarction in both normal and streptozotocin-induced type I diabetic rats. *J Pharm Pharmacol* 61**:** 1365-1374.

Anter E, Thomas SR, Schulz E, Shapira OM, Vita JA, Keaney JF, Jr. (2004). Activation of endothelial nitric-oxide synthase by the p38 MAPK in response to black tea polyphenols. *J Biol Chem* 279**:** 46637-46643.

Aoki H, Kang PM, Hampe J, Yoshimura K, Noma T, Matsuzaki M, *et al.* (2002). Direct activation of mitochondrial apoptosis machinery by *c-jun* N-terminal kinase in adult cardiac myocytes. *J Biol Chem* 277**:** 10244-10250.

Balligand JL, Kelly RA, Marsden PA, Smith TW, Michel T (1993). Control of cardiac muscle cell function by an endogenous nitric oxide signaling system. *Proc Natl Acad Sci U S A* 90**:** 347-351.

Bandyopadhyay D, Chattopadhyay A, Ghosh G, Datta AG (2004). Oxidative stress-induced ischemic heart disease: protection by antioxidants. *Curr Med Chem* 11**:** 369-387.

Bartekova M, Carnicka S, Pancza D, Ondrejcakova M, Breier A, Ravingerova T (2010). Acute treatment with polyphenol quercetin improves postischemic recovery of isolated perfused rat hearts after global ischemia. *Can J Physiol Pharmacol* 88**:** 465-471.

Bartling B, Holtz J, Darmer D (1998). Contribution of myocyte apoptosis to myocardial infarction? *Basic Res Cardiol* 93**:** 71-84.

Bassenge E, Fink N, Skatchkov M, Fink B (1998). Dietary supplement with vitamin C prevents nitrate tolerance. *J Clin Invest* 102**:** 67-71.

Bassi R, Heads R, Marber MS, Clark JE (2008). Targeting p38-MAPK in the ischaemic heart: kill or cure? *Curr Opin Pharmacol* 8**:** 141-146.

Bates ER, Krell MJ, Dean EN, O'Neill WW, Vogel RA (1986). Demonstration of the "no-reflow" phenomenon by digital coronary arteriography. *Am J Cardiol* 57**:** 177-178.

Baumann G, Riess G, Erhardt WD, Felix SB, Ludwig L, Blumel G, *et al.* (1981). Impaired beta-adrenergic stimulation in the uninvolved ventricle post-acute myocardial infarction: reversible defect due to excessive circulating catecholamine-induced decline in number and affinity of beta-receptors. *Am Heart J* 101**:** 569-581.

Baumann J, von Bruchhausen F, Wurm G (1980). Flavonoids and related compounds as inhibition of arachidonic acid peroxidation. *Prostaglandins* 20**:** 627-639.

Becatti M, Taddei N, Cecchi C, Nassi N, Nassi PA, Fiorillo C (2012). SIRT1 modulates MAPK pathways in ischemic-reperfused cardiomyocytes. *Cell Mol Life Sci* 69**:** 2245-2260.

Bell JR, Vila-Petroff M, Delbridge LM (2014). CaMKII-dependent responses to ischemia and reperfusion challenges in the heart. *Front Pharmacol* 5**:** 96.

Bell JR, Curl CL, Ip WT, Delbridge LM (2012). Ca^{2+}/calmodulin-dependent protein kinase inhibition suppresses post-ischemic arrhythmogenesis and mediates sinus bradycardic recovery in reperfusion. *Int J Cardiol* 159**:** 112-118.

Bell RM, Yellon DM (2003). Bradykinin limits infarction when administered as an adjunct to reperfusion in mouse heart: the role of PI3K, Akt and eNOS. *J Mol Cell Cardiol* 35**:** 185-193.

Bhamra GS, Hausenloy DJ, Davidson SM, Carr RD, Paiva M, Wynne AM, *et al.* (2008). Metformin protects the ischemic heart by the Akt-mediated inhibition of mitochondrial permeability transition pore opening. *Basic Res Cardiol* 103**:** 274-284.

Bhuiyan MS, Shibuya M, Shioda N, Moriguchi S, Kasahara J, Iwabuchi Y, *et al.* (2007). Cytoprotective effect of bis(1-oxy-2-pyridinethiolato)oxovanadiun(IV) on myocardial

ischemia/reperfusion injury elicits inhibition of Fas ligand and Bim expression and elevation of FLIP expression. *Eur J Pharmacol* 571**:** 180-188.

Bian YF, Hao XY, Gao F, Yang HY, Zang N, Xiao CS (2011). Adiponectin attenuates hypoxia/reoxygenation-induced cardiomyocyte injury through inhibition of endoplasmic reticulum stress. *J Investig Med* 59**:** 921-925.

Boengler K, Hilfiker-Kleiner D, Drexler H, Heusch G, Schulz R (2008). The myocardial JAK/STAT pathway: from protection to failure. *Pharmacol Ther* 120**:** 172-185.

Bogoyevitch MA, Kobe B (2006). Uses for JNK: the many and varied substrates of the *c-jun* N-terminal kinases. *Microbiol Mol Biol Rev* 70**:** 1061-1095.

Bogoyevitch MA, Gillespie-Brown J, Ketterman AJ, Fuller SJ, Ben-Levy R, Ashworth A, *et al.* (1996). Stimulation of the stress-activated mitogen-activated protein kinase subfamilies in perfused heart. p38/RK mitogen-activated protein kinases and *c-jun* N-terminal kinases are activated by ischemia/reperfusion. *Circ Res* 79**:** 162-173.

Bolli R (1988). Oxygen-derived free radicals and postischemic myocardial dysfunction ("stunned myocardium"). *J Am Coll Cardiol* 12**:** 239-249.

Bolli R (1990). Mechanism of myocardial "stunning". *Circulation* 82**:** 723-738.

Bolli R, Jeroudi MO, Patel BS, DuBose CM, Lai EK, Roberts R, *et al.* (1989). Direct evidence that oxygen-derived free radicals contribute to postischemic myocardial dysfunction in the intact dog. *Proc Natl Acad Sci U S A* 86**:** 4695-4699.

Bonaventura D, de Lima RG, da Silva RS, Bendhack LM (2011). NO donors-relaxation is impaired in aorta from hypertensive rats due to a reduced involvement of K^+ channels and sarcoplasmic reticulum Ca^{2+}-ATPase. *Life Sci* 89**:** 595-602.

Brady AJ, Warren JB, Poole-Wilson PA, Williams TJ, Harding SE (1993). Nitric oxide attenuates cardiac myocyte contraction. *Am J Physiol* 265**:** H176-182.

Braunwald E, Kloner RA (1985). Myocardial reperfusion: a double-edged sword? *J Clin Invest* 76**:** 1713-1719.

Brookes PS, Digerness SB, Parks DA, Darley-Usmar V (2002). Mitochondrial function in response to cardiac ischemia-reperfusion after oral treatment with quercetin. *Free Radic Biol Med* 32**:** 1220-1228.

Bui AL, Horwich TB, Fonarow GC (2011). Epidemiology and risk profile of heart failure. *Nat Rev Cardiol* 8**:** 30-41.

Bullen ML, Miller AA, Dharmarajah J, Drummond GR, Sobey CG, Kemp-Harper BK (2011). Vasorelaxant and antiaggregatory actions of the nitroxyl donor isopropylamine NONOate are maintained in hypercholesterolemia. *Am J Physiol* 301**:** H1405-1414.

Burger AJ, Elkayam U, Neibaur MT, Haught H, Ghali J, Horton DP, *et al.* (2001). Comparison of the occurrence of ventricular arrhythmias in patients with acutely decompensated congestive heart failure receiving dobutamine versus nesiritide therapy. *Am J Cardiol* 88**:** 35-39.

Cain BS, Meldrum DR, Meng X, Dinarello CA, Shames BD, Banerjee A, *et al.* (1999). p38 MAPK inhibition decreases TNF-alpha production and enhances postischemic human myocardial function. *J Surg Res* 83**:** 7-12.

Canty JM, Jr., Suzuki G (2012). Myocardial perfusion and contraction in acute ischemia and chronic ischemic heart disease. *J Mol Cell Cardiol* 52**:** 822-831.

Capano M, Crompton M (2006). Bax translocates to mitochondria of heart cells during simulated ischaemia: involvement of AMP-activated and p38 mitogen-activated protein kinases. *Biochem J* 395**:** 57-64.

Caramori PR, Adelman AG, Azevedo ER, Newton GE, Parker AB, Parker JD (1998). Therapy with nitroglycerin increases coronary vasoconstriction in response to acetylcholine. *J Am Coll Cardiol* 32**:** 1969-1974.

Carnicer R, Crabtree MJ, Sivakumaran V, Casadei B, Kass DA (2013). Nitric oxide synthases in heart failure. *Antioxid Redox Signal* 18**:** 1078-1099.

Cawley SM, Kolodziej S, Ichinose F, Brouckaert P, Buys ES, Bloch KD (2011). sGCα1 mediates the negative inotropic effects of NO in cardiac myocytes independent of changes in calcium handling. *Am J Physiol* 301**:** H157-163.

Chambers JW, Pachori A, Howard S, Iqbal S, LoGrasso PV (2013). Inhibition of JNK mitochondrial localization and signaling is protective against ischemia/reperfusion injury in rats. *J Biol Chem* 288**:** 4000-4011.

Chan EC, Pannangpetch P, Woodman OL (2000). Relaxation to flavones and flavonols in rat isolated thoracic aorta: mechanism of action and structure-activity relationships. *J Cardiovasc Pharmacol* 35**:** 326-333.

Chan EC, Drummond GR, Woodman OL (2003). 3', 4'-dihydroxyflavonol enhances nitric oxide bioavailability and improves vascular function after ischemia and reperfusion injury in the rat. *J Cardiovasc Pharmacol* 42**:** 727-735.

Chau VQ, Salloum FN, Hoke NN, Abbate A, Kukreja RC (2011). Mitigation of the progression of heart failure with sildenafil involves inhibition of RhoA/Rho-kinase pathway. *Am J Physiol* 300**:** H2272-2279.

Chen X, Zhang X, Kubo H, Harris DM, Mills GD, Moyer J, *et al.* (2005). Ca2+ influx-induced sarcoplasmic reticulum Ca^{2+} overload causes mitochondrial-dependent apoptosis in ventricular myocytes. *Circ Res* 97**:** 1009-1017.

Cheong E, Tumbev V, Abramson J, Salama G, Stoyanovsky DA (2005). Nitroxyl triggers Ca^{2+} release from skeletal and cardiac sarcoplasmic reticulum by oxidizing ryanodine receptors. *Cell Calcium* 37**:** 87-96.

Chin KY, Qin C, Cao N, Kemp-Harper BK, Woodman OL, Ritchie RH (2014). The concomitant coronary vasodilator and positive inotropic actions of the nitroxyl donor Angeli's salt in the intact rat heart: contribution of soluble guanylyl cyclase-dependent and -independent mechanisms. *Br J Pharmacol* 171**:** 1722-1734.

Cho JY, Dutton A, Miller T, Houk KN, Fukuto JM (2003a). Oxidation of N-hydroxyguanidines by copper(II): model systems for elucidating the physiological chemistry of the nitric oxide biosynthetic intermediate N-hydroxyl-L-arginine. *Arch Biochem Biophys* 417**:** 65-76.

Cho SY, Park SJ, Kwon MJ, Jeong TS, Bok SH, Choi WY, *et al.* (2003b). Quercetin suppresses proinflammatory cytokines production through MAP kinases and NF-kappaB pathway in lipopolysaccharide-stimulated macrophage. *Mol Cell Biochem* 243**:** 153-160.

Christensen FH, Hansen T, Stankevicius E, Buus NH, Simonsen U (2007). Elevated pressure selectively blunts flow-evoked vasodilatation in rat mesenteric small arteries. *Br J Pharmacol* 150**:** 80-87.

Comalada M, Ballester I, Bailon E, Sierra S, Xaus J, Galvez J, *et al.* (2006). Inhibition of pro-inflammatory markers in primary bone marrow-derived mouse macrophages by naturally occurring flavonoids: analysis of the structure-activity relationship. *Biochem Pharmacol* 72**:** 1010-1021.

Cos P, Ying L, Calomme M, Hu JP, Cimanga K, Van Poel B, *et al.* (1998). Structure-activity relationship and classification of flavonoids as inhibitors of xanthine oxidase and superoxide scavengers. *J Nat Prod* 61**:** 71-76.

Couchonnal LF, Anderson ME (2008). The role of calmodulin kinase II in myocardial physiology and disease. *Physiology (Bethesda)* 23**:** 151-159.

Cowan KJ, Storey KB (2003). Mitogen-activated protein kinases: new signaling pathways functioning in cellular responses to environmental stress. *J Exp Biol* 206**:** 1107-1115.

Cowie MR, Wood DA, Coats AJ, Thompson SG, Poole-Wilson PA, Suresh V, *et al.* (1999). Incidence and aetiology of heart failure; a population-based study. *Eur Heart J* 20**:** 421-428.

Crompton M (1999). The mitochondrial permeability transition pore and its role in cell death. *Biochem J* 341 (Pt 2)**:** 233-249.

Dai T, Tian Y, Tocchetti CG, Katori T, Murphy AM, Kass DA, *et al.* (2007). Nitroxyl increases force development in rat cardiac muscle. *J Physiol* 580**:** 951-960.

Darra E, Shoji K, Mariotto S, Suzuki H (2007). Protective effect of epigallocatechin-3-gallate on ischemia/reperfusion-induced injuries in the heart: STAT1 silencing flavonoid. *Genes Nutr* 2**:** 307-310.

Das A, Salloum FN, Durrant D, Ockaili R, Kukreja RC (2012). Rapamycin protects against myocardial ischemia-reperfusion injury through JAK2-STAT3 signaling pathway. *J Mol Cell Cardiol* 53**:** 858-869.

Das S, Tosaki A, Bagchi D, Maulik N, Das DK (2006). Potentiation of a survival signal in the ischemic heart by resveratrol through p38 mitogen-activated protein kinase/mitogen- and stress-activated protein kinase 1/cAMP response element-binding protein signaling. *J Pharmacol Exp Ther* 317**:** 980-988.

Davis RJ (1993). The mitogen-activated protein kinase signal transduction pathway. *J Biol Chem* 268**:** 14553-14556.

De Witt BJ, Marrone JR, Kaye AD, Keefer LK, Kadowitz PJ (2001). Comparison of responses to novel nitric oxide donors in the feline pulmonary vascular bed. *Eur J Pharmacol* 430**:** 311-315.

Del Re DP, Miyamoto S, Brown JH (2008). Focal adhesion kinase as a RhoA-activable signaling scaffold mediating Akt activation and cardiomyocyte protection. *J Biol Chem* 283**:** 35622-35629.

Derici K, Samsar U, Demirel-Yilmaz E (2012). Nitric oxide effects depend on different mechanisms in different regions of the rat heart. *Heart Vessels* 27**:** 89-97.

Di Carlo MN, Said M, Ling H, Valverde CA, De Giusti VC, Sommese L, *et al.* (2014). CaMKII-dependent phosphorylation of cardiac ryanodine receptors regulates cell death in cardiac ischemia/reperfusion injury. *J Mol Cell Cardiol* 74**:** 274-283.

Ding W, Li Z, Shen X, Martin J, King SB, Sivakumaran V, *et al.* (2011). Reversal of isoflurane-induced depression of myocardial contraction by nitroxyl via myofilament sensitization to Ca^{2+}. *J Pharmacol Exp Ther* 339**:** 825-831.

Duarte J, Andriambeloson E, Diebolt M, Andriantsitohaina R (2004). Wine polyphenols stimulate superoxide anion production to promote calcium signaling and endothelial-dependent vasodilatation. *Physiol Res* 53**:** 595-602.

Duilio C, Ambrosio G, Kuppusamy P, DiPaula A, Becker LC, Zweier JL (2001). Neutrophils are primary source of O_2 radicals during reperfusion after prolonged myocardial ischemia. *Am J Physiol* 280**:** H2649-2657.

DuMond JF, King SB (2011). The chemistry of nitroxyl-releasing compounds. *Antioxid Redox Signal* 14**:** 1637-1648.

Eeckhout E, Kern MJ (2001). The coronary no-reflow phenomenon: a review of mechanisms and therapies. *Eur Heart J* 22**:** 729-739.

Efthymiou CA, Mocanu MM, Yellon DM (2005). Atorvastatin and myocardial reperfusion injury: new pleiotropic effect implicating multiple prosurvival signaling. *J Cardiovasc Pharmacol* 45**:** 247-252.

El-Armouche A, Wahab A, Wittkopper K, Schulze T, Bottcher F, Pohlmann L, *et al.* (2010). The new HNO donor, 1-nitrosocyclohexyl acetate, increases contractile force in normal and beta-adrenergically desensitized ventricular myocytes. *Biochem Biophys Res Commun* 402**:** 340-344.

Elkayam U, Mehra A, Shotan A, Ostrzega E (1992). Nitrate resistance and tolerance: potential limitations in the treatment of congestive heart failure. *Am J Cardiol* 70**:** 98b-104b.

Ellis A, Li CG, Rand MJ (2000). Differential actions of L-cysteine on responses to nitric oxide, nitroxyl anions and EDRF in the rat aorta. *Br J Pharmacol* 129**:** 315-322.

Entman ML, Smith CW (1994). Postreperfusion inflammation: a model for reaction to injury in cardiovascular disease. *Cardiovasc Res* 28**:** 1301-1311.

Fang F, Li D, Pan H, Chen D, Qi L, Zhang R, *et al.* (2011). Luteolin inhibits apoptosis and improves cardiomyocyte contractile function through the PI3K/Akt pathway in simulated ischemia/reperfusion. *Pharmacology* 88**:** 149-158.

Farber NE, Pieper GM, Gross GJ (1988). Postischemic recovery in the stunned myocardium after reperfusion in the presence or absence of a flow-limiting coronary artery stenosis. *Am Heart J* 116**:** 407-420.

Farmer PJ, Sulc F (2005). Coordination chemistry of the HNO ligand with hemes and synthetic coordination complexes. *J Inorg Biochem* 99**:** 166-184.

Favaloro JL, Kemp-Harper BK (2007). The nitroxyl anion (HNO) is a potent dilator of rat coronary vasculature. *Cardiovasc Res* 73**:** 587-596.

Favaloro JL, Kemp-Harper BK (2009). Redox variants of NO (NO• and HNO) elicit vasorelaxation of resistance arteries via distinct mechanisms. *Am J Physiol* 296**:** H1274-1280.

Feng J, Lucchinetti E, Ahuja P, Pasch T, Perriard JC, Zaugg M (2005). Isoflurane postconditioning prevents opening of the mitochondrial permeability transition pore through inhibition of glycogen synthase kinase 3beta. *Anesthesiology* 103**:** 987-995.

Ferrandi C, Ballerio R, Gaillard P, Giachetti C, Carboni S, Vitte PA, *et al.* (2004). Inhibition of *c-jun* N-terminal kinase decreases cardiomyocyte apoptosis and infarct size after myocardial ischemia and reperfusion in anaesthetized rats. *Br J Pharmacol* 142**:** 953-960.

Ferrari R, Ceconi C, Curello S, Alfieri O, Visioli O (1993). Myocardial damage during ischaemia and reperfusion. *Eur Heart J* 14 Suppl G**:** 25-30.

Ferrari R, Alfieri O, Curello S, Ceconi C, Cargnoni A, Marzollo P, *et al.* (1990). Occurrence of oxidative stress during reperfusion of the human heart. *Circulation* 81**:** 201-211.

Feuerstein GZ, Young PR (2000). Apoptosis in cardiac diseases: stress- and mitogen-activated signaling pathways. *Cardiovasc Res* 45**:** 560-569.

Follath F, Yilmaz MB, Delgado JF, Parissis JT, Porcher R, Gayat E, *et al.* (2011). Clinical presentation, management and outcomes in the Acute Heart Failure Global Survey of Standard Treatment (ALARM-HF). *Intensive Care Med* 37**:** 619-626.

Fox KF, Cowie MR, Wood DA, Coats AJ, Gibbs JS, Underwood SR, *et al.* (2001). Coronary artery disease as the cause of incident heart failure in the population. *Eur Heart J* 22**:** 228-236.

French JP, Quindry JC, Falk DJ, Staib JL, Lee Y, Wang KK, *et al.* (2006). Ischemia-reperfusion-induced calpain activation and SERCA2a degradation are attenuated by exercise training and calpain inhibition. *Am J Physiol* 290**:** H128-136.

Frias MA, Pedretti S, Hacking D, Somers S, Lacerda L, Opie LH, *et al.* (2013). HDL protects against ischemia reperfusion injury by preserving mitochondrial integrity. *Atherosclerosis* 228**:** 110-116.

Frodin M, Gammeltoft S (1999). Role and regulation of 90 kDa ribosomal S6 kinase (RSK) in signal transduction. *Mol Cell Endocrinol* 151**:** 65-77.

Froehlich JP, Mahaney JE, Keceli G, Pavlos CM, Goldstein R, Redwood AJ, *et al.* (2008). Phospholamban thiols play a central role in activation of the cardiac muscle sarcoplasmic reticulum calcium pump by nitroxyl. *Biochemistry* 47**:** 13150-13152.

Fujigaki T, Nakamura H, Fukui S, Miyako M, Haseba S, Gotoh Y (1989). Comparison of the effects of amrinone and dobutamine on hemodynamics and myocardial oxygen balance in dogs with experimental left ventricular failure. *J Cardiothorac Anesth* 3**:** 433-440.

Fukami Y, Toki Y, Numaguchi Y, Nakashima Y, Mukawa H, Matsui H, *et al.* (1998). Nitroglycerin-induced aortic relaxation mediated by calcium-activated potassium channel is markedly diminished in hypertensive rats. *Life Sci* 63**:** 1047-1055.

Fukuto JM, Carrington SJ (2011). HNO signaling mechanisms. *Antioxid Redox Signal* 14**:** 1649-1657.

Fukuto JM, Wallace GC, Hszieh R, Chaudhuri G (1992a). Chemical oxidation of N-hydroxyguanidine compounds. Release of nitric oxide, nitroxyl and possible relationship to the mechanism of biological nitric oxide generation. *Biochem Pharmacol* 43**:** 607-613.

Fukuto JM, Chiang K, Hszieh R, Wong P, Chaudhuri G (1992b). The pharmacological activity of nitroxyl: a potent vasodilator with activity similar to nitric oxide and/or endothelium-derived relaxing factor. *J Pharmacol Exp Ther* 263**:** 546-551.

Galiuto L, Lombardo A, Maseri A, Santoro L, Porto I, Cianflone D, *et al.* (2003). Temporal evolution and functional outcome of no reflow: sustained and spontaneously reversible patterns following successful coronary recanalisation. *Heart* 89**:** 731-737.

Gao F, Yue TL, Shi DW, Christopher TA, Lopez BL, Ohlstein EH, *et al.* (2002). p38 MAPK inhibition reduces myocardial reperfusion injury via inhibition of endothelial adhesion molecule expression and blockade of PMN accumulation. *Cardiovasc Res* 53**:** 414-422.

Geleijnse JM, Launer LJ, Van der Kuip DA, Hofman A, Witteman JC (2002). Inverse association of tea and flavonoid intakes with incident myocardial infarction: the Rotterdam Study. *Am J Clin Nutr* 75**:** 880-886.

Gerritsen ME, Carley WW, Ranges GE, Shen CP, Phan SA, Ligon GF, *et al.* (1995). Flavonoids inhibit cytokine-induced endothelial cell adhesion protein gene expression. *Am J Pathol* 147**:** 278-292.

Gheorghiade M, Pang PS (2009). Acute heart failure syndromes. *J Am Coll Cardiol* 53**:** 557-573.

Gheorghiade M, Abraham WT, Albert NM, Greenberg BH, O'Connor CM, She L, *et al.* (2006). Systolic blood pressure at admission, clinical characteristics, and outcomes in patients hospitalized with acute heart failure. *JAMA* 296**:** 2217-2226.

Gonzalez DR, Beigi F, Treuer AV, Hare JM (2007). Deficient ryanodine receptor S-nitrosylation increases sarcoplasmic reticulum calcium leak and arrhythmogenesis in cardiomyocytes. *Proc Natl Acad Sci U S A* 104**:** 20612-20617.

Gonzalez DR, Fernandez IC, Ordenes PP, Treuer AV, Eller G, Boric MP (2008). Differential role of S-nitrosylation and the NO-cGMP-PKG pathway in cardiac contractility. *Nitric Oxide* 18**:** 157-167.

Gori T, Mak SS, Kelly S, Parker JD (2001). Evidence supporting abnormalities in nitric oxide synthase function induced by nitroglycerin in humans. *J Am Coll Cardiol* 38**:** 1096-1101.

Grocott-Mason R, Fort S, Lewis MJ, Shah AM (1994). Myocardial relaxant effect of exogenous nitric oxide in isolated ejecting hearts. *Am J Physiol* 266**:** H1699-1705.

Grzybowski M, Welch RD, Parsons L, Ndumele CE, Chen E, Zalenski R, *et al.* (2004). The association between white blood cell count and acute myocardial infarction in-hospital mortality: findings from the National Registry of Myocardial Infarction. *Acad Emerg Med* 11**:** 1049-1060.

Halestrap AP (2010). A pore way to die: the role of mitochondria in reperfusion injury and cardioprotection. *Biochem Soc Trans* 38**:** 841-860.

Halestrap AP, McStay GP, Clarke SJ (2002). The permeability transition pore complex: another view. *Biochimie* 84**:** 153-166.

Hansen PR (1995). Role of neutrophils in myocardial ischemia and reperfusion. *Circulation* 91**:** 1872-1885.

Harris GK, Qian Y, Leonard SS, Sbarra DC, Shi X (2006). Luteolin and chrysin differentially inhibit cyclooxygenase-2 expression and scavenge reactive oxygen species but similarly inhibit prostaglandin-E2 formation in RAW 264.7 cells. *J Nutr* 136**:** 1517-1521.

Hausenloy DJ, Yellon DM (2004). New directions for protecting the heart against ischaemia-reperfusion injury: targeting the Reperfusion Injury Salvage Kinase (RISK)-pathway. *Cardiovasc Res* 61**:** 448-460.

Hausenloy DJ, Yellon DM (2007). Reperfusion injury salvage kinase signalling: taking a RISK for cardioprotection. *Heart Fail Rev* 12**:** 217-234.

Hausenloy DJ, Tsang A, Yellon DM (2005). The reperfusion injury salvage kinase pathway: a common target for both ischemic preconditioning and postconditioning. *Trends Cardiovasc Med* 15**:** 69-75.

Hearse DJ, Bolli R (1992). Reperfusion induced injury: manifestations, mechanisms, and clinical relevance. *Cardiovasc Res* 26**:** 101-108.

Hein TW, Zhang C, Wang W, Chang CI, Thengchaisri N, Kuo L (2003). Ischemia-reperfusion selectively impairs nitric oxide-mediated dilation in coronary arterioles: counteracting role of arginase. *The FASEB J* 17**:** 2328-2330.

Heinemann A, Stauber RE (1996). Vasodilator responses to nitric oxide are enhanced in mesenteric arteries of portal hypertensive rats. *Eur J Clin Invest* 26**:** 824-826.

Heinrich TA, da Silva RS, Miranda KM, Switzer CH, Wink DA, Fukuto JM (2013). Biological nitric oxide signalling: chemistry and terminology. *Br J Pharmacol* 169**:** 1417-1429.

Heitzer T, Just H, Brockhoff C, Meinertz T, Olschewski M, Munzel T (1998). Long-term nitroglycerin treatment is associated with supersensitivity to vasoconstrictors in men with stable coronary artery disease: prevention by concomitant treatment with captopril. *J Am Coll Cardiol* 31**:** 83-88.

Herrera MD, Zarzuelo A, Jimenez J, Marhuenda E, Duarte J (1996). Effects of flavonoids on rat aortic smooth muscle contractility: structure-activity relationships. *Gen Pharmacol* 27**:** 273-277.

Hertog MG, Feskens EJ, Kromhout D (1997). Antioxidant flavonols and coronary heart disease risk. *Lancet* 349**:** 699.

Hertog MG, Feskens EJ, Hollman PC, Katan MB, Kromhout D (1993). Dietary antioxidant flavonoids and risk of coronary heart disease: the Zutphen Elderly Study. *Lancet* 342**:** 1007-1011.

Hilfiker-Kleiner D, Hilfiker A, Fuchs M, Kaminski K, Schaefer A, Schieffer B, *et al.* (2004). Signal transducer and activator of transcription 3 is required for myocardial capillary growth,

control of interstitial matrix deposition, and heart protection from ischemic injury. *Circ Res* 95**:** 187-195.

Hill MF, Singal PK (1996). Antioxidant and oxidative stress changes during heart failure subsequent to myocardial infarction in rats. *Am J Pathol* 148**:** 291-300.

Huang C, Gu H, Zhang W, Manukyan MC, Shou W, Wang M (2011). SDF-1/CXCR4 mediates acute protection of cardiac function through myocardial STAT3 signaling following global ischemia/reperfusion injury. *Am J Physiol* 301**:** H1496-1505.

Huang MH, Knight PR, 3rd, Izzo JL, Jr. (1999). Ca^{2+}-induced Ca^{2+} release involved in positive inotropic effect mediated by CGRP in ventricular myocytes. *Am J Physiol* 276**:** R259-264.

Huk I, Brovkovych V, Nanobash Vili J, Weigel G, Neumayer C, Partyka L, *et al.* (1998). Bioflavonoid quercetin scavenges superoxide and increases nitric oxide concentration in ischaemia-reperfusion injury: an experimental study. *Br J Surg* 85**:** 1080-1085.

Hunt SA, Abraham WT, Chin MH, Feldman AM, Francis GS, Ganiats TG, *et al.* (2009). 2009 focused update incorporated into the ACC/AHA 2005 Guidelines for the Diagnosis and Management of Heart Failure in Adults: a report of the American College of Cardiology Foundation/American Heart Association Task Force on Practice Guidelines: developed in

collaboration with the International Society for Heart and Lung Transplantation. *Circulation* 119**:** e391-479.

Ikeda Y, Miura T, Sakamoto J, Miki T, Tanno M, Kobayashi H, *et al.* (2006). Activation of ERK and suppression of calcineurin are interacting mechanisms of cardioprotection afforded by delta-opioid receptor activation. *Basic Res Cardiol* 101**:** 418-426.

Irvine JC, Favaloro JL, Kemp-Harper BK (2003). NO- activates soluble guanylate cyclase and Kv channels to vasodilate resistance arteries. *Hypertension* 41**:** 1301-1307.

Irvine JC, Kemp-Harper BK, Widdop RE (2011). Chronic administration of the HNO donor Angeli's salt does not lead to tolerance, cross-tolerance, or endothelial dysfunction: comparison with GTN and DEA/NO. *Antioxid Redox Signal* 14**:** 1615-1624.

Irvine JC, Favaloro JL, Widdop RE, Kemp-Harper BK (2007). Nitroxyl anion donor, Angeli's salt, does not develop tolerance in rat isolated aortae. *Hypertension* 49**:** 885-892.

Irvine JC, Ravi RM, Kemp-Harper BK, Widdop RE (2013a). Nitroxyl donors retain their depressor effects in hypertension. *Am J Physiol* 305**:** H939-945.

Irvine JC, Ritchie RH, Favaloro JL, Andrews KL, Widdop RE, Kemp-Harper BK (2008). Nitroxyl (HNO): the Cinderella of the nitric oxide story. *Trends Pharmacol Sci* 29**:** 601-608.

Irvine JC, Cao N, Gossain S, Alexander AE, Love JE, Qin C, *et al.* (2013b). HNO/cGMP-dependent antihypertrophic actions of isopropylamine-NONOate in neonatal rat cardiomyocytes: potential therapeutic advantages of HNO over NO. *Am J Physiol* 305**:** H365-377.

Jackson MI, Han TH, Serbulea L, Dutton A, Ford E, Miranda KM, *et al.* (2009). Kinetic feasibility of nitroxyl reduction by physiological reductants and biological implications. *Free Radic Biol Med* 47**:** 1130-1139.

Jalili T, Carlstrom J, Kim S, Freeman D, Jin H, Wu TC, *et al.* (2006). Quercetin-supplemented diets lower blood pressure and attenuate cardiac hypertrophy in rats with aortic constriction. *J Cardiovasc Pharmacol* 47**:** 531-541.

Javadov S, Jang S, Agostini B (2014). Crosstalk between mitogen-activated protein kinases and mitochondria in cardiac diseases: therapeutic perspectives. *Pharmacol Ther* 144**:** 202-225.

Jennings RB, Sommers HM, Smyth GA, Flack HA, Linn H (1960). Myocardial necrosis induced by temporary occlusion of a coronary artery in the dog. *Arch Pathol* 70**:** 68-78.

Jeroudi MO, Hartley CJ, Bolli R (1994). Myocardial reperfusion injury: role of oxygen radicals and potential therapy with antioxidants. *Am J Cardiol* 73**:** 2b-7b.

Jin HB, Yang YB, Song YL, Zhang YC, Li YR (2012). Protective roles of quercetin in acute myocardial ischemia and reperfusion injury in rats. *Mol Biol Rep* 39**:** 11005-11009.

Joiner ML, Koval OM, Li J, He BJ, Allamargot C, Gao Z, *et al.* (2012). CaMKII determines mitochondrial stress responses in heart. *Nature* 491**:** 269-273.

Jonassen AK, Sack MN, Mjos OD, Yellon DM (2001). Myocardial protection by insulin at reperfusion requires early administration and is mediated via Akt and p70s6 kinase cell-survival signaling. *Circ Res* 89**:** 1191-1198.

Jordan JE, Zhao ZQ, Vinten-Johansen J (1999). The role of neutrophils in myocardial ischemia-reperfusion injury. *Cardiovasc Res* 43**:** 860-878.

Kaiser RA, Bueno OF, Lips DJ, Doevendans PA, Jones F, Kimball TF, *et al.* (2004). Targeted inhibition of p38 mitogen-activated protein kinase antagonizes cardiac injury and cell death following ischemia-reperfusion in vivo. *J Biol Chem* 279**:** 15524-15530.

Kalin R, Righi A, Del Rosso A, Bagchi D, Generini S, Cerinic MM, *et al.* (2002). Activin, a grape seed-derived proanthocyanidin extract, reduces plasma levels of oxidative stress and adhesion molecules (ICAM-1, VCAM-1 and E-selectin) in systemic sclerosis. *Free Radic Res* 36**:** 819-825.

Karim CB, Stamm JD, Karim J, Jones LR, Thomas DD (1998). Cysteine reactivity and oligomeric structures of phospholamban and its mutants. *Biochemistry* 37**:** 12074-12081.

Katori T, Hoover DB, Ardell JL, Helm RH, Belardi DF, Tocchetti CG, *et al.* (2005). Calcitonin gene-related peptide in vivo positive inotropy is attributable to regional sympatho-stimulation and is blunted in congestive heart failure. *Circ Res* 96**:** 234-243.

Khan M, Varadharaj S, Ganesan LP, Shobha JC, Naidu MU, Parinandi NL, *et al.* (2006). C-phycocyanin protects against ischemia-reperfusion injury of heart through involvement of p38 MAPK and ERK signaling. *Am J Physiol* 290**:** H2136-2145.

Khong FL, Zhang Y, Edgley AJ, Qi W, Connelly KA, Woodman OL, *et al.* (2011). 3′, 4′-Dihydroxyflavonol antioxidant attenuates diastolic dysfunction and cardiac remodeling in streptozotocin-induced diabetic m (Ren2) 27 rats. *PloS one* 6**:** e22777.

Kim DS, Ha KC, Kwon DY, Kim MS, Kim HR, Chae SW, *et al.* (2008). Kaempferol protects ischemia/reperfusion-induced cardiac damage through the regulation of endoplasmic reticulum stress. *Immunopharmacol Immunotoxicol* 30**:** 257-270.

Kim JK, Pedram A, Razandi M, Levin ER (2006). Estrogen prevents cardiomyocyte apoptosis through inhibition of reactive oxygen species and differential regulation of p38 kinase isoforms. *J Biol Chem* 281**:** 6760-6767.

Kimata M, Shichijo M, Miura T, Serizawa I, Inagaki N, Nagai H (2000). Effects of luteolin, quercetin and baicalein on immunoglobulin E-mediated mediator release from human cultured mast cells. *Clin Exp Allergy* 30**:** 501-508.

Klabunde RE, Ritger RC (1991). NG-monomethyl-l-arginine (NMA) restores arterial blood pressure but reduces cardiac output in a canine model of endotoxic shock. *Biochem Biophys Res Commun* 178**:** 1135-1140.

Kloner RA, Ganote CE, Jennings RB (1974). The "no-reflow" phenomenon after temporary coronary occlusion in the dog. *J Clin Invest* 54**:** 1496-1508.

Kloner RA, Przyklenk K, Whittaker P (1989). Deleterious effects of oxygen radicals in ischemia/reperfusion. Resolved and unresolved issues. *Circulation* 80**:** 1115-1127.

Knekt P, Jarvinen R, Reunanen A, Maatela J (1996). Flavonoid intake and coronary mortality in Finland: a cohort study. *BMJ* 312**:** 478-481.

Kohr MJ, Kaludercic N, Tocchetti CG, Dong Gao W, Kass DA, Janssen PM, *et al.* (2010). Nitroxyl enhances myocyte Ca^{2+} transients by exclusively targeting SR Ca^{2+}-cycling. *Front Biosci (Elite Ed)* 2**:** 614-626.

Kojda G, Kottenberg K, Noack E (1997). Inhibition of nitric oxide synthase and soluble guanylate cyclase induces cardiodepressive effects in normal rat hearts. *Eur J Pharmacol* 334**:** 181-190.

Kojda G, Kottenberg K, Nix P, Schluter KD, Piper HM, Noack E (1996). Low increase in cGMP induced by organic nitrates and nitrovasodilators improves contractile response of rat ventricular myocytes. *Circ Res* 78**:** 91-101.

Kojda G, Brixius K, Kottenberg K, Nix P, Schluter KD, Piper HM, *et al.* (1995). The new NO donor SPM3672 increases cGMP and improves contraction in rat cardiomyocytes and isolated heart. *Eur J Pharmacol* 284**:** 315-319.

Krug A, Du Mesnil de R, Korb G (1966). Blood supply of the myocardium after temporary coronary occlusion. *Circ Res* 19**:** 57-62.

Lancel S, Zhang J, Evangelista A, Trucillo MP, Tong X, Siwik DA, *et al.* (2009). Nitroxyl activates SERCA in cardiac myocytes via glutathiolation of cysteine 674. *Circ Res* 104**:** 720-723.

Langer M, Luttecke D, Schluter KD (2003). Mechanism of the positive contractile effect of nitric oxide on rat ventricular cardiomyocytes with positive force/frequency relationship. *Pflugers Arch* 447**:** 289-297.

Layland J, Li JM, Shah AM (2002). Role of cyclic GMP-dependent protein kinase in the contractile response to exogenous nitric oxide in rat cardiac myocytes. *J Physiol* 540**:** 457-467.

Leblanc N, Wan X, Leung PM (1994). Physiological role of Ca^{2+}-activated and voltage-dependent K+ currents in rabbit coronary myocytes. *Am J Physiol* 266**:** C1523-1537.

Lecour S (2009). Activation of the protective Survivor Activating Factor Enhancement (SAFE) pathway against reperfusion injury: Does it go beyond the RISK pathway? *J Mol Cell Cardiol* 47**:** 32-40.

Lecour S, Smith RM, Woodward B, Opie LH, Rochette L, Sack MN (2002). Identification of a novel role for sphingolipid signaling in TNF alpha and ischemic preconditioning mediated cardioprotection. *J Mol Cell Cardiol* 34**:** 509-518.

Lefer AM, Tsao PS, Lefer DJ, Ma X (1991). Role of endothelial dysfunction in the pathogenesis of reperfusion injury after myocardial ischemia. *The FASEB J* 5**:** 2029-2034.

Lei K, Davis RJ (2003). JNK phosphorylation of Bim-related members of the Bcl2 family induces Bax-dependent apoptosis. *Proc Natl Acad Sci U S A* 100**:** 2432-2437.

Lemasters JJ, Nieminen AL, Qian T, Trost LC, Elmore SP, Nishimura Y, *et al.* (1998). The mitochondrial permeability transition in cell death: a common mechanism in necrosis, apoptosis and autophagy. *Biochim Biophys Acta* 1366**:** 177-196.

Leo C-H, Hart JL, Woodman OL (2011). 3′, 4′-Dihydroxyflavonol reduces superoxide and improves nitric oxide function in diabetic rat mesenteric arteries. *PloS one* 6**:** e20813.

Leo CH, Joshi A, Hart JL, Woodman OL (2012). Endothelium-dependent nitroxyl-mediated relaxation is resistant to superoxide anion scavenging and preserved in diabetic rat aorta. *Pharmacol Res* 66**:** 383-391.

Liao PH, Hung LM, Chen YH, Kuan YH, Zhang FB, Lin RH, *et al.* (2011). Cardioprotective effects of luteolin during ischemia-reperfusion injury in rats. *Circ J* 75**:** 443-450.

Lim NR, Thomas CJ, Silva LS, Yeap YY, Yap S, Bell JR, *et al.* (2013). Cardioprotective 3',4'-dihydroxyflavonol attenuation of JNK and p38(MAPK) signalling involves CaMKII inhibition. *Biochem J* 456**:** 149-161.

Lima B, Forrester MT, Hess DT, Stamler JS (2010). S-nitrosylation in cardiovascular signaling. *Circ Res* 106**:** 633-646.

Lin EQ, Irvine JC, Cao AH, Alexander AE, Love JE, Patel R, *et al.* (2012). Nitroxyl (HNO) stimulates soluble guanylyl cyclase to suppress cardiomyocyte hypertrophy and superoxide generation. *PLoS One* 7**:** e34892.

Lin LL, Wartmann M, Lin AY, Knopf JL, Seth A, Davis RJ (1993). cPLA2 is phosphorylated and activated by MAP kinase. *Cell* 72**:** 269-278.

Lindahl M, Tagesson C (1993). Selective inhibition of group II phospholipase A2 by quercetin. *Inflammation* 17**:** 573-582.

Ling H, Gray CB, Zambon AC, Grimm M, Gu Y, Dalton N, *et al.* (2013). Ca^{2+}/Calmodulin-dependent protein kinase II delta mediates myocardial ischemia/reperfusion injury through nuclear factor-kappaB. *Circ Res* 112**:** 935-944.

Lotito SB, Frei B (2006). Dietary flavonoids attenuate tumor necrosis factor alpha-induced adhesion molecule expression in human aortic endothelial cells. Structure-function relationships and activity after first pass metabolism. *J Biol Chem* 281**:** 37102-37110.

Lubbe WF, Podzuweit T, Opie LH (1992). Potential arrhythmogenic role of cyclic adenosine monophosphate (AMP) and cytosolic calcium overload: implications for prophylactic effects of beta-blockers in myocardial infarction and proarrhythmic effects of phosphodiesterase inhibitors. *J Am Coll Cardiol* 19**:** 1622-1633.

Luo Y, Sun G, Dong X, Wang M, Qin M, Yu Y, *et al.* (2015). Isorhamnetin attenuates atherosclerosis by inhibiting macrophage apoptosis via PI3K/AKT activation and HO-1 induction. *PLoS One* 10**:** e0120259.

Ma XL, Gao F, Liu GL, Lopez BL, Christopher TA, Fukuto JM, *et al.* (1999a). Opposite effects of nitric oxide and nitroxyl on postischemic myocardial injury. *Proc Natl Acad Sci U S A* 96**:** 14617-14622.

Ma XL, Kumar S, Gao F, Louden CS, Lopez BL, Christopher TA, *et al.* (1999b). Inhibition of p38 mitogen-activated protein kinase decreases cardiomyocyte apoptosis and improves cardiac function after myocardial ischemia and reperfusion. *Circulation* 99**:** 1685-1691.

Magnani L, Gaydou EM, Hubaud JC (2000). Spectrophotometric measurement of antioxidant properties of flavones and flavonols against superoxide anion. *Analytica Chimica Acta* 411**:** 209-216.

Magrini F, Niarchos AP (1980). Ineffectiveness of sublingual nitroglycerin in acute left ventricular failure in the presence of massive peripheral edema. *Am J Cardiol* 45**:** 841-847.

Mahn K, Borras C, Knock GA, Taylor P, Khan IY, Sugden D, *et al.* (2005). Dietary soy isoflavone induced increases in antioxidant and eNOS gene expression lead to improved endothelial function and reduced blood pressure in vivo. *The FASEB J* 19**:** 1755-1757.

Maier LS, Bers DM (2007). Role of Ca^{2+}/calmodulin-dependent protein kinase (CaMK) in excitation-contraction coupling in the heart. *Cardiovasc Res* 73**:** 631-640.

Malakul W, Ingkaninan K, Sawasdee P, Woodman OL (2011). The ethanolic extract of Kaempferia parviflora reduces ischaemic injury in rat isolated hearts. *J Ethnopharmacol* 137**:** 184-191.

Mann DL (2003). Stress-activated cytokines and the heart: from adaptation to maladaptation. *Annu Rev Physiol* 65**:** 81-101.

Manning AS, Hearse DJ (1984). Reperfusion-induced arrhythmias: mechanisms and prevention. *J Mol Cell Cardiol* 16**:** 497-518.

Mansuri ML, Parihar P, Solanki I, Parihar MS (2014). Flavonoids in modulation of cell survival signalling pathways. *Genes Nutr* 9**:** 400.

Martin S, Andriambeloson E, Takeda K, Andriantsitohaina R (2002). Red wine polyphenols increase calcium in bovine aortic endothelial cells: a basis to elucidate signalling pathways leading to nitric oxide production. *Br J Pharmacol* 135**:** 1579-1587.

Martindale JJ, Wall JA, Martinez-Longoria DM, Aryal P, Rockman HA, Guo Y, *et al.* (2005). Overexpression of mitogen-activated protein kinase kinase 6 in the heart improves functional

recovery from ischemia in vitro and protects against myocardial infarction in vivo. *J Biol Chem* 280**:** 669-676.

Matsui T, Tao J, del Monte F, Lee KH, Li L, Picard M, *et al.* (2001). Akt activation preserves cardiac function and prevents injury after transient cardiac ischemia in vivo. *Circulation* 104**:** 330-335.

Mattiazzi A, Kranias EG (2014). The role of CaMKII regulation of phospholamban activity in heart disease. *Front Pharmacol* 5**:** 5.

McLaughlin MM, Kumar S, McDonnell PC, Van Horn S, Lee JC, Livi GP, *et al.* (1996). Identification of mitogen-activated protein (MAP) kinase-activated protein kinase-3, a novel substrate of CSBP p38 MAP kinase. *J Biol Chem* 271**:** 8488-8492.

McMurray JJ, Adamopoulos S, Anker SD, Auricchio A, Bohm M, Dickstein K, *et al.* (2012). ESC guidelines for the diagnosis and treatment of acute and chronic heart failure 2012: The Task Force for the Diagnosis and Treatment of Acute and Chronic Heart Failure 2012 of the European Society of Cardiology. Developed in collaboration with the Heart Failure Association (HFA) of the ESC. *Eur J Heart Fail* 14**:** 803-869.

Means CK, Xiao CY, Li Z, Zhang T, Omens JH, Ishii I, *et al.* (2007). Sphingosine 1-phosphate S1P2 and S1P3 receptor-mediated Akt activation protects against in vivo myocardial ischemia-reperfusion injury. *Am J Physiol* 292**:** H2944-2951.

Mebazaa A, Parissis J, Porcher R, Gayat E, Nikolaou M, Boas FV, *et al.* (2011). Short-term survival by treatment among patients hospitalized with acute heart failure: the global ALARM-HF registry using propensity scoring methods. *Intensive Care Med* 37**:** 290-301.

Mebazaa A, Nieminen MS, Packer M, Cohen-Solal A, Kleber FX, Pocock SJ, *et al.* (2007). Levosimendan vs dobutamine for patients with acute decompensated heart failure: the SURVIVE Randomized Trial. *JAMA* 297**:** 1883-1891.

Miao W, Luo Z, Kitsis RN, Walsh K (2000). Intracoronary, adenovirus-mediated Akt gene transfer in heart limits infarct size following ischemia-reperfusion injury in vivo. *J Mol Cell Cardiol* 32**:** 2397-2402.

Milano G, Morel S, Bonny C, Samaja M, von Segesser LK, Nicod P, *et al.* (2007). A peptide inhibitor of *c-jun* NH_2-terminal kinase reduces myocardial ischemia-reperfusion injury and infarct size in vivo. *Am J Physiol* 292**:** H1828-1835.

Mink PJ, Scrafford CG, Barraj LM, Harnack L, Hong CP, Nettleton JA, *et al.* (2007). Flavonoid intake and cardiovascular disease mortality: a prospective study in postmenopausal women. *Am J Clin Nutr* 85**:** 895-909.

Miranda KM, Nagasawa HT, Toscano JP (2005a). Donors of HNO. *Curr Top Med Chem* 5**:** 649-664.

Miranda KM, Yamada K, Espey MG, Thomas DD, DeGraff W, Mitchell JB, *et al.* (2002). Further evidence for distinct reactive intermediates from nitroxyl and peroxynitrite: effects of buffer composition on the chemistry of Angeli's salt and synthetic peroxynitrite. *Arch Biochem Biophys* 401**:** 134-144.

Miranda KM, Nims RW, Thomas DD, Espey MG, Citrin D, Bartberger MD, *et al.* (2003a). Comparison of the reactivity of nitric oxide and nitroxyl with heme proteins. A chemical discussion of the differential biological effects of these redox related products of NOS. *J Inorg Biochem* 93**:** 52-60.

Miranda KM, Paolocci N, Katori T, Thomas DD, Ford E, Bartberger MD, *et al.* (2003b). A biochemical rationale for the discrete behavior of nitroxyl and nitric oxide in the cardiovascular system. *Proc Natl Acad Sci U S A* 100**:** 9196-9201.

Miranda KM, Dutton AS, Ridnour LA, Foreman CA, Ford E, Paolocci N, *et al.* (2005b). Mechanism of aerobic decomposition of Angeli's salt (sodium trioxodinitrate) at physiological pH. *J Am Chem Soc* 127**:** 722-731.

Mitra A, Ray A, Datta R, Sengupta S, Sarkar S (2014). Cardioprotective role of P38 MAPK during myocardial infarction via parallel activation of alpha-crystallin B and Nrf2. *J Cell Physiol* 229**:** 1272-1282.

Mizukami Y, Yoshioka K, Morimoto S, Yoshida K (1997). A novel mechanism of JNK1 activation. Nuclear translocation and activation of JNK1 during ischemia and reperfusion. *J Biol Chem* 272**:** 16657-16662.

Monrad ES, Baim DS, Smith HS, Lanoue AS (1986). Milrinone, dobutamine, and nitroprusside: comparative effects on hemodynamics and myocardial energetics in patients with severe congestive heart failure. *Circulation* 73**:** Iii168-174.

Mosawy S, Jackson DE, Woodman OL, Linden MD (2013). Treatment with quercetin and 3',4'-dihydroxyflavonol inhibits platelet function and reduces thrombus formation in vivo. *J Thromb Thrombolysis* 36**:** 50-57.

Muller-Strahl G, Kottenberg K, Zimmer HG, Noack E, Kojda G (2000). Inhibition of nitric oxide synthase augments the positive inotropic effect of nitric oxide donors in the rat heart. *J Physiol* 522 Pt 2**:** 311-320.

Munzel T, Daiber A, Mulsch A (2005). Explaining the phenomenon of nitrate tolerance. *Circ Res* 97**:** 618-628.

Munzel T, Sayegh H, Freeman BA, Tarpey MM, Harrison DG (1995). Evidence for enhanced vascular superoxide anion production in nitrate tolerance. A novel mechanism underlying tolerance and cross-tolerance. *J Clin Invest* 95**:** 187-194.

Münzel T, Genth-Zotz S, Hink U (2007). Targeting Heme-Oxidized Soluble Guanylate Cyclase Solution for All Cardiorenal Problems in Heart Failure? *Hypertension* 49**:** 974-976.

Nagao A, Seki M, Kobayashi H (1999). Inhibition of xanthine oxidase by flavonoids. *Biosci Biotechnol Biochem* 63**:** 1787-1790.

Nagasawa HT, DeMaster EG, Redfern B, Shirota FN, Goon DJ (1990). Evidence for nitroxyl in the catalase-mediated bioactivation of the alcohol deterrent agent cyanamide. *J Med Chem* 33**:** 3120-3122.

Naughton P, Hoque M, Green CJ, Foresti R, Motterlini R (2002). Interaction of heme with nitroxyl or nitric oxide amplifies heme oxygenase-1 induction: involvement of the transcription factor Nrf2. *Cell Mol Biol* 48**:** 885-894.

Niccoli G, Burzotta F, Galiuto L, Crea F (2009). Myocardial no-reflow in humans. *J Am Coll Cardiol* 54**:** 281-292.

Nieminen MS, Brutsaert D, Dickstein K, Drexler H, Follath F, Harjola VP, *et al.* (2006). EuroHeart Failure Survey II (EHFS II): a survey on hospitalized acute heart failure patients: description of population. *Eur Heart J* 27**:** 2725-2736.

Nijveldt RJ, van Nood E, van Hoorn DE, Boelens PG, van Norren K, van Leeuwen PA (2001). Flavonoids: a review of probable mechanisms of action and potential applications. *Am J Clin Nutr* 74**:** 418-425.

Niketic V, Stojanovic S, Nikolic A, Spasic M, Michelson AM (1999). Exposure of Mn and FeSODs, but not Cu/ZnSOD, to NO leads to nitrosonium and nitroxyl ions generation which cause enzyme modification and inactivation: an in vitro study. *Free Radic Biol Med* 27**:** 992-996.

O'Connor CM, Gattis WA, Uretsky BF, Adams Jr KF, McNulty SE, Grossman SH, *et al.* (1999). Continuous intravenous dobutamine is associated with an increased risk of death in patients with advanced heart failure: insights from the Flolan International Randomized Survival Trial (FIRST). *Amer Heart J* 138**:** 78-86.

Okumura H, Nagaya N, Itoh T, Okano I, Hino J, Mori K, *et al.* (2004). Adrenomedullin infusion attenuates myocardial ischemia/reperfusion injury through the phosphatidylinositol 3-kinase/Akt-dependent pathway. *Circulation* 109**:** 242-248.

Opie LH (1989). Reperfusion injury and its pharmacologic modification. *Circulation* 80**:** 1049-1062.

Orallo F, Camina M, Alvarez E, Basaran H, Lugnier C (2005). Implication of cyclic nucleotide phosphodiesterase inhibition in the vasorelaxant activity of the citrus-fruits flavonoid (+/-)-naringenin. *Planta Med* 71**:** 99-107.

Osada M, Netticadan T, Tamura K, Dhalla NS (1998). Modification of ischemia-reperfusion-induced changes in cardiac sarcoplasmic reticulum by preconditioning. *Am J Physiol* 274**:** H2025-2034.

Otsu K, Yamashita N, Nishida K, Hirotani S, Yamaguchi O, Watanabe T, *et al.* (2003). Disruption of a single copy of the p38alpha MAP kinase gene leads to cardioprotection against ischemia-reperfusion. *Biochem Biophys Res Commun* 302**:** 56-60.

Ottani A, Galantucci M, Ardimento E, Neri L, Canalini F, Calevro A, *et al.* (2013). Modulation of the JAK/Erk/STAT signaling in melanocortin-induced inhibition of local and systemic responses to myocardial ischemia/reperfusion. *Pharmacol Res* 72**:** 1-8.

Pagliaro P, Mancardi D, Rastaldo R, Penna C, Gattullo D, Miranda KM, *et al.* (2003). Nitroxyl affords thiol-sensitive myocardial protective effects akin to early preconditioning. *Free Radic Biol Med* 34**:** 33-43.

Panneerselvam M, Tsutsumi YM, Bonds JA, Horikawa YT, Saldana M, Dalton ND, *et al.* (2010). Dark chocolate receptors: epicatechin-induced cardiac protection is dependent on delta-opioid receptor stimulation. *Am J Physiol* 299**:** H1604-1609.

Paolocci N, Katori T, Champion HC, St John ME, Miranda KM, Fukuto JM, *et al.* (2003). Positive inotropic and lusitropic effects of HNO/NO^- in failing hearts: independence from beta-adrenergic signaling. *Proc Natl Acad Sci U S A* 100**:** 5537-5542.

Paolocci N, Ekelund UE, Isoda T, Ozaki M, Vandegaer K, Georgakopoulos D, *et al.* (2000). cGMP-independent inotropic effects of nitric oxide and peroxynitrite donors: potential role for nitrosylation. *Am J Physiol* 279**:** H1982-1988.

Paolocci N, Saavedra WF, Miranda KM, Martignani C, Isoda T, Hare JM, *et al.* (2001). Nitroxyl anion exerts redox-sensitive positive cardiac inotropy in vivo by calcitonin gene-related peptide signaling. *Proc Natl Acad Sci U S A* 98**:** 10463-10468.

Parissis JT, Farmakis D, Nieminen M (2007). Classical inotropes and new cardiac enhancers. *Heart Fail Rev* 12**:** 149-156.

Paulus WJ, Vantrimpont PJ, Shah AM (1994). Acute effects of nitric oxide on left ventricular relaxation and diastolic distensibility in humans. Assessment by bicoronary sodium nitroprusside infusion. *Circulation* 89**:** 2070-2078.

Petronilli V, Sileikyte J, Zulian A, Dabbeni-Sala F, Jori G, Gobbo S, *et al.* (2009). Switch from inhibition to activation of the mitochondrial permeability transition during

hematoporphyrin-mediated photooxidative stress. Unmasking pore-regulating external thiols. *Biochim Biophys Acta* 1787**:** 897-904.

Pierce GN, Meng H (1992). The role of sodium-proton exchange in ischemic/reperfusion injury in the heart. Na^+-H^+ exchange and ischemic heart disease. *Am J Cardiovasc Pathol* 4**:** 91-102.

Pietta PG (2000). Flavonoids as antioxidants. *J Nat Prod* 63**:** 1035-1042.

Poderoso JJ, Carreras MC, Schopfer F, Lisdero CL, Riobo NA, Giulivi C, *et al.* (1999). The reaction of nitric oxide with ubiquinol: kinetic properties and biological significance. *Free Radic Biol Med* 26**:** 925-935.

Podzuweit T, Dalby AJ, Cherry GW, Opie LH (1978). Cyclic AMP levels in ischaemic and non-ischaemic myocardium following coronary artery ligation: relation to ventricular fibrillation. *J Mol Cell Cardiol* 10**:** 81-94.

Putcha GV, Le S, Frank S, Besirli CG, Clark K, Chu B, *et al.* (2003). JNK-mediated BIM phosphorylation potentiates Bax-dependent apoptosis. *Neuron* 38**:** 899-914.

Qin CX, Williams SJ, Woodman OL (2011). Antioxidant activity contributes to flavonol cardioprotection during reperfusion of rat hearts. *Free Radic Biol Med* 51**:** 1437-1444.

Qin CX, Chen X, Hughes RA, Williams SJ, Woodman OL (2008). Understanding the cardioprotective effects of flavonols: discovery of relaxant flavonols without antioxidant activity. *J Med Chem* 51**:** 1874-1884.

Qvigstad E, Moltzau LR, Aronsen JM, Nguyen CH, Hougen K, Sjaastad I, *et al.* (2010). Natriuretic peptides increase beta1-adrenoceptor signalling in failing hearts through phosphodiesterase 3 inhibition. *Cardiovasc Res* 85**:** 763-772.

Rafiee P, Shi Y, Su J, Pritchard KA, Jr., Tweddell JS, Baker JE (2005). Erythropoietin protects the infant heart against ischemia-reperfusion injury by triggering multiple signaling pathways. *Basic Res Cardiol* 100**:** 187-197.

Rahman S, Li J, Bopassa JC, Umar S, Iorga A, Partownavid P, *et al.* (2011). Phosphorylation of GSK-3beta mediates intralipid-induced cardioprotection against ischemia/reperfusion injury. *Anesthesiology* 115**:** 242-253.

Rani N, Bharti S, Manchanda M, Nag T, Ray R, Chauhan S, *et al.* (2013). Regulation of heat shock proteins 27 and 70, p-Akt/p-eNOS and MAPKs by naringin dampens myocardial injury and dysfunction in vivo after ischemia/reperfusion. *PloS one* 8**:** e82577.

Rastaldo R, Pagliaro P, Cappello S, Penna C, Mancardi D, Westerhof N, *et al.* (2007). Nitric oxide and cardiac function. *Life Sci* 81**:** 779-793.

Reffelmann T, Kloner RA (2002). The "no-reflow" phenomenon: basic science and clinical correlates. *Heart* 87**:** 162-168.

Renaud S, de Lorgeril M (1992). Wine, alcohol, platelets, and the French paradox for coronary heart disease. *Lancet* 339**:** 1523-1526.

Rice-Evans CA, Miller NJ, Bolwell PG, Bramley PM, Pridham JB (1995). The relative antioxidant activities of plant-derived polyphenolic flavonoids. *Free Radic Res* 22**:** 375-383.

Ritchie RH, Zeitz CJ, Wuttke RD, Hii JT, Horowitz JD (2006). Attenuation of the negative inotropic effects of metoprolol at short cycle lengths in humans: comparison with sotalol and verapamil. *J Am Coll Cardiol* 48**:** 1234-1241.

Ritchie RH, Irvine JC, Rosenkranz AC, Patel R, Wendt IR, Horowitz JD, *et al.* (2009). Exploiting cGMP-based therapies for the prevention of left ventricular hypertrophy: NO• and beyond. *Pharmacol Ther* 124**:** 279-300.

Rodrigo R, Rivera G, Orellana M, Araya J, Bosco C (2002). Rat kidney antioxidant response to long-term exposure to flavonol rich red wine. *Life Sci* 71**:** 2881-2895.

Rodriguez-Sinovas A, Abdallah Y, Piper HM, Garcia-Dorado D (2007). Reperfusion injury as a therapeutic challenge in patients with acute myocardial infarction. *Heart Fail Rev* 12**:** 207-216.

Romero M, Jimenez R, Sanchez M, Lopez-Sepulveda R, Zarzuelo MJ, O'Valle F, *et al.* (2009). Quercetin inhibits vascular superoxide production induced by endothelin-1: Role of NADPH oxidase, uncoupled eNOS and PKC. *Atherosclerosis* 202**:** 58-67.

Rose BA, Force T, Wang Y (2010). Mitogen-activated protein kinase signaling in the heart: angels versus demons in a heart-breaking tale. *Physiol Rev* 90**:** 1507-1546.

Ruiz-Meana M, Garcia-Dorado D (2009). Translational cardiovascular medicine (II). Pathophysiology of ischemia-reperfusion injury: new therapeutic options for acute myocardial infarction. *Rev Esp Cardiol* 62**:** 199-209.

Russo A, Acquaviva R, Campisi A, Sorrenti V, Di Giacomo C, Virgata G, *et al.* (2000). Bioflavonoids as antiradicals, antioxidants and DNA cleavage protectors. *Cell Biol Toxicol* 16**:** 91-98.

Said M, Vittone L, Mundina-Weilenmann C, Ferrero P, Kranias EG, Mattiazzi A (2003). Role of dual-site phospholamban phosphorylation in the stunned heart: insights from phospholamban site-specific mutants. *Am J Physiol* 285**:** H1198-1205.

Said M, Becerra R, Valverde CA, Kaetzel MA, Dedman JR, Mundina-Weilenmann C, *et al.* (2011). Calcium-calmodulin dependent protein kinase II (CaMKII): a main signal responsible for early reperfusion arrhythmias. *J Mol Cell Cardiol* 51**:** 936-944.

Said M, Becerra R, Palomeque J, Rinaldi G, Kaetzel MA, Diaz-Sylvester PL, *et al.* (2008). Increased intracellular Ca^{2+} and SR Ca^{2+} load contribute to arrhythmias after acidosis in rat heart. Role of Ca^{2+}/calmodulin-dependent protein kinase II. *Am J Physiol* 295**:** H1669-1683.

Salah N, Miller NJ, Paganga G, Tijburg L, Bolwell GP, Rice-Evans C (1995). Polyphenolic flavanols as scavengers of aqueous phase radicals and as chain-breaking antioxidants. *Arch Biochem Biophys* 322**:** 339-346.

Salas MA, Valverde CA, Sanchez G, Said M, Rodriguez JS, Portiansky EL, *et al.* (2010). The signalling pathway of CaMKII-mediated apoptosis and necrosis in the ischemia/reperfusion injury. *J Mol Cell Cardiol* 48**:** 1298-1306.

Saleem M, Ohshima H (2004). Xanthine oxidase converts nitric oxide to nitroxyl that inactivates the enzyme. *Biochem Biophys Res Commun* 315**:** 455-462.

Sanada S, Komuro I, Kitakaze M (2011). Pathophysiology of myocardial reperfusion injury: preconditioning, postconditioning, and translational aspects of protective measures. *Am J Physiol* 301**:** H1723-1741.

Sanada S, Asanuma H, Tsukamoto O, Minamino T, Node K, Takashima S, *et al.* (2004). Protein kinase A as another mediator of ischemic preconditioning independent of protein kinase C. *Circulation* 110**:** 51-57.

Sanchez M, Lodi F, Vera R, Villar IC, Cogolludo A, Jimenez R, *et al.* (2007). Quercetin and isorhamnetin prevent endothelial dysfunction, superoxide production, and overexpression of p47phox induced by angiotensin II in rat aorta. *J Nutr* 137**:** 910-915.

Sandirasegarane L, Diamond J (1999). The nitric oxide donors, SNAP and DEA/NO, exert a negative inotropic effect in rat cardiomyocytes which is independent of cyclic GMP elevation. *J Mol Cell Cardiol* 31**:** 799-808.

Sarkar D, Vallance P, Amirmansour C, Harding SE (2000). Positive inotropic effects of NO donors in isolated guinea-pig and human cardiomyocytes independent of NO species and cyclic nucleotides. *Cardiovasc Res* 48**:** 430-439.

Sato N, Uechi M, Asai K, Patrick T, Kudej RK, Vatner SF (1997). Effects of a novel inotropic agent, BAY y 5959, in conscious dogs: comparison with dobutamine and milrinone. *Am J Physiol* 272**:** H753-759.

Scarabelli TM, Mariotto S, Abdel-Azeim S, Shoji K, Darra E, Stephanou A, *et al.* (2009). Targeting STAT1 by myricetin and delphinidin provides efficient protection of the heart from ischemia/reperfusion-induced injury. *FEBS Lett* 583**:** 531-541.

Schofer J, Montz R, Mathey DG (1985). Scintigraphic evidence of the "no reflow" phenomenon in human beings after coronary thrombolysis. *J Am Coll Cardiol* 5**:** 593-598.

Schwartz BG, Kloner RA (2012). Coronary no reflow. *J Mol Cell Cardiol* 52**:** 873-882.

Schwertz H, Carter JM, Abdudureheman M, Russ M, Buerke U, Schlitt A, *et al.* (2007). Myocardial ischemia/reperfusion causes VDAC phosphorylation which is reduced by cardioprotection with a p38 MAP kinase inhibitor. *Proteomics* 7**:** 4579-4588.

Seal JB, Gewertz BL (2005). Vascular dysfunction in ischemia-reperfusion injury. *Ann Vasc Surg* 19**:** 572-584.

Seko Y, Tobe K, Ueki K, Kadowaki T, Yazaki Y (1996). Hypoxia and hypoxia/reoxygenation activate Raf-1, mitogen-activated protein kinase kinase, mitogen-activated protein kinases, and S6 kinase in cultured rat cardiac myocytes. *Circ Res* 78**:** 82-90.

Seko Y, Takahashi N, Tobe K, Kadowaki T, Yazaki Y (1997). Hypoxia and hypoxia/reoxygenation activate p65PAK, p38 mitogen-activated protein kinase (MAPK), and stress-activated protein kinase (SAPK) in cultured rat cardiac myocytes. *Biochem Biophys Res Commun* 239**:** 840-844.

Sha X, Isbell TS, Patel RP, Day CS, King SB (2006). Hydrolysis of acyloxy nitroso compounds yields nitroxyl (HNO). *J Am Chem Soc* 128**:** 9687-9692.

Shafirovich V, Lymar SV (2002). Nitroxyl and its anion in aqueous solutions: spin states, protic equilibria, and reactivities toward oxygen and nitric oxide. *Proc Natl Acad Sci U S A* 99**:** 7340-7345.

Shaulian E, Karin M (2002). AP-1 as a regulator of cell life and death. *Nat Cell Biol* 4**:** E131-136.

Shimizu S, Yokoshiki H, Sperelakis N, Paul RJ (2000). Role of voltage-dependent and Ca^{2+}-activated K^{+} channels on the regulation of isometric force in porcine coronary artery. *J Vasc Res* 37**:** 16-25.

Shintani-Ishida K, Inui M, Yoshida K (2012). Ischemia-reperfusion induces myocardial infarction through mitochondrial Ca^{2+} overload. *J Mol Cell Cardiol* 53**:** 233-239.

Shiraishi J, Kohno Y, Sawada T, Ito D, Kimura M, Ariyoshi M, *et al.* (2011). Systolic blood pressure at admission, clinical manifestations, and in-hospital outcomes in patients with acute myocardial infarction. *J Cardiol* 58**:** 54-60.

Skrzypiec-Spring M, Grotthus B, Szelag A, Schulz R (2007). Isolated heart perfusion according to Langendorff---still viable in the new millennium. *J Pharmacol Toxicol Methods* 55**:** 113-126.

Smith CC, Dixon RA, Wynne AM, Theodorou L, Ong SG, Subrayan S, *et al.* (2010). Leptin-induced cardioprotection involves JAK/STAT signaling that may be linked to the mitochondrial permeability transition pore. *Am J Physiol* 299**:** H1265-1270.

Smith JA, Shah AM, Lewis MJ (1991). Factors released from endocardium of the ferret and pig modulate myocardial contraction. *J Physiol* 439**:** 1-14.

Solaini G, Harris DA (2005). Biochemical dysfunction in heart mitochondria exposed to ischaemia and reperfusion. *Biochem J* 390**:** 377-394.

Song DK, Jang Y, Kim JH, Chun KJ, Lee D, Xu Z (2010a). Polyphenol (-)-epigallocatechin gallate during ischemia limits infarct size via mitochondrial K_{ATP} channel activation in isolated rat hearts. *J Korean Med Sci* 25**:** 380-386.

Song JQ, Teng X, Cai Y, Tang CS, Qi YF (2009). Activation of Akt/GSK-3beta signaling pathway is involved in intermedin(1-53) protection against myocardial apoptosis induced by ischemia/reperfusion. *Apoptosis* 14**:** 1299-1307.

Song MJ, Baek I, Seo M, Kim SH, Suk K, Woodman OL, *et al.* (2010b). Effects of 3',4'-dihydroxyflavonol on vascular contractions of rat aortic rings. *Clin Exp Pharmacol Physiol* 37**:** 803-810.

Song ZF, Ji XP, Li XX, Wang SJ, Wang SH, Zhang Y (2008). Inhibition of the activity of poly (ADP-ribose) polymerase reduces heart ischaemia/reperfusion injury via suppressing JNK-mediated AIF translocation. *J Cell Mol Med* 12**:** 1220-1228.

Sonnenblick EH, Frishman WH, LeJemtel TH (1979). Dobutamine: a new synthetic cardioactive sympathetic amine. *N Engl J Med* 300**:** 17-22.

Stasch JP, Schmidt PM, Nedvetsky PI, Nedvetskaya TY, H SA, Meurer S, *et al.* (2006). Targeting the heme-oxidized nitric oxide receptor for selective vasodilatation of diseased blood vessels. *J Clin Invest* 116**:** 2552-2561.

Steinberg SF (1999). The molecular basis for distinct beta-adrenergic receptor subtype actions in cardiomyocytes. *Circ Res* 85**:** 1101-1111.

Stephanou A (2004). Role of STAT-1 and STAT-3 in ischaemia/reperfusion injury. *J Cell Mol Med* 8**:** 519-525.

Stephanou A, Scarabelli TM, Brar BK, Nakanishi Y, Matsumura M, Knight RA, *et al.* (2001). Induction of apoptosis and Fas receptor/Fas ligand expression by ischemia/reperfusion in cardiac myocytes requires serine 727 of the STAT-1 transcription factor but not tyrosine 701. *J Biol Chem* 276**:** 28340-28347.

Stephanou A, Brar BK, Scarabelli TM, Jonassen AK, Yellon DM, Marber MS, *et al.* (2000). Ischemia-induced STAT-1 expression and activation play a critical role in cardiomyocyte apoptosis. *J Biol Chem* 275**:** 10002-10008.

Stokoe D, Engel K, Campbell DG, Cohen P, Gaestel M (1992). Identification of MAPKAP kinase 2 as a major enzyme responsible for the phosphorylation of the small mammalian heat shock proteins. *FEBS Lett* 313**:** 307-313.

Sugamura K, Keaney JF, Jr. (2011). Reactive oxygen species in cardiovascular disease. *Free Radic Biol Med* 51**:** 978-992.

Sun D, Huang J, Zhang Z, Gao H, Li J, Shen M, *et al.* (2012). Luteolin limits infarct size and improves cardiac function after myocardium ischemia/reperfusion injury in diabetic rats. *PLoS One* 7**:** e33491.

Szobi A, Rajtik T, Carnicka S, Ravingerova T, Adameova A (2014). Mitigation of postischemic cardiac contractile dysfunction by CaMKII inhibition: effects on programmed necrotic and apoptotic cell death. *Mol Cell Biochem* 388**:** 269-276.

Takahashi N, Hayano T, Suzuki M (1989). Peptidyl-prolyl cis-trans isomerase is the cyclosporin A-binding protein cyclophilin. *Nature* 337**:** 473-475.

Takatani T, Takahashi K, Uozumi Y, Matsuda T, Ito T, Schaffer SW, *et al.* (2004). Taurine prevents the ischemia-induced apoptosis in cultured neonatal rat cardiomyocytes through Akt/caspase-9 pathway. *Biochem Biophys Res Commun* 316**:** 484-489.

Takeishi Y, Abe J, Lee JD, Kawakatsu H, Walsh RA, Berk BC (1999). Differential regulation of p90 ribosomal S6 kinase and big mitogen-activated protein kinase 1 by ischemia/reperfusion and oxidative stress in perfused guinea pig hearts. *Circ Res* 85**:** 1164-1172.

Tan Y, Rouse J, Zhang A, Cariati S, Cohen P, Comb MJ (1996). FGF and stress regulate CREB and ATF-1 via a pathway involving p38 MAP kinase and MAPKAP kinase-2. *Embo J* 15**:** 4629-4642.

Tang L, Peng Y, Xu T, Yi X, Liu Y, Luo Y, *et al.* (2013). The effects of quercetin protect cardiomyocytes from A/R injury is related to its capability to increasing expression and activity of PKCepsilon protein. *Mol Cell Biochem* 382**:** 145-152.

Tani M, Neely JR (1989). Role of intracellular Na^+ in Ca^{2+} overload and depressed recovery of ventricular function of reperfused ischemic rat hearts. Possible involvement of H^+-Na^+ and Na^+-Ca^{2+} exchange. *Circ Res* 65**:** 1045-1056.

Tao J, Zhu W, Li Y, Xin P, Li J, Liu M, *et al.* (2011). Apelin-13 protects the heart against ischemia-reperfusion injury through inhibition of ER-dependent apoptotic pathways in a time-dependent fashion. *Am J Physiol* 301**:** H1471-1486.

Tavazzi L, Maggioni AP, Lucci D, Cacciatore G, Ansalone G, Oliva F, *et al.* (2006). Nationwide survey on acute heart failure in cardiology ward services in Italy. *Eur Heart J* 27**:** 1207-1215.

Temsah RM, Dyck C, Netticadan T, Chapman D, Elimban V, Dhalla NS (2000). Effect of beta-adrenoceptor blockers on sarcoplasmic reticular function and gene expression in the ischemic-reperfused heart. *J Pharmacol Exp Ther* 293**:** 15-23.

Testai L, Martelli A, Marino A, D'Antongiovanni V, Ciregia F, Giusti L, *et al.* (2013). The activation of mitochondrial BK potassium channels contributes to the protective effects of naringenin against myocardial ischemia/reperfusion injury. *Biochem Pharmacol* 85**:** 1634-1643.

Thomas CJ, Lim NR, Kedikaetswe A, Yeap YY, Woodman OL, Ng DC, *et al.* (2015). Evidence that the MEK/Erk but not the PI3K/Akt pathway is required for protection from myocardial ischemia-reperfusion injury by 3',4'-dihydroxyflavonol. *Eur J Pharmacol* 758**:** 53-59.

Thomas CJ, Ng DC, Patsikatheodorou N, Limengka Y, Lee MW, Darby IA, *et al.* (2011). Cardioprotection from ischaemia-reperfusion injury by a novel flavonol that reduces activation of p38 MAPK. *Eur J Pharmacol* 658**:** 160-167.

Tocchetti CG, Stanley BA, Murray CI, Sivakumaran V, Donzelli S, Mancardi D, *et al.* (2011). Playing with cardiac "redox switches": the "HNO way" to modulate cardiac function. *Antioxid Redox Signal* 14**:** 1687-1698.

Tocchetti CG, Wang W, Froehlich JP, Huke S, Aon MA, Wilson GM, *et al.* (2007). Nitroxyl improves cellular heart function by directly enhancing cardiac sarcoplasmic reticulum Ca^{2+} cycling. *Circ Res* 100**:** 96-104.

Toledo-Pereyra LH, Lopez-Neblina F, Toledo AH (2008). Protein kinases in organ ischemia and reperfusion. *J Invest Surg* 21**:** 215-226.

Toufektsian MC, de Lorgeril M, Nagy N, Salen P, Donati MB, Giordano L, *et al.* (2008). Chronic dietary intake of plant-derived anthocyanins protects the rat heart against ischemia-reperfusion injury. *J Nutr* 138**:** 747-752.

Townsend PA, Scarabelli TM, Pasini E, Gitti G, Menegazzi M, Suzuki H, *et al.* (2004). Epigallocatechin-3-gallate inhibits STAT-1 activation and protects cardiac myocytes from ischemia/reperfusion-induced apoptosis. *The FASEB J* 18**:** 1621-1623.

Unverferth DA, Blanford M, Kates RE, Leier CV (1980). Tolerance to dobutamine after a 72 hour continuous infusion. *Am J Med* 69**:** 262-266.

Valverde CA, Mundina-Weilenmann C, Reyes M, Kranias EG, Escobar AL, Mattiazzi A (2006). Phospholamban phosphorylation sites enhance the recovery of intracellular Ca2+ after perfusion arrest in isolated, perfused mouse heart. *Cardiovasc Res* 70**:** 335-345.

van Dam H, Wilhelm D, Herr I, Steffen A, Herrlich P, Angel P (1995). ATF-2 is preferentially activated by stress-activated protein kinases to mediate *c-jun* induction in response to genotoxic agents. *Embo J* 14**:** 1798-1811.

Vanoverschelde JL, Wijns W, Essamri B, Bol A, Robert A, Labar D, *et al.* (1993). Hemodynamic and mechanical determinants of myocardial O2 consumption in normal human heart: effects of dobutamine. *Am J Physiol* 265**:** H1884-1892.

Vila-Petroff M, Salas MA, Said M, Valverde CA, Sapia L, Portiansky E, *et al.* (2007). CaMKII inhibition protects against necrosis and apoptosis in irreversible ischemia-reperfusion injury. *Cardiovasc Res* 73**:** 689-698.

Vittone L, Mundina-Weilenmann C, Said M, Ferrero P, Mattiazzi A (2002). Time course and mechanisms of phosphorylation of phospholamban residues in ischemia-reperfused rat hearts. Dissociation of phospholamban phosphorylation pathways. *J Mol Cell Cardiol* 34**:** 39-50.

Vleeming W, van Rooij HH, Wemer J, Porsius AJ (1991). Cardiovascular responses to the stereoisomers of dobutamine in isolated rat hearts 48 hours after acute myocardial infarction. *J Cardiovasc Pharmacol* 17**:** 634-640.

Wadsworth TL, McDonald TL, Koop DR (2001). Effects of Ginkgo biloba extract (EGb 761) and quercetin on lipopolysaccharide-induced signaling pathways involved in the release of tumor necrosis factor-alpha. *Biochem Pharmacol* 62**:** 963-974.

Walker MJ, Curtis MJ, Hearse DJ, Campbell RW, Janse MJ, Yellon DM, *et al.* (1988). The Lambeth Conventions: guidelines for the study of arrhythmias in ischaemia infarction, and reperfusion. *Cardiovasc Res* 22**:** 447-455.

Wan LL, Xia J, Ye D, Liu J, Chen J, Wang G (2009). Effects of quercetin on gene and protein expression of NOX and NOS after myocardial ischemia and reperfusion in rabbit. *Cardiovasc Ther* 27**:** 28-33.

Wang H, Kohr MJ, Traynham CJ, Wheeler DG, Janssen PM, Ziolo MT (2008). Neuronal nitric oxide synthase signaling within cardiac myocytes targets phospholamban. *Am J Physiol* 294**:** C1566-1575.

Wang L, Tu YC, Lian TW, Hung JT, Yen JH, Wu MJ (2006). Distinctive antioxidant and antiinflammatory effects of flavonols. *J Agric Food Chem* 54**:** 9798-9804.

Wang S, Dusting GJ, May CN, Woodman OL (2004). 3',4'-Dihydroxyflavonol reduces infarct size and injury associated with myocardial ischaemia and reperfusion in sheep. *Br J Pharmacol* 142**:** 443-452.

Wang S, Fei K, Xu YW, Wang LX, Chen YQ (2009). Dihydroxyflavonol reduces post-infarction left ventricular remodeling by preventing myocyte apoptosis in the non-infarcted zone in goats. *Chin Med J (Engl)* 122**:** 61-67.

Wang Y, Zhang ZZ, Wu Y, Ke JJ, He XH, Wang YL (2013). Quercetin postconditioning attenuates myocardial ischemia/reperfusion injury in rats through the PI3K/Akt pathway. *Braz J Med Biol Res* 46**:** 861-867.

Wanstall JC, Jeffery TK, Gambino A, Lovren F, Triggle CR (2001). Vascular smooth muscle relaxation mediated by nitric oxide donors: a comparison with acetylcholine, nitric oxide and nitroxyl ion. *Br J Pharmacol* 134**:** 463-472.

Weiss JN, Korge P, Honda HM, Ping P (2003). Role of the mitochondrial permeability transition in myocardial disease. *Circ Res* 93**:** 292-301.

Weiss SJ (1989). Tissue destruction by neutrophils. *N Engl J Med* 320**:** 365-376.

Westerhof N, Boer C, Lamberts RR, Sipkema P (2006). Cross-talk between cardiac muscle and coronary vasculature. *Physiol Rev* 86**:** 1263-1308.

Weyrich AS, Ma XL, Buerke M, Murohara T, Armstead VE, Lefer AM, *et al.* (1994). Physiological concentrations of nitric oxide do not elicit an acute negative inotropic effect in unstimulated cardiac muscle. *Circ Res* 75**:** 692-700.

White HD, Chew DP (2008). Acute myocardial infarction. *Lancet* 372**:** 570-584.

Williams SJ, Thomas CJ, Boujaoude M, Gannon CT, Zanatta SD, Jarrott B, *et al.* (2011). Water soluble flavonol prodrugs that protect against ischaemia-reperfusion injury in rat hindlimb and sheep heart. *MedChemComm* 2**:** 321-324.

Wilson RF, Laxson DD, Lesser JR, White CW (1989). Intense microvascular constriction after angioplasty of acute thrombotic coronary arterial lesions. *Lancet* 1**:** 807-811.

Wit AL, Janse MJ (2001). Reperfusion arrhythmias and sudden cardiac death: a century of progress toward an understanding of the mechanisms. *Circ Res* 89**:** 741-743.

Wong PS, Hyun J, Fukuto JM, Shirota FN, DeMaster EG, Shoeman DW, *et al.* (1998). Reaction between S-nitrosothiols and thiols: generation of nitroxyl (HNO) and subsequent chemistry. *Biochemistry* 37**:** 5362-5371.

Woodman OL, Chan E (2004). Vascular and anti-oxidant actions of flavonols and flavones. *Clin Exp Pharmacol Physiol* 31**:** 786-790.

Woodman OL, Malakul W (2009). 3′, 4′-Dihydroxyflavonol prevents diabetes-induced endothelial dysfunction in rat aorta. *Life Sci* 85**:** 54-59.

Woodman OL, Meeker WF, Boujaoude M (2005). Vasorelaxant and antioxidant activity of flavonols and flavones: structure-activity relationships. *J Cardiovasc Pharmacol* 46**:** 302-309.

Woodman OL, Long R, Pons S, Eychenne N, Berdeaux A, Morin D (2014). The cardioprotectant 3',4'-dihydroxyflavonol inhibits opening of the mitochondrial permeability transition pore after myocardial ischemia and reperfusion in rats. *Pharmacol Res* 81**:** 26-33.

Wu X, Xu T, Li D, Zhu S, Chen Q, Hu W, *et al.* (2013). Erk/PP1a/PLB/SERCA2a and JNK pathways are involved in luteolin-mediated protection of rat hearts and cardiomyocytes following ischemia/reperfusion. *PLoS One* 8**:** e82957.

Wynne BM, Labazi H, Tostes RC, Webb RC (2012). Aorta from angiotensin II hypertensive mice exhibit preserved nitroxyl anion mediated relaxation responses. *Pharmacol Res* 65**:** 41-47.

Yamamoto K, Ichijo H, Korsmeyer SJ (1999). BCL-2 is phosphorylated and inactivated by an ASK1/Jun N-terminal protein kinase pathway normally activated at G(2)/M. *Mol Cell Biol* 19**:** 8469-8478.

Yamazaki KG, Romero-Perez D, Barraza-Hidalgo M, Cruz M, Rivas M, Cortez-Gomez B, *et al.* (2008). Short- and long-term effects of (-)-epicatechin on myocardial ischemia-reperfusion injury. *Am J Physiol* 295**:** H761-767.

Yamazaki KG, Andreyev AY, Ortiz-Vilchis P, Petrosyan S, Divakaruni AS, Wiley SE, *et al.* (2014). Intravenous (-)-epicatechin reduces myocardial ischemic injury by protecting mitochondrial function. *Int J Cardiol* 175**:** 297-306.

Yanagi S, Matsumura K, Marui A, Morishima M, Hyon SH, Ikeda T, *et al.* (2011). Oral pretreatment with a green tea polyphenol for cardioprotection against ischemia-reperfusion injury in an isolated rat heart model. *J Thorac Cardiovasc Surg* 141**:** 511-517.

Yang XM, Krieg T, Cui L, Downey JM, Cohen MV (2004). NECA and bradykinin at reperfusion reduce infarction in rabbit hearts by signaling through PI3K, Erk, and NO. *J Mol Cell Cardiol* 36**:** 411-421.

Yao YT, Li LH, Chen L, Wang WP, Li LB, Gao CQ (2010). Sevoflurane postconditioning protects isolated rat hearts against ischemia-reperfusion injury: the role of radical oxygen species, extracellular signal-related kinases 1/2 and mitochondrial permeability transition pore. *Mol Biol Rep* 37**:** 2439-2446.

Yellon DM, Hausenloy DJ (2007). Myocardial reperfusion injury. *N Engl J Med* 357**:** 1121-1135.

Yin T, Sandhu G, Wolfgang CD, Burrier A, Webb RL, Rigel DF, *et al.* (1997). Tissue-specific pattern of stress kinase activation in ischemic/reperfused heart and kidney. *J Biol Chem* 272**:** 19943-19950.

Yoo J, Fukuto JM (1995). Oxidation of N-hydroxyguanidine by nitric oxide and the possible generation of vasoactive species. *Biochem Pharmacol* 50**:** 1995-2000.

Yu D, Li M, Tian Y, Liu J, Shang J (2015). Luteolin inhibits ROS-activated MAPK pathway in myocardial ischemia/reperfusion injury. *Life Sci* 122**:** 15-25.

Yue TL, Wang C, Gu JL, Ma XL, Kumar S, Lee JC, *et al.* (2000). Inhibition of extracellular signal-regulated kinase enhances ischemia/reoxygenation-induced apoptosis in cultured cardiac myocytes and exaggerates reperfusion injury in isolated perfused heart. *Circ Res* 86**:** 692-699.

Yuill KH, Yarova P, Kemp-Harper BK, Garland CJ, Dora KA (2011). A novel role for HNO in local and spreading vasodilatation in rat mesenteric resistance arteries. *Antioxid Redox Signal* 14**:** 1625-1635.

Zahradnikova A, Minarovic I, Venema RC, Meszaros LG (1997). Inactivation of the cardiac ryanodine receptor calcium release channel by nitric oxide. *Cell Calcium* 22**:** 447-454.

Zaidi NF, Lagenaur CF, Abramson JJ, Pessah I, Salama G (1989). Reactive disulfides trigger Ca^{2+} release from sarcoplasmic reticulum via an oxidation reaction. *J Biol Chem* 264**:** 21725-21736.

Zamzami N, Kroemer G (2001). The mitochondrion in apoptosis: how Pandora's box opens. *Nat Rev Mol Cell Biol* 2**:** 67-71.

Zeller A, Wenzl MV, Beretta M, Stessel H, Russwurm M, Koesling D, *et al.* (2009). Mechanisms underlying activation of soluble guanylate cyclase by the nitroxyl donor Angeli's salt. *Mol Pharmacol* 76**:** 1115-1122.

Zenebe W, Pechanova O, Andriantsitohaina R (2003). Red wine polyphenols induce vasorelaxation by increased nitric oxide bioactivity. *Physiol Res* 52**:** 425-432.

Zhang J, Li XX, Bian HJ, Liu XB, Ji XP, Zhang Y (2009). Inhibition of the activity of Rho-kinase reduces cardiomyocyte apoptosis in heart ischemia/reperfusion via suppressing JNK-mediated AIF translocation. *Clin Chim Acta* 401**:** 76-80.

Zhang N, Pei F, Wei H, Zhang T, Yang C, Ma G, *et al.* (2011). Isorhamnetin protects rat ventricular myocytes from ischemia and reperfusion injury. *Exp Toxicol Pathol* 63**:** 33-38.

Zhang T, Brown JH (2004). Role of Ca^{2+}/calmodulin-dependent protein kinase II in cardiac hypertrophy and heart failure. *Cardiovasc Res* 63**:** 476-486.

Zhao ZQ (2004). Oxidative stress-elicited myocardial apoptosis during reperfusion. *Curr Opin Pharmacol* 4**:** 159-165.

Zhao ZQ, Nakamura M, Wang NP, Wilcox JN, Shearer S, Ronson RS, *et al.* (2000). Reperfusion induces myocardial apoptotic cell death. *Cardiovasc Res* 45**:** 651-660.

Ziolo MT (2008). The fork in the nitric oxide road: cyclic GMP or nitrosylation? *Nitric Oxide* 18**:** 153-156.

Zou H, Li Y, Liu X, Wang X (1999). An APAF-1.cytochrome c multimeric complex is a functional apoptosome that activates procaspase-9. *J Biol Chem* 274**:** 11549-11556.

Zucchi R, Ronca F, Ronca-Testoni S (2001). Modulation of sarcoplasmic reticulum function: a new strategy in cardioprotection? *Pharmacol Ther* 89**:** 47-65.

Zweier JL, Talukder MA (2006). The role of oxidants and free radicals in reperfusion injury. *Cardiovasc Res* 70**:** 181-190.

Zweier JL, Flaherty JT, Weisfeldt ML (1987). Direct measurement of free radical generation following reperfusion of ischemic myocardium. *Proc Natl Acad Sci U S A* 84**:** 1404-1407.